ADDIS ABABA UNIVERSITY

ADDIS ABABA INSTITUTE OF TECHNOLOGY

School of Civil and Environmental Engineering

Flood Change Detection, Attribution and Management Implication in Data-Scarce Watersheds: A Case of Wabi Shebele River Basin, Ethiopia

By

Fraol Abebe Wudineh

Thesis for the Degree of Doctor of Philosophy

March 2022

FLOOD CHANGE DETECTION, ATTRIBUTION AND MANAGEMENT IMPLICATION IN DATA-SCARCE WATERSHEDS: A CASE OF WABI SHEBELE RIVER BASIN, ETHIOPIA

Ph.D. Dissertation

By:

Fraol Abebe

Under supervision of:

Dr. Belete Berhanu

Associate Professor, School of Civil and Environmental Engineering, Addis Ababa Institute of Technology, AAU, Ethiopia

Dr. Semu Ayalew

Associate Research Professor, School of Civil and Environmental Engineering, University of Connecticut, USA

A dissertation submitted to Addis Ababa University, Addis Ababa Institute of Technology, School of Civil and Environmental Engineering in Partial Fulfillment of the Doctor of Philosophy (Ph.D.) in Civil (Hydraulic) Engineering.

March 2022

Addis Ababa, Ethiopia

Addis Ababa University (AAU), Addis Ababa Institute of Technology (AAiT)

Doctoral Dissertation Approval Sheet

Flood Change Detection, Attribution and Management Implication in Data-Scarce Watersheds: A Case of Wabi Shebele River Basin, Ethiopia

By:

Fraol Abebe Wudineh — 3/21/2022 — Date

APPROVED BY

BOARD OF EXAMINERS:

Supervisor 1: - Dr. Belete Berhanu Kidanewold (Assoc. Prof.) — 22/03/2022 — Date

Supervisor 2: - Dr. Semu Ayalew Moges (Assoc. Prof.) — March 26,2022 — Date

External Examiner: - Prof. Assefa M. Melesse — March 23, 2022 — Date

Internal Examiner 1: - Prof. Yilma Seleshi — March 24, 2022 — Date

Internal Examiner 2: - Dr. Dereje Hailu (Assoc. Prof.) — March 25,2022 — Date

Chairperson: - Dr. Ebrahim Mohammed (Assoc. Prof.) — Date

Mebrahtu Mohammed (Dr.-Ing.)
Dean, School of Civil & Environmental Engineering

ABSTRACT

Trends and variability of hydroclimatic extremes have received excessive attention in many hydrological modeling studies. However, many scientists are still uncertain to attribute the proportion of hydrologic variability is driven by climate change/variability and anthropogenic factors, particularly in tropical catchments. Wabi Shebele River Basin in Ethiopia experiences flooding with limited availability of the type data is used as a case study to investigate changes in flood discharges and potential driving factors affecting hydrologic response changes and management implication of understanding flood variabilities. Both statistical non-parametric tests and SWAT hydrologic model are used in flood change detection and attribution process. Among the discharge-based flood indicators, annual maximum series (AMS) and peak over threshold (POT) are used to analysis flood time series. Overview of flood discharge analysis indicates the increasing tendency of flood events throughout the basin since 2000. The seasonality analysis reveals cycles of significant extreme high river flows at five to ten-year intervals in the river basin. Precipitation extremes show an increasing trend in the western and eastern upper basin and a decreasing trend in the middle between 1980-2018. The assessment upon driving forces of floods: rainfall, drainage area, elevation, slope, sand soil, forest, and agricultural land coverage identified as the most influential variables in flood formation of the basin. The correlation analysis between extreme streamflow with precipitation and global climate indices reveals a moderate to high correlation value. The semi-distributed hydrological model (i.e., SWAT) conducted to disentangle the impact of climate change and LULC change on flood hazard showed that precipitation and agricultural land coverage led to increment in flood indices. In the middle and upper parts of the Wabi Shebele basin, streamflow increases with increases in agricultural land, and forest coverage decrease. The simulation of hydrologic response to climate change in the future (i.e., 2041-2060 and 2081-2100) showed that the river basin is likely to experience an increase in flood hazard with an increase in precipitation in the future as temperatures increase less than 2^{o}C. Finally, the study on the implication of flood variability revealed that socio-economic damages follow a similar trend tendency to flood variabilities in the river basin. In such cases, development-based climate adaptation mechanisms and flood risk management strategies need to placed. In transboundary river basins like Wabi Shebele, floods have transboundary consequences which need cooperation between riparian countries for Integrated Flood Management (IMF).

TABLE OF CONTENTS

LIST OF TABLES

LIST OF FIGURES

DECLARATION OF AUTHORSHIP

I, **Fraol Abebe Wudineh**, declare that the thesis entitled **Flood Change Detection, Attribution and Management Implication in Data-Scarce Watersheds: A Case of Wabi Shebele River Basin, Ethiopia,** and the work presented in the thesis are my own, original work. I confirm that: this work was done wholly or mainly while in candidature for a Ph.D. degree at Addis Ababa University. Where I have quoted from the work of others, the sources are given. Except for such quotations, this thesis is entirely my work, and I have also acknowledged all sources of help.

Parts of this work have been published as:

I. Abebe Wudineh F., Ayalew Moges S., Berhanu Kidanewold B. (2021a) Trend and Variability in Flood Discharge and Attribution to Climate Change in Wabi Shebele River Basin, Ethiopia. In: Delele M.A., Bitew M.A., Beyene A.A., Fanta S.W., Ali A.N. (eds) Advances of Science and Technology. ICAST 2020, vol 385. Springer, Cham. https://doi.org/10.1007/978-3-030-80618-7_7

II. F. A. Wudineh, S. A. Moges and B. B. Kidanewold (2021b) Detecting hydrological variability in precipitation extremes: Application of reanalysis climate product in data-scarce Wabi-Shebele basin of Ethiopia. J. Hydrol. Eng., ASCE, 2021. https://doi.org/10.1061/(ASCE)HE.1943-5584.0002156

III. Wudineh, F.A., Moges, S.A. and Kidanewold, B.B. (2022) Flood Generation Mechanisms and Potential Drivers of Flood in Wabi-Shebele River Basin, Ethiopia. Natural Resources, 13, 38-51. https://doi.org/10.4236/nr.2022.131003

IV. Wudineh, F.A., Moges, S.A. and Kidanewold, B.B. (2021c) Flood Change Detection and Attribution Using Simulation Approach in Data-Scarce Watersheds: A Case of Wabi Shebele River Basin, Ethiopia. Journal of Water Resource and Protection, 13, 362-393. https://doi.org/10.4236/jwarp.2021.135023

V. F. A. Wudineh, S. A. Moges and B. B. Kidanewold (2021d) Management Implication of Understanding Flood Variabilities in Transboundary Rivers for Future: A Case of Wabi Shebele River Basin, Ethiopia. Pp 151-179 in: Melesse, Assefa M., Abtew, Wossenu, Moges, Semu A. (Eds.) Nile and Grand Ethiopian Renaissance Dam; Past, Present and Future. Springer Geography, https://doi.org/10.1007/978-3-030-76437-1_9

Signed: 

Date: March 28, 2022

ACKNOWLEDGEMENTS

First and foremost, thanks to God, all praises to Almighty God for his merciful and giving me the strength and making this possible.

The supervisors of this thesis at the Addis Ababa University (Addis Ababa Institute of Technology) were Dr. Belete Berhanu and Dr. Semu Ayalew. I am thankful for their guidance and comments, which improved the content of this thesis considerably. My deepest gratitude is to my adviser, Dr. Semu Ayalew. He has been commenting on my views and helping me understand and enrich my ideas, and gave me his guidance to recover when my steps faltered.

The PhD was sponsored by Debre Berhan University, Ethiopian Ministry of Education and I am very grateful to my managers for agreeing to this, supporting me through the years.

I would like to thank the following persons for their comments and cooperation: Dr. Fiseha Behulu from Addis Ababa University for generously given his time and valuable advice; Dr. Endalu Tadele from Addis Ababa Science and Technology University for facilitated office during my study; Surafel Mamo (Ph.D. classmate) for his help with the CHIRPS climate product and Ethiopian Ministry of Water, Irrigation and Energy (MoWIE'), Hydrology Department staffs for their cooperation, which enabled me the use of observed hydrology data and soil data in this study; and Water and Land Resource Center (WLRC) staffs for provided me land use and land cover maps, used in the study. The climate data used in this work was provided by the Ethiopian National Meteorology Agency (NMA), whose support is gratefully acknowledged.

Most importantly, none of this would have been possible without the love and patience of my family. I would like to express my heartfelt gratitude to my mom, Likitu Gemtessa, and my brothers. Finally, my gratitude also goes to my beloved wife Elizabeth T/tsadik and my son, Oliyad Fraol. They have been a constant source of love, concern, support, and strength for me in all these years.

ABBREVATIONS

95PPU	95 Percent Prediction Uncertainty
AMAX	Annual Maximum Discharge
AMS	Annual Maximum Series
AR4	IPCC Fourth Assessment Report
ArcGIS	Aeronautical Reconnaissance Coverage Geographical Information System
BCM	Billion Cubic Meters
CDF	Cumulative Distribution Function
CFSR	Climate Forecast System Reanalysis
CHIRPS	Climate Hazards Group InfraRed Precipitation with Stations
CMIP5	Climate Model Inter-Comparison Project Phase 5
CORDEX-Africa	Coordinated Regional Climate Downscaling Experiment Africa Domain
DEM	Digital Elevation Model
EDA	Exploratory Data Analysis
EM-DAT	Emergency Events Database
ENACTS	Enhancing National Climate Services
EPIs	Extreme Precipitation Indices
ERCS	Ethiopian Red Cross Society
FDC	Flow Duration Curve
FEPI	Flood exceedance probability Index
FFI	Flood Frequency Index
GCM	Global Climate Model
GDP	Gross Domestic Product
GHG	Greenhouse Gases
GWI	Global Water Initiative
HI	Flood Hazard Index
HRU	Hydrologic Response Unit
ICAST	International Conference on Advances of Science and Technology
IDW	Inverse Distance Weights
IFM	Integrated Flood Management

IPCC	Intergovernmental Panel on Climate Change
ITCZ	Intertropical Convergence Zone
IWMI	International Water Management Institute
IWRM	Integrated Water Resource Management
LULC	Land use and Land Cover
MAR	Mean Annual Rainfall
MLR	Multiple Linear Regression
MoWR	Ministry of Water Resources
NBI	Nile Basin Initiative
NDRMC	National Disasters Risk Management Commission
NMA	National Meteorological Agency
OFDA	Office of U.S. Foreign Disaster Assistance
PCA	Principal Component Analysis
POT	Peak Over Threshold
QMPF	Mean Peak Flow Discharge
QPM	Quantile Perturbation Method
RCM	Regional Climate Model
RCP	Representative Concentration Pathways
SCS-CN	Soil Conservation Service Curve Number
SRES	Special Report on Emission Scenarios
SRTM	Shuttle Radar Topography Mission
SST	Sea Surface Temperature
SUFI2	Sequential Uncertainty Fitting Version 2
SWAT	Soil and Water Assessment Tool
SWAT-CUP	SWAT- Calibration and University Programs
UNOCHA	United Nations Office for the Coordination of Humanitarian Affairs
WLRC	Water and Land Resource Center
WMO	World Meteorological Organization

1. INTRODUCTION

1.1. Background and Motivation

Flooding is a natural hazard that is one of the most disastrous and widespread occurrences around the world. It varies in terms of magnitude, duration, and frequency, resulting in varying degrees of damage to human lives and properties. Based on World Meteorological Organization (WMO 2014) reports, flooding is found to be the second most common natural disaster due to weather, water, and climate extremes contributing to high numbers of deaths and economic losses. Globally, the number of inland flood catastrophes between 1996 and 2005 was twice as large as between 1950 and 1980, while the property losses increased by a factor of five (Merz et al. 2012; 2014). In tropical countries, floods occur almost every year, whereas, in other basins, the frequency of occurrence may vary dramatically. Although floods are an integral part of the dynamics of any river channel, flood hazards are rising throughout the world. Historical records of flooding have shown that the impacts of flooding on people's livelihood indicate increasing trends since the 1950s (Adnan 2010; IPCC 2014).

As the watershed changes, it also becomes more hydrologically active, changing the streamflow components and origin of discharge. Consequently, these can increase the extent of the floodplain and the risk of flooding imposed on surrounding areas. Hall et al. (2014) indicated in their studies that flood damage in Europe is rising, mainly due to an increase in the value of assets on floodplains and also changes in flood discharges. The frequency of floods during pre-development periods has become more severe due to the transformation of the watersheds from rural to urban land uses (Eleutério et al., 2012). The floodplains are still attractive for several purposes, e.g., geomorphologic advantages for developing industrial facilities, agriculture, river transportation capabilities, entertainment potential for living and tourism exploitation, the well-being of living near water-bodies, resource availability, sanitation potential, etc. Although several techniques were developed to control water bodies and modify the water dynamics by hydraulic structures like dams and dikes, climate change has been continuing to aggravating flood hazards in riverine societies.

EM-DAT: The OFDA/CRED International Disaster Database provided the lists of natural disasters in Ethiopia over the last century and early 21st century (EM-DAT 2021). According to IPCC (2001), extreme climate events, including floods and droughts, have been increasingly frequent

and severe in Africa, particularly in the Horn of Africa. Among these floods is one of the two most frequently occurring types of disaster in Ethiopia. The projected trends by World Bank (2020) indicate that through the end of the 20th century, there is a likely 20% increase in extreme high rainfall events in Ethiopia. The spatial distribution of flood events between 1980 and 2021 is summarized in Appendix A (i.e., Table A.1 and Figure A-1), in which 31.4 % of flood events occurred in the Wabi Shebele River Basin.

Some initiatives started in recent decades to reduce the negative impacts and take advantage of possible opportunities of climate change in the region. For instance, the Global Water Initiative (GWI) East Africa was established in 2006 to reduce vulnerability to water-related shocks within the region and improve livelihoods, health, and overall welfare through Integrated Water Resource Management (GWI 2010). However, the program includes a limited area (i.e., the Rift Valley and Borana areas) while the climate change vulnerable areas in the country are vast. Similarly, NDRMC (2018) of Ethiopia has already put in place policies, strategies, and programs that enhance the adaptive capacity and reduce the vulnerabilities to extreme weather and climate events. But the country needs financial and technological support and capacity building to implement these policies and strategies.

Limited understanding of flood generation mechanisms aggravates disasters to human life and properties. The studies concerning changes in water resources and floods at a global or continental scale have been carried out using large-scale (global and continental) hydrological models (Dankers et al. 2014; Ruiz-Villanueva et al. 2016; Teshome and Zhang 2019; Adnan 2010). At catchment scale (i.e., the scale of most rivers and catchments, usually less than 300,000 km^2) however, the precision and reliability of these results have not been demonstrated still. A reliable estimate of the impacts of driving forces on water resources in watersheds is hard to infer from large-scale results or by analogy from nearby locations. Moreover, the assumption of stationarity has long served as the basis for statistical analysis of hazards by defining the magnitude of events with a given frequency of occurrences, such as the probable maximum precipitation (PMP) or stationary 100-year design flood (e.g., McCuen 2003; Salas et al., 2018; Slater et al. 2021). If this assumption is incorrect, there is a danger that systems are over or under-designed and either do not serve their purpose adequately or are overly costly. In reality, hydroclimatic extremes exhibit multiple forms of natural non-stationarity depending on the chosen timescales (e.g., Slater et al. 2021; Hall et al. 2014; Merz et al. 2012; Delgado et al., 2009). The major water-related problems

have been always related to having too much water (floods) or too little water (low flows or droughts).

Management of natural hazards, like a flood, requires a thorough understanding of the temporal and spatial factors that contribute to the generations of the flood (Meng et al., 2016; Taye and Willems 2012; Adnan 2010). The growing climate change uncertainty and increased anthropogenic activities require better flood monitoring, management, and mitigation tools. Currently, many predictions and monitoring of extreme weather events such as numerical weather prediction, coupled weather and hydrological models, and radars-based real-time warning systems are emerging. Hydrological models are the main forecasting tools used to predict flooding hazards' magnitude, extent, and level. Studies on a local scale can use data available in national archives (e.g., the discharge observations and meteorological data) and hydrological models developed at the regional scale. It provides the knowledge needed by planners, managers, and policy-makers to assess mitigation possibilities and direct adaptation efforts to the most vulnerable geographic regions and societal sectors.

In this study, assessment of flooding events, including flood generation mechanism, variabilities, and attribution is explored in one of the flood-prone areas in Ethiopia. The study intended to contribute to understanding of mechanisms, changes, and variabilities in the flood hazard to facilitate flood forecasting models and assess the management implication in data-scarce watersheds, in the case of Wabi Shebele River Basin, Ethiopia. Wabi Shebele river is one of the remote river basins in Ethiopia with little study in the area of flood generation, changes and attribution studies this study addressed. The area is known with very limited data that are ideally required in hydrologic modeling and flood risk management. Compared to recommended minimum densities of stations by WMO (2013), the total hydrometric networks in the river basin account only 1/4 for weather stations and about ½ for stream gauging stations. The lack of accessibility, security problems, budgetary constraints, and lack of skilled human resources were reported to cause data limitation in the river basin (Awass 2009; MoWR 2003; Pickford 1999). The existing hydrometric network in the river basin lacks proper consideration of the variability of the hydro-meteorological elements (mainly rainfall and discharge) to be measured. Therefore, an alternative approach through hydrologic models, supported by statistical treatments of existing data is required to overcome data inconsistency in the river basin.

The terms detection and attribution are used in this study as are given by IPCC (2010) and Merz et al. (2012): "detection" as demonstrating a change that has been observed which is statistically different from what can be explained by natural internal variability and "attribution" as the process of establishing the most likely causes for the detected change with some defined level of confidence. The terms change and trend are synonymously used in studies owing that trend is not necessarily a gradual change (Merz et al. 2012; Hundecha and Merz 2012; Yue et al., 2019). Similarly, this study used a similar definition for both terms.

1.2. Research Questions

This study intended to address the following questions: Is flood hazard shows increasing trend in the Wabi Shebele basin? If so, what are the most influential drivers for flood generation and changes? Detection and attribution of changes in flood hazard is decision-based frame work that are important in flood management activities.

1.3. Objective of the thesis

The overall objective of this thesis is to contribute toward the understanding of mechanisms, changes, and variabilities in the flood hazard that can be attributed to external driving forces to facilitate flood forecasting models and understanding the implication of management of flood variabilities in the Wabi Shebele River Basin, Ethiopia.

The specific objectives are:

1) To detect temporal changes in extreme high discharges and attribution based on statistical and model-based approach
2) To detect variabilities in precipitation extremes using reanalysis climate product in the data-scarce watersheds
3) To assess potential drivers of flood events and identifying the influential drivers on floods generations in an effort to predict flood peak discharges in ungagged watersheds
4) To quantify the impacts of climate change and land-use/land cover change on streamflow and flood hazard in the Wabi Shebele River Basin using a model-based approach
5) To investigate associated impacts and management implications of understanding flood variabilities in the Wabi Shebele River Basin, Ethiopia

1.4. Thesis Organization

This thesis is organized into three sections. The first section deals with a general introduction under chapters (Chapter 1-2). Following the introduction under chapter 1, the study area description is presented in chapter 2. The study's analysis, results, and panels are under five chapters (Chapter 3-8). In chapter 3, trends and variabilities in flood discharges and attribution to climate variables using available observed data. In chapter 4, variabilities in precipitation extremes in data-scarce watersheds are investigated using reanalysis rainfall data sets. Flood generation mechanics and potential driving forces are addressed in chapter 5. In chapter 6, flood change detection and attribution using the model-based approach in the data-scarce watershed. Chapter 7 discusses climate change and land use/cover changes impact on flood hazards. Both observed data and climate models with the hydrological model are used to explore the climate change impact on flood magnitude and frequency. Land use and land cover change analysis and impacts on flood occurrence is also presented in this section. The assessment on the implication of understanding flood variabilities in flood risk management is discussed under chapter 8.

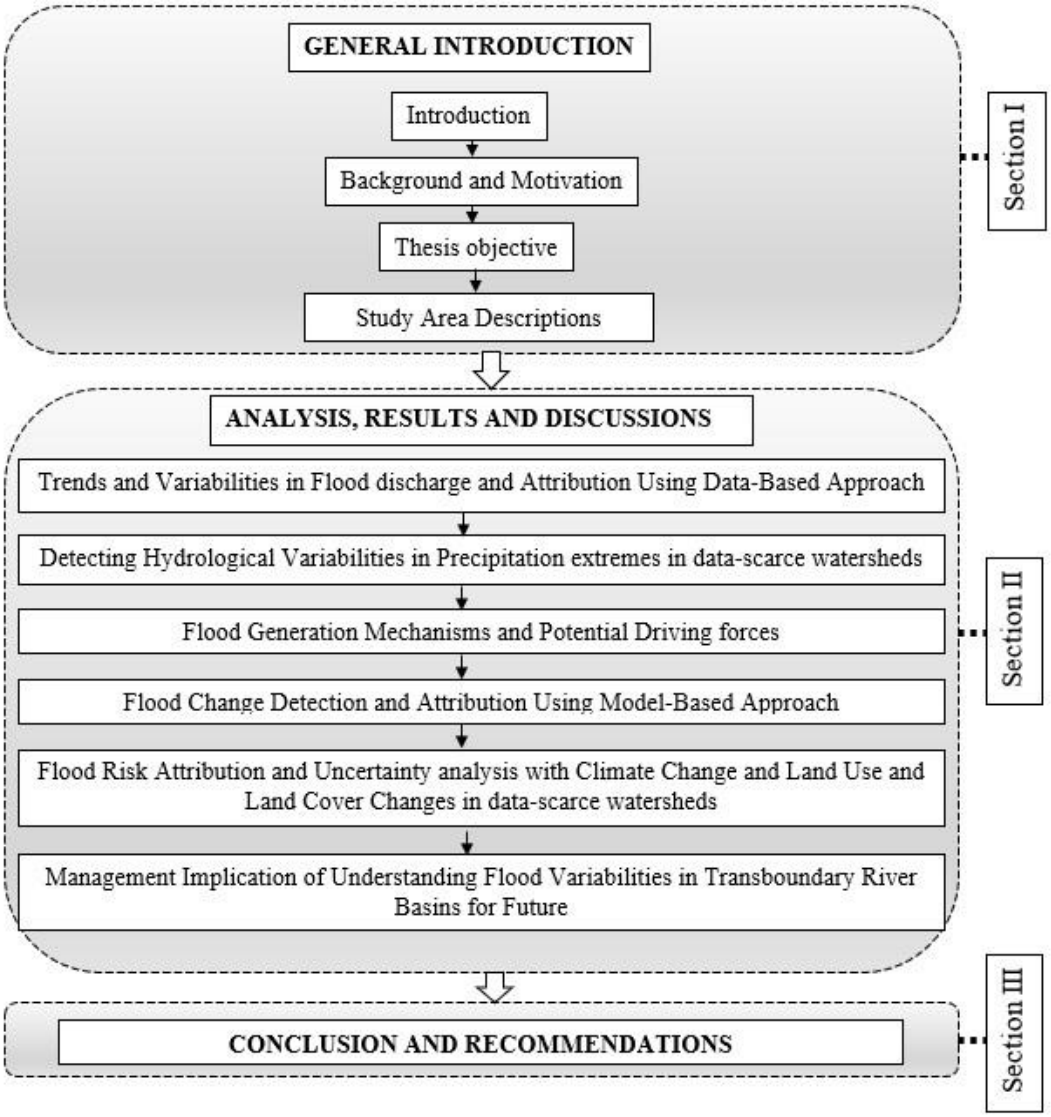

Figure 1-1 Conceptual framework of the research

2. STUDY AREA DESCRIPTIONS

2.1. Introduction

Wabi Shebele River Basin, one of the major river basins in Ethiopia is selected as the study site for this thesis. This chapter introduces the location and physiographic characteristics of the Wabi Shebele River Basin in terms of topography, geology, soils, land use and land cover, climate, hydrology, and specific water infrastructure developments existent in the area.

2.2. Location

The Wabi Shebele basin is a transboundary river basin located in the Horn of Africa, between Ethiopia and the Republic of Somalia. It originates from Bale highlands ranges of the Galama to Ahmar of Ethiopia, about 4,000 m altitudes, and drains a portion of Somalia before draining to the Indian Ocean. More than 70% of the catchment (202,220 km^2) is falls in Ethiopia, covering about 19% of the total areas of the country. The Wabi Shebele basin in this study represents the catchment in Ethiopia, within 4°45' N to 9°45' N latitude and 38°45' E to 45°45' E longitude (Figure 2-1). The river basin is bounded: by Genale-Dawa Basin on the southwest, Rift Valley Basin on the west and north-west, Aysha-Dewele Basin on the northeast, and Ogaden Basin on the east. The basin crosses four administrative regions. 98 % of the study area falls in the Somali and Oromia regions, and the remaining 2% falls within Harari and SNNP regional states.

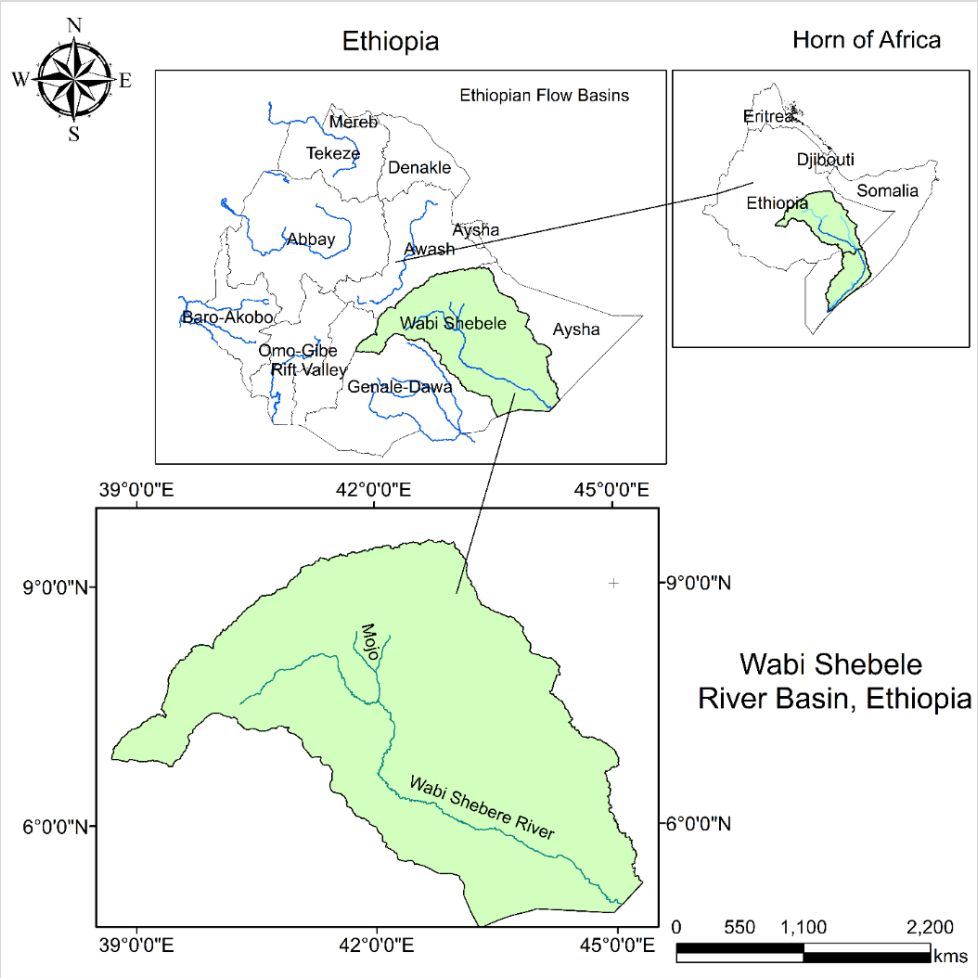

Figure 2-1 Location Map of the study area, Wabi Shebele River Basin

2.3. Topography

The Wabi Shebele River flows south in the upper catchment, then in the eastern direction, and subsequently changes its course towards the northeastern, and the river finds its path towards the south in the central areas of the river basin and to the Indian Ocean. A 90 m grid digital elevation model (DEM) of Shuttle Radar Topography Mission (SRTM) is obtained from http://srtm.csi.cgiar.org used for all subsequent terrain analysis. The highest altitude within the catchment, above 4,000 m, is at the northwestern borders of the basin. The northwest to the eastern boundary of the river basin has high elevation due to Galama and Ahmar ranges. The catchment elevation ranges from about 200 meters above sea level, where the Wabi Shebele crosses the Republic of Somalia border, to 4000 meters above sea level in the highlands of the northwestern boundary of the basin (Figure 2-2). The basin's 11% coverage is highland. The alluvial plain of lower valley which is stretched up to the Somalia border is very gentle slope of 0.25 to 0.35 m/km.

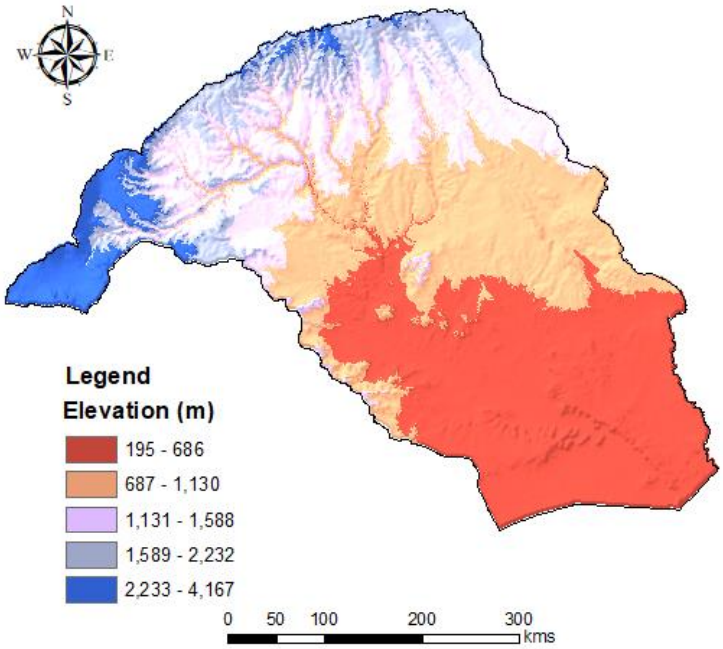

Figure 2-2 Elevation of the Wabi Shebele River Basin (derived from SRTM 90 m digital elevation data)

Slope analysis is conducted for the catchment using the ArcGIS Spatial Analyst. The northwest and north of the Wabi Shebele basin have steep slopes of greater than 15% due to the hilly landscape at the foot of the Bale and Ahmar ranges (Figure 2-3). The middle and lower parts of the basin are generally flat and rolling types ranging from 0 to 7.5%.

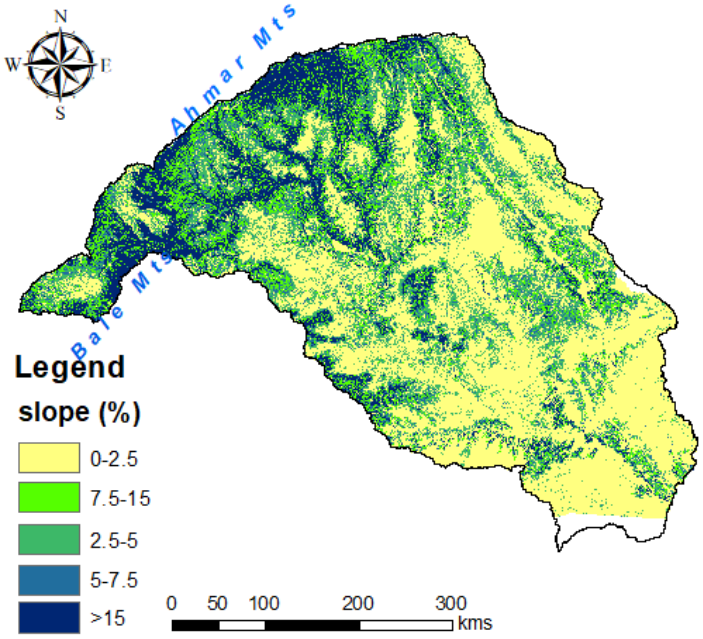

Figure 2-3 Slope Analysis for the Wabi Shebele River Basin (derived from SRTM 90 m digital elevation data)

2.4. Geology and Soils

Geologically, the study area is dominated by Mesozoic sedimentary formations. The Precambrian base is located in the northeast part of the basin around the Harar to Babile region consists of granite, granitic migmatite, and gneiss. There are also volcanic rocks at the northwest of the basin. Highly fractured volcanic rocks in the northwest part of the basin at Arsi-Bale basalt bordering the rift valley are the areas where numerous springs outcrops along faults and form a substantial baseflow of the Wabi Shebele river. This crystalline substratum is impervious and favorable to runoff. Alluvial deposits are distributed linearly along the Wabi Shebele river course, Jerer and Fafen rivers, and fan deposits of seasonal floods and stream beds (Awass 2009).

The soils in the basin are influenced by the interaction of the soil-forming factors of climate, parent material, relief/topography, and organisms (flora and fauna). About 50% of the soils in the basin are soils of calcareous or gypseous differentiation types (Figure 2-4). These are highly drained loamy sand soils (i.e., Calcisols, Solonchaks, Gypsisols, and Arenosols) distributed over flat and gently undulating lands of middle and downstream of the basin in Jijiga, Korahe, Fik, Afder, and Gode zones. Vertisols (clay) comprise 18.1% of the Wabi Shebele basin, covering significant areas at the middle belt. Poorly drained and shallow profile soils (i.e., Vertisols and Leptosols (sandy loam)) distributed over the upstream of Wabi Shebelle river basin, especially in most areas Arsi, west, and east Harerge, western Arsi, and Bale zones. The soil data used in this research was obtained from the Ethiopian Ministry of Water, Irrigation, and Energy (MoWIE') (MoWR 2004b).

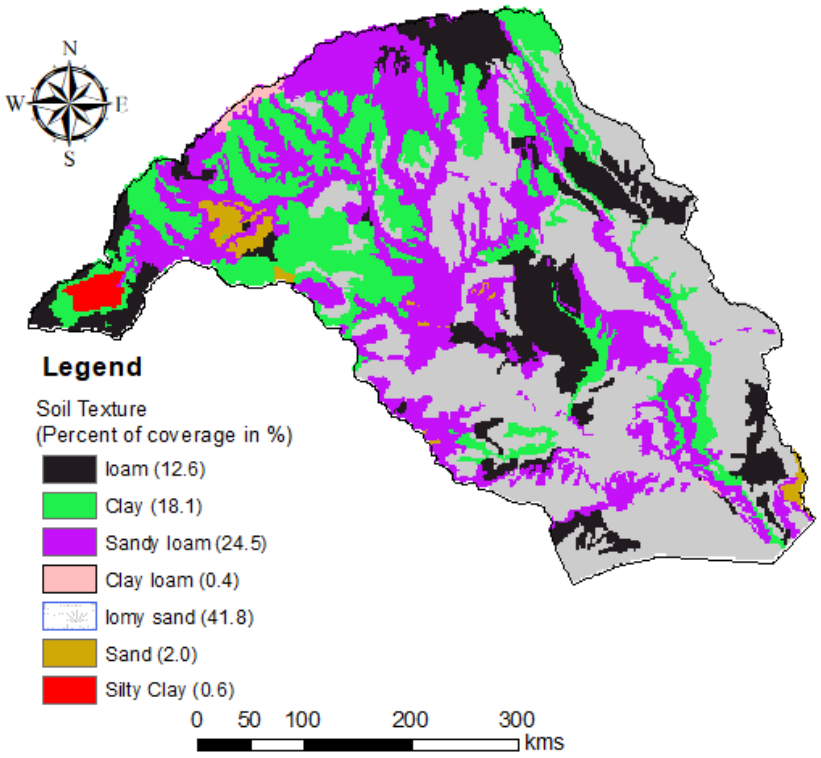

Figure 2-4 Dominant Soil classes in the Wabi Shebele River Basin

2.5. Land Use and Land Cover

Land use and land cover map information in three decades at 1986, 1997 and 2016 is used in the study (Figure 2-5). The LULC classes are presented in Table 2-1. Based on recent land use map information (LULC in 2016) analysis, there are ten main classes of LULC information identified in the Wabi Shebele basin. It is found that the main categories are Shrubs, grassland, and agricultural land. The major is agricultural cultivation, covering about 12.5% of the catchment area (Figure 2-6). Shrubland and woodland are predominant land cover with 36.90% and 31.69% area of coverage respectively from the total catchment area.

Table 2-1 land use/land cover classification (%) in 1986, 1997 and 2016

Year	Forest	Woodland	Shrubland	Agricultural land	Grassland	Bare land	Wetland	Water body	Afroalpine	Settlement
1986	5.21	43.30	31.56	8.41	9.06	1.95	0.23	0.00	0.21	0.05
1997	0.71	1.13	28.20	12.41	42.74	14.08	0.55	0.01	0.15	0.07
2016	2.65	31.69	36.90	12.50	11.40	4.49	0.10	0.02	0.17	0.08

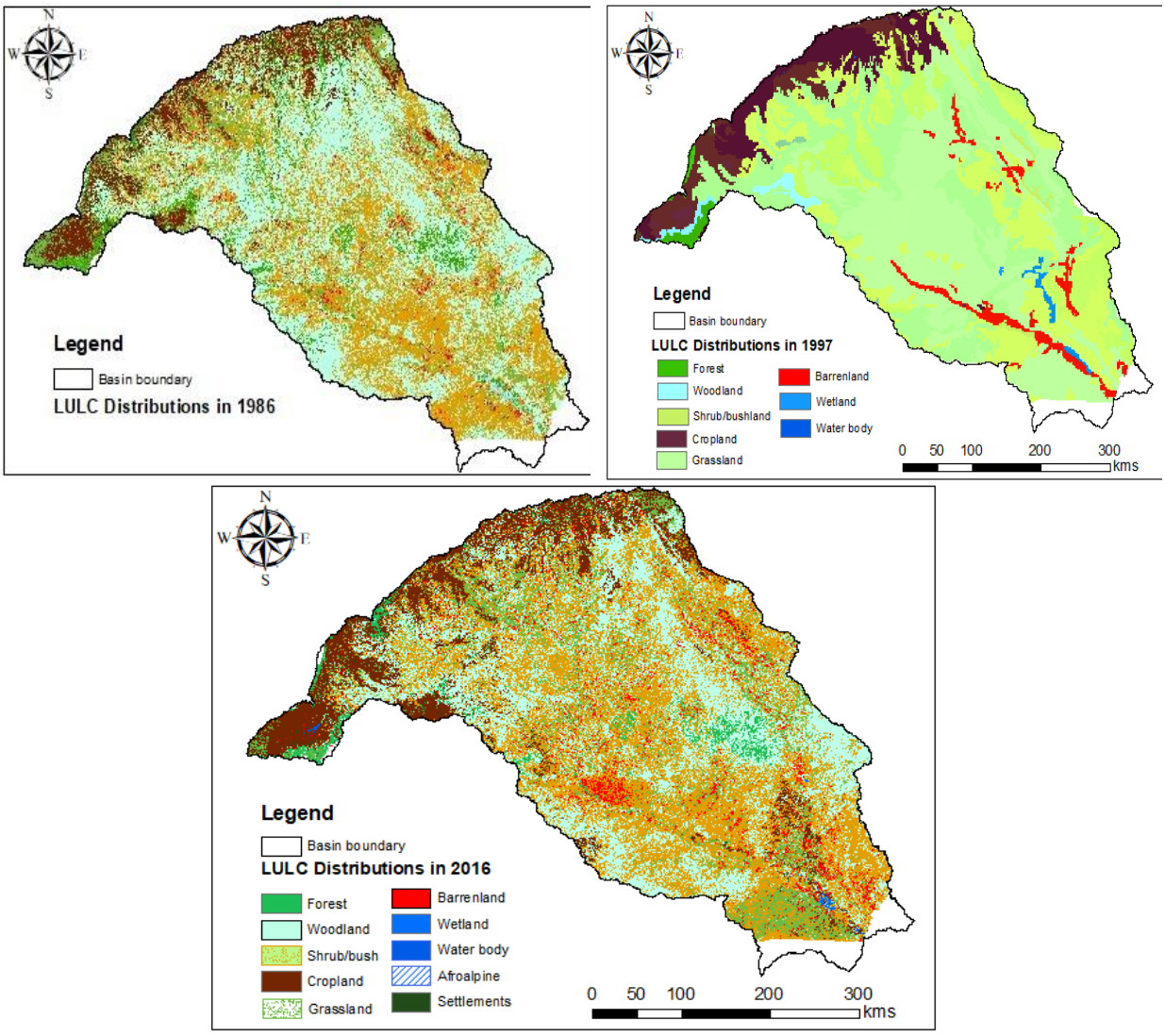

Figure 2-5 Land use within the Wabi Shebele basin (Source: WLRC 2016)

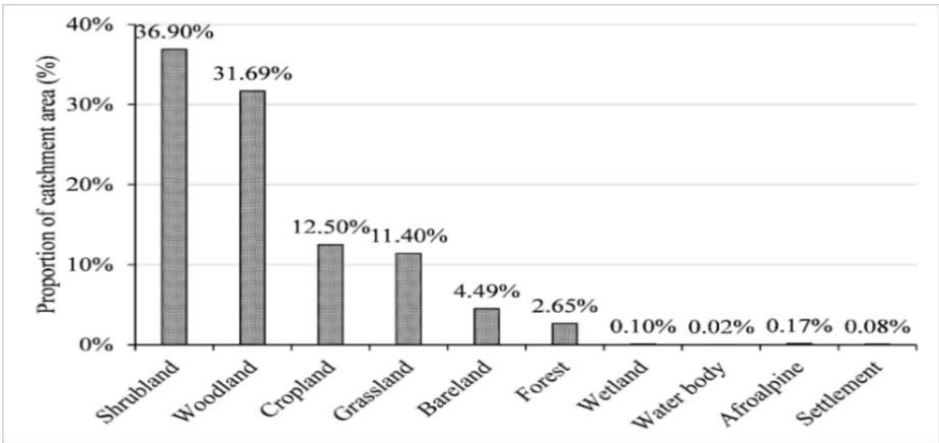

Figure 2-6 Land Use/ Land Cover Distribution Proportionate to Catchment Area

2.6. Climate and Hydrology

The climate of Ethiopia is controlled by the seasonal migration of the Intertropical Convergence Zone (ITCZ) and associated atmospheric circulations (Seleshi and Zanke 2004). There are three different seasons in Ethiopia: the rainy season from June to September, the dry season from October to January, and the less rainy season from February to May (NMA 1996; Seleshi and Zanke 2004). The climate of the Wabi Shebele basin is dependent on the altitude and latitudinal movement of the ITCZ (Awass 2009). The highlands are cold, while the lowlands are arid with a recorded annual rainfall of 1213 mm and 268 mm, respectively (MoWR 2003; Awass 2009).

The hydrology of the Wabi Shebele River Basin is complex, and each sub-catchment responds differently. In the upper basin (northwestern basin), the specific discharges are relatively low due to the long but not very intense rainfall conditions and considerable perviousness of soils. A significant tributary in this region is the Maribo River, which joins the Wabi River from the right bank. In the middle of the basin, Wabi Shebele receives substantial inflow from the wet watersheds of Ulul, Robe, and Siyanan rivers with flood conditions (MoWR 2003). Relatively the watersheds are characterized by intense rainfall and large impervious watersheds. From Imi to the frontier, the Wabi Shebele flows in a vast alluvial plain with a very gentle slope of 0.25 to 0.35 m/km. In the lower catchment, runoff moderated by lower topography, floodplain storage, and length of stream reach, producing times to peak is more than 48 hours. While having the largest area coverage, the basin's annual runoff estimate to be 3.4 BCM, which is low relative to major river basins in Ethiopia (Awass 2009).

2.6.1. Precipitation

Rainfall in the Wabi Shebele River Basin shows high temporal and spatial variability. The mean annual rainfall in the Wabi Shebele River Basin ranges between 213-1283 mm. It indicates that high spatial variation, with maximum rainfall, is more than six times the minimum rainfall. Areas with higher elevation show higher annual rainfall. An example for illustration of spatial variation in annual rainfall is shown in Figure 2-7. The mean annual rainfall at the stations with the complete records was summarized, and spatial interpolation is performed over the entire basin using Ordinary kriging interpolation methods for 1980-2013 on the selected gauging stations. The monthly values in Figure 2-8 show the seasonality of rainfall within the year. The quality station data are checked before using in analysis (Appendix C).

According to National Meteorological Agency (NMA 1996) report, the rainfall in the Wabi Shebele basin is characterized by two rainfall regimes: i) the area characterized by a quasi-double maximum rainfalls pattern with a small peak in April and maximum peak in August, bimodal type I (covers the west-east highland of the basin), and ii) the area dominated by double maximum rainfall pattern with peaks during April and October, bimodal type II (cover the south-eastern lowland of the Wabi Shebele basin).

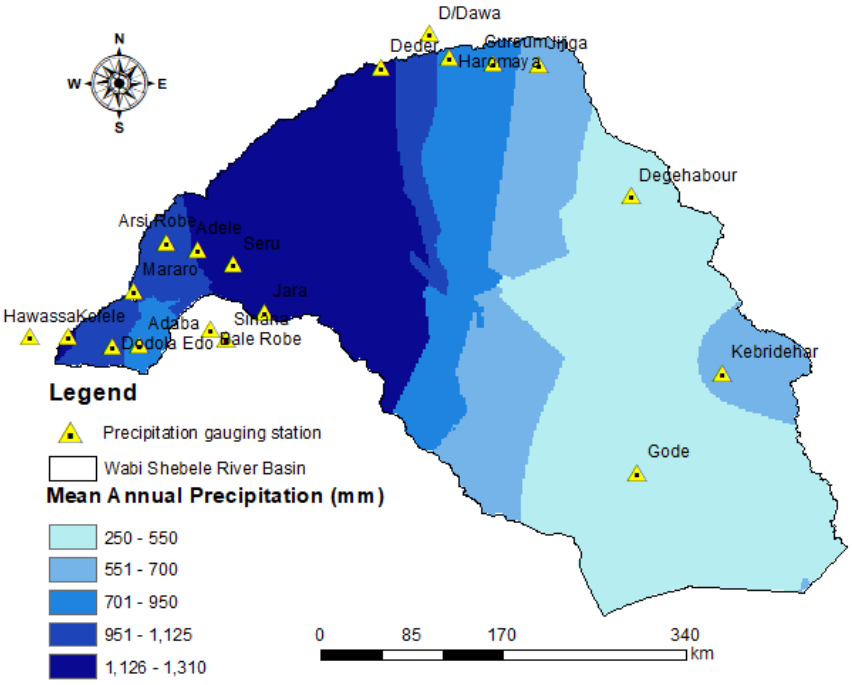

Figure 2-7 Mean annual rainfall variation in Wabi Shebele River Basin

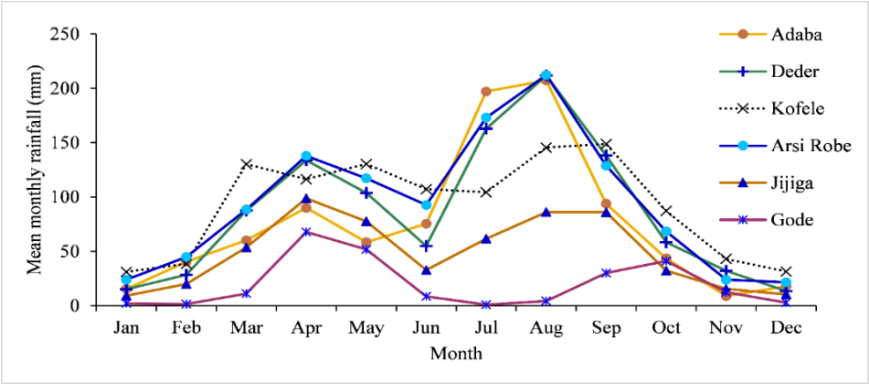

Figure 2-8 Long-term (1980–2013) average monthly rainfall on selected meteorological stations

Correlation with Elevation

The Mean Annual Precipitation (MAP) of 19 stations in the Wabi Shebele basin was computed and correlated with their respective elevations. It found that the stations' MAP was positively

correlated with elevation as indicated by the scatter plot in Figure 2-9. A linear trend line gives the best R^2 coefficient of 0.6403.

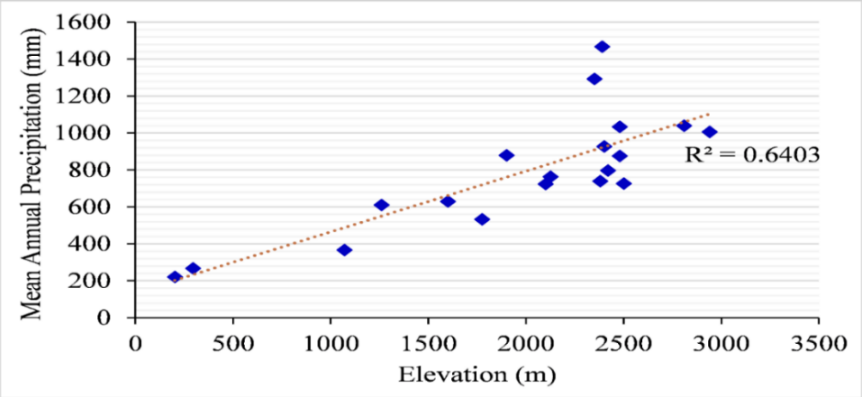

Figure 2-9 Correlation of Station Mean Annual Precipitation with Elevation (Source: Computed from data from NMA)

2.6.2. Temperature

The Mean Annual Temperature (MAT) in the Wabi Shebele basin is in the range of 12-29^{o}C. Maximum and minimum temperatures are usually experienced in March and January consecutively. The MAT was calculated for each station and extrapolated over the area to see the spatial variabilities in temperature time series across the region (Figure 2-10). The temperatures are lower in the northwestern and get higher towards the southeast part of the basin.

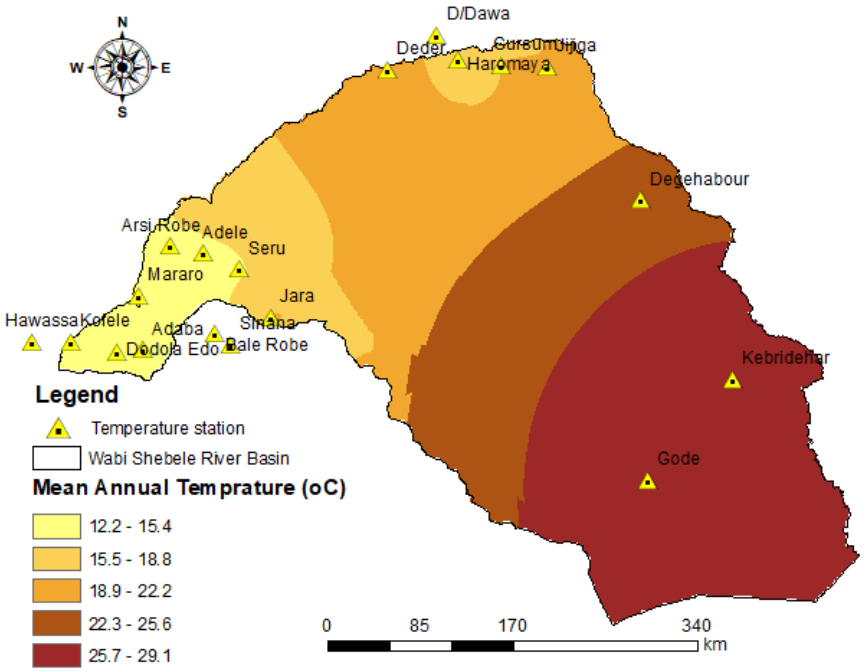

Figure 2-10 Mean Annual Temperature in the Wabi Shebele River Basin (Source: Computed from NMA Temperature Data)

Figure 2-11 shows the monthly maximum, minimum, and mean at four northwest, middle, northeast, and southeast stations for the same period. The mean annual maximum temperatures for the basin range from 20.1 to 36.9 ^{o}C, and mean minimum yearly temperatures range from 1.8 to 25.1^{o}C. Monthly statistics for temperature over 34 years for different stations also computed.

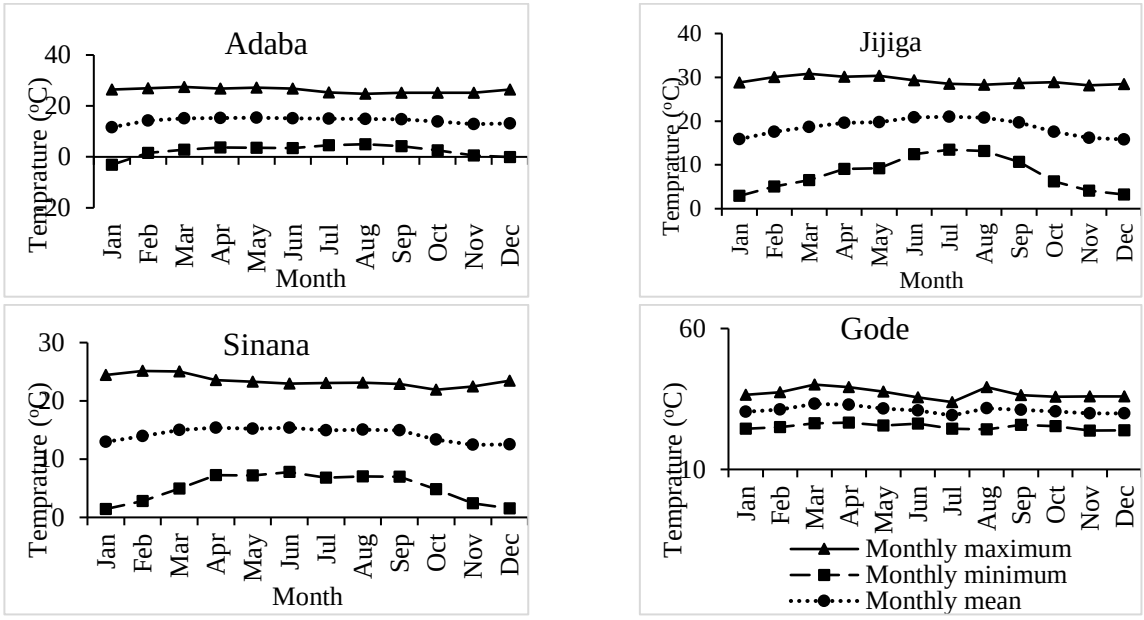

Figure 2-11 Monthly Statistics of Temperature at four stations (Computed from NMA gauge data)

2.6.3. Evaporation

Mean Annual Evaporation (MAE) increases from less than 1,400 mm in the north highland part to more than 2,000 mm in the southern lowland part of the basin (MoWR 2003). Figure 2-12 shows the monthly distribution of evaporation at different weather stations in the Wabi Shebele River Basin. The spatial distribution of potential evaporation is presented in Figure 2-13. The highest (115.3 mm to 200.2 mm) and lowest (98.7 mm to 146.3 mm) evaporation occurs in March and December (MoWR 2003).

2.6.4. Streamflow

The river flow is analyzed based on mean monthly distribution of discharges in selected rivers (Figure 2-14). In all rivers, the discharge was recorded as maximum in the wet season (July to September) and minimum in the dry season (October - March). Around 60% of the annual discharge in all sampled rivers is from the heavy summer (June-September) rains, whereas 19% of the streamflow in a year is from spring (February-May) rains.

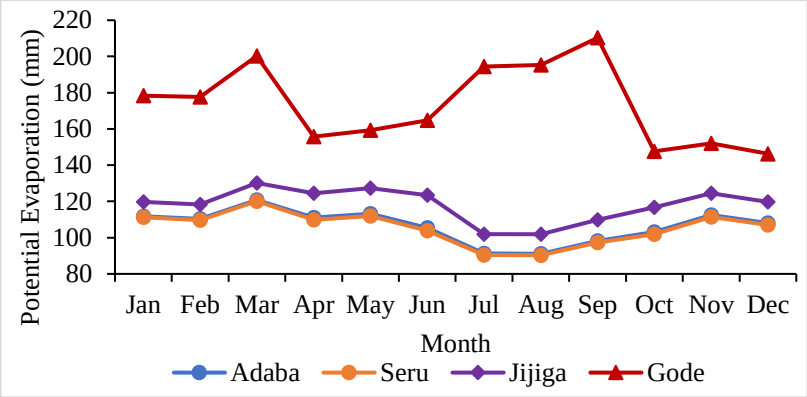

Figure 2-12 Long-term average monthly Evaporation on selected meteorological stations (Source: MoWR 2003)

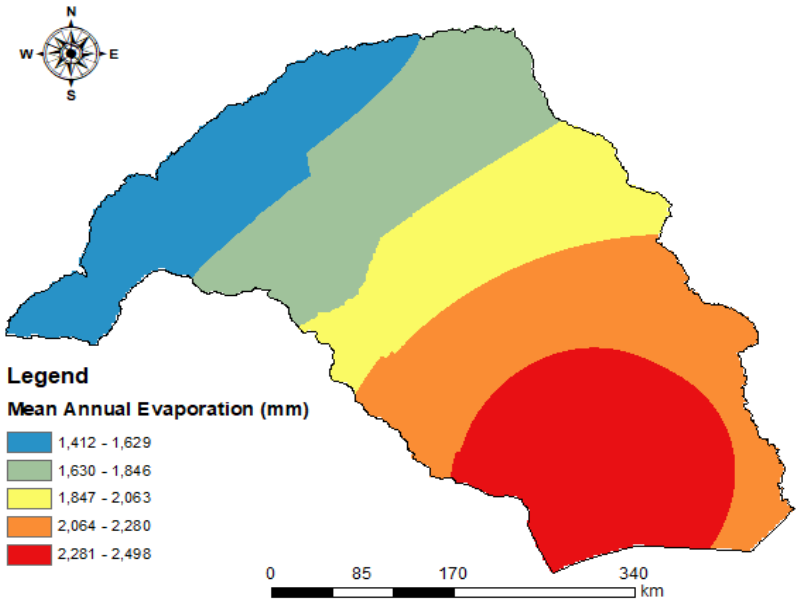

Figure 2-13 Mean Annual Evaporation (Source: MoWR 2003)

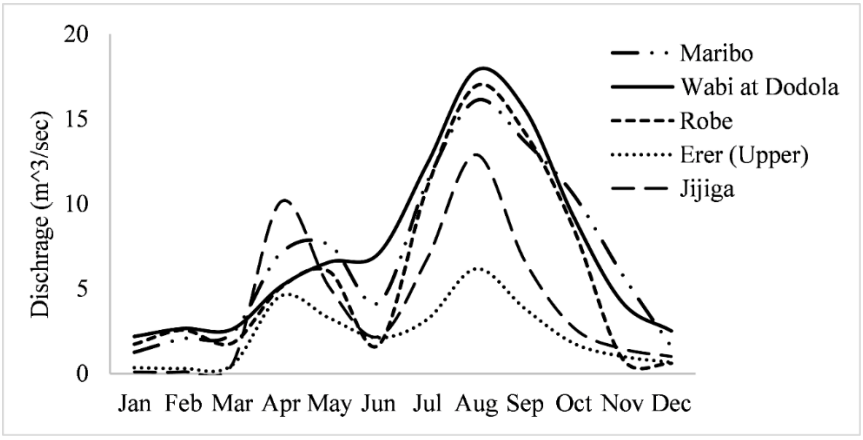

Figure 2-14 Mean monthly discharge distributions at selected gauging stations in record length

2.7. Demography

The total population in the Wabi Shebele basin is about 5.884 million as per the census of 1997 (MoWR 1998). About 88.4% of the population resides in the rural parts. Population density is highest in the highland area of the basin in Arsi (56.9 people/km^2), while the lowest lowland area is in the Afder zone (5.1 people/km^2) (Figure 2-15). A large percentage of the population in the highlands depends on agriculture, and whereas the lowlanders, in general, are pastoralists.

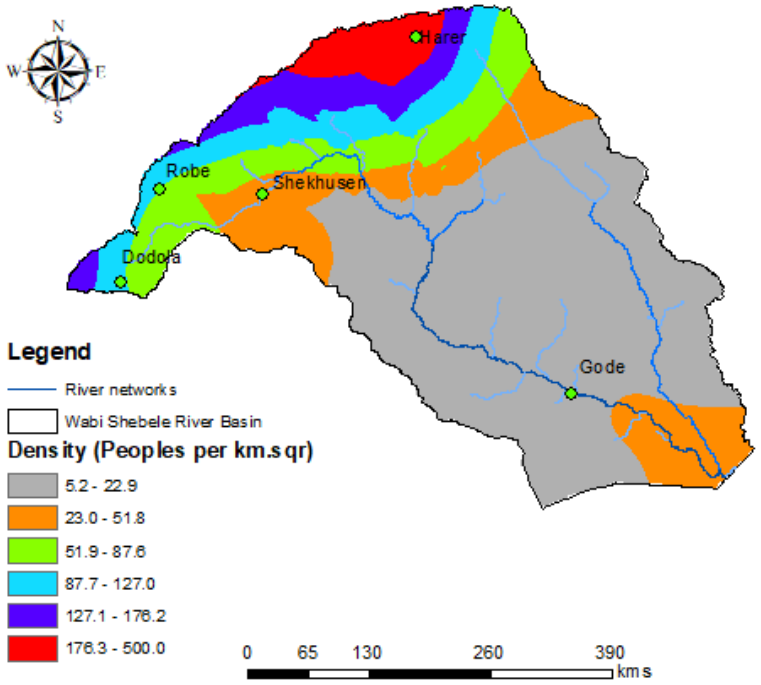

Figure 2-15 Population Densities in the Wabi Shebele River Basin (Source: MoWR 1998)

2.8. Water Resources Development

In the Wabi Shebele basin, there are over 334 traditional irrigation schemes covering an estimated 12,000 ha, and 72 small and medium modern irrigation schemes with an estimated irrigable area of 7045 ha (MoWR 2003; Awulachew et al., 2007; Awass 2009). The only existing dam under operation on the Wabi Shebele river is the Melka Wakena hydropower dam. There is a large-scale irrigation project at Gode, but it is not functional.

A total of 149 potential irrigation sites with estimated irrigable area of 237,905 ha identified during the basin master plan study (MoWR 2003). More recently, Somali Regional State, regional task force identified potential irrigable area in Wabi Shebele basin estimated to 500, 000 ha based on the basis of area coverage of potential soil classes suitable for crop production (LCRDB, 2013), which is more than twice the area estimated by MoWR (2003) and Awulachew et al. (2007).

3. TRENDS AND VARIABILITY IN FLOOD DISCHARGE AND ATTRIBUTION TO CLIMATE CHANGE

Abstract

Using a data-based statistical system, this study attempted to examine trends and variabilities in mean and extreme hydroclimatic variables in Wabi Shebele River Basin. Linear trend investigation and Mann-Kendall trend significance tests are performed as preliminary analyses to see trends on mean discharges and climate variables. In contrast, Quantile Perturbation Method (QPM) analysis is conducted to detect clear oscillating patterns and trends in extremes. The result indicates a less increase in mean annual discharge in the basin in between 1975 and 2015 up to 0.58Mm^3/yr, 1.49Mm^3/yr, 0.94Mm^3/yr, and 11.06Mm^3/yr in Maribo, Wabi at Dodola, Robe, and Erer river respectively. Mean temperature shows a significant increasing trend in the upper and middle part of the basin, but a decreasing trend in the lower basin. Similarly, a less increasing trend is observed in annual rainfall in the western and eastern upper basin, whereas the decreasing trend is in the middle and lower part of the basin. The QPM analysis in flood and precipitation extremes indicates a five-year frequency of significant anomalies and general increasing trends in floods. In the early 1980s, significant negative perturbation was observed in Maribo, Robe, and Erer rivers. The extreme precipitation anomalies increase at Adaba station and decrease at Robe (Arsi) station. Extreme discharge and precipitation anomalies follow a similar oscillation pattern with small average correlation values (R^2), i.e., 0.23%, 0.027%, 0.02%, and 0.08% in Maribo, Robe, Tebel, and Erer watersheds respectively.

Keywords: Attribution, River Basin, Discharge, Flood, Trend, Variability, Wabi Shebele

---

[1] Abebe Wudineh F., Ayalew Moges S., Berhanu Kidanewold B. (2021) Trend and Variability in Flood Discharge and Attribution to Climate Change in Wabi Shebele River Basin, Ethiopia. In: Delele M.A., Bitew M.A., Beyene A.A., Fanta S.W., Ali A.N. (eds) Advances of Science and Technology. ICAST 2020, vol 385. Springer, Cham. https://doi.org/10.1007/978-3-030-80618-7_7

3.1. Introduction

Both changes and variability in the water resources have severely threatened sustainable water resources development, particularly in the downstream part of the watershed. Therefore,

determining the variability of stream runoff is an essential task in water resources management and ecosystem restoration (Taye and Willems 2012; Meng et al. 2016). The mean annual discharge provides a measure of the potential supply; intra-annual and multi-annual variation offers information that can be used to determine the probability of experiencing deficiencies under natural conditions and the amount of storage required (Zuo et al. 2015; Zhang et al. 2000; Meng et al. 2016). In current situations, the hydrology of the earth is shifting with the potential to make floods and droughts more extreme (Charles et al., 2011). There is now a high need for decision-makers to better understand the continuing change and variation in hydroclimatic extremes to make preparations for the possibility of changing conditions.

Understanding changes in flood events and their probable causes have both scientific and practical significance in reviewing existing flood risk management practices and adapting future practices. Flood discharges and their exceedance probabilities, together with changes in the time of flood occurrence within the year, are the main variables needed to prepare future flood management strategies (Taye and Willems 2012; Meng et al., 2016). The need to understand the impact that man is having on 'nature' is also another importance. A river discharge gives an entire picture of a catchment response for water resource planning and management among hydrological variables (Adnan 2010; Taye and Willems 2012).

In Ethiopia, flooding is the most natural disaster that frequently occurred between 1906 and 2007, with average damages estimated to 321,000$ per event (Tadesse et al. 2016). There is an argument in the literature that a large number of flood events which caused many fatalities and large properties in Ethiopia are associated with climate change, intense monsoon rainfall in a short time during the rainy season, summer (Getahun and Gebre, 2015; Tadesse et al., 2016; NDRMC, 2018; Akola et al., 2018; Admassu et al., 2010). The Wabi Shebele River Basin is the frequently affected basin by hydrological extremes in the Horn of Africa (MoWR 2003; Tadesse et al. 2016). For instance, in 1996, 1999 unexpected floods destroyed homes and crops especially in three districts, i.e., Kelafo, Mustahil, and Burkur (UNDP 1999). According to the local authorities, 34 people and 750 livestock died, with 70,000 affected by the floods in these areas. The flood of April 2005 was considered the worst flood in the past 40 years by locals when floodwaters surrounded 30,000 persons, and 6000 live stocks were washed away (Tadesse et al. 2016). The Ethiopian Ministry of Water, Irrigation, and Energy (MoWIE') study of the Wabi Shebele River Basin master plan shows that severe hydrologic extremes in the basin, especially in 1973, 1979, 1984-85 is caused by harsh

hydrologic extremes natural atmospheric variability (MoWR 2003). Previous studies have focused on water resources potential assessment than trends and variabilities of hydroclimatic elements in the basin (BCEOM 1973; Houghton-Carr et al. 2011; Amer et al. 2013; Awulachew et al. 2007). A few studies conducted on climate characteristics show significant declines of annual and summer (June-September) rainfall total since 1982 in southeastern Ethiopia, using progressive Man-Kendall test on the yearly rainfall of Jijiga and Negele climate gauging stations (Seleshi and Zanke 2004). Upper Wabi Shebele basin streamflow is affected by rainfall conditions more similar to those of the high Ethiopian plateaus than those of the downstream Wabi Shebelle basin (BCEOM 1973).

The most frequently used to describe river runoff variability are the standard deviation variability of river runoff and the coefficient of variation. Mann-Kendall test and Spearman tests are the most non-parametric trend tests used in hydroclimatic variables. However, the results of these statistical tests are often influenced by serial correlation and increase the chance of incorrectly rejecting the null hypothesis of no trend or vice versa in most hydro climatological data. To overcome this problem, a relatively novel approach, the quantile perturbation method (QPM) (Ntegeka and Willems 2008; Williams et al. 2012), which is not dependent on the assumptions mentioned above, is utilized for analyzing temporal trend and variabilities in extreme hydroclimatic variables in this study. The study of temporal changes in extreme events identifies anomalies that can be attributed to different phenomena.

This study aims to detect temporal changes in extremely high discharges and attribute them to climate change using the data-based approach in the Wabi Shebele River Basin. Specifically, the study aims at 1) analyzing variabilities in extreme hydroclimatic variables and 2) investigating the correlation between extreme discharge and extreme precipitation anomalies for better communicating the science to water resource practitioners.

3.2. Methods

Data: Meteorological data including precipitation and temperature were collected from the National Meteorological Agency (NMA). Daily rainfall and temperature (maximum and Minimum) records for seven stations (Table 3-1), with a good spatial distribution, were used to see the characteristics of precipitation and temperatures in this study. These stations are selected based on quality of data (i.e., length of the record and spatial distribution of stations in the basin). The distribution of rainfall between watersheds shows variations (Figure 3-1). Significant variation

occurs during the rainy season (i.e., June to September). Considerable variation is also observed from April to June and from September to October.

Table 3-1. Annual summary of data used in the study

Data Source	Type of Data	Period	Station Name	Mean Annual	Extreme mean	Missing data (%)	Remark
MoWIE	Discharge	1975-2008	Maribo	3.18	16.01	9.27	Catch. Area=192km^2
		1975-2015	Wabi at Dodola	7.32	36.14	4.45	Catch. Area=1040km^2
		1979-2006	Robe	5.91	24.3	19.97	Catch. Area=169km^2
		1983-2006	Tebel	1.2	2.07	11.75	Catch. Area=79km^2
		1984-1999	Erer (upper)	2.51	12.7	9.07	Catch. Area=494km^2
NMA	Rainfall	1980-2013	Adaba	892.3	182	21.1	Elev.=2420m
		2000-2018	Kofele	1107.5	165	6.4	Elev.=2620m
		1980-2013	Robe (Arsi)	1113.7	201.5	1.7	Elev.=2400m
		1980-2013	Gindhir	1090.7	201.5	11.51	Elev.=1920m
		1980-2013	Diredawa	665.4	130.4	1.92	Elev.=1260m
		1980-2011	Jijiga	585.5	112.6	2.87	Elev.=1775m
		1980-2011	Degahabour	349.6	91.9	5.64	Elev.=1070m

Q=Discharge in m^3/s, RF=Rainfall in mm

The discharge data in this study were collected from the Hydrology Department of the Ministry of Water, Irrigation, and Electricity (MoWIE). The measurements of river levels follow the World Metrological Organization (WMO) (MoWR 2003). Five stations from the upper, middle, and lower part of the basin, relatively which have long records, one on the main river and others on major tributaries of the basin, were selected. The monthly database contains maximum and minimum discharges of each month and the monthly average runoff, which assisted in constructing the extremes time series. The main features of discharge gauging chosen stations are described in Table 3-1 and Table 3-2.

The missed data in discharge is maximum in the dry season (October-January) in Wabi Shebele River Basin (Table 3-2). This may be due to the inappropriate placing of the discharge gauging station. Awass (2009) reported that some the gauging stations in Wabi Shebele River Basin are installed on raised structures anchored to bridges, while others are off-setted in pockets of the main course of the stream. Due to these, most of the stations have shown that stations are not reliable enough to capture the low discharge situation in the basin. Therefore, such a gauging station placing problem may cause missed data, especially in the dry season. For existing gaps in between data, a multiple regression method with adjacent discharge data and rain-fall data is used to fill.

Table 3-2. Seasonal summary of data used in the study

Type of Data	Station/River	Season	Extreme Mean	Missing data (%)
Discharge	Maribo	Dry	10.47	11.43
		Wet	16.01	4.9
	Wabi at Dodola	Dry	24.73	6.14
	Bridge	Wet	36.14	2.99
	Robe	Dry	6.52	18.3
		Wet	20.98	22.4
	Erer	Dry	3.9	11.7
		Wet	12.25	6.4
Rainfall	Adaba	Dry	56.86	23.2
		Wet	178.88	21.3
	Kofele	Dry	96.86	10.5
		Wet	155.14	4.6
	Robe (Arsi)	Dry	77.83	2.4
		Wet	195.5	0.6
	Diredawa	Dry	56.9	1.8
		Wet	178.9	1.3
	Jijiga	Dry	46.7	2.6
		Wet	104	3.1
	Degehabour	Dry	33.9	4.8
		Wet	78.2	6.5

Dry=October – March, Wet= April -September

Peak Over Threshold selection (POT): This study uses the three highest values for each year from the wet season to see annual and monthly hydroclimatic variability. To see extreme variability in rainfall and streamflow at the weekly aggregation level, at least 5 POT values are selected. In the case of daily precipitation analysis, at least 15 extreme measurements per year is selected. In the case of extreme discharge, similar procedures in precipitation are followed to select monthly and extreme annual discharge.

Change Detection

The starting point of any change detection in observed time series is to hypothesize about the type of potential changes. These may include step-changes in the mean of a series at a particular point in time (regime shift), gradual changes (trend) in the average of the series over time, or changes in the variability of the series. After formulating the hypothesis, the data series of one or many stations are used to test whether the null hypothesis be rejected or not at a chosen significance level

(e.g., 5 or 10 %), which is the probability of incorrectly rejecting the null hypothesis. Both parametric and non-parametric tests are commonly used for trend detection. Parametric trend tests are more powerful than nonparametric ones, but they require data to be independent and normally distributed. On the other hand, non-parametric trend tests require only that the data be independent and can tolerate outliers in the data. One of the widely used non-parametric tests for detecting trends in the time series is the Mann Kendall test (Mann 1945; Kendall 1975).

Mann-Kendall (MK) trend test: The MK trend test statistics, S is defined as:

$$S = \sum_{i=1}^{n-1} \sum_{j=i+1}^{n} sgn(X_j - X_i) \tag{3.1}$$

Where n is length of the sample, *Xi* and *Xj* are sample values from i= 1,2, …, n-1 and j= i+1, …, n. and:

$$sgn(X_j - X_i) = \begin{cases} 1 \; for \; X_j > X_i \\ 0 \; for \; X_j = X_i \\ -1 \; for \; X_j < X_i \end{cases} \tag{3.2}$$

Under the null hypothesis that Xj and Xi are independent and randomly ordered, the statistic S tends to normality for large n, i.e., n≥ 8, with mean E(S)=0 and variance V(S) given by:

$$V(S) = \frac{n(n-1)(2n+5) - \sum_{l=1}^{n} t_i(l-1)(2l+5)l}{18} \tag{3.3}$$

where:

ti is the number of ties of length *l*.

The trend test statistic S is then standardized (Z_{mk}; equation 3.4), and its significance is estimated from normal cumulative distribution.

$$Z_{mk} = \begin{cases} \dfrac{S-1}{\sqrt{Var(S)}} \; for \; S > 0 \\ 0 \quad for \; S = 0 \\ \dfrac{S+1}{\sqrt{Var(S)}} \; for \; S < 0 \end{cases} \tag{3.4}$$

The standardized Mann-Kendall statistic (Z_{mk}) follows the standard normal distribution with a mean of 0 and variance of 1 under the null hypothesis of no trend (Mann 1945; Welch 1959). A positive Z_{mk} value reveals an upward trend, while a negative one reveals a downward trend. The null hypothesis is rejected if $|Z_{mk}|>1.96$ at a confidence level of 0.05; thus, the time series has significant trends.

Both "Z_{mk}" and "p" values were obtained to characterize trends and statistical significance. "p" value is the probability value of the MK statistic also referred to the statistical significance (%). The value of near to zero regression gradient indicates strong evidence against the null hypothesis, so you reject the null hypothesis (no trend), whereas the value of regression gradient very different from zero indicates weak evidence against the null hypothesis, so you fail to reject the null hypothesis.

The p-value of the MK statistic S of sample data can be estimated using the normal cumulative distribution function:

$$p = 0.5 - \emptyset(|Z_{mk}|) \ \ where \ \emptyset(|Z_{mk}|) = \frac{1}{\sqrt{2\pi}} \int_0^{|Z|} e^{\frac{r^2}{2}} dt \tag{3.5}$$

If the P-value is small enough, the trend is quite unlikely to be caused by random sampling. At the significance level of 0.05, if $p \leq 0.050$, the statistically significant.

Quantile Perturbation Method (QPM): is an empirical statistical analysis used to study trends and multi-decadal oscillations in extreme values (Ntegeka and Willems 2008). It uses ranks of time series to detect frequency and perturbation of extreme time series. The perturbation is the ratio of similarly ranked data from the two series i.e., series in block length and refence series (Equation 3.6). The reference series is the long-term expected series while the other series is taken as the actual series within a particular block (sub-period). Based on Tabari, et al. (2014) recommendations, QPM is applied on different block length; 5, 7 and 10-years to select appropriate value of sub-period (block length) in between 5- and 15-years as preliminary analysis. From preliminary analysis the block length which shows better oscillation patterns (high and low) of extreme value is selected for the whole time series variability analysis. For each block of years, a single perturbation is calculated as the average of all perturbations above a particular threshold. Repeating the averaging over the different blocks assigns one factor to each block which eventually leads to a temporal variation of the perturbation factor.

The same quantiles above the threshold from the sub-series and the full series were compared by:

$$\frac{Y_1 - X_1}{X_1}, \frac{Y_2 - X_2}{X_2}, \frac{Y_3 - X_3}{X_3}, \dots, \frac{Y_n - X_n}{Y_n} \tag{3.6}$$

where, Y_1, Y_2, Y_3, . . ., Y_n were extracted from a sub-series based on their values, which were larger than the threshold, and they were arranged in descending order; X_1, X_2, X_3, . . ., X_n are the corresponding quantiles from the full series. The linear interpolation was used to estimate quantiles

that could not the trend of the sub-period. The sub-period was assigned by moving window, which firstly put the sub-period at the beginning of the full series and subsequently shifted by 1 year at a time. Consequently, this procedure provided a large number of anomaly indices. The ultimate anomalies from the different moving window positions are considered to characterize the variability of the extreme quantiles in the series. Moreover, the moving window technique made the anomaly indices change smoothly with time.

The statistical significance of the anomalies was tested by confidence intervals, which were estimated by a nonparametric bootstrap method. The confidence interval (CI) is calculated and superimposed on the plot to identify periods of significant perturbations. The values in the full time series at each site are randomly resampled to make a new series with different sequence, and the anomalies are recalculated for the resampled series based on the QPM method. The anomaly calculations are repeated 1000 times, leading to 1000 anomaly values for each block period. After ranking of the 1000 anomaly factors, the 25^{th} and 975^{th} values define the 95% CI for each block period. It is then graphically possible to identify periods of significant variations that the perturbation factors between the upper and lower limits of the confidence interval (the region of acceptance of the null hypothesis) are considered insignificant, whereas those outside the region of acceptance of the null hypothesis are defined as statistically significant.

Change Attribution

Two general classes of approaches are identified for attributing detected changes in flood hazard: data-based approach and model-based approach. Merz et al. (2012) suggest a framework based on proof of consistency, inconsistency, and provision of a statement of confidence for "hard" attribution. Jia et al. (2012) and Viglione et al. (2016) used a fingerprint-based method to attribute observed changes in the water resource amounts to local human activities rather than climate variability in the Hai catchment of China and Germany watersheds respectively. Seleshi and Zanke (2004) used correlation analysis to attributes rainfall variability to atmospheric circulation indices based on observed data. Other studies (e.g., Schreider et al., 2002; Andréassian et al., 2003; Seibert and McDonnell, 2010; Fenicia et al., 2009) used the hydrologic model to identify the causal effects of the different causes of changes in flood hazards. The application of models is always associated with the uncertainty which emanated from the assumptions made on the structure of the models and issues related to scaling. Therefore, interpretation of the results needs caution.

Pearson's correlation coefficient: is used to see the strength of linear relationship between two variables. If the two variables are linearly related, the correlation coefficient will be near 1 or -1. The sign depends on whether the variables are positively or negatively related. The correlation coefficient related to zero (0) if there is poor relationship between the variables. Between rainfall in the Wabi Shebele basin and runoff in main and tributary rivers were determined at daily and annual time scales. The effect of seasonality in precipitation on river discharge was investigated separately by using data from the wet period from April - September (6 months).

3.3. Results and Discussion

The spatial and temporal variabilities in hydro-climate of Wabi Shebele River Basin is observed using data based statistical approach. Linear regression test, Mann-Kendall trend test and quantile perturbation method (QPM) are used to investigate possible trends and oscillation patterns in river discharge and climate variables. The linear trend test and Mann-Kendall trend test are performed to see trends on mean discharges, total rainfall and mean temperatures and then compare with previous results, while the QPM analysis was used to see trends and variabilities in hydroclimatic extremes due to its capacity to detect clear oscillating patterns and trends in extremes. As observed on Figure 3-1, the Wabi Shebele basin rainfall is bimodal type taking place from February-May and June-September on high land area and from March-May and September-November in lowland. In western-eastern upper and middle basin, the months from June-September (Summer) is the periods in which largest precipitation record exist, the months from march -may (Spring) is the period in which significant precipitation record exist. But in lowland around Gindhir, Gode and Degehabour, the months from March-May (Spring) and September-November (Autumn) are periods in which largest and significant rainfall records exist respectively (Figure 3-1). Therefore, in highland and lowland of Wabi Shebele River Basin has two regimes of wet and dry season categories are exist. The months in which less precipitation is record exist collectively categorized as dry season in both regions. Accordingly, the highland part of the basin around Adaba, Merero, Robe (Arsi), Seru, Deder, Harar and Jijiga have dry season in between October and March, and wet season in between April and September. Whereas the lowland area of the basin around Gindhir, Degehabour, Gode have wet season (March to May; September to November) and dry season (December to February; June to August). The low-lying areas of Wabi Shebelle Basin around Degehabour, Gode, Kebridehar, and Kelafo rains from March to May is caused by moisture from the Indian Ocean, while the October to November rains is associated with the retreat of the

ITCZ in a southward direction (Amer et al. 2013). The temperature situation of sub basins shows that wet season is the season in which maximum temperature record exist specially February up to May, and the dry is the season in which minimum temperature record exist (Figure 3-1).

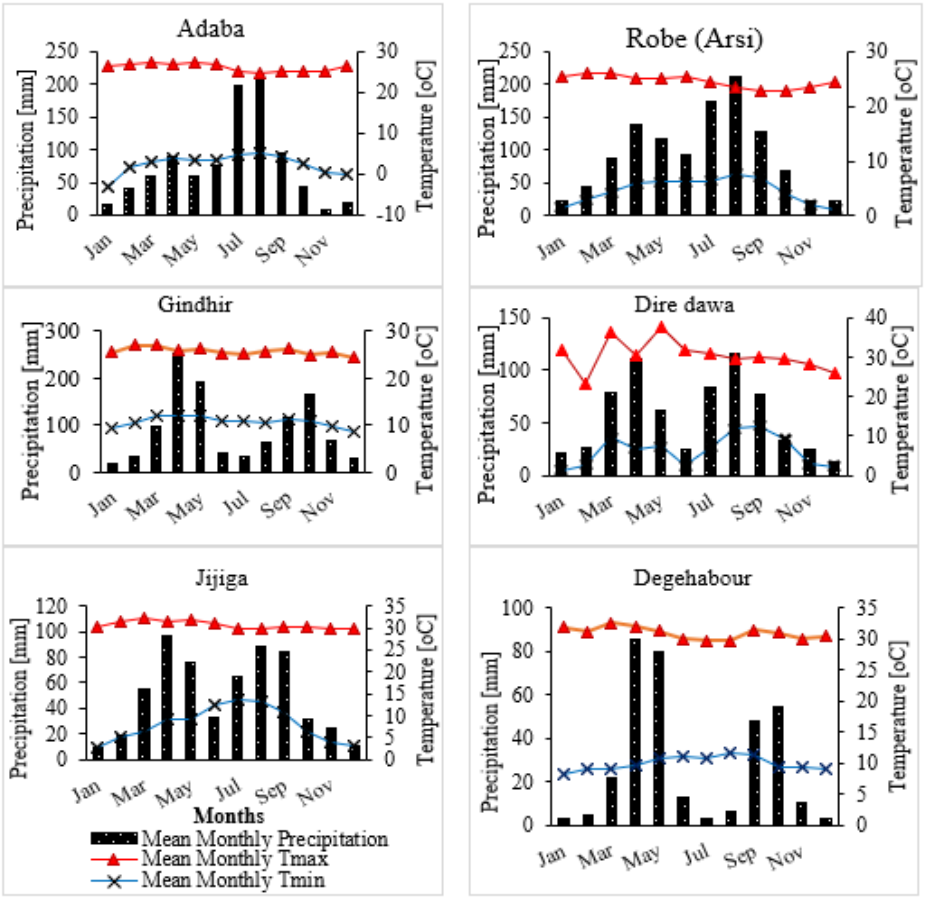

Figure 3-1. Mean monthly precipitation and temperatures distributions at selected gauging stations for 30 years in average (1980-2013)

3.3.1. The trend analysis

In this study linear regression and Mann-Kendall trend test are performed to see trends and verify its significance on mean discharge, total rainfall and mean temperatures and then compare with previous results. A linear trend analysis to the annual mean runoff at all stations revealed an increasing trend at values of 1.45 Mm^3, 0.58 Mm^3 and 0.94 Mm^3 on Wabi at Dodola bridge, Maribo and Robe respectively. The verification analysis on trend using Mann-Kendall trend test shows insignificant trends for the selected stations at annual and seasonal discharge levels (Table 3-3). In some stations significant increasing trend in discharge are observed in wet season, for example, in Wabi river at Dodola bridge and Erer river at western and eastern upper basin.

Trends in mean river discharge follows similar trends with rainfall exist in western and eastern upper basin sample gauging stations. The spatial and temporal distribution of rainfall governs amount and intra and inter annual variability of discharges. This indicates that, Wabi Shebele River flow exhibits typical characteristics of tropical rainfall-dependent discharge regimes. Similar result was obtained from trend analysis on mean river discharge in between 1975 and 2015 in Wabi Shebele River Basin shows less or insignificant trends.

Table 3-3. Statistical summary of trend test in mean annual discharge

Stations	Period	Average (Mm^3)	St. dev. (Mm^3)	Slope	S	α	Z_{mk}	p-value
Maribo	1975-2008	100.2	24.32	0.581	587	0.05	1.48	0.092
Wabi at Dodola	1975-2015	230.9	64.44	1.485	164	0.05	1.83	0.619
Robe	1979-2006	48.5	28.19	0.944	74	0.05	1.44	0.086
Tebel	1983-2006	3.00	1.66	0.179	192	0.05	4.73	0.001
Erer	1984-1999	87.5	78.29	11.07	48	0.05	2.03	0.018

Table 3-4. Statistics summary of trend in annual rainfall

Stations	Period	Average (mm)	St. dev. (mm)	Slope	S	α	Z_{mk}	p-value
Adaba	1980-2013	892.3	303.2	0.8	99	0.05	1.48	0.44
Kofele	2000-2018	1097.6	107.6	-7.62	-55	0.05	-1.97	0.17
Robe (Arsi)	1980-2013	1113.7	339.8	-19.3	-169	0.05	-2.52	0.04
Gindhir	1980-2013	1090.7	455.4	-10.9	-1	0.05	-0.03	0.39
Diredawa	1980-2013	665.4	151.0	2.38	39	0.05	0.56	0.64
Jijiga	1980-2013	585.5	108.8	1.6	57	0.05	0.91	0.33
Degehabour	1980-2011	349.6	155.3	-3.8	-85	0.05	-1.39	0.304

Trend analysis on annual, seasonal and monthly rainfall indicates less or insignificant increasing trends in record length (1980-2013) at western and eastern upper Wabi Shebele basin on Bale, Arsi and Harar highlands. But, significant decreasing trends in rainfalls is observed at middle and lowland area of the basin around Arsi robe, Gindhir and Degehabour in Wabi Sheble basin (Table 3-4). The wet season (April to September) rainfall has shown insignificant increasing trend in the basin. The study conducted by Shiferaw et al (2015) also indicates insignificant trend of summer rainfall which range from +4 up to -5mm/decade and substantial decreasing trends in spring rainfall during the last three decades from 1975-2007 in the basin.

Temperature trend analysis shows significant increasing trends in most of gauging stations located in upper and middle part of the basin except lower part of the basin around Degahabour which shows significant decreasing trend (Table 3-5). The south-eastern part of the low-lying areas of the basin around Degehabur, Gode, Kebridehare, and Kelafo receives no rainfall in July and August and has two rainy seasons (Amer et al. 2013). The first is from March to May, and the second is from October to November. As explained under section 2.6.2, max temperature in the basin is recorded in wet season and minimum temperature is in dry season. The temperature trend difference from other part of the basin probably tied to rainfall distribution difference from others.

Table 3-5. Statistics summary of trend in mean temperature

Stations	Period	Average (°C)	St. dev. (°C)	Slope	S	α	Z_{mk}	p-value
Adaba	1980-2013	14.66	0.714	0.05	239	0.05	3.5	0.001
Kofele	2000-2018	19.56	0.527	0.01	55	0.05	1.9	0.397
Robe (Arsi)	1980-2013	14.85	0.689	0.06	339	0.05	5.0	0.001
Gindhir	1980-2013	18.32	0.70	0.02	115	0.05	1.7	0.139
Diredawa	1980-2013	25.54	0.40	0.03	330	0.05	4.9	0.002
Jijiga	1980-2013	19.50	0.654	0.04	194	0.05	3.1	0.002
Degehabour	1980-2011	19.30	6.333	-0.3	-161	0.05	2.8	0.005

3.3.2. Trends and variabilities in annual extremes

Quantile perturbation method (QPM) is used to see possible trends and variabilities in extreme discharge and climatic variables. The method has a capacity to explore clear oscillating patterns and trends in hydroclimatic extremes. The method has also the option of identifying the statistical significance of the variability observed and thus the statistical significance of the variability identified. The mean perturbation is assigned to a year which is approximately in the middle of the block. The value of confidence interval is superimposed on the same plot of extreme perturbations to identify the periods of significant variations.

From preliminary analysis conducted, 5 (five) year block of periods shows better oscillation patterns (high and low) of extreme discharges and precipitation in comparison to 7- and 10-years block lengths as shown on Figure 3-2. Hence a 5-year block was used as block length of variability analysis in this study.

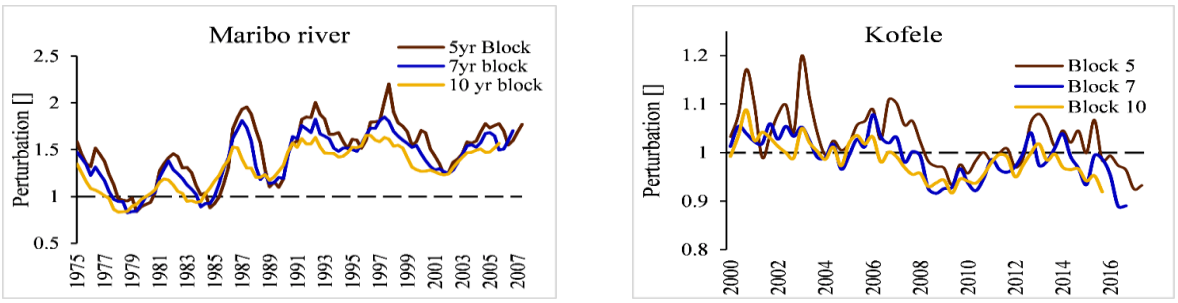

Figure 3-2. Extreme perturbations at different block lengths on both discharge and precipitation

Extreme discharge: When considering extreme high discharges in annual time steps, most of perturbation values varies within confidence interval. Among gauging stations increasing trend is observed on Maribo river (Figure 3-3). In early 1980s, significant negative perturbation up to -26.5%, -17.8%, -25% and -20% was observed in Maribo, Robe, Tebel and Erer watersheds respectively. Whereas, maximum significant perturbations up to 88.3%, 95.6%, 610% and 482% are observed respectively in watersheds in between 1986-1989. High oscillation pattern in annual extreme high discharges were observed in upper basin watersheds. Generally, extreme high discharge quantile perturbation shows increasing trend in Wabi Shebele River Basin from 1975 to 2015. The estimated confidence intervals are wide enough excluding the possibility of statistically significant changes. These significant anomalies of extreme discharges can be due to major driving factors like climate variables or catchment characteristics.

The oscillation pattern of extreme discharge quantiles changes within half a decade in both directions negatively and positively, which shows existence of external factors effects with in a given interval of years. For instance, the sea surface temperature change (SST) occurrence over the globe will occur within two to seven years interval in the form of El-Nino and La-Nino (Siam et al. 2014). The effect this climate change indices is high over the world including our country. There is a consequence of flood and drought in Ethiopia during the occurrence year of these indices (UNOCHA 2015). Most of positive significant anomalies of extreme discharge quantiles in Wabi Shebele River Basin occurred in moderate to very strong El-Nino years (Table 3-6). Contrary most of negative significant anomalies in the basin occurred in week to strong La Nino years. This study coincided with FAO study report in 2000 that in some parts of Ethiopia, periods of above-average rainfall are triggered at certain times by the warm phase of the El Niño Southern Oscillation (ENSO), while droughts are associated with the cold phase disturbance, or La Niña (http://www.fao.org/3/x8406e/X8406e00.htm#TopOfPage). This indicates global climate change

indices are a probable cause for changes of extreme discharge quantiles in Wabi Shebele River Basin. The impact of El Niño and La Niña are surprisingly increasing over the globe especially in developing countries like Ethiopia which their economies are dependent on regularly occurring seasonal weather conditions.

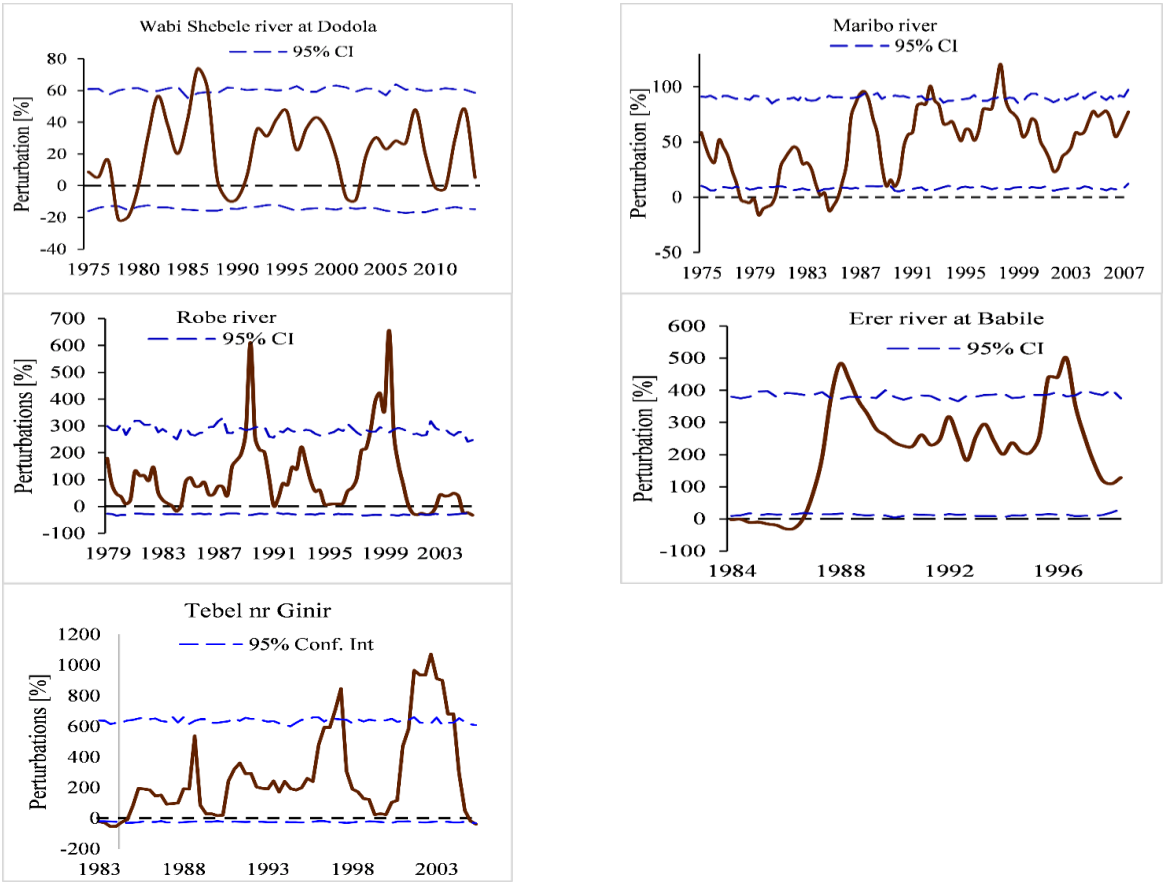

Figure 3-3. Extreme discharge variability with confidence interval in Wabi Shebele River Basin

El Niño refers to the large-scale ocean-atmosphere climate interaction linked to a periodic warming in sea surface temperatures across the central and east-central Equatorial Pacific and La Niña represent periods of below-average sea surface temperatures across the east-central Equatorial Pacific (https://www.nrdc.org/stories/flooding-and-climate-change-everything-you-need-know).The humanitarian impact of La-Niña is greater when it immediately follows an El-Niño. In 1988 El Niño year's floods affected 2.5 million peoples, whereas the 1999 and 2011 drought years occurred following La-Niña events affected 31.5 million and 14 million peoples respectively in the region including Wabi Shebele basin (UNOCHA 2015).

Table 3-6. Summary of QPM analysis in annual extreme discharge

Sub basin	Magnitude of highest anomaly (%)	Time of highest anomaly	Remark
Maribo	-11.9	1984	WL
	+95.6	1987	SE
	100.5	1992	SE
	120.5	1997	VSE
Wabi at Dodola	+61.5	1982	VSE
	+85.3	1987	SE
	-15.5	1990	SL
	-20.1	2002	ME
Robe	+610.5	1989	SL
	+655.7	1999	SL
Tebel	-53.2	1983	VSE
	+846.9	1997	VSE
	+1071.3	2002	ME
Erer	-31.1	1985	WL
	+482.5	1988	SE
	+501.1	1996	ML

WE=Weak El Niño, SE= Strong El Niño, VSE= Very strong El Niño, WL= Weak La-Niña, SL= Strong La-Niña years.

Precipitation extremes: The perturbation in precipitation extreme varies within confidence interval in most of stations of the basin taken in consideration. But unique result is observed on Adaba and Robe (Arsi) stations record (Figure 3-4). An increasing and decreasing trend of precipitation extremes is observed in Adaba and Robe (Arsi) stations respectively. In early 1980s significant negative anomaly up to -10.4% is observed at Adaba station, but maximum positive perturbation of +38.2% is observed at Robe station. In 2000s significant positive anomaly of +137.8% is observed at Adaba and significant negative anomaly of -39.2% at Robe (Arsi) rainfall stations are observed. In the other side most rainfall stations indicate significant positive precipitation anomalies in early 1980s specially between 1982-1983 and immediate decreasing trend in between 1984 and 1985 (Table 3-7 and Figure 3-4). Generally, most of rainfall perturbation analysis indicates decreasing trends in middle Wabi Shebele basin.

Table 3-7. Characteristics of highest anomaly in precipitation extremes

Station Name	Magnitude of highest anomaly (%)	Time of highest anomaly
Adaba	-14.4	1983
	+76.8	1990
	-18.3	2000
	137.8	2009
Kofele	+42.2	2006
	-9.7	2017
Robe (Arsi)	+38.2	1982
	+34.5	1987
	-47.1	1993
	-36.9	2001
Gindhir	+170.7	1980
	-33.5	1994
	-38.6	2003
Diredawa	-20.06	1984
Jijiga	+47.3	1986
	-19	2008
Degehabour	+210.4	1982
	+215.5	1986
	-20.8	1990
	+201.2	2000

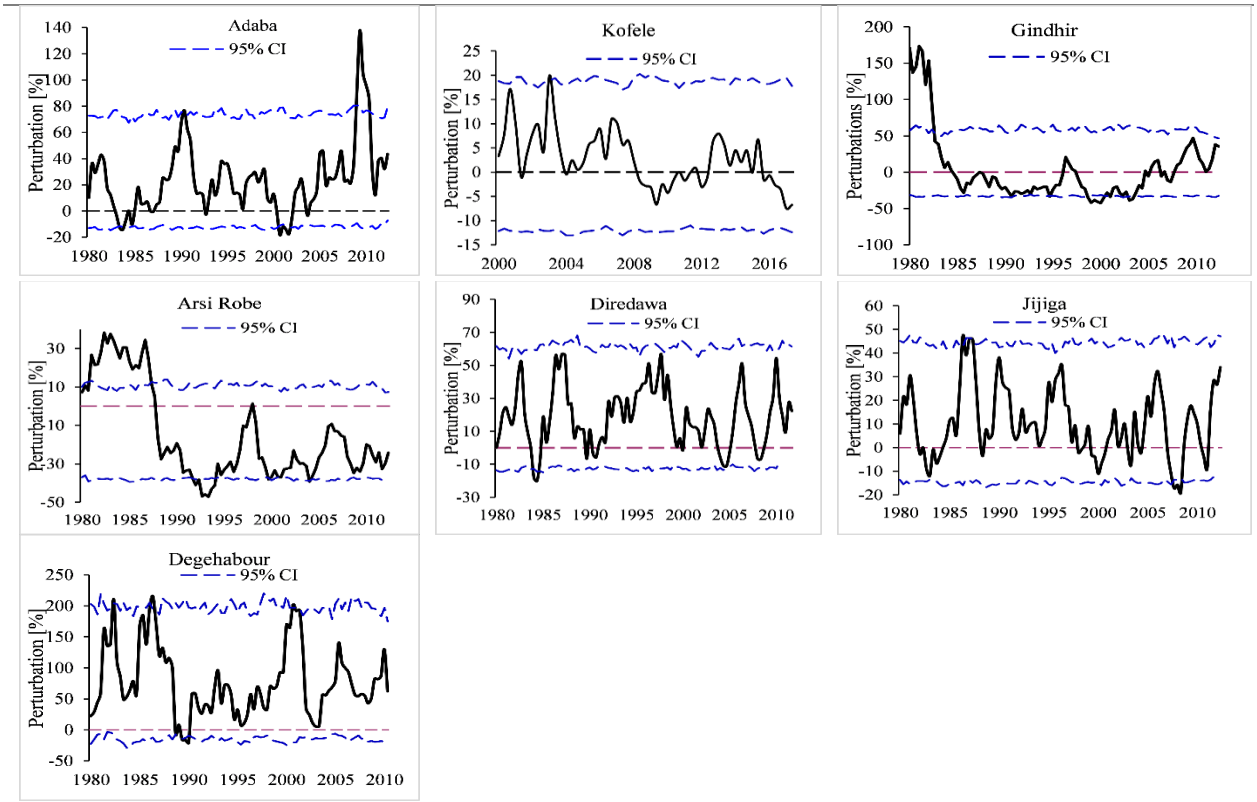

Figure 3-4. Annual precipitation extreme perturbations using 5-year block length with 95% Confidence interval at seven gauging stations of Wabi Shebele River Basin

In Ethiopia, droughts and floods are occurred frequently at every 3-5 years for last 50-years (World Bank 2006). The actual power generated from Melka Wakena Dam, the hydro-power plant exist in this sub basin, shows power decrement in 1991, 1996 and 2000 by 32%, 21% and 38% relative to their Preceded years (MoWR 2003). In other side western and eastern upper Wabi Shebele basin indicates significant positive anomaly in precipitation extremes in 2000s. This also coincided with the recent study result (Moges et al. 2010; Tadesse et al. 2016; UNOCHA 2015; IWMI 2015; Awass 2009) which indicates several devastating floods in Wabi Shebele River Basin. The destructive flood in August 2005 on the basin affected 100,000, 154 deaths and the flood occurred starting November 2008, in basin caused around 52,000 human displacements from 14 kebeles (small admirative unit), 185 villages and 164-hectare farm lands washed away (IWMI 2015).

Temperature extremes: Temperature anomalies were analyzed based on the long-term average perturbation. High temperatures in Wabi Shebele River Basin perturbation analysis shows general increasing trends in the basin particularly in upper and middle of the basin but less decreasing trend in lower part of the basin (Figure 3-5). Starting 1990 significant increasing trends are observed in Adaba, Kofele, Robe gauging stations record.

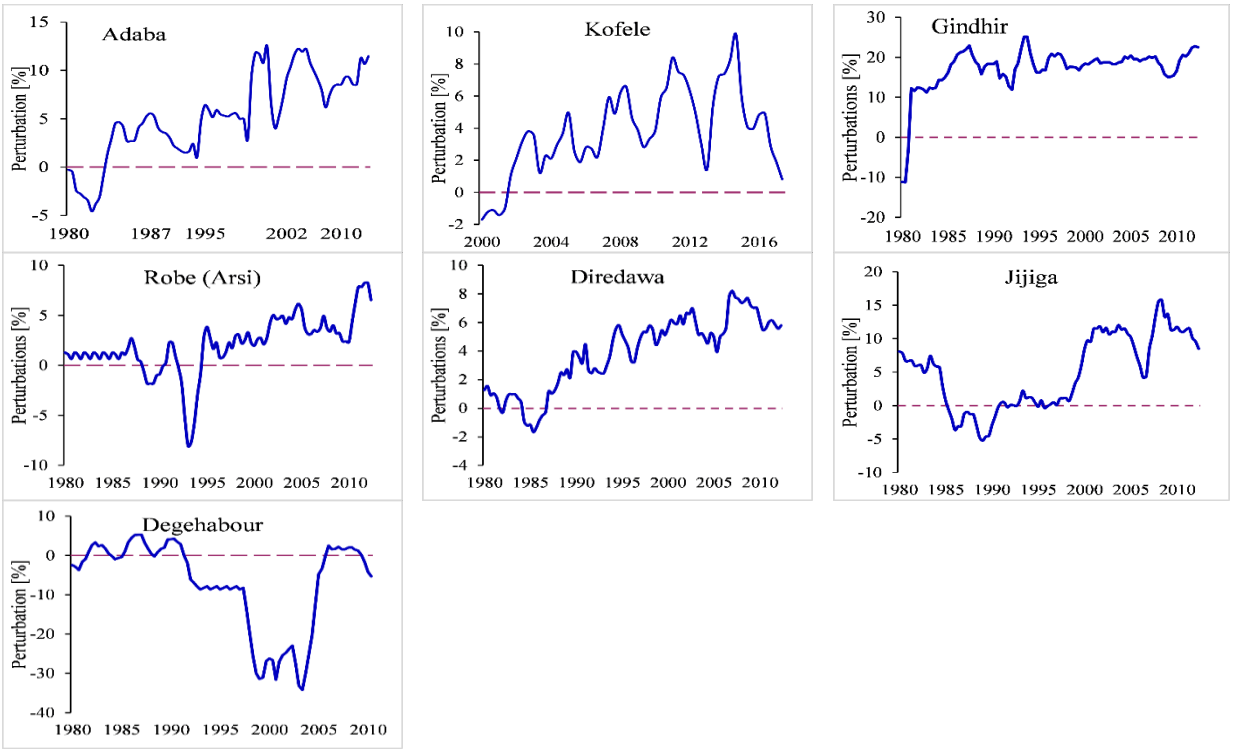

Figure 3-5. Extreme high-Temperature average perturbations using 5-year block length at selected gauging stations in Wabi Shebele basin

There are a few limitations in the application of the frequency perturbation method for temperature compared to rainfall. First, the independence criterion is difficult to ascertain as there are correlation in daily value similar to river discharge. For this study, the independence criterion was ignored. Instead, only a threshold for the peaks was selected. Second, temperature significance periods were not based on 95% confidence intervals because there was no reasonable distribution valid for all the periods in temperatures (Ntegeka and Willems 2008).

3.3.3. Trends and variabilities in seasonal extremes

The QPM approach is applied to extreme value at seasonal aggregation level. Three maximum events are selected from each season to see temporal variability in extreme seasonal flood events. Two seasons, i.e., dry (October- March) and Wet (April- September), are used to see extreme quantiles in this study.

Extreme discharge: QPM analysis conducted on extreme seasonal discharges indicates significant positive anomalies in dry season streamflow of upper Wabi Shebele basin at five years interval in average i.e., 1977,1982,1987, 1997, and 2008 (Table 3-8). These years have directly coincided with weak to very strong El-Nino years.

For Wet season quantile perturbation analysis also shows similar dry season perturbation oscillation patterns. There are both negative and positive significant anomalies that occurred in upper Wabi Shebele river discharge extremes at half a decade interval. Accordingly, the years 1976, 1982, 1986, 1995, and 2010 are the years in which significant positive anomalies were observed in the wet season. Whereas the years like 1978-80, 1984-85, 1990, and 2001-02 are the years in which significant decrement of extreme discharge was observed in upper Wabi Shebele River Basin. Similar to the dry season, wet season significant positive anomalies are separately observed in moderate to very strong scale El-Nino years. Whereas negatively significant anomalies are observed in La-Nina years.

Table 3-8. Characteristics of highest anomaly in seasonal discharges

Station/River name	Magnitude of highest anomaly (%)	Season of occurrence	Year
Maribo	+370	Dry	1997
Wabi at Dodola	+265.1	Dry	1997
Robe	+967.3	Dry	1989
Tebel	+1029.7	Wet	2001
Erer	+1318.9	Dry	1998

Precipitation extremes: In wet season (April- September), the extreme precipitation anomalies followed decreasing trend in between 1980-1990 and less increasing trends between 1990 to 2013

(Table 3-9). The early 1980s and 1990s are years in which significant positive and negative anomalies are observed respectively in most stations.

Except for the years like 1988 and 1997, most of the extreme precipitation over the Wabi Shebele River Basin changes within the confidence interval. 1988 rainfall across the basin shows significant positive anomalies in the basin during the dry season. It is also evident that there is an increasing trend in extreme precipitation on Adaba station rainfall. 1988 was when high flood disasters occurred in the horn of Africa as a whole (UNOCHA 2015). Similar results are reported by MoWR (2003) on the upper Wabi Shebele basin around Adaba. In the early 1990s and late 2000s, a significant increasing trend is observed in the dry season.

Table 3-9. Characteristics of highest anomaly in seasonal extreme precipitation

Station name	Magnitude of highest anomaly (%)	Season of occurrence	Year
Adaba	+666.6	Dry	1990
Kofele	+32.9	Wet	2004
Robe (Arsi)	+5948.9	Dry	1982
Gindhir	+777.1	Dry	1992
Diredawa	+1493	Dry	1997
Jijiga	-23.7	Wet	1999
Degehabour	+251.7	Wet	1985

Temperature extremes: QPM analysis on seasonal high temperatures indicates an increasing trend in both dry and wet seasons (Table 3-10). The size of positive trends decreases from western to eastern upper basin and indicates the general decreasing trend downstream of Wabi Shebele River Basin around Degehabour and Gode area. There are strong arguments in literature that, results for more water vapor, and heat in the atmosphere high storms (Williams et al., 2012; Dettinger et al. 2009; Hall et al. 2014).

Table 3-10. Characteristics of highest anomaly in seasonal high temperatures

Station name	Magnitude of highest anomaly (%)	Season of occurrence	Year
Adaba	+15.8	Wet	2004
Kofele	+11.9	Wet	2014
Robe (Arsi)	+12.8	Dry	2002
Gindhir	+18.9	Dry	1990
Diredawa	+12.9	Dry	2012
Jijiga	+17.9	Wet	2008
Degehabour	-35.6	Dry	2003

3.3.4. Effect of Aggregation level on detected Anomalies

The effects of time aggregation on variability analysis are investigated based on daily, monthly and annual anomalies in the study area. In extreme discharge perturbation analysis, anomalies at daily aggregation level are less than both monthly and yearly perturbation (Figure 3-6). Whereas, the extreme precipitation perturbation at daily aggregation level is higher than both monthly and annual aggregation level (Figure 3-7) which coincided with the study result of Ntegeka and Willems (2008). This indicates that, the extreme discharge perturbation conducted by QPM at different aggregation level gives completely opposite result with the study result of Ntegeka and Willems (2008) in which the perturbations of smaller aggregation level are greater than larger level. It is known that the first day discharge has significant effect on the next day or lack of independency in daily discharge may be the cause for less anomaly in small time aggregation level.

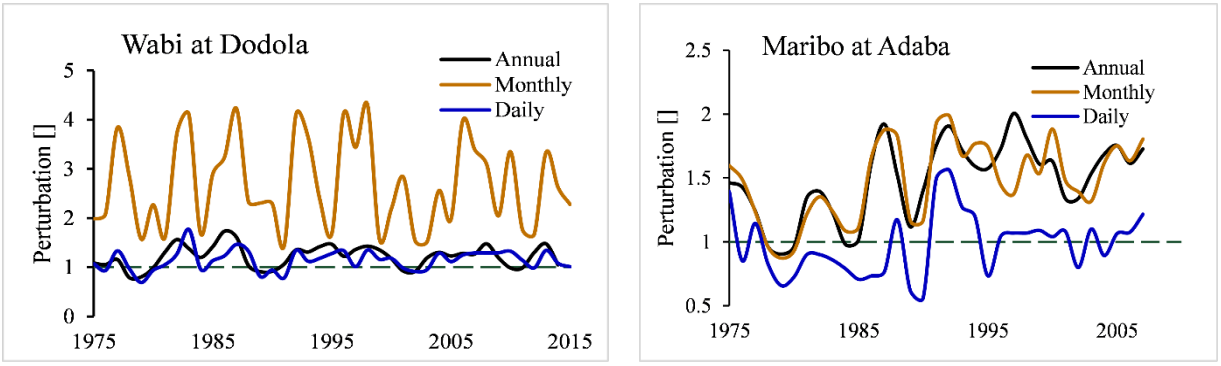

Figure 3-6. Comparison between extreme discharge perturbations at different aggregation levels

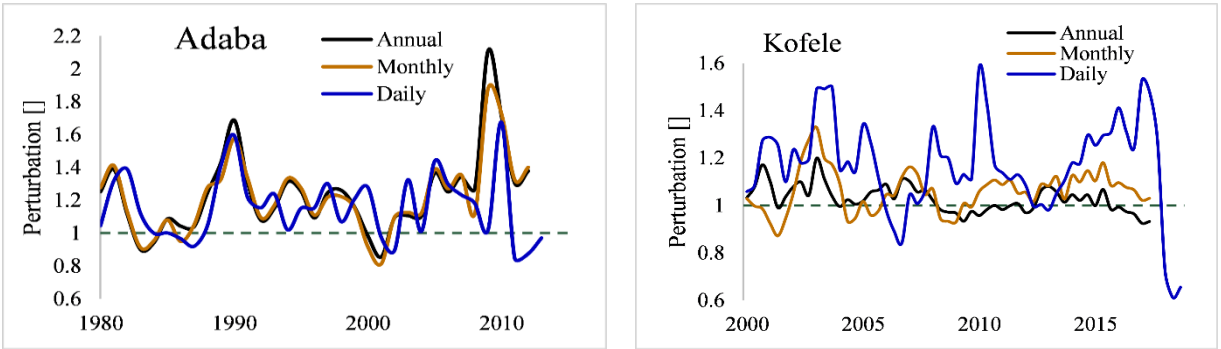

Figure 3-7. Comparison between precipitation perturbations at different aggregation levels

3.3.5. Correlation Analysis

Intergovernmental Panel on Climate Change (IPCC) indicated that climate change "has detectably influenced" several of the water-related variables that contribute to floods, such as rainfall and snowmelt (https://www.nrdc.org/stories/flooding-and-climate-change-everything-you-need-know). In this study, the rainfall variability in Wabi Shebele basin was taken as one of the major

driving factors for flood change in the basin. To verify this hypothesis, Pearson's correlation analysis is conducted on extreme anomalies of discharge and precipitation in different watersheds of the basin. The statistical significance of correlation value is checked using student test at 5% significance error.

The result indicates that oscillation pattern of both variables, i.e., extreme discharge and precipitation anomalies follows similar pattern with small correlation value. From Table 3-11, it is evident that in dry season a better positive correlation value in between extreme discharge and precipitation up to 62 %, 20%, 30%, 53% and 65% are observed at Maribo, Wabi at Dodola, Robe, Tebel and Erer watersheds respectively.

Furthermore, the tendency of anomalies in annual and wet season extremes follow similar direction which indicates that extreme discharge in the study area is attributed to wet season rainfall changes. In general, statistical correlation using Pearson's correlation coefficient method shows, less than 50% correlation value in average in between extreme discharge and precipitation anomalies. High variability and a low signal-to-noise ratio in flood time series are often occurred within a usually available series of observations (Merz et al. 2012). This may also be interpreted those changes in extreme discharge in Wabi Shebele River Basin are caused by multiple driving factors in addition to climate elements. There was study result by MoWR (2003), in upper Wabi Shebele River Basin (upstream of Melka wakena) strong flood only occurs when soil has been previously saturated with water after the first rainy phase. This is because of not very intense rainfall conditions and considerable perviousness of soil in sub basin.

Table 3-11. Annual and seasonal correlation coefficient between discharges and rainfall anomalies

Station name	Annual	Dry season (October – March)	Wet season (April -September)
Maribo	0.03	0.62*	0.004
Wabi at Dodola	-0.20	0.20	-0.18
Robe river	-0.09	0.3	-0.13
Tebel river	-0.18	0.53*	-0.29
Erer river	-0.14	0.65*	-0.27

*****=Statistically significant at 5% significant error

3.4. Conclusion

Temporal variabilities in hydroclimate variables were examined for Wabi Shebele River Basin for 1975-2015. The trend detection analysis done on runoff at five river locations using linear trend regression test at annuals scale indicates insignificant increasing trend over the study period. While

the annual rainfall in the middle and lower part of the basin showed a significant decreasing trend, and an insignificant increasing trend in the western and eastern highlands. The major runoff is generated from the western and eastern highlands of the basin. At the annual time scale, the runoff variability is consistent with the annual rainfall variability. The mean temperature over the basin showed a significant increasing trend in the basin consistent with the national and global trends.

The temporal trend and variability analysis done on extreme high discharge using the QPM approach indicates a significant increasing trend in the Maribo river from the western upper basin and Erer river discharge from the eastern upper basin. The other most extreme discharge anomalies vary within the confidence interval. The dry and wet season anomalies mostly follow a similar oscillation pattern with annual extreme discharge anomalies. Most of the positive and significant anomalies of extreme discharge quantiles in the river basin occurred in moderate to very-strong El-Nino years whereas, the most negative significant anomalies occurred in weak to strong La Nino years. The large-scale climate oscillation contributes to the flooding situation in the basin. The precipitation extreme perturbations analysis shows an increasing trend at all aggregation levels in the western and eastern upper basin and a decreasing trend in the middle between 1980 and 2018. QPM analysis on high temperature indicates a significant increasing trend with a high oscillation pattern. The study conducted by Shiferaw et al (2015) reveals a similar result that a substantial increasing trend in rainfall over southeastern highlands of Ethiopia and a warming trend of about 0.4°C/decade in the region. The correlation analysis done between extreme discharge and precipitation indicates a strong correlation of dry season extreme discharge and precipitation anomaly up to 65% in some watersheds, even though it falls below 50% in other sample watersheds.

Wabi Shebele River Basin is the largest basin in Ethiopia with ungagged hydrologic characteristics. It is hard to characterize the whole basin's extreme hydroclimatic variabilities with only five sub-basins which most of it confined at the upper highland area of the river basin, while the basin has more than 11 sub-basins with larger than 500 km^2 catchment area. Therefore, an extension of river discharges and precipitations in un-gagged sub-basin using robust model and analysis can explore better information on trends, temporal variabilities, correlations, and periodicities in extreme hydroclimate variabilities of the basin.

4. DETECTING VARIABILITY IN PRECIPITATION EXTREMES: APPLICATION OF REANALYSIS CLIMATE PRODUCT IN DATA-SCARCE WATERSHEDS

Abstract

Understanding climate data is essential for water resource management, flood risk assessment, agricultural planning, ecological modeling, and climate change adaptation. This study investigated the trends and variability of precipitation extremes to explore statistically significant trends in extreme hydrological conditions over the last 35 years in the Wabi Shebele basin of Ethiopia. Two reanalysis climate products: ENACTS (i.e., Enhancing National Climate Services) and CHIRPS (i.e., Climate Hazards Group InfraRed Precipitation with Stations) are evaluated against ground observations using cumulative distribution function and statistical measures. The result shows that the CHIRPS dataset performed well and captured the precipitation extremes measured by rain gauges. The Mann-Kendall trend test analysis conducted using three extreme precipitation indices, i.e., AMP (i.e., annual highest 1-day precipitation amount), R10 (i.e., the yearly count of days when precipitation >=10 mm), and R95P (i.e., 95% percentile precipitation events). The result indicates an increasing tendency over the western-eastern highland and southern part of the basin; In contrast, it indicates decreasing trends over the middle of the study area. The Quantile Perturbation analysis using R95P reveals high oscillations at five years intervals within a confidence interval, particularly at the basin's western-eastern highlands and southern lowlands. Since the 2000s, a periodicity analysis of maximum yearly precipitation using the auto-correlation function has revealed cycles at 2 to 5-year intervals over western-eastern highlands of the basin.

Keywords: CHIRPS, Cumulative distribution function (CDF), ENACTS, Extreme precipitation Indices (EPI), and Trends

---

[2]F. A. Wudineh, S. A. Moges and B. B. Kidanewold Detecting hydrological variability in precipitation extremes: Application of reanalysis climate product in data-scarce Wabi-Shebele basin of Ethiopia. J. Hydrol. Eng., ASCE, 2021. https://doi.org/10.1061/(ASCE)HE.1943-5584.0002156

4.1. Introduction

The amount of carbon dioxide (CO_2) in the atmosphere has increased by more than 40% since 1850 and is now higher ~407 ppm than during the past 2-2.5 million years (Podesta and Holdren

2014; Emeribe et al. 2019). This increasing CO_2 concentrations and other emissions caused by human activity was the cause for an observed increasing trend in average temperature from 1951 to 2010 on the earth (IPCC 2014; Shiferaw et al. 2015). Since the advent of this warming, there are increased concerns regarding extreme weather events. For example, findings by Dankers et al. (2014) and Wanders (2015) revealed that heavy precipitation, which is above moderate value, and rain-induced inland flooding have become strong since the 20th century in many regions.

Understanding observational and historical hydro climatological data is essential for water resource management, flood risk assessment, agricultural planning, ecological modeling, and climate change adaptation. Knowledge about changes in hydrological data (i.e., precipitation, temperature, and streamflow) is fundamental to understand flooding risk and to allow preparation for mitigation. Rainfall is the leading cause of large floods in the horn of Africa, including Ethiopia (Tadesse et al. 2016). In Ethiopia, severe hydrological extremes have been endemic with high spatial variabilities since the 1950s: extreme floods in the eastern and southeastern of the country at different times, e.g., (Tadesse et al. 2016; UNDP 1999; MoWR 2003). In recent years, Wabi Shebele River Basin has been marked by frequent destructive hydrologic extremes (MoWR 2003; IWMI 2015; ERCS 2005). The Ethiopian Ministry of Water, Irrigation and Energy (MoWIE') (MoWR 2003) during the basin master plan study reveal the severe hydrologic extremes in the Wabi Shebele basin, especially in 1973, 1979, 1984-1985, were caused by natural atmospheric variability. Other studies constantly show decreasing rainfall trends over the Wabi Shebele basin since the 1950s (Gebru 2016). Some studies used stochastic and hydrologic models, e.g., (Abebe and Förch 2006; IPCC 2001; Amer et al. 2013; Awulachew et al. 2007) to characterize the Wabi Shebele basin hydroclimatic variables due to the limitation of ground-based observed data.

Ground-based observed data with broad coverage and record length are crucial to understanding the variabilities and impacts of climate change at the regional and local scales. In developing countries, the vulnerability to severe climate threats is due to a lack of ground-based observations (Wilby et al., 2002; Gebrechorkos et al., 2018). Therefore, in data-scarce watersheds, like the Wabi Shebele basin, searching for other representative climate products is necessary to assess variabilities accurately in hydrological extremes. Currently, there are different reanalysis climate products available in Africa (Gebrechorkos et al., 2018). Among these, CHIRPS (i.e., Climate Hazards Group InfraRed Precipitation with Stations product from the Climate Hazard Group) (Dinku et al. 2014), ENACTS (i.e., Enhancing National Climate Services) (Funk et al. 2015) are

selected with ground-based observed data to see temporal and spatial variabilities in extreme precipitations in this study.

This chapter aims to detect variabilities in precipitation extremes using reanalysis climate product in the data-scarce watershed, Wabi Shebele basin, Ethiopia. First, preliminary analysis compares CHIRPS and ENACTS climate products against available field-based observed data based on distribution and extreme precipitation values. Then, the climate product, which indicates corresponding values with the observed dataset in terms of extremes and distributions, is used for detailed variability analysis in the study area.

4.2. Materials and Methods

4.2.1. Precipitation characteristics in the study area

There are two types of rainfall regimes in the Wabi Shebele basin (NMA 1996): bimodal type I and bimodal type II. Rainfall in bimodal type I has a quasi-double maximum rainfall pattern, with a modest peak in April and a significant peak in August (i.e., covers the west-east highland of the Wabi Shebele basin). On the other hand, a twofold peak pattern defines the rainfall pattern of bimodal type II with peaks in April and October (i.e., covers the low-lying southeastern areas of the basin). Furthermore, MoWR (2003) identified five rainfall zones in the Wabi Shebele basin during the basin master plan study. These rainfall zones are defined based on the magnitude and intensity of precipitation in the region. Additional, one rainfall zone at lowland areas of the middle basin, which not incorporated in the previous studies, is defined as Rainfall Zone 6 for extreme precipitation analysis in this study (Figure 4-1):

- Rainfall Zone 1: occupies large volcanic groups around Arena mountains and the Ticho and Minne-Gololcha mountains with uninterrupted rainfall from March to November (e.g., Ticho, Sagure, Arsi Robe stations);
- Rainfall Zone 2: occupies high plateaus of Arsi, Bale, and Chercher with an annual depth of rainfall greater than 900mm in two seasons (e.g., Deder, Goba, Gelemso, Assassa, Sire, Kofelle stations);
- Rainfall Zone 3: occupies the Guedeb plain, that hemmed in by mountains with annual depth varies from 900mm to 700mm (e.g., Adaba, Dodola stations);

- Rainfall Zone 4: occupies the northern area of the limestone plateau, as well as the granite group of Harar with annual rainfall, varies from 900mm to 500mm (e.g., Diredawa, Harar, Jijiga, Fugnanbira stations);
- Rainfall Zone 5: occupies all southern areas of the basin with an annual rainfall of less than 500mm (e.g., Degahabour, Kebridehar, Gode, Kelefo stations);
- Rainfall Zone 6: occupies the wettest region at the middle basin with an annual rainfall of more than 900 mm (e.g., Seru, Sinana, Jara, Shekhusen).

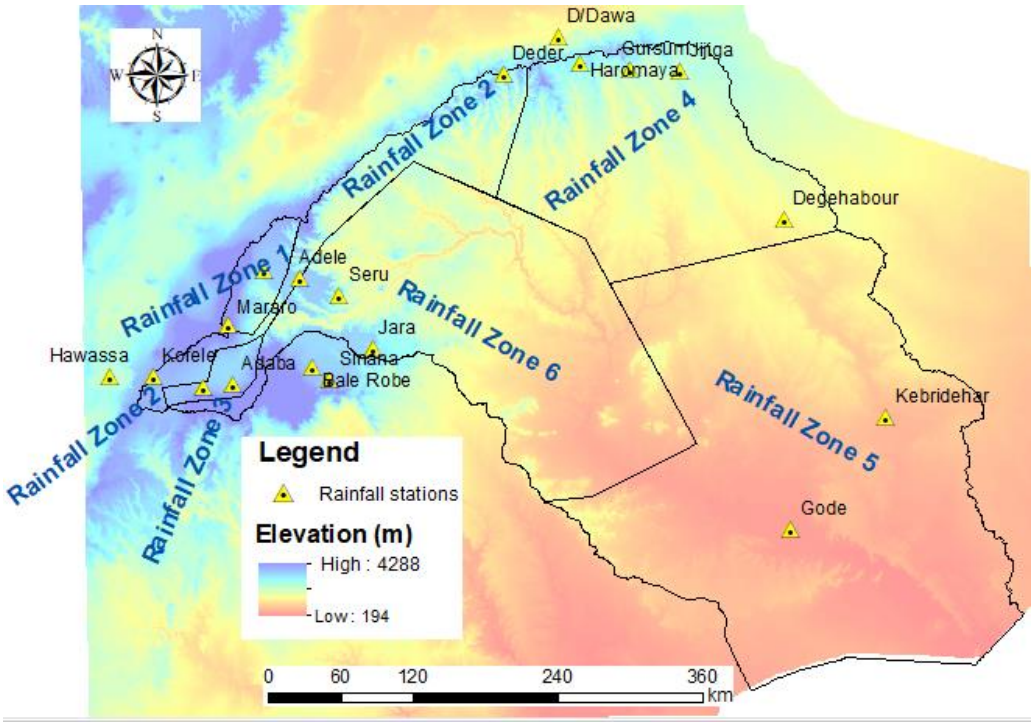

Figure 4-1 Rainfall Zones in Wabi Shebele River Basin

Data

In this study, three weather datasets: 1) observed data set from ground rain gauge stations, 2) grid-based reanalysis precipitation data from ENACTS approach product, and 3) CHIRPS products covering 1981-2019. I collected both observed and ENACTS precipitation datasets from Ethiopian National Meteorological Agency (NMA). In addition, the CHIRPS precipitation dataset is freely downloaded from the Climate Hazards Center University of California website (ftp://ftp.chg.ucsb. Edu/pub/org/chg/products/CHIRPS-2.0).

Ground-based gauged precipitation dataset: is measured precipitation data used in analysis after a quality check. Several studies used this manner widely in precipitation extremes analysis for the case data limitation is not an issue, e.g., (Emeribe et al. 2019; Talchabhadel et al. 2018). In

this study, I used a ground-based observed precipitation dataset to validate the reanalysis of climate products for the study area. The gauged precipitation dataset has rainfall at a daily aggregation level from ten climatic stations (Table 4-1) for 1980- 2013. The stations are selected based on data quality (i.e., length of the record, minimum percent of missing data, and spatial distribution of stations in the basin). Before data analysis, existing gaps in-between data are filled using multiple regression analysis with adjacent station data (Mfwango et al., 2018). This dataset hereafter referred to as "observed precipitation."

ENACTS data set: is a reanalysis data set, a merged data set of rain gauge observations, and a locally calibrated version of tropical applications of meteorology using satellite data (TAMSAT) and ground-based observations. The data set is estimated using the simple bias adjustment (ADJ) method over Ethiopia (Dinku et al. 2014). The ENACTS weather data set provides precipitation daily time series covering 34 years (1983–2016) at 4-km grid intervals (NMA 1996). The daily precipitation data set obtained from the ENACTS product was named ENACTS precipitation in this study.

CHIRPS data set: is a quasi-global satellite-based precipitation data set developed for managing and monitoring extreme events and trend analysis (Gebrechorkos et al.,2018). It is available at multiple time scales, daily and monthly, from 1981 to the present at a high spatial resolution of 0.05°. The CHIRPS data set is freely available at the Climate Hazards Center University of California, Santa Barbara (CHG) (ftp://ftp.chg.ucsb). This study prepares CHIRPS data at 37 points for analysis throughout the basin, and the data obtained was called CHIRPS precipitation.

Table 4-1. Inventory of rainfall stations with the observed dataset used in the study

Station Code/Name	Location			Data Availability		
	Latitude	Longitude	Altitude	Length (Years)	Missing data (%)	Mean annual rainfall (mm)
Adaba	7.0	39.4	2420	31	21.12%	892.3
Arsi Robe	7.9	39.6	2400	31	1.70	1113.7
Kofele	7.1	38.8	2620	14	6.40%	1107.5
Deder	9.3	41.5	2350	31	22.40%	1029.4
Jijiga	9.3	42.8	1175	29	2.87%	585.5
Degehabour	8.2	43.6	1070	29	5.64%	349.6
Gode	5.9	43.6	295	29	8.62%	268.0
Diredawa	9.6	41.8	1260	31	1.92%	665.4

4.2.2. Methods

Evaluation methods

Cumulative Distribution Function (CDF): is used to compare the cumulative frequency and distribution of precipitation values for an overlapping period of different datasets (1983-2013). The method used to compare distributions of climate data ensembles over other regions, e.g. (Kay et al. 2011; Jenkins et al. 2009). Since the stations are too sparse in the basin, I selected only ten weather stations (Table 4-1) for comparison. Among different approaches used to compare reanalysis data products with ground observation (Gebrechorkos et al. 2018), point to pixel analysis is commonly used. Therefore, I extracted gridded data for the point-based station location and used it. In this study, the frequency is evaluated based on the rainfall intensity classification of the World Meteorological Organization (WMO) guide (WMO 2013): (1) rain <2.5 mm hr^{-1} (light rain), (2) 2.5 mm hr^{-1} ≤ rain <10 mm hr^{-1} (moderate rain), (3) 10 mm hr^{-1} ≤ rain < 50 mm hr^{-1} (heavy rain) and (4) rain ≥50 mm hr^{-1} (violent rain).

Additionally, reanalysis rainfall products were quantitatively evaluated against ground observations using four statistical indices: the relative Percent of Bias (PBIAS), Root Mean Square Error (RMSE), Pearson Correlation Coefficient (r), and Mean Absolute Error (MAE) (Table 4-3). The statistical value between estimates and observations is considered satisfactory for PBIAS and r values ±25% and > 0.5, respectively (Moriasi et al., 2007). The lower the RMSE and MAE values, the closer the reanalysis estimates are to the ground measurements. The unit of RMSE and MAE is mm/ period time.

Defining precipitation extremes: represent extreme precipitation in this study; a total of eight Extreme Precipitation Indices (EPIs) selects from the Expert Team on Climate Change Detection and Indices (http://etccdi.pacificclimate.org/list_27_indices.shtml). EPIs computed at both annual and seasonal time scales (Table 4-2).

Table 4-2. Extreme precipitation Indices (EPIs) used in this study

Extreme Precipitation Indices (EPIs)	Explanation
AMP (mm)	Annual highest 1-day precipitation amount
R10 (days)	Annual count of days when precipitation>=10mm
PRCPTOT (mm)	Annual total precipitation in wet (precipitation>=1mm) days
R95PTOT (mm)	Annual total precipitation when precipitation > 95^{th} percentile
R95P (mm)	95% percentile precipitation events
SMW (mm)	Seasonal maximum daily precipitation for winter
SMSp (mm)	Seasonal maximum daily precipitation for spring
SMSu (mm)	Seasonal maximum daily precipitation for summer

Table 4-3. Evaluation statistical measures

Statistical measure	Formula	Value range	Perfect score
Percent of Bias (PBIAS)	$PBIAS = \frac{\sum_{1=1}^{n}(Y_i - X_i)}{\sum_{i=1}^{n} X_i} * 100$	0 to ∞	0
Root Mean Square Error	$RMSE = \sqrt{\frac{1}{n}\sum_{i=1}^{n}(Y_i - X_i)^2}$	0 to ∞	0
Pearson Correlation Coefficient	$r = \frac{\sum_{i=1}^{n}(Y_i - \bar{Y})(X_i - \bar{X})}{\sqrt{\sum_{i=1}^{n}(Y_i - \bar{Y})^2}\sqrt{\sum_{i=1}^{n}(X_i - \bar{X})^2}}$	-1 to 1	1
Mean Absolute Error	$MAE = \frac{1}{n}\sum_{i=1}^{n}(Y_i - X_i)$	∞ to ∞	0
Nasch and Sutcliffe Efficiency	$NSE = 1 - \frac{\sum_{i=1}^{n}(X_i - Y_i)^2}{\sum_{i=1}^{n}(X_i - \bar{X})^2}$	-∞ to 1	1
Coefficient of Determination	$R^2 = \left[\frac{\sum_{i=1}^{n}(X_i - \bar{X})(Y_i - \bar{Y})}{\sqrt{\sum_{i=1}^{n}(X_i - \bar{X})^2}\sqrt{\sum_{i=1}^{n}(Y_i - \bar{Y})^2}}\right]^2$	0 to 1	1

Xi is observed value, Yi is estimated value, n is the number of data pairs, *Xbar* and *Ybar* are the average observed and estimated data, respectively.

Trend and Variability tests

Two nonparametric tests (i.e., Mann- Kendall trend test and Quantile perturbation method) are used to analyze trends and variabilities in extreme precipitations in this study. These tests yield results based on the rank numbers of the elements in the series. In addition, the cycles and periodicity observe using correlogram analysis in rainfall time series (Emeribe et al., 2019; Higashino and Stefan, 2019). Finally, the spatial distribution of trends is prepared and analyzed using Inverse Distance Weighting (IDW) method in Arc GIS (Li et al. 2020). These tests are briefly described below.

Mann-Kendall (MK) trend test: is a rank-based nonparametric statistical test (Mann 1945; Welch 1959) which commonly used to assess the significance of trends in hydro-meteorological time series, e.g., (Emeribe et a. 2019; Kay et al. 2011; Meng et al. 2016; Sen 1968; Seleshi and Zanke 2004; Yue et al. 2019). The power of the test increases with sample size, the slope of trend, and pre-assigned significance level, while it is decreasing function of the variation of time series (Yue et al. 2019). Therefore, additional discussion requires during trend analysis of a small sample size using the Mann-Kendall trend test.

One of the assumptions in the MK trend test is the serial independent time series. However, hydrometeorological series often contaminated by serial correlation. Several studies proposed pre-whitening procedures (Von Storch, 1999; Yue et al., 2003; Talchabhadel et al. 2018; Yue et al., 2002) to limit the effect of serial correlation on MK trend results. Pre-whitening is the process of minimizing or eliminating short-term stochastic persistence to enable detection of deterministic change (Razavi and Vogel 2018). It consists of fitting time series models such as autoregressive (AR) or autoregressive moving average (ARMA) models to an ‘‘original” time series and separating out the time series of residuals from the original series, which becomes the ‘‘pre-whitened” series. The difference between the underlying original (presumably true) process and a prescribed model process will result in a realization of ‘‘some” new process, which inherits ‘‘some” properties from the original process excluding (partly or fully) the short-term persistence, which was removed by fitting and effectively removing the AR or ARMA process. If significant autocorrelation (lag-1 autocorrelation) exists in the data series, the trend test results may contain an error. The lag-1 autocorrelation is computed and removed. Yue et al. (2003) used a 90% Confidence Interval (CI) to identify significant auto-correlation and remove it. In this study, the MK trend test was performed after pre-whitening data for those stations that showed serial correlations above 95% confidence interval following studies like Talchabhadel et al. (2018) and Ahmad et al. (2015).

The detail of the Mann-Kendall trend test is presented in section 3.2. In this study, the method to test the statistical significance of trends in three extreme precipitation Indices: AMP (mm), R10 (days), and R95PTOT (mm).

Autocorrelation function (ACF): represents the correlation between a time series and the same series at a later interval (Emeribe et al., 2019). A serial correlation is to refer to persistence in the form of autoregressive noise, typically first-order, lag-1:

$$X_i = r_1 X_{i-1} + \varepsilon_i(\mu, \sigma) \quad (4.1)$$

where *Xi* is the present (i^{th}) measurement of the hydrological quantity under consideration, x_{i-1} is the previous ($i\text{-}1^{th}$) measurement ε_i is white (serially independent and normally-distributed) random noise with mean, μ, and standard deviation, σ, and r_1 is the lag-1 serial correlation coefficient, given by:

$$r_1 = \frac{\sum_{i=1}^{N-1}(X_i - \bar{X})(X_{i+1} - \bar{X})}{\sum_{i-1}^{N}(X_i - \bar{X})\text{^}2} \quad (4.2)$$

Where N is the amount of data, to identify whether the correlation is significant or not, r_1 was tested against the null hypothesis at a 95% confidence interval, using a two-tailed test:

$$r_1(95\%) = \frac{-1 \pm 1.96\sqrt{(N-2)}}{N-1} \quad (4.3)$$

If the value of correlation coefficient r(1) is beyond the boundary limit, single-stage pre-whitening or deserialization (Talchabhadel et al. 2018) requires before proceeding to the Mann-Kendall trend test in this study.

$$X_j = X_i - r_1 X_{i-1} \quad (4.4)$$

Xj is the pre-whitened data used in the subsequent trend analysis, and r_1 is the lag-1 serial correlation coefficient as determined directly from the data using Equation 4.2.

The Quantile Perturbation method (QPM): is designed for analyzing extreme conditions (Ntegeka and Willems 2008; Taye and Willems 2012; Moges et al. 2014; Onyutha 2016; Tabari et al., 2014). QPM method compares the long-term baseline period extreme value quantiles with those of a selected sub-period to explore. It uses the given series directly (i.e., without rescaling) to obtain quantile anomalies. Further description of the method is incorporated in section 3.2 of this study.

4.3. Results

4.3.1. Evaluation of precipitation datasets

The reanalysis of climate products comparison takes place in daily and monthly time scales in ten rainfall stations. The daily rainfall of both products compared with observed daily rainfall using CDF at rainfall stations. First, rainfall data were arranged according to rainfall rates proposed by WMO: 0 mm hr^{-1} (dry), < 2.5 mm hr^{-1} (light rain), 2.5 ≤ rainfall < 10 mm hr^{-1} (moderate rain), 10 mm hr^{-1} ≤ rainfall ≤ 50 mm hr^{-1} (heavy rain) and > 50 mm hr^{-1} (violent rain). To analyze precipitation extremes further, I chose a reanalysis climate product that captures rainfall distribution related to available observed data. Figure 4-2 presents the relative probability distribution of all daily precipitations for all climate products based on different stations in the subbasin. Table 4-4 shows the summary of CDF of extreme precipitation occurrence for datasets. From Figure 4-2, both reanalysis precipitation datasets showed very closely related cumulative distribution function with ground-based observed precipitation. However, CHIRPS and observed datasets are more consistent in describing extreme precipitation values (> 10 mm hr^{-1}) than ENACTS. In most sample stations (i.e., 60%), the CHIRPS climate dataset estimates precipitation

extremes values related to ground-based observed values. The goodness-of fit test analysis on CDF using Chi-Square statistics (X^2) showed that small X^2 value in most of sample stations for CHIRPS product which mean that there is high correlation between the product and expected observed value (Appendix C, Table C.1). It is also evident from Table 4-4 that ENACTS reanalysis products presented dry, light rains, and moderate rainfalls values related to ground-based observed rainfall data in the study area.

Furthermore, reanalysis climate products are evaluated against ground observation at a monthly time scale using four statistical indices. As presented in Table 4-5, the average value of PBIAS for all stations was -1.396% and -0.369% for ENACTS and CHIRPS, respectively. Similarly, the r-value of these products was ≥ 0.5 in most stations, with an average value of 0.866 and 0.870, respectively. Figure 4-3 shows that CHIRPS datasets estimate precipitation with the better statistical value it has with observed precipitation in most the gauging stations. The RMSE and MAE, which evaluate the average magnitude error between reanalysis estimates and ground stations, showed the same trend as PBIAS and r that CHIRPS datasets estimated values related to observed data. Therefore, we can conclude that the CHIRPS rainfall product performed well and captured extreme precipitations gauged on the ground in Wabi Shebele basin. Thus, I used the CHIRPS precipitation dataset for further precipitation analysis in this study.

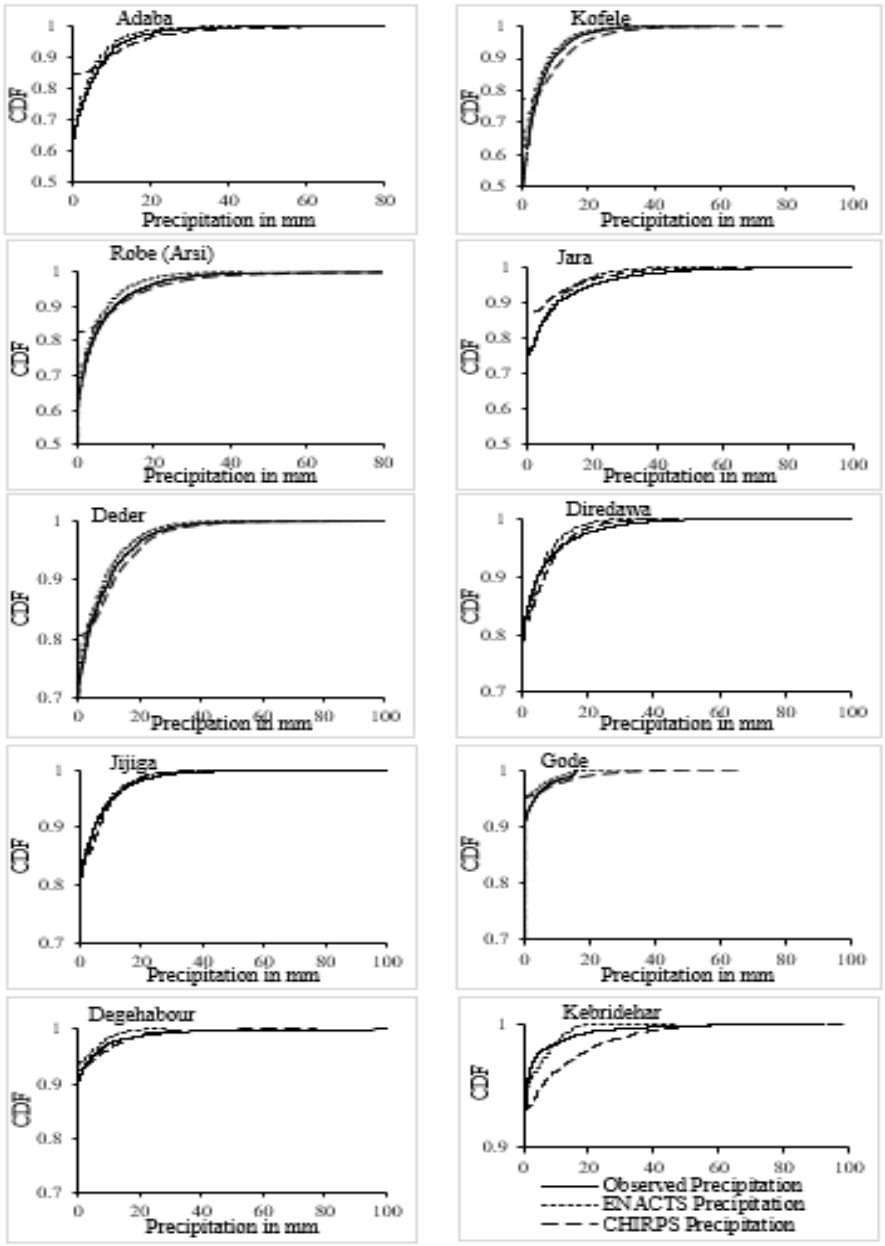

Figure 4-2 Distribution of daily precipitation values for three different precipitation datasets using CDF in the Wabi Shebele basin at sample stations

Table 4-4. Comparison of rainfall products based on daily precipitation distribution (dry, moderate rain, and extreme values). Bold numbers represent corresponding values of precipitation distribution

Stations	Datasets	Dry (%)	Light to moderate precipitation (%)	Extreme (heavy and violent) rainfall (%)
Adaba	Observed	**62.7**	28.8	**8.4**
	CHIRPS	84.8	6.0	**9.2**
	ENACTS	**70.1**	**23.2**	6.7
Arsi Robe	Observed	**60.6**	**29.5**	**9.9**
	CHIRPS	82.7	6.8	**10.5**
	ENACTS	**69.3**	**23.1**	7.7
Jara	Observed	**74.7**	**15.6**	**9.6**
	CHIRPS	87.2	5.6	7.3
	ENACTS	**76.7**	**13.7**	**9.5**
Deder	Observed	**72.37**	**16.95**	**10.68**
	CHIRPS	80.57	8.54	**10.89**
	ENACTS	**75.96**	**16.12**	7.92
Jijiga	Observed	**80.4**	**14.3**	**5.3**
	CHIRPS	84.1	10.1	**5.7**
	ENACTS	**81.9**	**12.8**	5.9
Diredawa	Observed	76.7	17.4	**5.9**
	CHIRPS	**82.8**	10.8	**6.5**
	ENACTS	**80.7**	14.4	4.9
Degehabour	Observed	90.48	6.73	**2.79**
	CHIRPS	**92.41**	**4.00**	**3.59**
	ENACTS	**93.34**	**4.88**	1.78
Gode	Observed	90.86	7.42	**1.72**
	CHIRPS	**95.14**	**2.40**	2.46
	ENACTS	**95.04**	**3.47**	**1.44**
Kebridehar	Observed	**92.7**	5.7	**1.6**
	CHIRPS	**93.1**	**3.1**	3.9
	ENACTS	94.6	**3.8**	**1.6**

Table 4-5. The average of r, PBIAS, RMSE, and MAE between two reanalysis precipitation datasets and gauged precipitation data on a monthly time scale during 1980 to 2013 over the Wabi Shebele River Basin, Ethiopia

Index	ENACTS	CHIRPS
r	0.866	0.870
PBIAS	-1.396	-0.369
RAMSE	4.942	1.842
MAE	-1.498	1.230

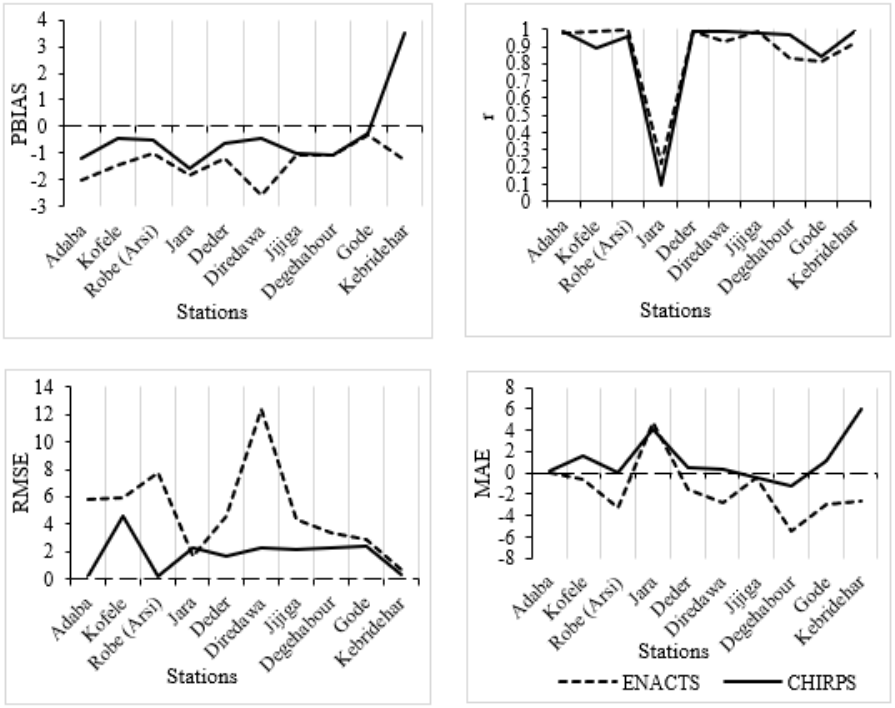

Figure 4-3 Comparison of monthly reanalysis rainfall estimate with ground measurements using four statistical indices

Trend analysis: The MK trend test was used to identify trends in annual precipitation between 1983 and 2013 using all data sets. Before the MK trend test, a serial correlation is checked to verify the independence of precipitation values. The result shows a significant serial correlation in precipitation time series at Robe (Arsi), Jara, and Deder stations, Figure 4-4. The impact of observed precipitation on ENACTS precipitation is significant in these stations. ENACTS climate is a blended climate product from available station data with satellite measurements and reanalysis products using the IRI Climate Data Tools (CDT) (Dinku et al. 2020). Therefore, I made a pre-whitening process in the precipitation time series for both datasets at stations before the MK trend test. Whereas the serial correlation estimated using CHIRPS precipitation falls within 95% boundary limits in all sample stations, this means that rainfall in CHIRPS datasets fulfills the independence criteria for further trend analysis using the MK trend test.

The statistical verification of trends using the MK trend test conducted on annual precipitation using all rainfall products indicates no significant trends in most sample stations (Table 4-6). Instead, all products show a mix of positive and negative trend values at different stations. Stations situated at the upper and middle of the basin, i.e., Adaba, Robe (Arsi), and Jara stations, which had shown positive trends in observed precipitation, did not exhibit similar trend signs in both

reanalysis products. Similarly, some studies, e.g., (Shiferaw et al. 2015) revealed a less increasing trend in annual rainfall in the west and eastern upper part and a decreasing trend in the middle and lower part of the Wabi Shebele basin. In addition, stations located in the lower part of the basin, i.e., Degehabour, Gode, and Kebridehar, which show negative trends in observed precipitation, did not exhibit a similar tendency in both reanalysis products (i.e., ENACTS and CHIRPS). These may be taken as a limitation of using reanalysis climate products for trend analysis in the basin. Exceptionally, both reanalysis datasets captured a similar upward trend with ground-based observed datasets at the northeastern highland of the Wabi Shebele basin around Diredawa and Jijiga. Regarding the magnitude of statistical trend value (Z_{mk}), CHIRPS products estimate trend values related to observed precipitation.

Table 4-6. Statistical summary of trends in annual rainfall

Stations	Period	Z_{mk}, for annual precipitation		
		Observed	CHIRPS	ENACTS
Adaba	1983-2013	1.22	-0.78	-1.12
Kofele	2000-2018	-1.80	-0.54	-1.94
Robe (Arsi)	1983-2013	1.22	0.03	-0.75
Jara	1983-2013	0.41	-0.88	-2.62*
Deder	1983-2013	-0.85	0.51	-0.65
Diredawa	1983-2013	0.90	1.12	1.41
Jijiga	1983-2013	1.30	0.36	0.99
Degehabour	1983-2011	-1.40	0.06	1.46
Gode	1983-2011	-0.50	0.02	1.29
Kebridehar	1983-2011	-3.50*	-1.56	1.61

* Significant at 95% confidence level ($|Z_{mk}| \geq 1.96$)

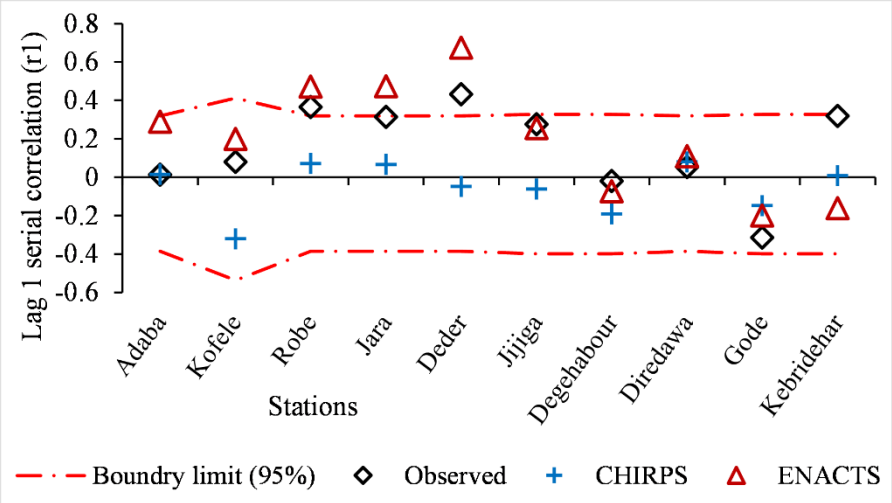

Figure 4-4. Serial correlation in annual precipitation using three rainfall products

4.3.2. Temporal variabilities and trends in precipitation extremes using CHIRPS dataset

Annual variation: The yearly variation of extreme precipitation is analyzed using four EPIs: AMP (mm), R10 (days), PRCPTOT (mm), and R95PTOT (mm) over six different rainfall zones (Figure 4-5).

From Figure 4-5, extreme precipitation indices; R10, PRCPTOT, and R95PTOT show the decreasing situation from upper highland to lower arid zones of the basin, from Rainfall 2 to 3, 1, 6, 4, and 5. The number of heavy rainfall (>10mm), total rain in a wet day, and amount of extreme precipitation exceeding 95% are maximum in the northwestern part of Wabi Shebele basin, i.e., Rainfall Zone 2, 3 & 1 and minimum in the lowland area of the basin, Rainfall Zone 5. However, the magnitude and range of annual maximum 1-day precipitation (AMP) are top in Rainfall zone 1 and minimum in Rainfall 4. The ranges of maximum yearly precipitation (AMP) are 54.7, 30.7, 46.7, 22.7, 32.3, 38.9 mm, corresponding to rainfall zones 1 to 6, respectively. These indicate that the magnitude and range of annual maximum 1-day rainfall is maximum on the highest altitude of the basin ranges from Galama mountains to Bale highlands, i.e., Rainfall Zone 1 & 3 and minimum at eastern upper basin around Harar and Jijiga highlands, i.e., Rainfall Zone 4.

The annual variabilities and trends in R95P are investigated using the quantile perturbation method (QPM). Based on the preliminary analysis, a block length of 5 years represents high oscillation patterns in precipitation extremes compared to other longer block lengths and was selected for variability analysis in this study. The perturbations observed in precipitation extremes using the CHIRPS dataset shown in Figure 4-6. Almost in all rainfall zones, the anomalies (%) of annual extreme precipitations fall within the confidence interval with weak significant negative anomalies in 1988 & 1989, particularly in Rainfall Zone 1, 2 & 3. However, the oscillation patterns of extreme precipitation decrease from the west to east highland part to the downstream lower basin. High oscillation patterns are observed within confidence intervals in Rainfall Zone 1 & 2. In Rainfall Zone 4 & 5 perturbation graph shows fewer oscillation patterns. In the 2000s, weak significant negative anomalies are observed in the northern highland part of the basin (Rainfall Zones 2, 3 & 4) with the maximum anomaly of 6.5%, 17.6%, and 13.4%, respectively, and fewer positive anomalies in the lowland of the basin (Rainfall Zone 5). In general, the QPM analysis on 95% maximum exceedance indicates oscillations within confidence intervals in most basin areas with insignificant increasing trend in zones 1, 2 & 5 and a decreasing trend in zones 3, 4, and 6. MoWR

(2003) also found a significant increasing trend in in-situ precipitation observations over the upper Wabi Shebele basin from 1980 to 1990 and 2000 to 2010. In the study area, significant negative anomalies occurred in 1988, 1994, and 2009, noticed moderate to strong La-Nina happened on the globe including our country (https://ggweather.com/enso/oni.htm).

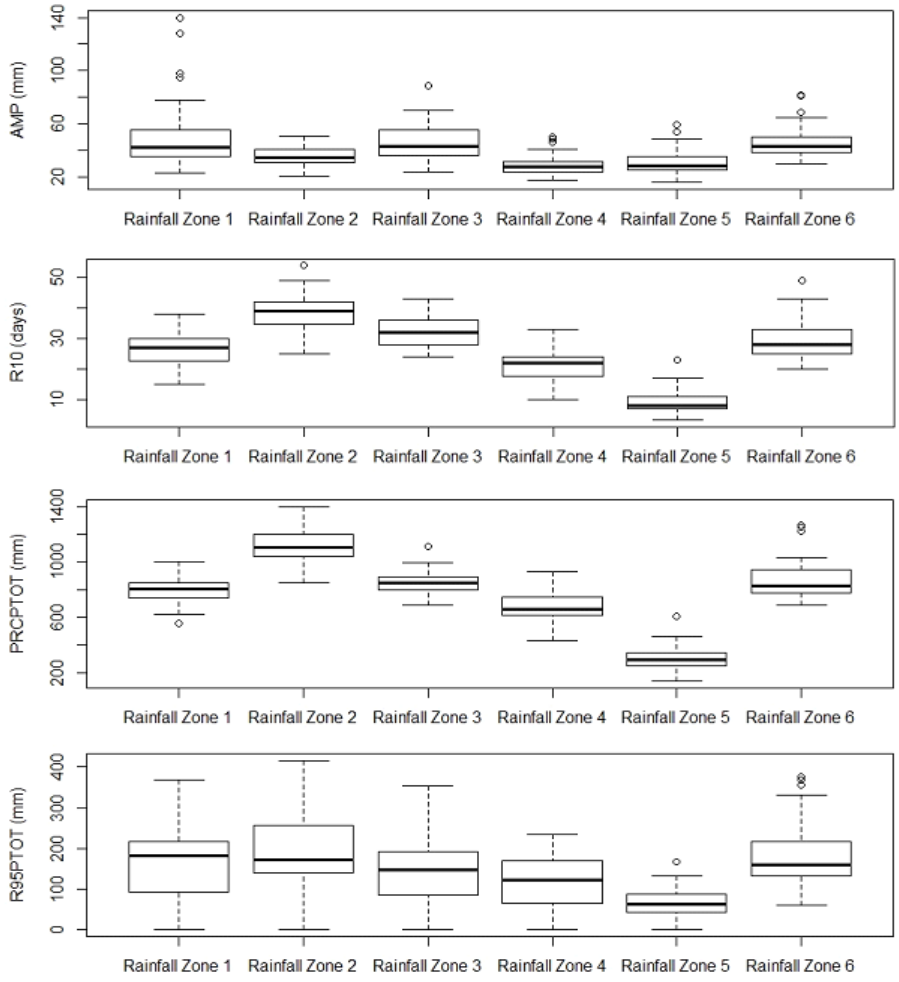

Figure 4-5. Annual variation of four EPIs in six rainfall zones of Wabi Shebele basin, 1981-2019. In each box, the central mark indicates the median, the bottom and top of the box indicates the 25th and 75th percentiles, respectively. The whiskers extend to the most extreme data points not considered outliers, and the outliers are plotted using the '°'symbol

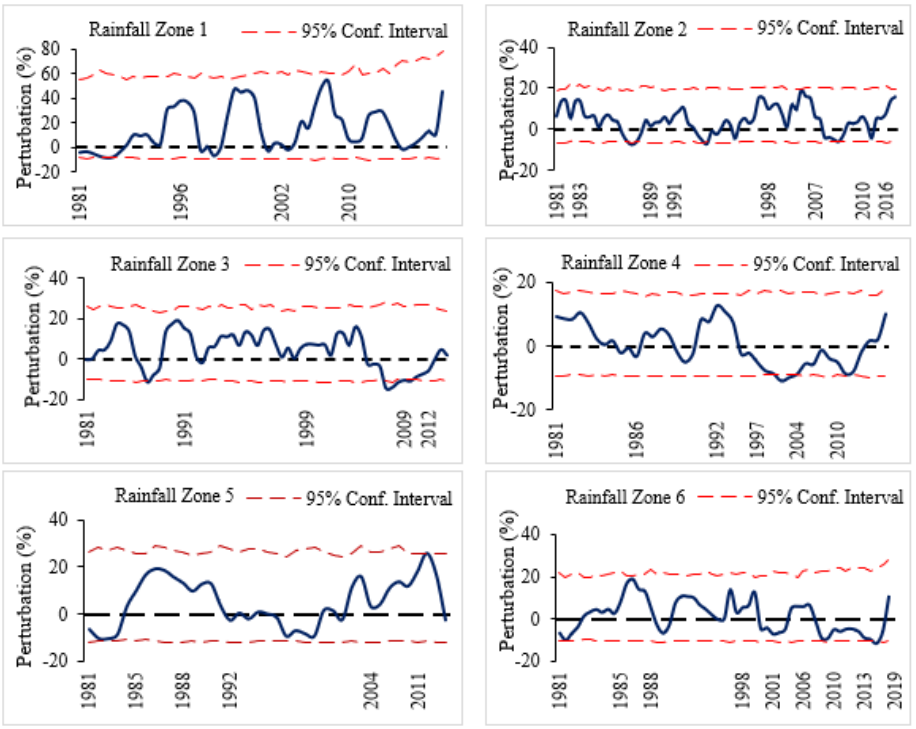

Figure 4-6. Annual extreme precipitation perturbations with 95% confidence intervals

Seasonal Variations: The perturbations in seasonal extreme precipitation quantiles are also identified (Figures 4-7 to 4-9). Figure 4-7 shows that there are weak significant anomalies for the winter period (October- January) over Rainfall zones 1, 2, 3, and 6. For the period 1981-2000, the winter precipitation quantiles show an increasing tendency throughout the basin. The late 1990s show a dominance of positive anomalies over the northern Wabi Shebele basin with changes up to around 200%, 80%, and 150% in Zone 1, 2, and 3, respectively. For the spring period (February-May), extreme precipitation in the basin varies within confidence intervals (Figure 4-8), decreasing trends in most rainfall zones. In the early 1980s, high oscillations in precipitation extremes were observed to be positive perturbations over most of the Wabi Shebele basin area in the spring season. Anomalies of extreme precipitation quantiles in the upper basin (Rainfall Zone 1& 2) indicates a less increasing trend within a confidence interval. For the summer period (July-September), QPM analysis shows weak significant perturbations at decade intervals in most Rainfall zones. At the north upper part of the basin (Rainfall Zone 1 & 2), significant positive anomalies were observed in the early 1990s and negative anomalies in the early 2000s. As presented in Figure 4-9, there is an increasing trend in extreme precipitation quantiles over the eastern upper part of the basin (Rainfall Zone 4) while indicating a decreasing trend in the middle basin (Rainfall Zone 6).

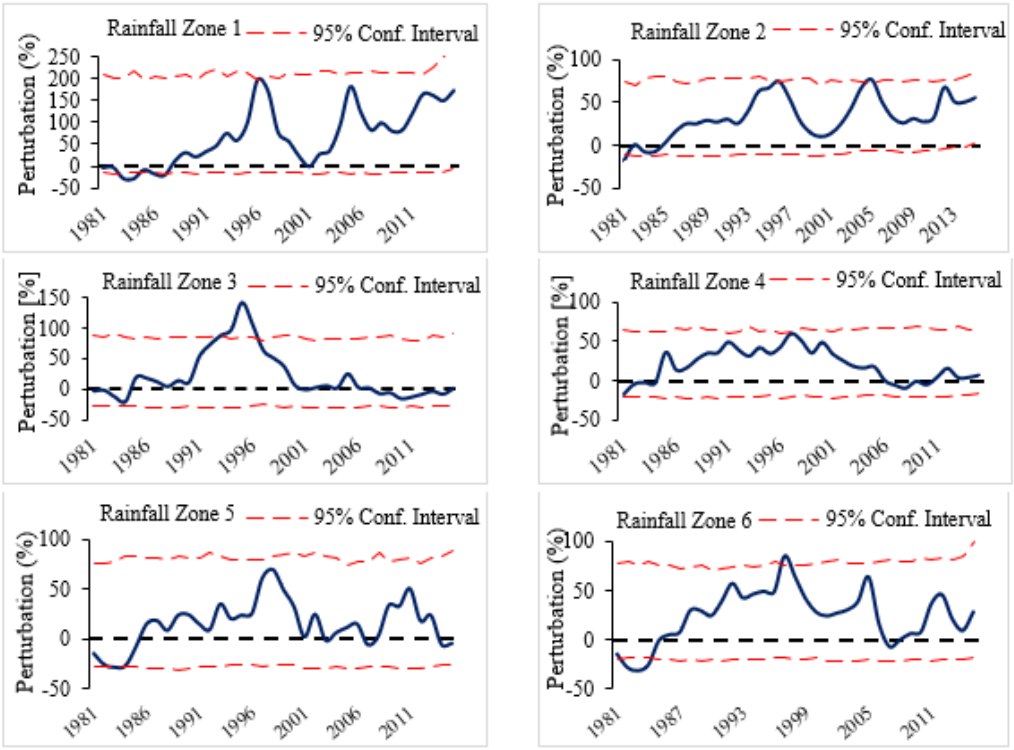

Figure 4-7. Seasonal extreme precipitation perturbations for the winter period with 95% confidence intervals

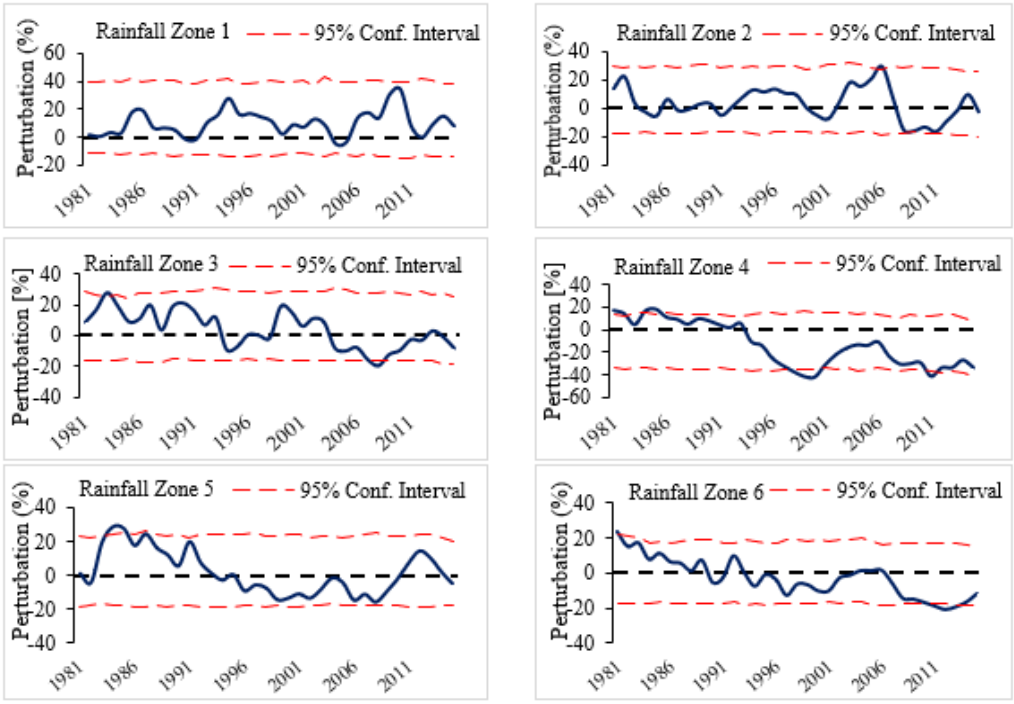

Figure 4-8. Seasonal extreme precipitation perturbations for the spring period with 95% confidence intervals

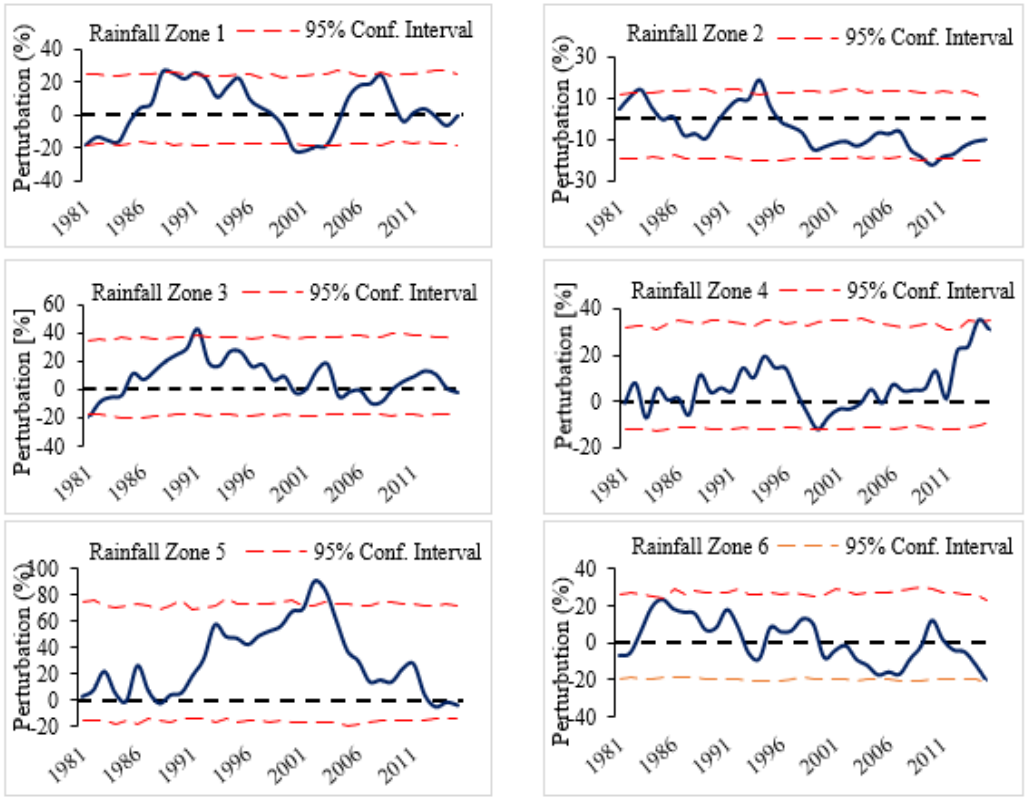

Figure 4-9. Seasonal extreme precipitation perturbations for the summer period with 95% confidence intervals

4.3.3. Spatial variability of extreme precipitation

Figure 4-10 shows the spatial distribution of trends in the 3 EPIs: AMP, R10 & R95P in the Wabi Shebele basin. The spatial distribution map of trend values uses to prepare using CHIRPS reanalysis data at 37 points throughout the Wabi Shebele basin. The MK trend test using extreme indices indicates an increasing tendency over the west-east highland and lowland area of the study area. On the other hand, the large middle part of the basin shows a decreasing trend in extreme precipitation indices. Further, extreme precipitation values in the northwestern basin, categorized as Rainfall Zone 1 by MoWR (MoWR 2003), indicate a significant increasing trend between 1981 and 2019. NMA (1996) and Seleshi and Zanke (2004) reported inconsistency caused by multiple weather conditions, like Subtropical Jet, Inter-tropical Convergence Zone, Red Sea Convergence Zone, Tropical Easterly Jet, and Somali Jet.

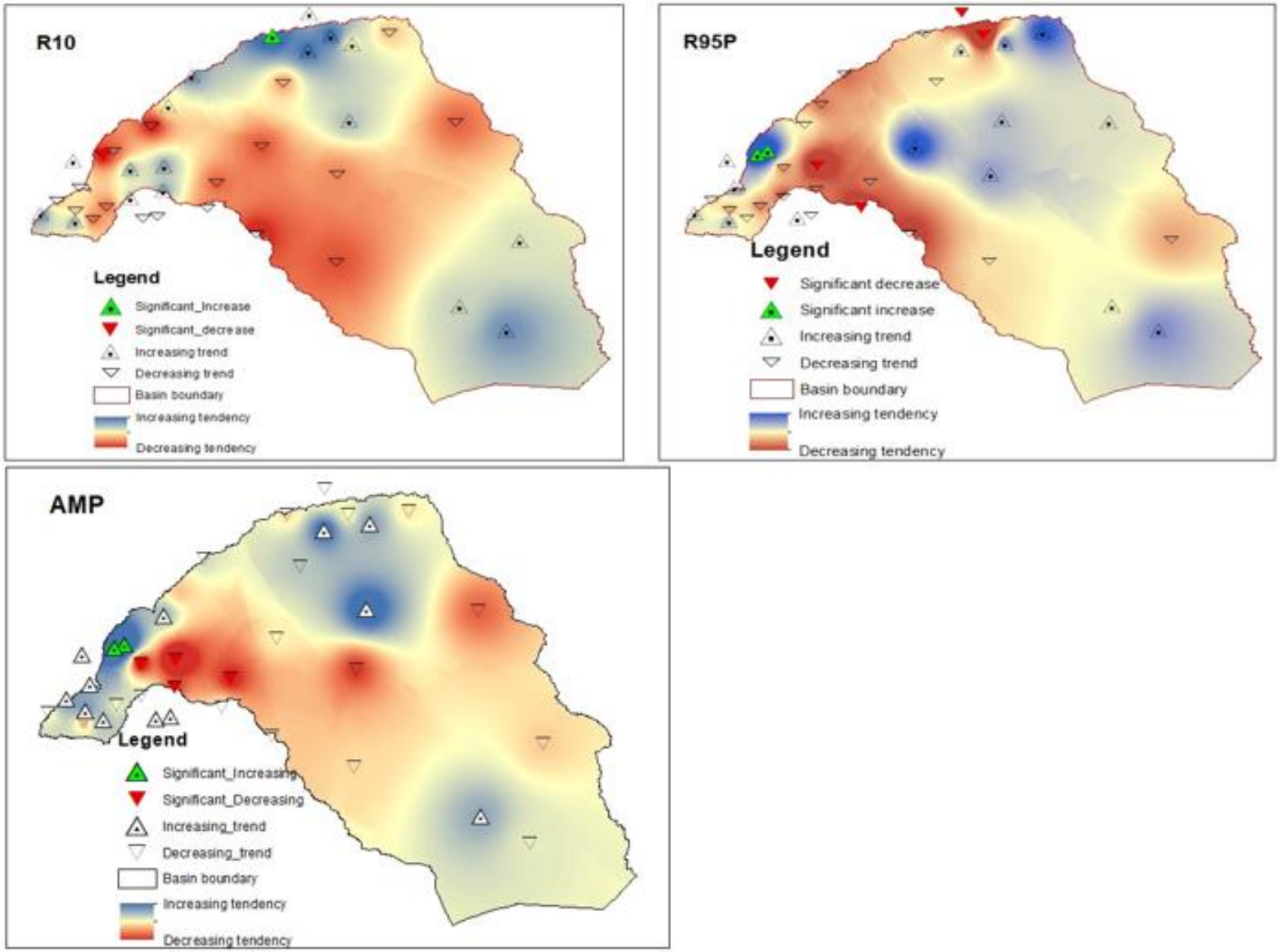

Figure 4-10. Spatial distribution of extreme precipitations trend values of Mann-Kendall test in Wabi Shebele basin

4.3.4. Periodicity and cycles in extreme precipitation

The correlogram is prepared to see periodic components of maximum annual daily rainfall from 1981 to 2019, Figure 4-11. The overall correlogram of residuals of precipitation extremes shows fluctuations over the lag-time and becomes larger or smaller depending on rainfall regime change. It is also evident from the analysis that the autocorrelation function in extreme precipitation varies above 95% probability at the north-west part of the basin (i.e., particularly in Rainfall Zone 1, around Arsi robe, Sagure, and Ticho area) since 2000. It is the sign of periodicity of precipitation extremes in the region in recent years. Similar periodicity was observed in precipitation in the lowland part of the basin (Rainfall Zone 5). The autocorrelation analysis on the northeastern highlands of the Wabi Shebele basin, particularly in Rainfall Zone 2 & 4, indicates oscillation patterns within a probability limit. When the autocorrelation function falls within 95% probability limits, the residuals of extreme precipitation appear to be random. As observed from Figure 4-11, the serial correlation in precipitation time series is not related to time in most rainfall zones, i.e., a positive residual is more likely to be followed by fewer residuals and vice versa, which is the sign of residual randomness.

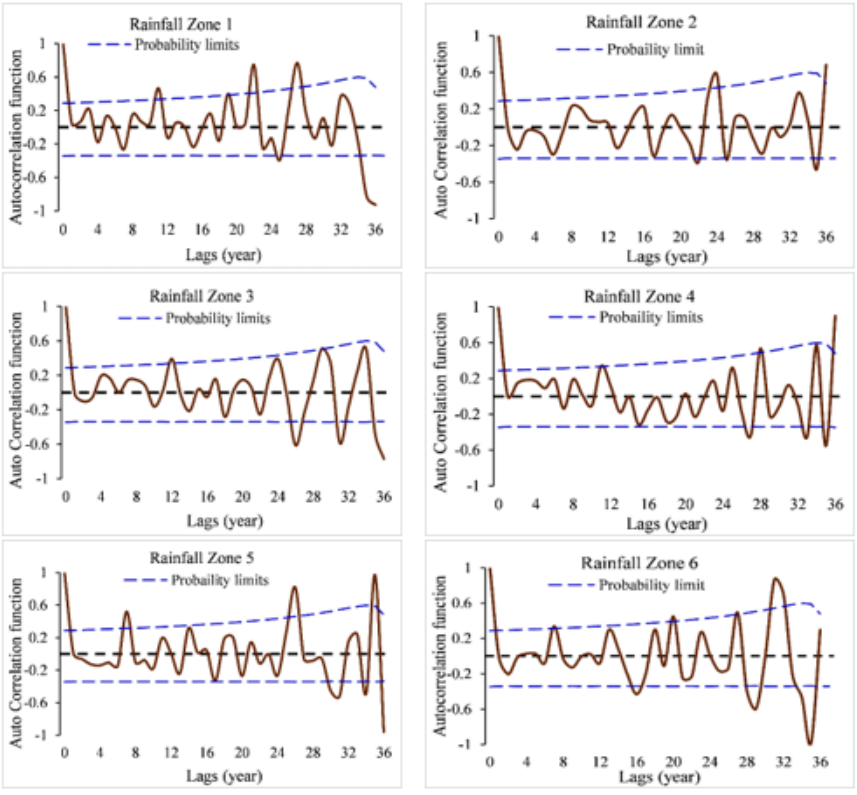

Figure 4-11 Correlogram of maximum annual daily rainfall in the Wabi Shebele River Basin from 1981 to 2019

4.4. Discussions

The results of correlogram in Rainfall Zones 1, 3, and 6 around Adaba, Robe (Arsi), Ticho, Seru, and Jara area show the probability of every two to a five-year extreme event since 2000. These suggest that the northern, western highland part of the Wabi Shebele basin has been highly vulnerable to extreme daily rainfall events in recent decades. These patterns are further proved by annual precipitation increasing trends observed in the region from ground-based measured precipitation trend analysis (Table 4-6). Ethiopian Panel on Climate Change (Shiferaw et al., 2015) reported similar results in rainfall trend analysis of the study area. The study indicates an insignificant trend of summer rainfall which ranges from +4 up to -5mm/decade in the Wabi Shebele River Basin. The frequency of precipitation extremes shows an increasing trend throughout the basin in recent decades (Figure 4-11), directly related to the flood event trends in the Wabi Shebele basin in the last two decades (Woldegebrael et al. 2019). CHIRPS reanalysis data is a quasi-global satellite product developed for managing and monitoring extreme events (e.g., droughts and floods) and trend analysis (Gebrechorkos et al. 2018). Precipitation analysis using extreme precipitation indices indicates low to moderate increasing trends in the study area's western to eastern highland and downstream lowland areas. It means decreasing trends in the middle part of the basin.

The current study results indicate rising extreme values in recent years, since 2000, particularly over northwestern to the eastern highland and lower part of the basin around Arsi Robe, Deder, Diredawa, Harar Jijiga, and Kebridehar area. These observed patterns of rising extreme precipitation events in the Wabi Shebele River Basin have implications for the design and development of climate change adaption and mitigation measures, especially in flood prevention, control, and post-disaster management (ERCS 2005; Akola et al., 2018; MoWR 2004a.). Furthermore, in the eastern upper basin around Deder, Jijiga, and Robe (Arsi), land productivity is decreasing from year to year due to erosion (MoWR 2004b). Therefore, the area needs to establish context-specific climate change adaptation and agricultural planning at the local level.

4.5. Conclusion

Using a robust reanalysis dataset, the study investigates trends and variabilities of extreme precipitation over the Wabi Shebele basin. First, the CDF and statistical measures like PBIAS, RMSE, r, and MAE analysis used to compare and contrast reanalysis data sets, i.e., CHIRPS and ENACTS, with ground-based gauged data based on the distribution of rainfall intensity and

magnitudes. Then the reanalysis data that shows related distribution and values with ground-based observed precipitation data was selected for trend and variability analysis entire the basin. The Mann Kendall trend test and Quantile Perturbation Method (QPM) investigate trends and variabilities in annual and seasonal precipitation extremes. The autocorrelation analysis also run to see cycles and periodicities of maximum 1-day yearly rainfall. Finally, the spatial trends and variability analysis of precipitation extremes perform using Inverse Distance Weighting (IDW) method integrated with GIS is applied.

Both CHIRPS and observed precipitation datasets indicate a corresponding value in probability distributions of precipitation extremes in the Wabi Shebele basin. In most sample stations, i.e., 66.7%, the CHIRPS climate dataset estimates precipitation extremes (above moderate rainfall) comparable to ground-based observed values. However, ENACTS precipitation data captures dry to light rainfall occurrence probability, more related to ground-based experimental occurrence probability. The trend analysis conducted on annual rainfall indicates a statistically no significant trend ($< |Z_{mk}|=1.96$) in most sample stations. On the other hand, the trend analysis conducted on annual precipitation using the CHIRPS dataset and ground-based observed dataset gives similar trend tendency and values in most sampled stations (50% of stations). Therefore, the CHIRPS dataset can supplement extreme precipitation based hydrological variability analysis than ENACTS in the Wabi Shebele basin.

The annual variations in extreme precipitation indicate decreasing situations from the western upper basin to lower arid zones, from Rainfall Zone 2 to 1, 3, 6, 4, and 5. The variability analysis in annual extreme precipitations indicates oscillation patterns within confidence intervals in most basin areas with a less increasing trend in the west to eastern highland part and downstream lowland of the Wabi Shebele basin (Rainfall Zones 1, 2, and 5). In all seasons, extreme precipitation QPM analysis indicates a weak to a strong increasing trend in the northern highland part of the basin (Rainfall Zone 1, 2, and 4) and a decreasing trend in the lower and middle part of the basin (Rainfall Zone 3, 5, and 6). In general, extreme precipitation indices (EPI) analysis indicates increasing trends and periodicities over the northwestern-eastern part and some pocket areas of lowlands. On the other hand, the middle part of the basin suggests a decreasing trend in all extreme indices. This result can provide relevant information on trends and occurrence cycles of extreme precipitations, which is the primary cause of extreme weather events. The study can support decision-makers in early flood risk prevention and development activities.

5. FLOOD GENERATION MECHANISMS AND POTENTIAL DRIVING FORCES IN WABI SHEBELE RIVER BASIN

Abstract

Flood is a natural process generated by the interaction of various driving factors. Flood peak flows, flood frequency at different return periods, and potential driving forces are analyzed in this study. The peak flow of six gauging stations, with a catchment area ranging from 169 - 124,108 km^2 and sufficient observed streamflow data, was selected to develop threshold (3^{rd} quartile) magnitude and frequency (POTF) that occurred over ten years of records. Sixteen Potential climatic, watershed and human driving factors of floods in the study area were identified and analyzed using GIS, Pearson's correlation, and Principal Correlation Analysis (PCA) to select the most influential factors. Eight of them (MAR, DA, BE, VS, sand, forest AGR, PD) are identified as the most significant variables in the flood formation of the basin. Moreover, mean annual rainfall (MAR), drainage area (DA), and lack of forest cover are explored as the principal driving factors for flood peak discharge in Wabi-Shebele River Basin. Finally, the study resulted in regression equations that helped plan and design different infrastructure works in the basin as ungauged catchment empirical equations to compute Q_{MPF}, Q_5, Q_{10}, Q_{50}, and Q_{100} using influential climate, watershed, and human driving factors. The results of these empirical equations are also statistically accepted with a high significance correlation ($R^2 > 0.9$).

Keywords: Flood Drivers, Climate Factors, Watershed Characteristics, Human Drivers, Principal Correlation Analysis (PCA), and Multiple Regression Model

---

[3] Wudineh, F.A., Moges, S.A. and Kidanewold, B.B. (2022) Flood Generation Mechanisms and Potential Drivers of Flood in Wabi-Shebele River Basin, Ethiopia. Natural Resources, 13, 38-51. https://doi.org/10.4236/nr.2022.131003

5.1. Introduction

Flood is a natural hazard that is most widespread around the globe both in terms of the occurrence and the resulting damages to human lives, environments and properties (Doocy et al. 2013). Based on a combination of sources, causes, and impacts, floods are categorized into river (or fluvial) floods, pluvial (or overland) floods, coastal floods, groundwater floods, or the failure of artificial water systems (Bloch et al., 2011). The major causes of floods therefore, include intensity, duration, and spatial distribution of rainfall on catchments; steep slopes, deforestation, and less

soil infiltration capacity; failure of hydrologic structures and sudden release of waters from dams; and landslides (Assefa 2018). Nied et al. (2013) also describes physical controlling factors of flood include: hydrological pre-conditions (e.g., soil saturation, snow cover), meteorological conditions (e.g., amount, intensity, and spatial and temporal distribution of precipitation), runoff generation processes as well as river routing (e.g., superposition of flood waves in the main river and its tributaries). These multi-dimensional causes of flood made it less predictable and aggravated its impacts worldwide (Erena and Worku 2018).

Floods are a complex function of different factors, for instance, a function of climatic variations over a range of time scales (Dettinger et al. 2009; Hall et al. 2014; Williams et al. 2012; Hamlet and Lettenmaier 2007; Tadesse et al. 2016; Yue et al., 2019) and land use and land cover change or natural changes in channel structure (Kundzewicz et al. 2018; Liu et al. 2017; Sutfin and Wohl 2019; Hall et al. 2014; Merz et al. 2012; Viglione et al. 2016). Atmospheric circulation also reported that triggers flood precipitation (Kundzewicz and Stoffel 2016; Niedźwiedź and Łupikasza 2016; Taye and Willems 2012; Moges et al. 2014; Seleshi and Zanke 2004). For instance, a possible correlation with climate change needs to be considered a given scenario, which may be changed in rainfall regimes (probably the most common). It is true in Ethiopia also; the climate/weather characteristics including torrential rainfall and summer thunderstorm are strongly linked with flooding in the country (NDRMC 2018; Tadesse et al. 2016). Similarly, the catchment characteristics, variability on drainage area, very short changeable topography, and low infiltration capacity of the ground surface exposes to high floods (Assefa 2018). Although, flood is a natural event, the human land use activities often involve clearing the natural vegetation (either for construction or for agriculture) and altering the characteristics of the ground cover can increase runoff substantially and the potential threat from flash floods and river floods (Broxton et al. 2014). However, the impact levels of flood drivers, the significance among the different elements of flood factors, and the relationship between peak discharges and potential drivers are still a critical knowledge gap in tropical river basins. Moreover, understanding the hydrological process of flooding in different regions and estimating the flood quintiles are important limitations in the basin since most rivers are ungauged.

Therefore, this study aimed to address the above knowledge gaps and development hindrance by identifying influential flood generations drivers and establishing relationships among drivers and peak flood indicators.

5.2. Flood Generating Mechanisms in Wabi Shebele basin

Floods that cause most damages in Wabi-Shebele River Basin are generated by a few days of heavy rainfalls with an average intensity of 10–200 mm/hr and a total sum of precipitation of a hundred millimeters (ERCS 2005). In the basin, flood events have occurred regularly as flash floods in the lowland sections, as to be seen from the state of river beds and evidence of sheet erosion (IWMI 2015). MoWR (2003) summarizes floods formation mechanisms in Wabi-Shebele River Basin under three general categories: i) high floods derived from a generalized runoff, occur after an average rainy phase of 10 days with a total rainfall depth exceeding 80 mm (e.g., northwest of the basin at upstream of Melka Wakena Hydropower); ii) floods caused by intense rainfall and on impervious soils (e.g., middle basin between Melka Wakena and Hamaro Hedad); and iii) floods in alluvial plains (e.g., lower basin between Hamero Hedad and Somalia border); short and violent floods (e.g., floods in Fafen watershed). Historical flood events in the basin are summarized in Table 5-1.

Table 5-1 Historical flood events in Wabi Shebele River Basin, 1980-2019

Date	Causalities Reported	Source
July 1993	Heavy Rain	http://floodobservatory.colorado.edu/Archives/index.html
1995	Heavy Rain	http://floodobservatory.colorado.edu/Archives/index.html
Oct. 1997	Torrential rain	http://www.fao.org/docrep/004/w7832e/w7832e00.HTM
Feb. 1998	Torrential rain	http://www.fao.org/docrep/004/w7832e/w7832e00.HTM
1999	Torrential rain	http://floodobservatory.colorado.edu/Archives/index.html
2003	Heavy Rain	ERCS: http://ifrc.org/where/country/check.asp/countryid=65
2005	Heavy Rain	ERCS: http://ifrc.org/where/country/check.asp/countryid=65
2006	Heavy Rain	http://floodobservatory.colorado.edu/Archives/index.html
May 2008	Heavy seasonal rains	http://www.irinnews.org/report/81526/ethiopia
2010	Heavy Rain	http://floodobservatory.colorado.edu/Archives/index.html
2015	Heavy Rain	http://floodobservatory.colorado.edu/Archives/index.html

5.3. Flood discharge characteristics in Wabi-Shebele River Basin

The peak flows over threshold (3rd quartile) magnitude and frequency (POTF) are analyzed. To ensure the time series independencies of extreme values, the analysis undertake with time interval approach. The successive peaks within the Time intervals between 5 to 14 days are used in this study (Keast and Ellison 2013; Moes 2015). The total 89 events consider in this POTF analysis. The mean peak flow (QMPF) was expressed as the arithmetic mean value of peak over threshold (3rd quartile) flows for the period of record.

The sampled watersheds exhibit less variability in flood-peak discharges. From Table 5-2, the standard deviation in QMPF is less than 35% of the mean except at the Jijiga station (i.e., a standard deviation related to 37% of the mean value). Studies (Enzel et al. 1993; Al-Rawas and Valeo 2010), were indicating the higher standard deviation of flood discharges indicating a potential for flash floods. Accordingly, only the northeastern part of the basin, in the Jijiga watershed, is identified as a potential flash flood area. Floods in other catchments are fall under riverine floods.

Table 5-2 Statistics of log flood-peak (QMPF) records

River/stations	Period of records	Log Q		Number of events	Mann Kendall trend test at 0.05 level
		Mean	St. dev.		
Maribo	1975-2008	0.87	0.17	18	2.45
Wabi at Dodola	1975-2015	1.21	0.15	13	2.42
Robe	1979-2006	0.48	0.34	18	0.13
Jijiga	1985-1996	0.40	0.37	14	3.71
Erer at Babile	1984-1999	0.77	0.20	16	-1.11
Wabi at Gode	1967-2002	2.44	0.20	10	2.76
	Total			89	

The Mann-Kendall test (Kendall 1975; Mann 1945), the common non-parametric trend detection, is used to detect trends in flood discharge. Most of the flood discharges indicate a significant trend ($p<0.05$) in gauging stations located in the northwestern (i.e., Wabi at Dodola and Maribo) and downstream part of the basin (i.e., Gode). However, flood discharge at Robe and Erer discharge has no significant trend, as shown in Table 5-2. Both rivers are located in a northern highland part of the basin. Flood discharges at Robe River indicate a less increasing trend while flood discharge of Erer river at Babile shows decreasing tendency. Some studies also found similar upward trends of flood events with the consequence of increases in deaths, injuries, stress-related disorders in the study area in the past six decades (Tadesse et al. 2016; Shiferaw et al. 2015; Woldegebrael et al. 2019).

5.4. Potential Flood Drivers in Wabi-Shebele River Basin

5.4.1. Climate factors

Precipitation with its different characteristics; intensity, duration, total amount, timing, or phase (whether liquid or solid), are an essential climate variable in shaping flood hazard (Shiferaw et al. 2015; Kundzewicz and Stoffel 2016; Williams and Funk 2011; Hall et al. 2014; Assefa 2018; Kundzewicz and Robson 2004). However, here due to the data scares in the basin, the relationship among climate factors and QMPF established based on annual and monthly rainfalls. The

correlation analysis is performed between rainfall in the rainy seasons, i.e., March to September (6 months), and flood discharge to see the impact of climate on flood events of the study area. The maximum water discharge in Wabi-Shebele River Basin is moderately correlated with the total annual rainfall over the watersheds (R^2=0.314 on average; Figure 5.1).

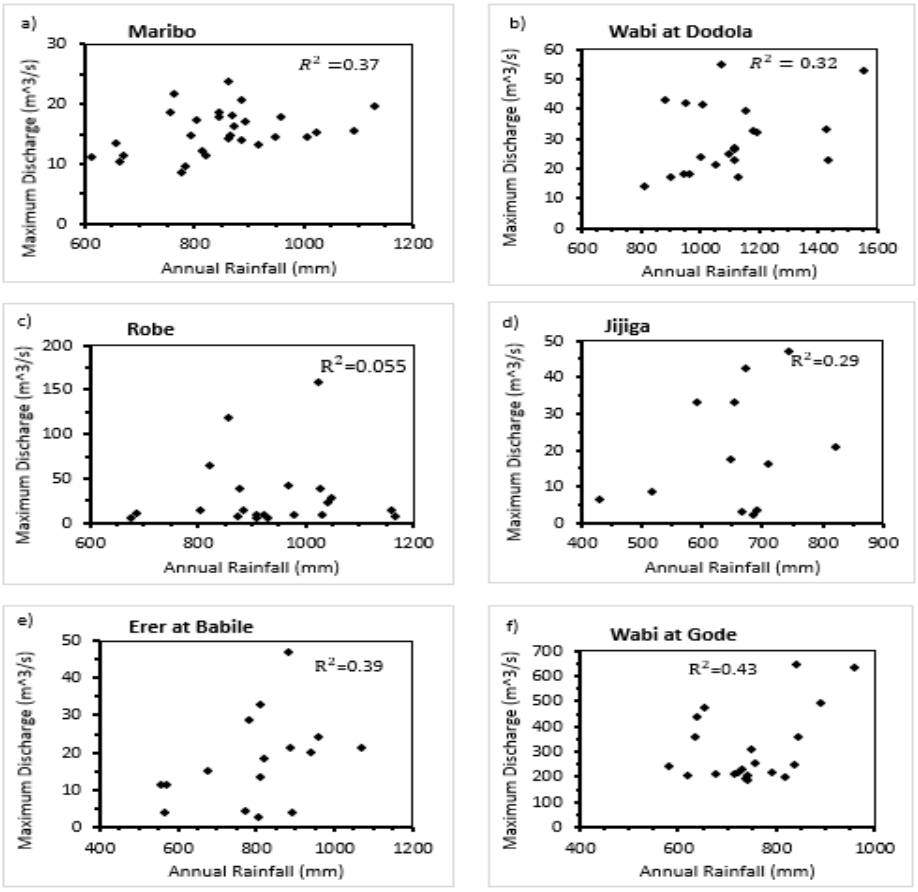

Figure 5-1 Relationship between annual rainfall (mm) and annual maximum of discharges (m^3/sec)

Although, the time lag between maximum annual precipitation and maximum annual flood is expected more than a day in Wabi-Shebele River Basin since it has the largest catchment size and complex land formation, the maximum number of consecutive wet days is positively correlated to peak daily discharges in a year, particularly on large watersheds like Wabi at Dodola Bridge and Gode stations at a correlation value of 0.49 and 0.7. It is noticed that the flooding in Wabi-Shebele basin significantly influenced with climate factors than other drivers. Moreover, the rain-bearing clouds coverage over the Wabi-Shebele River Basin is less intense than other basins like the Abay basin in Ethiopia (MoWR 2003). Therefore, flood events in the Wabi-Shebele basin are highly associated with the frequency of precipitation events.

5.4.2. Watershed factors

The multiple catchment characteristics that clearly identified as vital variables affecting flows (Al-Rawas and Valeo 2010; Stoffel et al. 2016; Patra 2010; Newson 2005) are considered as watershed factors. These variables are: Drainage area (DA; km^2), Mean basin elevation (BE; m), Basin slope (BS; %), Basin perimeter (BP; km), Basin shape factor (SF; dimensionless), Drainage density (DD; km/km^2), Valley slope (VS; m/km), and the elongation ratio (ER; dimensionless) (Appendix D). The mean peak flow (Q_{MPF}) in Wabi-Shebele River Basin is positively correlated with variables: DA, BP, VL, and SF, where maximum correlation with DA, BP, and VL with a correlation coefficient of 0.92, 0.93, and 0.96 respectively. It is also evident from Figure 5-1 above that the correlation value between flood discharge and annual rainfall increases with catchment size. Wabi watershed at Gode station has the largest catchment size showed maximum correlation value, and Robe watershed has the smallest catchment area in this study which exhibits minimum correlation value. Different studies also confirmed the impact of the size of watershed on peak flow. Al-Rawas and Valeo (2010) indicated that mean peak flow (Q_{MPF}) in arid watersheds is positively correlated with drainage size. Similarly, the study conducted by Huang (2020) showed that the drainage area affects not only the flow collection but also the time to peak flow. Moreover, the soil properties particularly the soil infiltration rate is another sensitive variable for surface runoff generation. Coarse textured soils have big well-connected spaces and allow more water to infiltrate through them quite rapidly, while fine-grained soils dominated by clay have low infiltration rates due to their smaller-sized pore spaces (Al-Rawas and Valeo 2010b). Soils containing a large amount of sand and silt have a habit of forming a crust and become more compacted that significantly reduces the infiltration rate. The mean peak flow (Q_{MPF}) in Wabi-Shebele River Basin is positively correlated with variables sand, and loam.

5.4.3. Human activities factor

The land use and population density and growth in the basin are consider as human activity drivers for flooding (MoWR 2004a; Kundzewicz and Stoffel 2016; Liu et al. 2017). The flood magnitude has high positive correlation with cultivated land and population density and strong negative correlation with forest cover.

5.4.4. Selection of Potential Flood Drivers in Wabi-Shebele

Using variables correlation matrix

The magnitude and type of correlation among the potential flood drivers from climate, watershed and human variables (i.e., MAR, DA, BS, VL, SF, DD, VS, ER, clay, sand, loam, forest, AGR, and PD) are estimated using the correlation matrix (Table 5-3) and scatter plot matrix (Figure 5.2). To identify significant predictors in watershed variables absolute value of correlation coefficient, R^2 exceeded 0.8, is selected.

MAR, the only climatic variable in the flood drivers, has a positive correlation with the variables with the watershed factors (BE, BS, SF, DD, VS, loam,) and human factors (forest, and AGR), with maximum correlation coefficients. Either positive or negative; the analysis indicates that MAR has strong relation with the flood indices (Q_{MPF}) and variables of both other factors, which push it to be one of the candidates for flood drivers in the basin. DA is correlated with BP (R^2=0.99) and VL (R^2=1.00). SF is negatively correlated with ER (R^2=-0.97), and BE is also significantly positively correlated with DD (R^2= 0.86). Both VS and BS do not exhibit any significant correlation with any watershed characteristics. Given these, five of the main variables were selected as independent watershed variables to avoid information redundancy or multi-col-linearity problems in the multiple regression analysis: DA, SF, BE, VS, and BS. The soil and human variables (Sand, Clay, loam, forest, AGR and PD) have less col-linearity, directly considered to be the member of the PCA analysis for further selection independent variables.

.

Table 5-3 Correlation matrix in between variables

Pearson's r	Q_{MPF}	DA	BE	BS	BP	VL	SF	DD	VS	ER	clay	sand	loam	MAR	forest	AGR	PD
Q_{MPF}	-																
DA	**0.999**	-															
BE	**-0.778**	-0.791	-														
BS	-0.018	-0.034	0.204	-													
BP	**0.999**	**0.999**	-0.803	-0.051	-												
VL	**1.000**	**1.000**	-0.791	-0.032	0.999	-											
SF	0.207	0.209	0.321	0.383	0.172	0.202	-										
DD	-0.594	-0.594	**0.859**	0.272	-0.624	-0.600	0.592	-									
VS	-0.560	-0.553	0.636	0.581	-0.583	-0.558	0.545	0.758	-								
ER	-0.295	-0.294	-0.223	-0.536	-0.257	-0.288	**-0.969**	-0.536	-0.517	-							
clay	-0.433	-0.413	0.257	-0.788	-0.414	-0.419	-0.173	0.314	-0.081	0.325	-						
sand	**0.613**	0.619	-0.754	0.468	0.615	0.619	-0.040	-0.537	-0.101	-0.146	-0.674	-					
loam	0.085	0.052	0.268	**0.681**	0.057	0.061	0.266	0.015	0.191	-0.319	-0.798	0.094	-				
MAR	-0.332	-0.348	**0.838**	0.412	-0.371	-0.349	0.738	**0.829**	0.624	-0.677	-0.058	-0.513	0.497	-			
forest	**-0.630**	-0.625	0.852	0.045	-0.648	-0.630	0.569	0.863	0.750	-0.408	0.390	-0.687	0.034	0.789	-		
AGR	-0.444	-0.446	0.347	**0.747**	-0.465	-0.448	0.093	0.499	0.655	-0.238	-0.257	0.259	0.135	0.250	0.154	-	
PD	-0.321	-0.317	-0.085	0.556	-0.318	-0.316	-0.361	-0.022	0.356	0.204	-0.313	0.530	-0.009	-0.297	-0.253	0.821	-

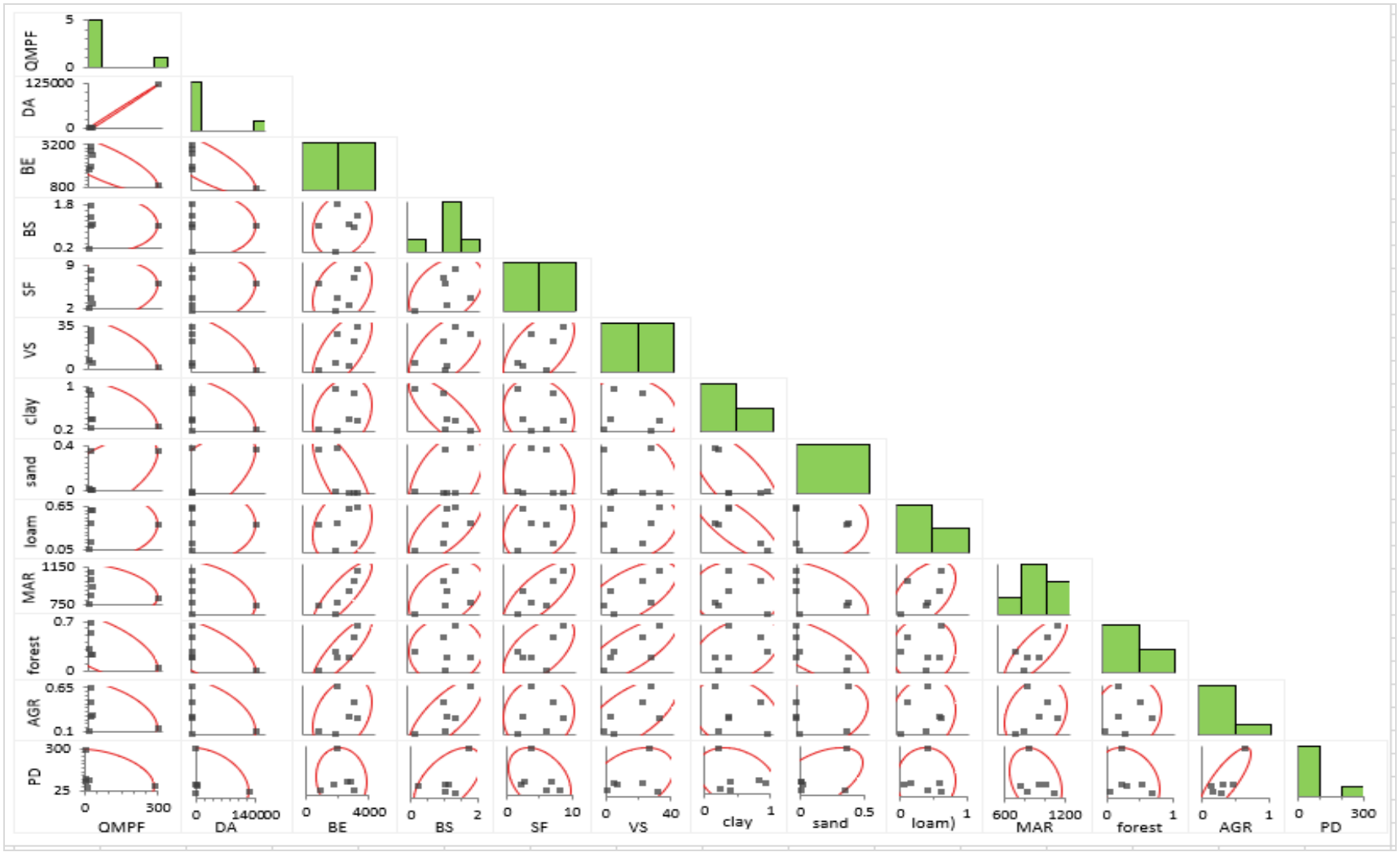

Figure 5-2 Scatter plot matrix for all pairs of variables

Note: Each plot shows the relationship between a pair of variables. The red ellipse contains the middle 75% of the neighborhoods and indicates whether the two variables are positively, negatively, or not correlated.

Principal Component Analysis (PCA)

Principal Component Analysis (PCA) is used to see multivariate relationships between potential driving factors and mean peak flow discharge (Q_{MPF}). PCA is one of the multivariate statistical techniques that can be used to deal with highly correlated variables in regression (Li et al. 2020; Rahman 2020) (see Appendix D). In this study, the PCA is further applied to select the most influential drivers among the twelve predictors (MAR, DA, SF, BE, VS, BS, Sand, Clay, loam, forest, AGR and PD) that sorted through correlation analysis to achieve uncorrelated six PCs.

The eigenvalues represent the quantity of variability in the data, and they are presented in Table 5-4. The first three PCs explain the maximum degree of variability of the data set with a proportion of 45% 26%, and 19% respectively and indicate about 90% the influence of the flood induces possible manage with the variables in these three PCs. Therefore, the variables in the three PCs are taken for the development the multiple linear regression equations among the flood drivers and flood indices.

Table 5-4 Principal correlation analysis: Eigen value analysis

Name	**PC1**	**PC2**	PC3	PC4	PC5	PC6
Eigenvalue	7.66	4.41	3.25	1.34	0.35	0.00
Proportion	0.45	0.26	0.19	0.08	0.02	0.00
Cumulative proportion	0.45	0.71	0.90	0.98	1	1

The coefficients in Table 5-5 show the linear combinations of variables that make each principal component. The absolute values near zero indicate that a variable contributes little to the PCs, whereas larger absolute values indicate variables that contribute more to the component. In the analysis, the first principal component has high negative associations with BE, VS, MAR, and forest and high positive association with DA and sand, so this component primarily measures the basin altitude difference and land cover. The second component has high positive associations with BS, SF, and loam, so this component primarily measures the slope and shape of the catchment. The third component has a high positive association with sand, AGR, and PD, so this component primarily measures the basin farmland and population density.

Table 5-5 Principal correlation analysis: Eigen vectors (coefficient) correlation matrix

Variables	PC1	PC2	PC3	PC4	PC5	PC6
Q_{MPF}	0.316	0.184	-0.153	-0.060	-0.106	-0.121
DA	**0.317**	0.179	-0.154	-0.089	-0.074	-0.392
BE	**-0.344**	0.023	-0.089	0.195	-0.210	-0.139
BS	-0.081	**0.395**	0.277	0.092	-0.096	0.300
BP	**0.323**	0.166	-0.149	-0.064	-0.074	0.211
VL	**0.318**	0.178	-0.152	-0.079	-0.076	-0.134
SF	-0.101	**0.357**	-0.299	-0.217	0.139	-0.059
DD	**-0.321**	0.114	-0.121	-0.220	**-0.346**	-0.372
VS	-0.281	0.210	0.096	-0.221	**0.550**	-0.194
ER	0.068	**-0.410**	0.212	0.241	0.075	-0.526
clay	-0.117	**-0.361**	-0.218	**-0.343**	-0.166	0.325
sand	0.234	0.222	0.292	-0.231	0.203	-0.074
loam	-0.033	**0.306**	0.056	**0.652**	0.058	0.007
MAR	-0.262	0.242	-0.222	0.170	-0.230	0.089
forest	**-0.317**	0.041	-0.223	-0.080	0.397	-0.048
AGR	-0.179	0.177	**0.382**	-0.240	-0.435	-0.228
PD	-0.044	0.042	**0.533**	-0.199	-0.011	0.172

The loading plot in Figure 5-3 visually shows the results for the first two components. From the graph, DA and sand indicate a small angle (< 90°) from the Q_{MPF} line, meaning the variables positively correlated to Q_{MPF}. The variables: forest, PD, BE, VS, and forest indicate angles related to 180°, meaning they are negatively correlated to Q_{MPF}. However, the variables: BS, SF, and loam have no significant correlation with Q_{MPF} in Wabi-Shebele River Basin.

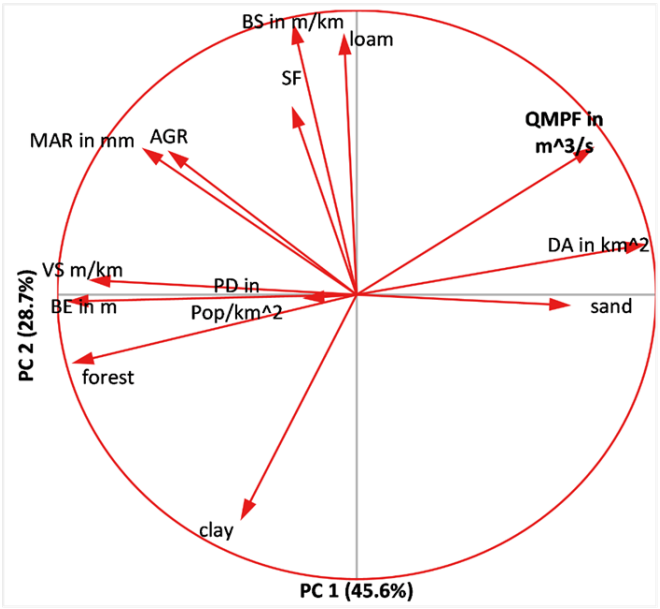

Figure 5-3 Two-dimensional correlation plot of coefficients of first two PCs (PC1 & PC2)

5.4.5. Relationship Development among drivers and flood magnitude

To select the most influential drivers, a significance level (p-value) for all drivers is examined (Table 5-6). The selection criterion is set to p <= 0.1 in regression analysis. Based on this criterion, DA, sand, MAR, and forest are found as the significant ones to be used in the development of regression equations to estimate the Q_{MPF}. Therefore, Q_{MPF} can well be estimated from Model 3 in Table 5-6, where adjusted R^2 has the highest value and p-value is significant (<0.05). The multiple regression equation is:

$$Q_{MPF} = 6.39MAR + 0.66DA + 0.35sand - 0.62forest - 19.64 \quad (5.1)$$

In the equation, climate factor (i.e., MAR), catchment size (i.e., DA), sand coefficient, and land use cover (i.e., forest) are the most influential exploratory factors on flood quantiles, Q_{MPF} in the study area. Furthermore, forest function is negatively related to Q_{MPF}, meaning watersheds with high forest coverage yields less flood discharge than watersheds with less forest coverage. Similarly, the relationship between flood frequency and principal drivers is examined.

For Q_5, Model 2 with only four variables of DA, BE, VS, and MAR was selected as the best model to represent Q_5 estimation. It is noticed from Table 5-6 that watershed characteristics are the most influential factors of flood-peak frequency at 5, and 10-year return periods, while climate factor and human influence factors are another most powerful to represent Q_{MPF} and flood-peak frequency at 20, 50, and 100-year return periods. The regression equations that describe the relationship between influential driving factors and different return periods flood-peak flows are:

$$Q_5 = 1.39MAR + 1.43DA + 2.98BE + 0.51VS - 17.67 \quad (5.2)$$

$$Q_{10} = 1.49DA + 2.44BE + 0.72VS - 0.59sand + 11.81 \quad (5.3)$$

$$Q_{20} = 3.63MAR + 0.76DA + 0.09AGR - 11.59 \quad (5.4)$$

$$Q_{50} = 8.05MAR - 4.70BE - 6.59 \quad (5.5)$$

$$Q_{100} = 8.23MAR - 4.59BE - 7.42 \quad (5.6)$$

Table 5-7 summarizes the evaluation statistics from the regression model to MAE, NSE, RMSE, and R^2 based on observed and predicted flood values for all the six flood quantiles. A value close to zero is preferable for MAE as zero indicates no error in prediction. It is seen that all the MAE values for all quantiles lie between 1 and 44. The smallest value of MAE is found in the case of Q_{MPF} and Q_{20} estimations. It is noted that except for Q_5 and Q_{100}, most flood quantiles estimations are evaluated as good values.

Figure 5.4 shows plots of predicted vs observed flood quantiles. These plots generally present a good agreement between the predicted and observed flood quantiles. For Q_5 there are a few cases of under estimation when the observed flows are in between 5.08 m3/s to 387.67 m^3/s, while predicted values ranges from 2.04 to 352 m^3/s.

Table 5-6 Selection of Regression model

Q	Model	R^2	Adj. R^2	ΔAdj.R^2	p-value	Variables Used
Q_{MPF}	1	0.999	0.996		0.040	DA, BE, MAR, forest
	2	0.999	0.996	0.001	0.040	DA, MAR, AGR, PD
	3	**0.999**	**0.996**	**0.003**	**0.020**	**DA, sand, MAR, forest**
	4	0.995	0.989	-0.007	0.006	DA, MAR, forest
Q_5	1	0.999	0.999		0.010	DA, BE, VS, sand
	2	**0.999**	**0.999**	**0.000**	**0.010**	**DA, BE, VS, MAR**
	3	0.999	0.995	-0.004	0.040	DA, BE, VS, AGR
	4	0.994	0.984	-0.009	0.009	DA, MAR, forest
Q_{10}	**1**	**0.999**	**0.999**		**0.004**	**DA, BE, VS, sand**
	2	0.998	0.991	-0.008	0.060	DA, BE, MAR, AGR
	3	0.997	0.994	0.003	0.003	DA, MAR, AGR
	4	0.996	0.993	-0.001	0.000	DA, MAR
Q_{20}	1	0.998	0.991		0.060	DA, BE, VS, sand
	2	0.999	0.995	0.004	0.040	DA, BE, VS, MAR
	3	0.998	0.994	-0.001	0.050	DA, BE, MAR, AGR
	4	**0.998**	**0.996**	**0.002**	**0.001**	**DA, MAR, AGR**
Q_{50}	1	0.986	0.932		0.174	DA, BE, VS, MAR
	2	0.982	0.955	-0.023	0.099	BE, sand, MAR
	3	0.935	0.838	-0.006	0.090	BE, MAR, forest
	4	**0.899**	**0.833**	**0.008**	**0.030**	**BE, MAR**
Q_{100}	1	0.964	0.821		0.279	DA, BE, VS, sand
	2	0.976	0.881	0.060	0.228	DA, BE, VS, MAR
	3	0.912	0.781	-0.100	0.128	BE, MAR, AGR
	4	**0.907**	**0.845**	**0.024**	**0.020**	**DA, MAR**

Table 5-7 Statistical evaluation for flood quantiles estimations

Quantiles	MAE	NSE	RMSE	R^2
Q_{MPF}	1.041	0.999	4.338	1.000
Q_5	10.102	0.987	248.416	0.999
Q_{10}	3.706	0.998	71.770	1.000
Q_{20}	1.119	0.999	2.622	1.000
Q_{50}	6.669	0.999	65.282	0.999
Q_{100}	43.602	0.953	7051.660	0.998

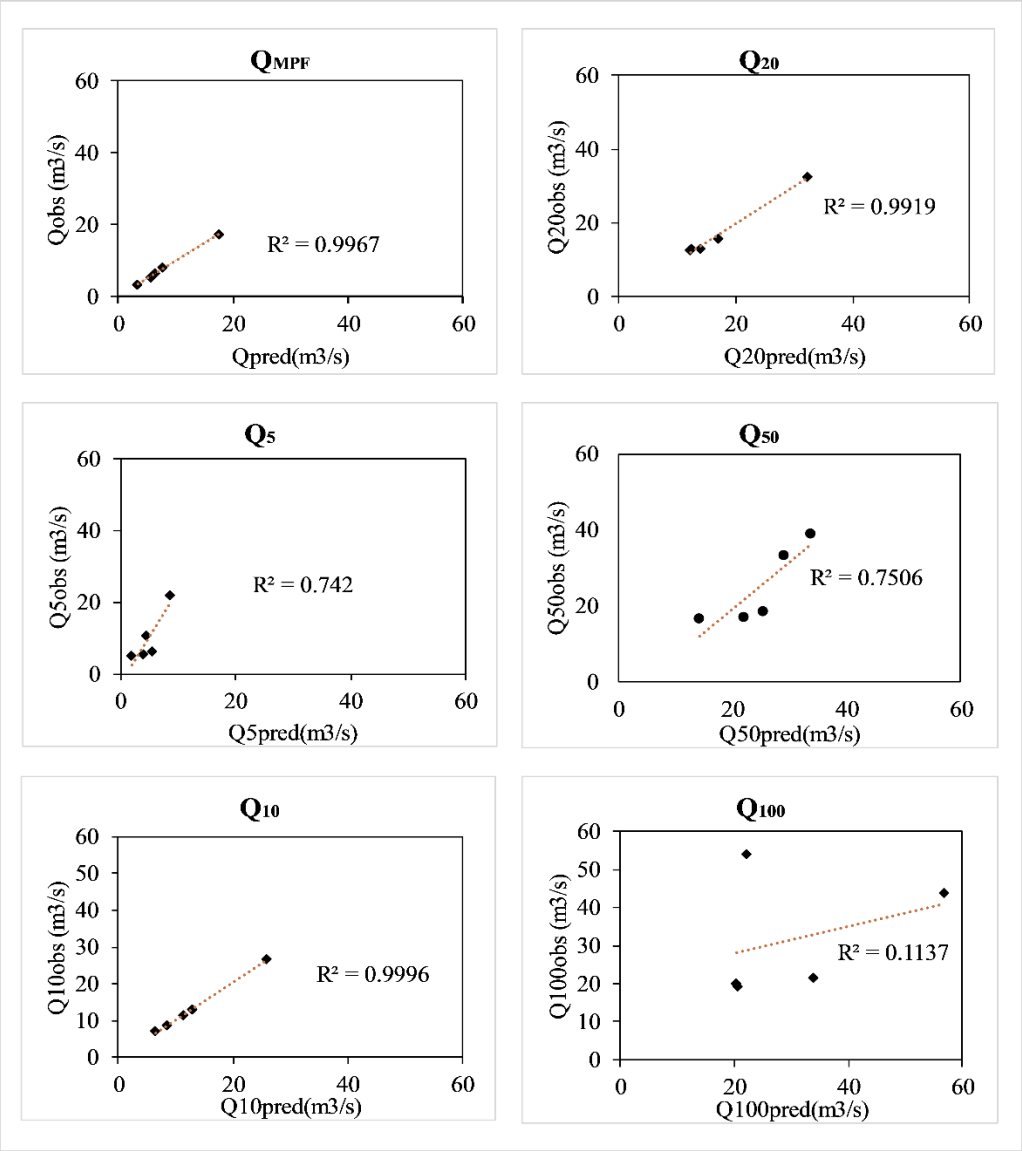

Figure 5-4 Comparison of observed and predicted flood quantiles of all quantiles and sample watersheds

5.5. Conclusion

The major flood drivers and flood generation mechanisms in Wabi Shebele River Basin assessed using observed mean peak streamflow observed at six hydrological gauging stations in the basin. The six gauging stations have varied catchment areas with a range of between 169 to 124,108 km^2). The threshold (3rd quartile) magnitude and frequency (POTF) that occurs over ten years of record are used to build the flood dataset. Sixteen climatic, watershed, and human factors were extracted and computed using GIS, Pearson's correlation analysis, Principal Correlation Analysis (PCA). Eight of them (Mean Annual Rainfall, Drainage Area, Basin Elevation, Valley Slope, sand,

forest, Agricultural land, Population Density) are identified as the most influential variables in flood formation of the basin. Moreover, mean annual rainfall (MAR), drainage area (DA), and lack of forest cover are explored as the principal driving factors for flood peak discharge in Wabi-Shebele River Basin. On the other hand, catchment shape factor (SF), a fraction of loam and clay soil coverages are separated as less influential factors, and the possibility of substituting them by the most influential factors during quantification modeling is ascertained. Moreover, larger watersheds with higher elevation and agricultural/ farmlands lead to larger flood-peak flow in all investigated return periods. Finally, regression equations are developed to estimate flood quantiles using identified driving factors that are used for different planning and designing of infrastructures in the basin.

6. FLOOD CHANGE DETECTION AND ATTRIBUTION USING SIMULATION APPROACH IN DATA-SCARCE WATERSHEDS

Abstract

Flood events vary with sub-regions, sites, and times and show complex characteristics. This study investigated temporal variabilities in flood discharges and relationships with principal driving factors in the Wabi Shebele River Basin based on simulated data using SWAT model. SWAT is calibrated using hydrometeorological data from 1990 to 1995 to obtain the optimum parameters and validated at a period between 1995–2000. The preliminary analysis using exploratory data analysis (EDA) on annual and seasonal maximum discharge reveals that there are cycles of extreme discharges at five- and ten-year intervals respectively throughout the basin. The statistical verification using Mann-Kendall test and Quantile perturbation method indicates a significant trend in flood magnitude and frequency entire the basin in early 21st century. For longest period (1980-2010) annual maximum streamflow shows significant positive trend (p-value<0.05) in middle catchments and negative trend (p-value<0.05) in eastern catchments. The years: 1986-1995, 2006-2010 are the years in which positive significant anomalies occurred in all seasons, while the years: 1980-1985, 1996-2005 are the occurrence years of significant negative anomalies. Rainfall from climate drivers; drainage area, elevation, slope and fraction of sand from environmental background drivers; fraction of forest and population density from external factors were identified as the powerful driving factors of flood variabilities in the Wabi Shebele River Basin.

Keywords: Flood events, Watersheds, Wabi Shebele River, Hydrological model, Driving factors of flood

---

[4] Wudineh, F.A., Moges, S.A. and Kidanewold, B.B. (2021) Flood Change Detection and Attribution Using Simulation Approach in Data-Scarce Watersheds: A Case of Wabi Shebele River Basin, Ethiopia. Journal of Water Resource and Protection, 13, 362-393. https://doi.org/10.4236/jwarp.2021.135023

6.1. Introduction

Flood is excessive water availability, which is caused by above normal streamflow, leading to inundation of areas which are normally not covered by water. In flood generation, antecedent conditions which refers to the saturation of natural storage in the catchment are critical factors

(Kay et al. 2011; Kundzewicz and Stoffel 2016). It is the consequence of earlier precipitation or snowmelt in the catchment. If the saturation is at maximum capacity, consecutive moderate amount of rain can also generate large floods (Bissolli et al. 2011). Further, low permeability of surface due to dry and crusted soil after a prolonged period without rain can also rapidly convert heavy rainfall to runoff which usually results in a flash flood (Li et al. 2020). Intense and/or long-lasting rainfall is the main cause of large flood events in tropical regions (Williams and Funk 2011; Shiferaw et al. 2015). In these regions, more water vapor and heat in the atmosphere brings storms and consequently floods will be become more intense (Hall et al. 2014).

Watersheds, by nature, are dynamic systems; therefore, they are in a constant state of change. Although many changes are not detectable over short periods, major storms and physical features of the watersheds can cause extreme changes in hydrology. Thus, natural changes to the land cover (e.g., afforestation) and the channel introduce non-stationarities into measured flood records (McCuen 2003). Studying the changes in river discharge and precipitation patterns has a critical importance as a climatic indicator for environmental risk problems such as droughts and floods. The study of trends in flood time series requires decision-makers to better understand the ongoing changes in hydrologic extremes to make preparations for the possibility of changing conditions. However, the lack of adequate observational data at the spatial and temporal resolution in several areas made changes and variabilities in floods are largely unknown (Kundzewicz and Stoffel 2016). Long-time series of good-quality data are not available in many areas, especially in developing countries. Thus, an alternative approach (hydrologic model) to generate discharges from weather and catchment variables is required in such areas.

In this study, SWAT model is used to generate stream flow from available meteorological and physiographic data in Wabi Shebele basin. This chapter aims to study multi-temporal trends in flood discharges through a flood simulation approach in watersheds, in conditions of data scarcity and correlations with potential driving forces. In Wabi Shebele River Basin obtaining historical river records are hardly difficult. Some gauging stations that exist in the upper part of the basin have inconsistent data which needs extra data extension mechanisms.

6.2. Materials

Wabi Shebele River Basin: is divided into four geographical areas based on morphometric characteristics and rainfall regimes (MoWR 2003; BCEOM 1973): upper catchments which characterized by a mountainous area with abrupt valleys; middle catchments which is wider

highland and rainy area; eastern catchments which characterized semi-arid areas and lower catchments which covers arid lowland area of the basin. The watershed characteristics analysis using Arc GIS indicate that flood characteristics of Wabi Shebele basin is related to basin and relief morphometric characteristics. The mean peak flow (Q_{MPF}) in Wabi Shebele basin has large positive association with linear morphometric parameters (like valley length, mean stream length) and with basin morphometric parameter (like drainage size, shape factor) and negative associations with relief morphometric characteristics (like basin elevation and valley slope). The basin has three climatological rainy seasons: spring (February- May), summer (June- September) and winter (October-January) (MoWR 2003; Ruiz-Villanueva et al. 2016; IWMI 2015). While having the largest area coverage, the basin's annual runoff is estimated to 3.4 BCM.

Data: Both ground-based station observations and gridded analysis data are utilized in this study. In Hydrologic model, digital elevation model (DEM), physio-graphic data of pedology, land use and occupation and classes of slopes and meteorological data were used to generate streamflow. Digital elevation model (DEM) with a spatial resolution of 90 meters was obtained from SRTM GDEM official website.

The soil information was acquired from FAO Digital Soil Map of the World (DSMW) at a scale of 1: 500000 downloaded from FAO Soil Map and Data-base website (htt://www.fao.org/soils-portal/soil-survey/soil-maps-and database/FAO-UNESCO-soil-map-of the world/en). The soil data with the resolution of 1km mainly include soil texture, soil depth, and soil drainage attributes needed for the SWAT model will be derived from Harmonized World Soil Databasev1.2, a database that combines existing regional and national soil information in combination with information provided by FAO-UNESCO soil map. Land-use and land cover data were obtained from Ministry of Water, Irrigation and Energy.

From the data described above, the hydrologic response units (HRU) were established. After HRU definition, the data from climatic stations located in the study basin were inserted on the SWAT model. These data refer to rain fall (mm), maximum and minimum air temperatures (°C), relative humidity (%), solar radiation ($MJ/m^2/day$) and wind speed (m/s). These data were obtained from the National Meteorology Agency (NMA). The data sets provide daily observations for stations exist in the basin. Table 6-1 shows fourteen weather stations selected in the study, which has good quality and spatial distribution in the basin with a minimum record length of 10 years in between

1980 to 2010. Five stations from upper catchments; six stations from middle catchments; two stations from Eastern catchments and one station from lower catchments (Table 6-1).

Table 6-2 shows measured discharge data used for model calibration and validation, collected from hydrology department of the Ministry of Water, Irrigation and Energy, Ethiopia (MoWIE). According to the Ministry, the measurements of river levels follow the guidelines of the World Metro-logical Organization (WMO) (MoWR 2003).

Table 6-1. Meteorological data stations used in SWAT model

S.No	Station Name	Controller	Period	Coordinates*		Altitude (m)	Station aspect	Missing data (%)
				Latitude	Longitude			
1	Adaba	NMA	1980-2013	543691	773113	2420	NW	21.12
2	Dodola	"	1988-2006	519746	772054	2580	NW	14.72
3	Kofele	"	2000-2018	479397	781976	2620	NW	6.40
4	Merero	"	1980-2013	538334	822503	2940	NW	27.80
5	Hawassa	"	1980-2013	443083	781757	1750	NW	0.60
6	Robe (Arsi)	"	1980-2013	568694	868627	2400	N	1.70
7	Sinana	"	1980-2013	624339	777736	2400	M	27.50
8	Deder	"	1980-2013	767132	1032669	2350	M	22.40
9	Jara	"	1986-2013	661100	804664	1960	M	3.92
10	Haromaya	"	1980-2011	832842	1040832	2125	N	14.12
11	Gursum	"	1984-2013	873588	1034746	1900	M	6.82
12	Jijiga	"	1980-2011	915127	1033159	1775	E	2.87
13	Gode	"	1980-2011	1006927	654440	295	S	8.62
14	Degehabour	"	1980-2013	1001635	911616	1070	E	5.64

*UTM, Zone 37N, NW=North western, N=North, M=Middle, E=East, S=South

Table 6-2. Discharge data used for calibration and validation of SWAT model

S. No	Station Name	Controller	Coordinates*		Altitude (m)	Catchment area (km^2)
			Latitude	Longitude		
1	Wabi @ Dodola	MoWIE	775521	503682	2618	1040
2	Maribo @ Adaba	"	773692	536818	3073	192
3	Wabi @ Legahida	"	881015	709436	2066	19793
4	Erer Nr. Babile	"	1021721	197816	1960	494
5	Wabi @ Gode	"	654138	341331	916	124108
6	Fafen @ Jijiga	"	1034208	258365	1813	731

* UTM, Zone 37N.

6.3. Methods

The methods implemented in this paper comprises a semi distributed macroscale hydrological modeling for the simulation of daily runoff, implementation of Exploratory data analysis (EDA)

to explore simulated data, data distributions and examine clusters in the data or relationships between variables and/or sample locations and a nonparametric trend test to detect trends in annual and seasonal maximum runoff.

6.3.1. Hydrological Model

A hydrological model offers a means of a mathematical simulation of the complex hydrological cycle to understand and approximate the hydrological response of river basins (Perrin et al., 2001; Adnan 2010). Hydrologic models are used for runoff estimation under different conditions. The runoff system is initiated by precipitation and takes place in different processes on a watershed (USACE 2000). A review of hydrological models is described briefly in Devia et al. (2015).

Soil and Water Assessment Tool (SWAT) is a continuous time, spatially distributed model designed to simulate water, sediment, nutrient and pesticide transport at a catchment scale on a daily time step. In this study, the model was used to generate flows. The model is driven by mereological data like precipitation, temperature, relative humidity, solar radiation and wind speed and physiographic data of pedology, land use and occupation, and classes of slopes.

It uses hydrologic response units (HRUs) that consist of specific land use, soil and slope characteristics. The HRUs are used to describe the spatial heterogeneity in terms of land cover, soil type and slope class within a watershed (Neitsch et al. 2005). The model estimates relevant hydrologic components such as evapotranspiration, surface runoff and peak rate of runoff, groundwater flow and sediment yield for each HRUs unit.

The water in each HRU in SWAT is stored in four storage volumes: snow, soil profile (0–2 m), shallow aquifer (typically 2–20 m), and deep aquifer. Surface runoff from daily rainfall is estimated using a modified SCS curve number method, which estimates the amount of runoff based on local land use, soil type, and antecedent moisture condition. Peak runoff predictions are based on a modification of the Rational Formula (Chow et at., 2013). The watershed concentration time is estimated using Manning's formula, considering both overland and channel flow. The SCS curve number is described by Equation (6.1).

$$Q_{surf} = \frac{(P_i - I_a)^2}{P_i - I_a + S} = \frac{(P_i - 0.2S)^2}{P_i + 0.8S} \quad (6.1)$$

In which, Qsurf is the accumulated runoff or rainfall excess (mm/day), Pi is the rainfall depth for the day (mm), Ia is the initial abstraction lost from canopy interception, surface storage, and

infiltration prior to runoff (mm H_2O; commonly approximated as 0.2 S), S is the retention parameter (mm). The retention parameter is defined by Equation (6.2).

$$S = 25.4\left(\frac{1000}{CN} - 1\right) \quad (6.2)$$

The SCS curve number is a function of the soil's permeability, land used and antecedent soil water conditions. Specifically, the CN values are based on the hydrologic soil group of the area, land use, management, and initial hydrologic condition; with the hydrologic soil group and land use being the most important variables.

For climate, SWAT uses the data from the station nearest to the centroid of each sub basin. Calculated streamflow, sediment yield, and nutrient loading obtained for each sub basin are then routed through the river system. Channel routing is simulated using the variable storage or Muskingum method. The soil percolation component of SWAT uses a water storage capacity technique to predict streamflow through each soil layer in the root zone. Downward flow occurs when field capacity of a soil layer is exceeded and the layer below is not saturated. Percolation from the bottom of the soil profile recharges the shallow aquifer. If the soil temperature in a particular layer reaches less than or equal 0^oC, no percolation is allowed from that layer. Groundwater flow contribution to total streamflow is simulated by routing a shallow aquifer storage component to the stream (Moriasi et al. 2007; Abbaspour et al. 2007). The model computes evaporation from soils and plants separately. Potential evapotranspiration can be modelled with the Penman–Monteith (Monteith 1965), Priestley– Taylor (Priestley 1972), or Hargreaves methods (Hargreaves and Samani 1985), depending on data availability. In this study, the Penman-Monteith method was used to determine potential evapotranspiration.

6.3.2. Defining an extreme event

Among the discharge-based flood indicators, annual maximum series (AMS) and peak over threshold (POT) are used to analysis flood time series. In this chapter six extreme hydrologic indices: Annual maximum discharge (AMAX), Peak over threshold (3^{rd} quartile) frequency (POTF), Peak over threshold (3^{rd} quartile) magnitude, seasonal maximum discharge for winter (SMW), Seasonal maximum discharge for spring (SMSp) and Seasonal maximum discharge for summer (SMSu) are used to define extreme high discharges. In extreme value analysis ensuring independence of samples is initial task. In this study the time interval approach is used to ensure the independence of flow discharges. Time intervals between 5 to 14 days between successive

peaks; 5 days for catchments <10000 km^2 and 14 days for catchments ≥10000, is used in this study. This approach is reported, a strong flood-frequency estimations approach e.g., (Keast and Ellison 2013; Malamud and Turcotte 2006).

6.3.3. Flood Change detection and Attribution

Flood Change Detection

Two distribution-free (nonparametric, e.g., rank-based) tests and exploratory data analysis (EDA) are used to detect changes in flood discharge. Exploratory data analysis (EDA) is used as preliminary analysis to explore initial hypotheses on changes in data time series to be confirmed by statistical analysis, nonparametric Mann-Kendall trend test to detect trends in flood discharges, and Quantile perturbation method (QPM) approach to see temporal variabilities in extreme discharges. In practice there is a continuum between "trend" and "change".

Exploratory data analysis (EDA): involves mainly plotting graphs, and allowed to explore some features in data and assess the first hypotheses to be confirmed by the statistical analysis. In addition, the linear regression gradient plot in the EDA allowed testing of potential trends data time series.

Mann-Kendall (MK) test: The MK test statistic, S is defined as (Kendall 1975; Mann 1945). The method's statistical equations are described in section 3.2 in detail. The Kendall rank coefficient is often used as a test statistic to establish whether two variables may be regarded as statistically dependent. Under the null-hypothesis of independence of Xi and Xj, the sampling distribution of 'tau' has an expected value of zero. The value of 'tau' ranges from -1(100% negative association, or perfect inversion) to +1(100% positive association or perfect agreement). A value of zero indicates the absence of association. P-value is used to verify if the trend quite to be caused by random sampling. The detail of the statistics is described under section 3.2.

Quantile Perturbation method (QPM): is used in this chapter to study trends and multi time period oscillation patterns in extreme flood discharges. The method has two concepts: (i), the frequency aspect which focuses on how often an extreme event (quantile) may occur and, (ii), the perturbation aspect which determines the changes in the extremes for a particular return period.

Flood Change Attribution

Studying trend and variability in hydroclimatic time series alone has no value unless the cause or driving factors of changes are followed. Merz et al (2012) reported in their research that the main

goal of trend and variability studies in hydroclimatic time series is to test hypothesis about the influence of driving forces of floods. The detected trends were explained by the correlation with changes in another variable (meteorological variables, maximum daily precipitation, large scale climate variabilities and external drivers). In the large-scale climate variability, four different climate indices were observed: Pacific Decadal Oscillation (PDO), Southern Oscillation Index (SOI), Indian ocean Dipole (IOD) and Atlantic Multidecadal Oscillation (AMO). The criterion for selection was the strength of the links between these indices and the flood variables found in east Africa, assessed in different literatures e.g.,(Moges et al. 2014; Taye and Willems 2012). In addition, Moges et al (2014) showed that the rainfall of the Ethiopian highlands has high correlations with Pacific Ocean Indices, i.e., PDO and SOI. Furthermore, an influence of the Indian Ocean index is reported as positively correlated to summer (June-September) rainfall over the northwest-east and central Ethiopian highlands (Segele and Lamb 2005; Seleshi and Zanke 2004).

Table 6-3. Potential driving factors flood changes analyzed in this study

Attributes	Abbreviation	Explanation	Sources
Meteorological index	MDP	Maximum daily precipitation	National Meteorological Agency (NMA)
Large scale climate indices	PDO	Pacific Decadal Oscillation	Joint Institute for the Study of the Atmosphere and Ocean (JISAO) (http://jisao.washington.edu/pdo/PDO.latest).
	SOI	Southern Oscillation Index	Climate Research Unit (CRU) database (http ://www.cru.uea.ac.uk/cru/data/soi/).
	IOD	Indian Ocean Dipole	http://iridl.ldeo.columbia.edu/SOURCES/.NOAA/.NCDC/.ERSST/.version4/.IOD/.C1981-2015/.iod/datafiles.html
	AMO	Atlantic Multidecadal Oscillation	From NOAA PSL1, http://ww.psl.noaa.gov/data/timeseries/AMO
Environmental background conditions	Elev.	Elevation	90m x 90m Digital Elevation Model (DEM) obtained from SRTM GDEM official website
	WS	Watershed slope	90m x 90m Digital Elevation Model (DEM) obtained from SRTM GDEM official website
	Soil	Soil	Ministry of Water, Irrigation and Energy (MoWIE)
External drivers	PD	Population density	Ministry of Water, Irrigation and Energy (MoWIE)
	Agricultural practices		Ministry of Water, Irrigation and Energy (MoWIE)
	Deforestation/ Afforestation		Ministry of Water, Irrigation and Energy (MoWIE)

For these large-scale climate indices, I used correlation with the flood parameters. In addition, changes in catchment and environmental background condition factors, deforestation and reforestation and alteration in agricultural management practices are analyzed. Table 6-3 summarizes all the factors analyzed in this study.

6.3.4. Flood Frequency Analysis

Parallel to changes in magnitudes, changes in the frequency of extreme events, which can be described by the occurrence rate has significant role in flood events. Changes in the occurrence rate reflect the clustering properties of flood events, caused by natural variability, regime shifts in the atmosphere (Camdevyren et al. 2005; Kerr 1992) or land use changes. For each sample watersheds, peak over threshold (3^{rd} quartile) time series was extracted to see trends in magnitude and number of occurrences in annual and seasonal time level.

6.4. Results and Discussion

6.4.1. Calibration and Validation of the Hydrological Model

For model calibration and validation, the observed daily and monthly streamflow data were used from 1988 to 2000 with three years warming period. To evaluate the model performance, three parameters have been used, namely R^2 and NSE and P-bias. NSE is a normalized statistic, ranges from $-\infty$ to 1, used to indicate the relative value of residual variance compared to the variance of the observed data and values close to one shows a perfect match of the modeled with the observed data (Nash and Sutcliffe 1970). R^2 is the proportion of the total variance in the observed data that can be explained by the model. The detail of these evaluation statics is presented under section 4.2.2, Table 4-3. Table 6-4 shows statistical evaluation of model performance.

During model initialization, minor land use/land cover, slope and soil types were ignored by setting a threshold of 10% in defining HRUs, to avoid unnecessary large number of HRUs in the analysis. Therefore, a total of 311 HRUs and 11 main sub basins are analyzed in this study. Based on the model, the physiographic characteristics of watersheds is presented in Table 6-5.

Table 6-4. Evaluation of model performance

Stations	Area (km^2)	Location		Ave. Annual Discharges (Mm^3)	Calibration			Validation		
		Lat	Long		R^2	NSE	Pbias (%)	R^2	NSE	Pbias (%)
Wabi at Dodola	1,040	7.01	39.02	230.9	0.7	0.7	-3.0	0.7	0.7	-2
Maribo	192	7.00	39.20	100.2	0.5	0.6	-19	0.4	0.5	-29
Robe	169	7.51	39.38	48.5	0.5	0.4	-30	0.4	0.4	-21
Wabi at L/Hida	19,793	7.58	40.54	1848.5	0.6	0.6	-0.9	0.6	0.7	1
Erer	494	9.14	42.15	87.5	0.4	0.4	-0.2	0.1	-0.4	-54
Jijiga	731	9.21	42.48	35.4	0.2	0.5	5.3	0.1	0.2	-59
Wabi at Gode	124,108	5.56	43.33	4523.2	0.4	0.2	-29	0.2	0.1	-38

Table 6-5. Physiographic characteristics of the eleven studied sub basins

S. No	Station (River)	Highest elevation (m.a.s.l)	Lowest elevation (m.a.s.l)	Relief (m)	Mean elevation (m.a.s.l)	Catchment area (Km^2)	Catchment Aspect	Mean catch. slope	Time Period analyzed
1	Wabi @ Dodola	3119	2473	646	2618	1,040	NW	0.11	1981-2010
2	Maribo @ Adaba	3743	2350	1393	3073	192	NW	0.14	1981-2010
3	Robe @ Robe	4055	2404	1651	2836	169	N	0.10	1981-2010
4	Wabi@ Legehidha	4153	765	3388	2066	19,793	M	0.12	1981-2010
5	Erer @ Babile	3004	1308	1696	1960	469	NE	0.18	1981-2010
6	Erer @ Hamaro	3388	503	2885	1357	14,760	M	0.14	1981-2010
7	Gololcha@Junction	2686	460	2226	1369	7,139	M	0.03	1981-2010
8	Fafem @ Jijiga	2482	1634	848	1813	910	NE	0.02	1981-2010
9	Fafem@ Kebridehar	3013	513	2500	1153	24,956	SE	0.03	1981-2010
10	Wabi @ Gode	3374	258	3116	916	124,108	S	0.105	1981-2010
11	Wabi @ Burkur	977	215	762	428	146,804	S	0.10	1981-2010

Relief is calculated as the difference between the highest and the lowest elevation, Aspect is the averaged aspect of the basin (m.a.s.l=meters above sea level; N=North; NE=North-East; S=South; SW South-West).

6.4.2. Annual Maximum Discharge

The presence of seasonal cycles and clusters in annual maximum discharges (AMAX) are examined using exploratory data analysis (EDA) (Figure 6-1). The magnitude of annual maximum discharge oscillates at 5–10-year intervals in most of sample stations. Annual maximum discharges indicate less than mean annual maximum values in 1990s for the middle and eastern catchments of Wabi Shebele basin. However, annual maximum discharge in 2000s is observed above mean maximum annual discharge in all gauging stations entire the basin.

The MK test applied at each site for the period 1981-2010 showed less decreasing trend in upper and lower catchments. For the longest period, 55% of the stations indicate weak to significant decreasing trends in annual maximum discharge. However, the watersheds in middle basin indicate a majority of significant increasing trend annual maximum discharge, $p<0.05$. Too see multi-temporal changes in annual maximum discharge Mann-Kendall trend tests are analyzed at 5, 10,15,25 and 30 years intervals.

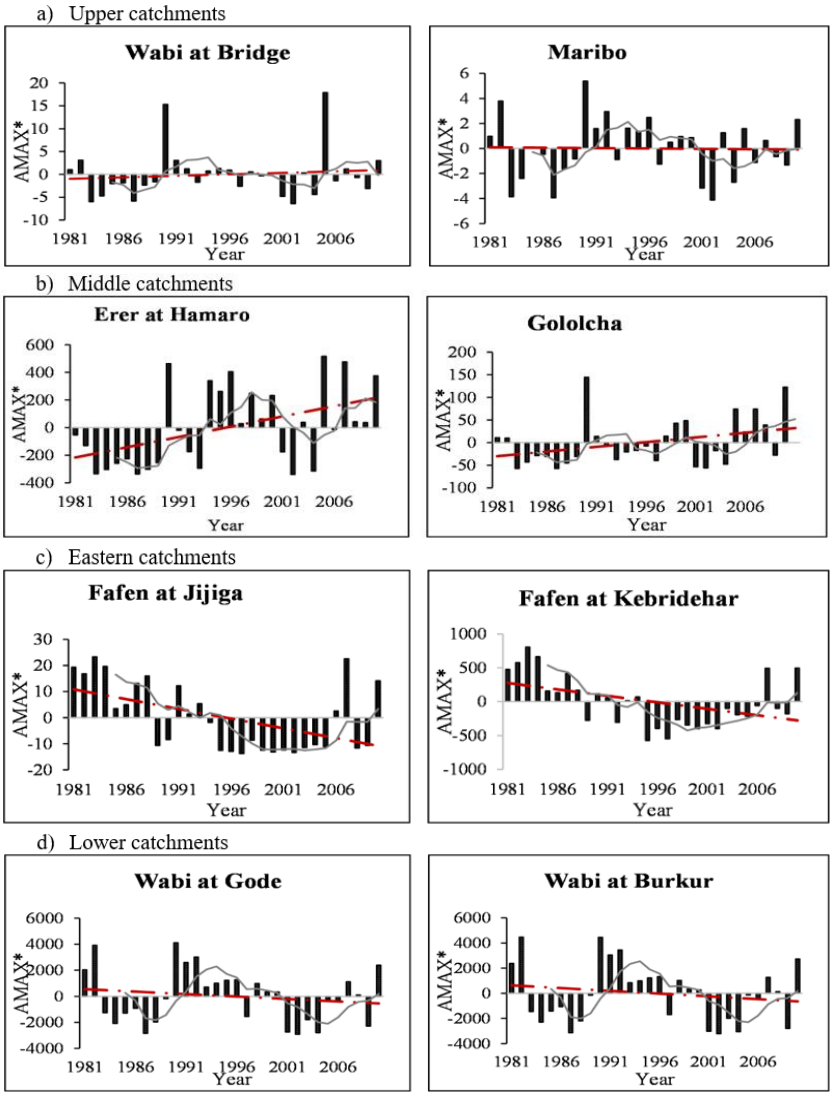

Figure 6-1 Standardized annual maximum discharge (AMAX*) averaged over the studied stations between 1981 and 2010. The broken line is the linear trend; the grey curve is the 5-year moving average in each sample sub-basins

From both Figures 6-1 & 6-2, some conclusions are extracted on multi-temporal trend analysis. First, blue colors are more frequent than red colors, meaning that positive trends are more frequent than negative, especially for the most recent period since 1996 in all stations (Figure 6-2). Second,

negative trends (red colors) appear more significantly in eastern Fafen catchments and lower stations of Wabi Shebele River Basin before 2000 (as shown on the Fafen @ Jijiga, Fafen @ Kebridehar, Wabi @ Gode and Wabi @ Burkur). Most of gauging stations in upper and middle catchments indicates weak to significant increasing trends and while stations in lower and eastern catchments showed weak to strong decreasing tendencies in annual maximum discharge during the past 30 years in Wabi Sheble River Basin. The years 1980s, and 2000s are the decades were weak to significant increasing flood discharges are occurring. For 1990s, most stations indicate decreasing trends in annual maximum discharge in the study area.

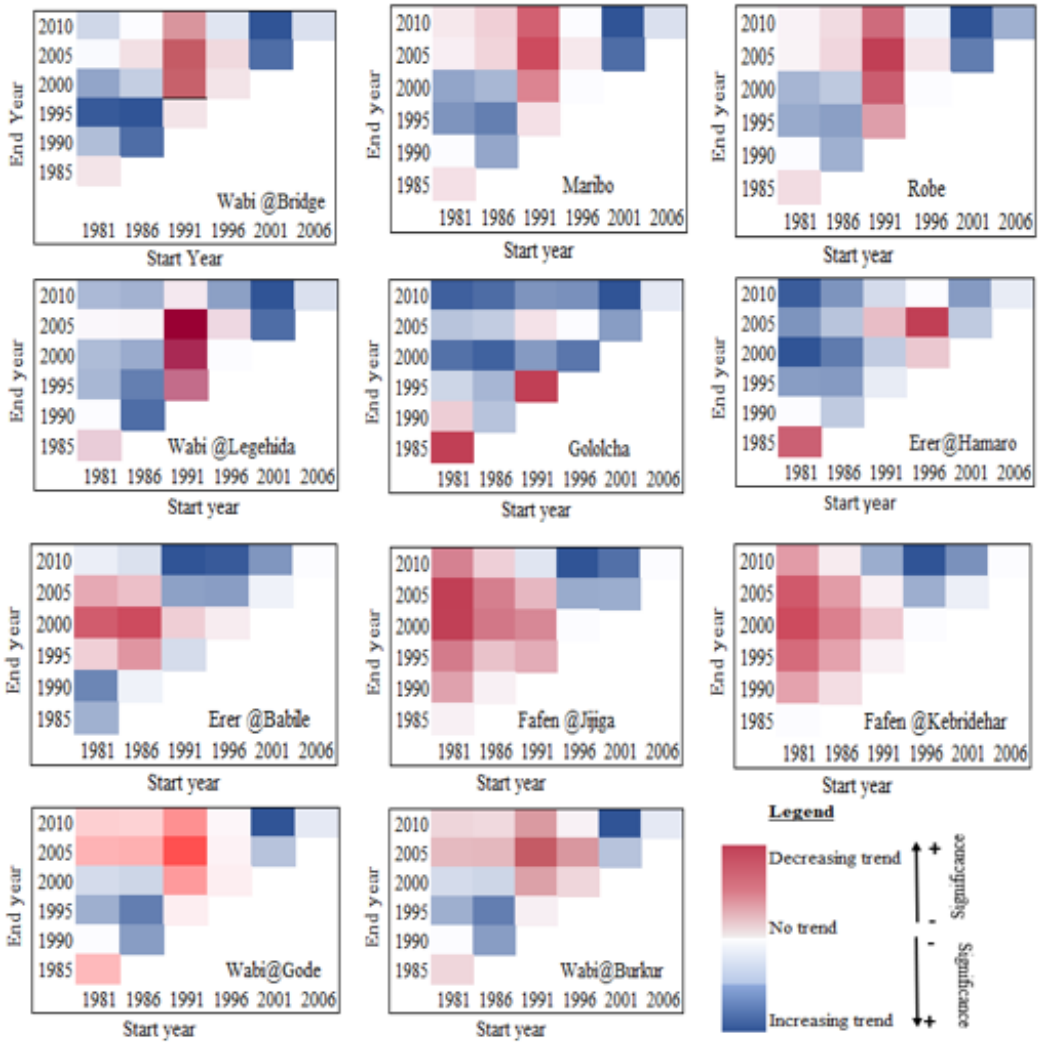

Figure 6-2. Multi-temporal trend analysis for the annual maximum discharge (AMAX) for river catchments in Wabi Shebele River Basin. Blue and red cells correspond to positive and negative tau values respectively (the darker the color the more significant the trend)

6.4.3. Flood Frequency and Seasonality

In Wabi Shebele basin, there are nine mean annual flood events, discharges greater than third quartile (3rd quartile). Some years (i.e., 1981, 1982, 1983, 1990, 1991, 2006, 2007 and 2010) were particularly rich in flood events, with more than 14 events on average. In contrast, in some other years (i.e., 1997, 2001, 2002 and 2004) only two to four events (POTF), was observed in the basin. The decades 1981-1990 and 2001-2010 are noticed as the decades of the richest flood events.

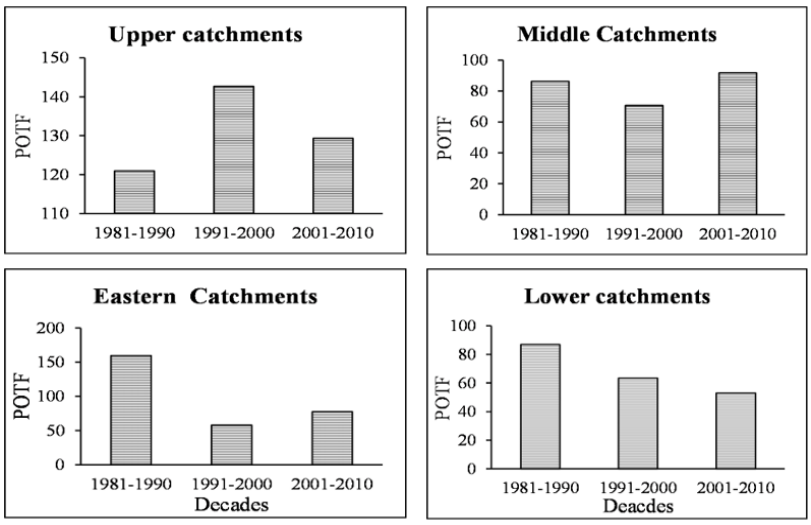

Figure 6-3. Decadal average POTF for periods 1981-2010 in different subbasins of Wabi Shebele

The averaged POTF in upper and middle catchments reveals increasing trends of flood events for longest time period, 1981-2010 (Figure 6-3). However average POTF in lower stations of Wabi Shebele basin and Fafen catchments indicates decreasing trends in number of events. At sample gauging stations the result of MK trend test for the long-term period (1981-2010) reveals positive trends of POTF for 55% of gauging stations. Among these significant increasing trends in POTF is observed over middle catchments (Erer watershed at Hamaro, and Golocha) and the rest 45% of stations indicates negative trends, mainly present in Fafen watershed and Wabi Shebele river at Gode and Burkur.

From Figure 6-4, the QPM analysis using peak over threshold (3rd quartile) indicates that most of extreme discharges varies within a confidence with high oscillation patterns in the entire the basin. Extreme discharges vary above reference line (above mean) in upper, middle and lower valley of Wabi Shebele river stations, whereas it varies below reference line in eastern catchments.

Figure 6-5, illustrates the importance of time windows in analysis of seasonal flood trends. The EDA of spring and winter discharge does not present trends in the longest period (1981-2010) in

most catchments of the basin. Almost in all sample catchments, seasonal maximum discharge indicates oscillation pattern at a decade interval. Like annual maximum discharge, maximum discharge in all seasons also indicates less than mean seasonal maximum discharge in 1990s.

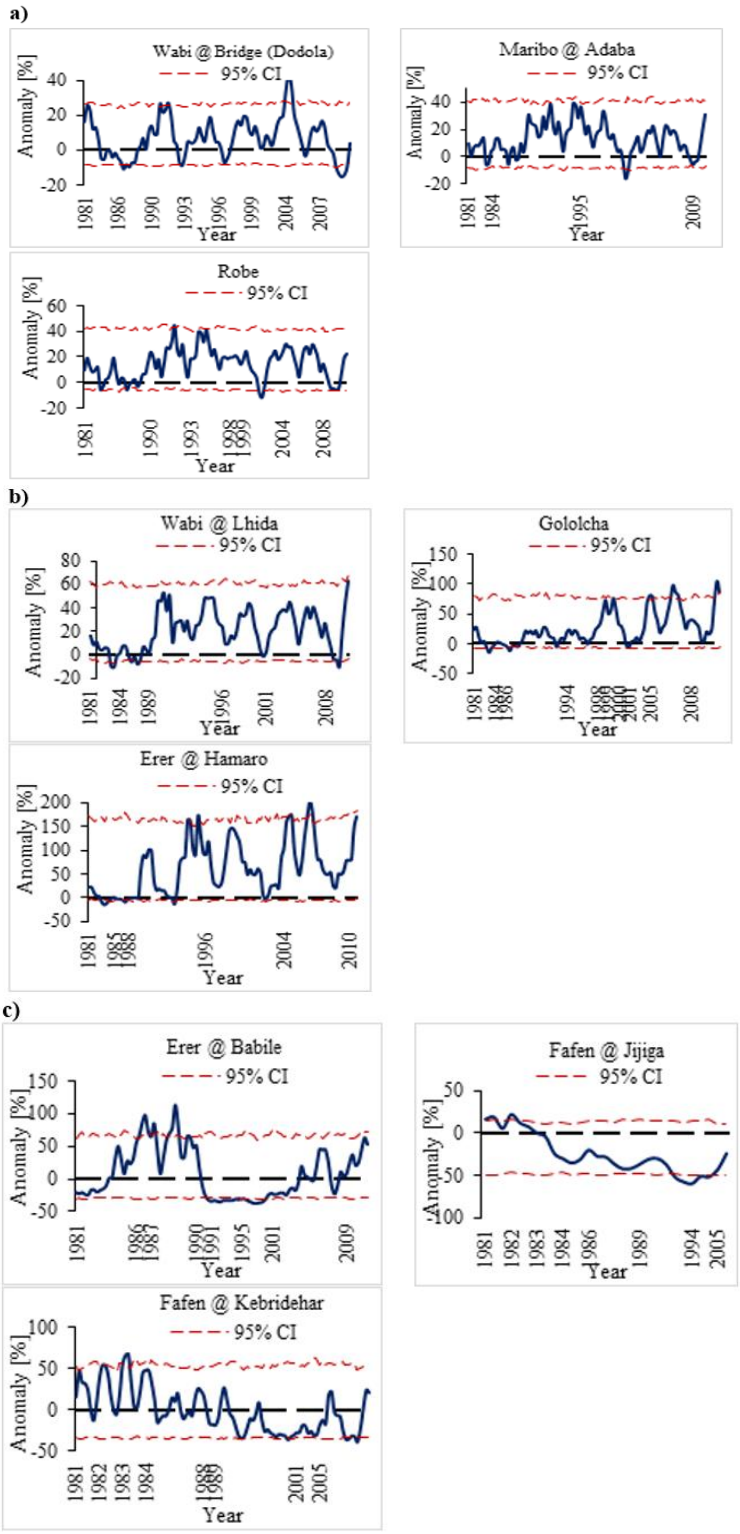

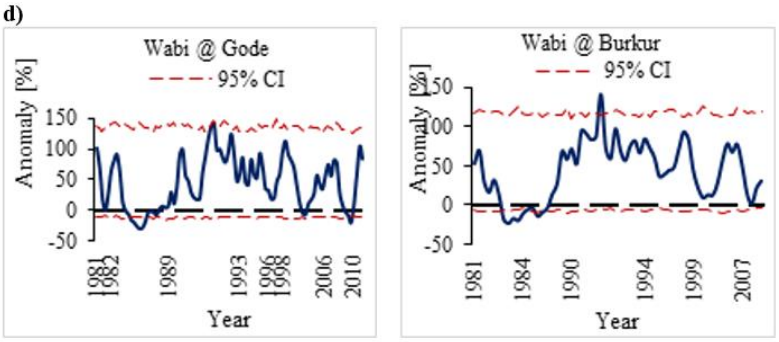

Figure 6-4. Temporal variability in extreme flood discharge using QPM with 95% CI (Confidence Interval) in Wabi Shebele River Basin using four different categories: a) Upper catchments, b) Middle catchments, c) Eastern catchments and d) Lower catchments

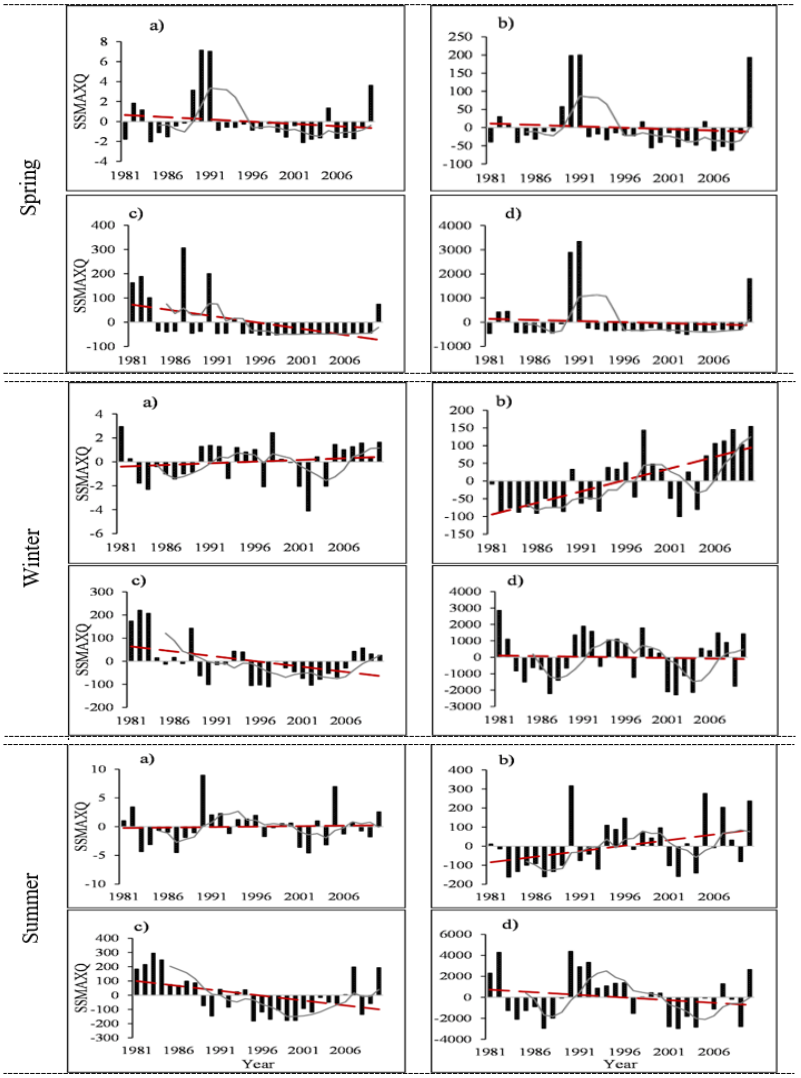

Figure 6-5. Standardized seasonal maximum discharge (SSMAXQ) averaged over the studied catchments for period 1981-2010: a) Upper catchments, b) Middle catchments, c) Eastern catchments, d) Lower catchments. Red broken line is the linear trend and grey curve is the 5-year moving average

From Figure 6-6, the multi-temporal analysis in seasonal flood discharge indicates similar patterns in summer and winter, and different in spring are observed in throughout the basin. In Fafen catchments spring flood discharge indicates weak increasing trend while indicates decreasing trend in summer and winter season for the last 30 years. Darker colors show statistically significant trends, and they are more frequent in summer and less in winter in eastern catchments. For 1990s, upper and lower Wabi Shebele basin flood discharge indicates significant decreasing trends in all seasons and weak decreasing trend in eastern catchments. In all catchments flood discharge indicates increasing tendency in 2000s. This pattern is stronger in summer and winter when 72% of stations showed significant increasing trends for the period 2001-2010. The same result was previously observed in the Wabi Shebele River Basin, where a significant increase in spring, summer and winter floods was identified (IWMI 2015).

Table 6-6, illustrates seasonal significant anomalies in extreme discharges investigated using QPM. In seasonal extreme variability analysis, significant anomaly occurrence season varies with catchments. In upper and middle catchments (Wabi at Dodola, Maribo, robe Wabi at Legehida and Gololcha watersheds), spring season is the season in which highest extreme variabilities are occurred. Similarly, in eastern catchments (Erer watersheds) highest extreme discharge anomalies are occurred in winter season and in lower Wabi Shebele catchments (at Gode and Burkur stations) during summer season.

The positive Kendall's Z values indicates increasing trend within analysis period (Table 6-7). Similar result is reported in literatures that the magnitude and frequency of floods indicates increasing trend in Wabi Shebele River Basin since 2000 (MoWR 2003; Tadesse et al. 2016; IWMI 2015). Extreme discharge variability analysis using peak over threshold (3^{rd} quartile) based on QPM showed significant increasing trend in early 1990s & 2000s and decreasing trends in 1980s particularly in upper and middle catchments (Table 6-8). Over eastern catchments 1980s is the decade in which significant increasing trends observed and decreasing trends in 1990s and 2000s. The lower Wabi Shebele river stations indicate general decreasing trend in analyses period, 1980-2010.

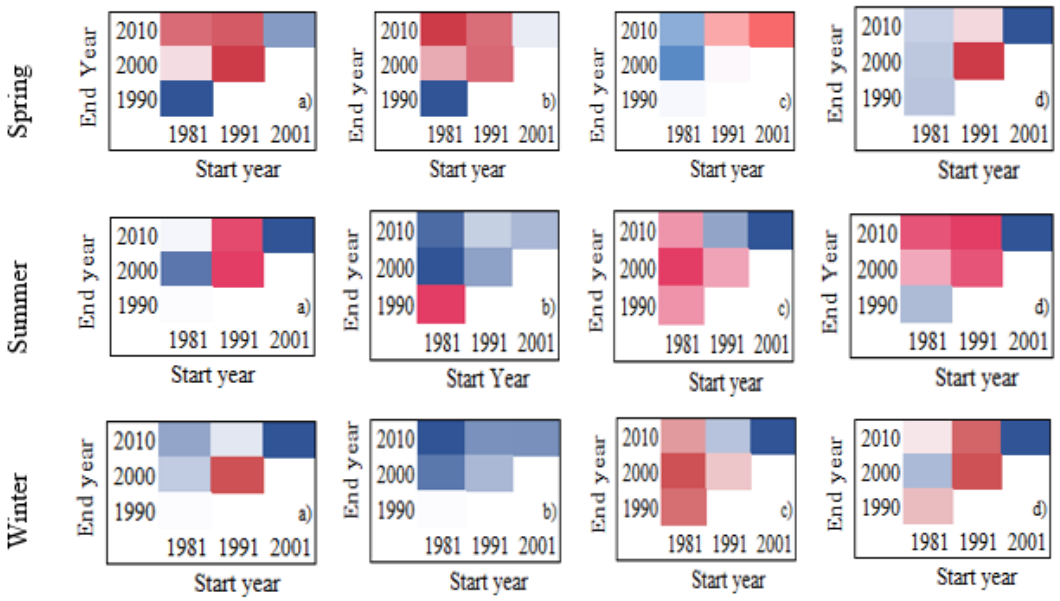

Figure 6-6. Multi-temporal trend analysis of seasonal maximum discharges for: (a)upper catchments, (b) middle catchments, (c) eastern catchments and (d) lower catchments. Legend is explained in Figure 6-2

Table 6-6. Characteristics of highest anomaly in seasonal extreme discharges

Station/River name	Highest +ve anomaly (%)	Season of occurrence	Year	Highest -ve anomaly (%)	Season of occurrence	Year
Wabi at Dodola	135	spring	1989	-29.7	summer	1983
Maribo	177	spring	1987	-60.5	spring	2004
Robe	193.2	spring	1987	-62.7	spring	2004
Wabi at Legehida	114.2	spring	1987	-49.1	spring	2004
Gololcha	116.5	spring	1987	-49.2	spring	2004
Erer at Hamaro	455.5	winter	2006	-57.4	spring	2004
Erer at Babile	296.8	winter	2006	-50.5	spring	1997
Fafen at Jijiga	177	spring	1981	-65.7	winter	1996
Fafen at Kebridehar	357.6	summer	1984	-65.2	spring	1996
Wabi at Gode	439.6	summer	1990	-61.5	summer	2001
Wabi at Burkur	438.7	summer	1990	-61.1	summer	2001

Table 6-7 Mann Kendall trend test summary extreme flood discharges in Wabi Shebele River Basin

Extreme Indices	Mann-Kendall Statistics	Upper catchments			Middle catchments			Eastern catchments			Lower catchments	
		Wabi @ Dodola	Maribo	Robe	Wabi @ Legehida	Erer @ Hamaro	Gololcha @ junction	Erer @ Babile	Fafen @ Jijiga	Fafen @ Kebridehar	Wabi @ Gode	Wabi @ Burkur
AMAX	Test statistcs (Z)	0.32	-0.18	-0.07	0.57	2.32	2.00	0.32	-2.64	-2.32	-0.82	0.41
	p-value (two-tailed)	0.75	0.86	0.94	0.57	0.02	0.05	0.75	0.01	0.02	0.41	0.45
	Mann-Kendall Stat (S)	19.0	-11.0	-5.0	33.0	131.0	113.0	19.0	-149.0	-131.0	-47.0	-43.0
	Kendall's tau	0.04	-0.03	0.09	0.08	0.30	0.26	0.04	-0.34	-0.30	-0.11	-0.10
	Alpha	0.05	0.05	0.05	0.05	0.05	0.05	0.05	0.05	0.05	0.05	0.05
	Trend	Not Significant	Not Significant	Not Significant	Not Significant	Increasing	Increasing	Not Significant	Decreasing	Decreasing	Not Significant	Not Significant
POTF	Test statistcs (Z)	1.471	0.969	1.149	0.997	2.41	2.046	-0.895	-3.207	-2.478	-1.208	-1.206
	p-value (two-tailed)	0.141	0.333	0.251	0.319	0.016	0.041	0.371	0.001	0.013	0.227	0.228
	Alpha	0.05	0.05	0.05	0.05	0.05	0.05	0.05	0.05	0.05	0.05	0.05
	Trend	Not Significant	Not Significant	Not Significant	Not Significant	Increasing	Increasing	Not Significant	Decreasing	Decreasing	Not Significant	Not Significant
SMW	Test statistcs (Z)	0.77	1.14	1.25	2.36	3.96	2.89	0.57	-2.36	-1.64	-0.04	-0.29
	p-value (two-tailed)	0.44	0.25	0.21	0.02	0.00	0.00	0.57	0.02	0.10	0.97	0.78
	Mann-Kendall Stat (S)	44.0	65.0	71.0	133.0	223.0	163.0	33.0	-133.0	-93.0	-3.0	-17.0
	Kendall's tau	0.10	0.15	0.16	0.31	0.51	0.38	0.08	-0.31	-0.21	-0.01	-0.04
	Alpha	0.05	0.05	0.05	0.05	0.05	0.05	0.05	0.05	0.05	0.05	0.05
	Trend	Not Significant	Not Significant	Not Significant	Increasing	Increasing	Increasing	Not Significant	Decreasing	Not Significant	Not Significant	Not Significant
SMSp	Test statistcs (Z)	0.82	-1.71	-1.82	-1.57	-1.61	-1.57	-2.61	-2.14	-2.53	0.57	0.57
	p-value (two-tailed)	0.41	0.09	0.07	0.12	0.11	0.12	0.01	0.03	0.01	0.57	0.57
	Mann-Kendall Stat (S)	47.0	-97.0	-103.0	-89.0	-91.0	-89.0	-147.0	-121.0	-143.0	33.0	33.0
	Kendall's tau	0.11	-0.22	-0.24	-0.21	-0.21	-0.21	-0.34	-0.28	-0.33	0.08	-0.08
	Alpha	0.05	0.05	0.05	0.05	0.05	0.05	0.05	0.05	0.05	0.05	0.05
	Trend	Not Significant	Not Significant	Not Significant	Not Significant	Not Significant	Not Significant	Decreasing	Decreasing	Decreasing	Not Significant	Not Significant
SMSu	Test statistcs (Z)	0.39	-0.18	0.00	0.54	2.21	1.68	0.00	-2.25	-2.21	-0.82	-0.89
	p-value (two-tailed)	0.70	0.86	1.00	0.59	0.03	0.09	1.00	0.02	0.03	0.41	0.37
	Mann-Kendall Stat (S)	23.0	-11.0	-1.0	31.0	125.0	95.0	-1.0	-127.0	-125.0	-47.0	-51.0
	Kendall's tau	0.05	-0.03	0.00	0.07	0.29	0.22	0.00	-0.30	-0.29	-0.11	-0.12
	Alpha	0.05	0.05	0.05	0.05	0.05	0.05	0.05	0.05	0.05	0.05	0.05
	Trend	Not Significant	Not Significant	Not Significant	Not Significant	Increasing	Not Significant	Not Significant	Decreasing	Decreasing	Not Significant	Not Significant

Table 6-8 Summary of QPM analysis in annual extreme discharges

Upper catchments			Middle catchments			Eastern Catchments			Lower catchments		
Sub basin	Magnitude of highest anomaly (%)	Time	Sub basin	Magnitude of highest anomaly (%)	Time	Sub basin	Magnitude of highest anomaly (%)	Time	Sub basin	Magnitude of highest anomaly (%)	Time
Wabi at Dodola	-10.9	1986	Wabi at Legehida	-6	1986	Erer at Babile	+96.9	1986	Wabi at Gode	-29.4	1983
	+27.3	1991		-7.9	1987		+112.3	1988		-19.4	2009
	+43.9	2004		-10	2009		+65.1	1989	Wabi at Burkur	-23.4	1983
	-15.4	2009	Gololcha	-14.6	1983		-34.5	1992		-14.2	1985
Maribo	-16.5	2000		-11.8	1987		-36.7	1998		+142.3	1991
Robe	-6.03	1982		+81	2005	Fafen at Jijiga	+19.4	1981			
	-6.3	1987		+98.4	2006		+22.5	1982			
	+45.3	1991		+105.4	2010		-58.6	1994			
	-12.3	2001	Erer at Hamaro	-14.2	1983	Fafen at Kebridehar	+68.4	1983			
				-8.5	1987		-37.02	1998			
				+165.3	1994		-39.6	2009			
				+174	1995						
				+203.6	2006						

6.4.4. Flood Change Attribution

The detected trends in flood discharge are explained with their correlation with changes in other variables; climate variables (meteorological variables and large-scale climate indices), environmental background condition variables, and external factors. Four large-scale climate indices; Pacific Decadal Oscillation (PDO), Southern Oscillation Index (SOI), The Indian Ocean Dipole (IOD), and Atlantic Multidecadal Oscillation (AMO), are selected to see the relationships with flood discharges in Wabi Shebele River Basin in this study. In addition, changes in the catchment and environmental background factors, deforestation and reforestation, Population density, and alteration in agricultural management practices are analyzed.

Flood change attribution to meteorological drivers

Most of the rivers in Ethiopia exhibit typical characteristics of tropical river flow regimes, dependent on rainfall. The spatial and temporal distribution of rainfall in Ethiopia governs the amount and inter-annual variability of water availability (Shiferaw et al. 2015). A general understanding of hydroclimatic variables such as precipitation, temperature, and discharge is essential for water resource planning and management. Among these, precipitation is the principal driving factor changes in streamflow, especially in tropical river basins like Wabi Shebele River Basin. Pearson's correlation test is performed between ground-based observed precipitation and flood discharges in the watersheds.

As presented in Table 6-9, flood discharges in the Wabi Shebele basin have a positive correlation value to rainfall in most of the stations in the study area at annual and seasonal time levels. The middle and eastern catchments indicate a moderate positive correlation value to areal rainfall in the catchments. It revealed that meteorological variables are among the major driving factors of flood change and frequency in the Wabi Shebele basin.

Table 6-9 Pearson correlation (R) computed between precipitation extremes and flood discharges changes for the studied period, 1980-2010

River/watersheds	Correlation (Pearson's R)			
	Annual	Spring	Summer	Winter
Upper catchments				
Wabi @ Dodola Bridge	-0.012	0.155	-0.056	0.123
Maribo	-0.014	0.254	-0.003	0.106
Robe	0.005	0.257	0.024	0.132
Middle Catchments				
Wabi @ Legehida	0.003	0.09	0.057	0.432
Erer @ Hamaro	0.038	0.136	0.100	0.284
Gololcha @ Wabi junction	0.186	0.141	0.172	0.369
Eastern Catchments				
Erer @ Babile	-0.042	0.08	0.187	-0.136
Fafen @ Jijiga	0.2	0.166	0.083	0.201
Fafen @ Kebridehar	0.062	0.133	0.235	0.202
Lower Catchments				
Wabi @ Gode	-0.018	-0.034	0.016	-0.214
Wabi @ Burkur	-0.016	-0.034	0.008	-0.216

Influence of natural variability

To explain extreme streamflow variabilities in the study area further, selected global climate indices are correlated to both precipitation and streamflow are conducted. The results of the correlation values are given in Tables 6-10 and 6-11. The results indicate that almost all rainfall stations have positively correlated to the Pacific and Atlantic Ocean indices, i.e., PDO and AMO (Table 6-10). However, rainfall stations in the eastern and lower parts of the Wabi Shebele basin have a high positive correlation with the Indian Ocean Index, i.e., IOD. This illustrates that the influence of Pacific, Atlantic, and Indian Oceans on the rainfall and river flow of the Wabi Shebele basin in the southeastern part of Ethiopia are considerable with different levels. The influence of the Indian Ocean is significant in the eastern extreme and lowland part of the basin compared to other oceans' influence. However, both Pacific and Atlantic Oceans have a considerable impact on the highland area of the study area. Southern Oscillation Index is not strong as others, particularly in the wet season and annual rainfall extremes and extreme streamflow in the basin.

Climate indices were also correlated with the flood parameters in Wabi Shebele River Basin. The result indicates that the annual flood discharges in the Wabi Shebele basin have a positive correlation with the Indian Ocean Dipole (IOD) and the Atlantic Multidecadal Oscillation (AMO) (Table 6-11). Particularly flood discharges in upper and middle watersheds indicate a strong

correlation value (R^2>0.5) with the AMO. However, in eastern catchments and the lower part of Wabi Shebele stations, flood discharges positively correlated to Pacific and Indian ocean indices (PDO, SOI, and IOD). The seasonal correlation analysis shows that summer and spring flood discharges positively correlated to the Pacific Ocean index, i.e., PDO in the Wabi Shebele basin. However, floods in the winter season have strong correlations with the AMO.

The results presented in Table 6-10 and 6-11 strengthen the study conducted by Seleshi and Zanke (2004) that during the spring season, the moist winds blow from the Gulf of Aden and the Indian Ocean to the Horn of Africa and produce main rains in southern and southeastern Ethiopia. The warmer atmosphere over the south Atlantic Ocean and the higher the pressure over the tropical eastern Pacific Ocean decreases summer rainfall over the lowlands of eastern, southern, and southeastern Ethiopia. Therefore, the global climate indices (i.e., Pacific, Atlantic, and Indian Oceans indices) affect extreme hydroclimatic variabilities in the Wabi Shebele basin.

Table 6-10. Annual and seasonal correlation coefficients between rainfall extremes and climate indices

	Annual				Dry Season (November-March)				Wet Season (April-September)			
	PDO	SOI	IOD	AMO	PDO	SOI	IOD	AMO	PDO	SOI	IOD	AMO
Adaba	**0.37**	-0.29	-0.06	-0.23	-0.33	-0.02	-0.14	**0.53***	**0.06**	0.07	-0.12	0.04
Kofele	**0.22**	-0.14	-0.10	-0.24	0.15	-0.27	-0.29	-0.11	**0.38**	-0.12	**0.40**	0.06
Arsi Robe	**0.37**	-0.18	**0.15**	-0.33	0.32	-0.12	0.19	-0.10	**0.34**	-0.01	**0.14**	-0.41
Gindhir	**0.06**	-0.03	**0.26**	-0.10	-0.22	0.11	0.01	**0.30**	**0.19**	0.04	**0.23**	-0.13
Diredawa	**0.32**	-0.10	**0.40**	0.05	0.04	0.01	0.41	**0.12**	**0.31**	-0.07	**0.15**	-0.01
Jijiga	**0.28**	-0.35	-0.16	-0.09	-0.23	0.03	-0.02	**0.56***	**0.51***	-0.05	-0.31	-0.21
Degehabour	-0.09	0.14	-0.06	-0.22	-0.01	0.03	**0.60***	**0.34**	**0.06**	-0.01	-0.01	0.08

*- statistically significant at 5% significance level

Table 6-11 Pearson correlation R computed between selected global climatic indices and analyzed flood discharges for the studied periods, 1980-2010

River/watersheds	Global Climate Indices															
	PDO				SOI				IOD				AMO			
	Annl	Spr	Sum	Wint	Annl	Spr	Sum	Wint	Annl	Spr	Sum	Wint	Annl	Spr	Sum	Wint
Upper catchments																
Wabi @ Dodola Bridge	-0.06	-0.43	**0.03**	-0.23	-0.04	-0.17	-0.05	-0.19	**0.10**	-0.14	-0.15	**0.06**	0.58	-0.12	**0.25**	0.08
Maribo	**0.07**	**0.04**	**0.16**	-0.02	-0.20	-0.36	-0.02	-0.22	**0.33**	**0.01**	-0.20	-0.17	**0.06**	-0.45	-0.02	**0.04**
Robe	-0.23	**0.05**	**0.12**	-0.04	**0.06**	-0.38	0.02	-0.18	**0.10**	0.02	-0.21	**0.06**	0.41	-0.44	-0.01	0.11
Middle Catchments																
Wabi @ Legehida	-0.23	-0.01	**0.03**	-0.23	0.06	-0.24	-0.01	0.05	**0.11**	-0.03	-0.12	**0.06**	0.41	-0.39	**0.31**	0.51
Erer @ Hamaro	-0.43	-0.02	-0.07	-0.22	**0.49**	-0.23	-0.07	**0.17**	**0.07**	-0.04	**0.03**	**0.14**	**0.60**	-0.37	**0.63**	**0.70**
Gololcha @ junction	-0.19	0.00	**0.08**	-0.15	**0.21**	-0.22	-0.25	**0.03**	**0.18**	-0.05	**0.07**	**0.24**	0.57	-0.34	**0.28**	0.56
Eastern Catchments																
Erer @ Babile	-0.13	0.20	**0.11**	0.02	0.23	-0.30	0.09	0.11	-0.29	-0.02	0.13	-0.14	0.00	-0.40	-0.18	0.13
Fafen @ Jijiga	**0.07**	**0.16**	**0.30**	**0.13**	**0.27**	-0.08	**0.08**	-0.09	**0.16**	0.00	**0.05**	-0.17	-0.19	-0.21	-0.39	-0.23
Fafen @ Kebridehar	0.35	**0.20**	**0.23**	0.06	-0.17	-0.19	0.04	**0.01**	**0.16**	0.02	**0.09**	-0.12	-0.28	-0.27	-0.31	-0.05
Lower Catchments																
Wabi @ Gode	-0.01	-0.10	**0.14**	-0.21	-0.21	-0.12	0.02	-0.30	**0.19**	-0.14	-0.28	-0.06	0.22	-0.12	-0.24	-0.36
Wabi @ Burkur	**0.04**	-0.11	**0.14**	-0.21	-0.26	-0.12	**0.02**	-0.27	**0.15**	-0.14	-0.28	**0.02**	**0.22**	-0.12	-0.24	-0.25

Annl =Annual, Spr =Spring (February – May), Sum =Summer (June-September), Wint =Winter (October-January)

Change attribution to environmental background conditions

The environmental background factors, i.e., elevation, slope, and soil type, can be considered static factors. Elevational differences of watersheds reflect differences in land cover type and associated hydrologic runoff response and geomorphic disturbance (Sutfin and Wohl 2019). Small land cover change results in rapid response to rainfall, increased flood magnitudes, increased potential for debris flows, abundant erosion, and consequently increase slope failures. The elevation varies largely in Wabi Shebele River Basin. Among the environmental background condition factors elevation is the critical factor in flood magnitude and frequency in the Wabi Shebele River Basin (Figure 6-7). Watershed slope (WS; %) is the mean watershed slope, measured by calculating the maximum rate of change between each cell. It indicates the steepness of the drainage area. As the slope decreases, catchment soils become more permeable, and thus the effect of infiltration becomes more significant (Al-Rawas and Valeo 2010). In the Wabi Shebele basin, the eastern and southern part is characterized by gentle slopes, and the northwestern part is characterized by higher slopes.

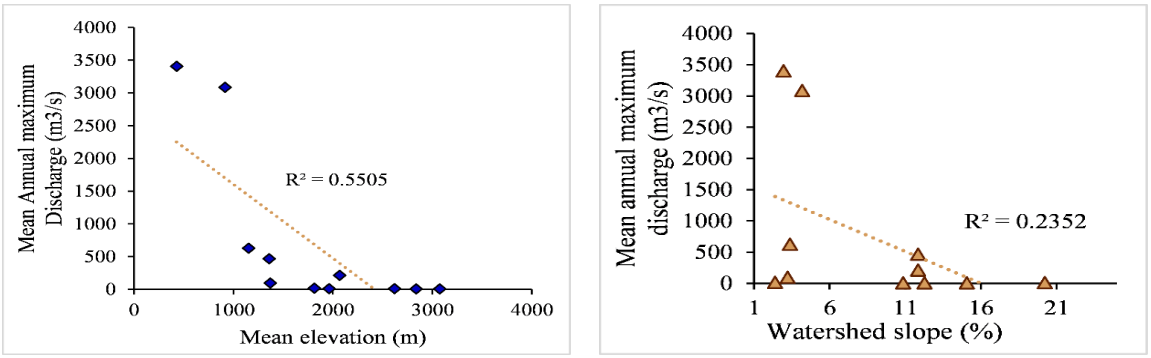

Figure 6-7 Scatter plot between Peak over threshold frequency (POTF) and (a) mean watershed elevation and (b) Watershed slope

In surface runoff generation, the soil infiltration rate is another sensitive variable. Coarse textured soils have wide well-connected spaces and allow more water to infiltrate through them quite rapidly, while fine-grained soils dominated by clay have low infiltration rates due to their smaller-sized pore spaces (Prachansri 2007). Soil containing a large amount of sand and silt tends to form a crust and become compacted. It significantly reduces the infiltration rate. The amount of organic matter in the soil surface can enhance infiltration because organic matter has more porous than mineral soil particles. It can also hold a much greater quantity of water. In the Wabi Shebele basin, soil distributions vary spatially; loamy sand in the east and downstream, clay in the middle, sandy loam in the middle, and silty clay in the northwest (Figure 2-4, section 2-4). The steep gradient

watersheds situated at the middle Wabi Shebele River Basin are dominated by clay soil type. These poorly drained and hillside soils at the upstream part of the basin may be the probable cause for flooding formation downstream of the Wabi Shebele basin due to low infiltration capacity in the upstream where high rainfall occurs. Contrary, highly drained soils and flat surfaces at the downstream part of the study area may be taken as the cause for surface water flow decrement and rise for underground water tables in the area.

Change attribution to human activities

The results presented under previous topics indicates the relationships between flood trends and changes in some atmospheric variables (i.e., meteorological and global climate indices). But these attributes explain the variability of flood discharge only at a partial level. Therefore, non-climatic changes in the catchment and river parameters are required to be taken into account.

During the last four decades, some environmental changes occurred in the studied catchments that influence the conditions of flood runoff (Table 6-12). Land use and land cover have been changing in the northern part of the Wabi Shebele River Basin. The extent of shrublands indicates significant increasing trends while grassland and cultivated area showed decreasing trends from 1984 to 1997 (MoWR 2004a). Similarly, the coverage of riparian woodland in the study area indicates decrement in the period. Shrubland class is the areas with an extensive physical limitation: like very steep slopes, shallow soils, rock outcrops, series of deeply dissected gorges, dry and rugged areas. Due to human activities and pressures in large semi-arid areas (middle and eastern upper catchments) of the basin, most of the coverages of Riparian Woodland, Grassland, and Perennial and seasonal Swamp and Marshland covers are changed to Shrubland in the Wabi Shebele basin in the past. Different land use and land cover types in the basin exhibit differences in hydrologic runoff response. Loss of land floor cover, thinner forest canopies, grasslands, and reduced infiltration of rainfall result in a rapid hydrologic response, increased flood magnitudes, and frequency (Sutfin and Wohl 2019). In the Wabi Shebele River Basin, magnitudes and frequency of flood events in middle watersheds indicate an increasing trend in recent decades (Section 6.4.2 and 6.4.3). In mountainous areas, increased intense convective storms, increase cultivated land, and more highly confined river valleys result in rapid runoff response and cause flood hazards.

Another potential driver of floods in watersheds is population density. The population growth and cultivated land density have a strong correlation (Liu et al., 2017). Increment of cultivated land results in an accelerated runoff process due to the rapid development of gullies (Kundzewicz et al.

2018). In the Wabi Shebele basin, human activities are concentrated in the west and eastern upper highland areas. As indicated in Figure 6-8, cultivation land coverage has a high correlation value with population density. The correlation graph is done using population density and cultivation land at five (5) zones: (1) western upper Wabi Shebele (Arsi and Bale zone highland areas), (2) eastern upper Wabi Shebele basin (west & east Hararghe zones and Jijiga district), (3) middle Wabi Shebele basin (lowland areas of east Bale zone, Hamaro, Fik, and Afder zones of Somali regional state), (4) Fafen Watersheds (around Deghabour and Kebridehar areas) and (5) lower Wabi Shebele basin (around Gode and Warder zones of Somali regional state).

Table 6-12 Land use/ land cover changes in Wabi Shebele basin between 1984 and 1997

S.No.	Land Use/Cover Type	1984	1994	Change (%)	
		Area (km^2)	Area (km^2)	Area (km^2)	%
1	Cultivated lands	26,989	23,507	-3,482	-13%
2	Afro-Alpine vegetation	167	397	230	138%
3	Forest lands	1691	1691	0	0%
4	Woodlands	4,301	7,409	3,108	72%
5	Riparian wood lands	1,080	241	-839	-78%
6	Shrub lands	51,406	138,396	86,990	169%
7	Grass lands	87,383	24,791	-62,592	-72%
8	Wet lands	1,052	68	-984	-94%
9	Bare lands	27,954	6,882	-21,072	-75%
10	Water bodies	39	32	-7	-18%
Total		**202,220**	**202,220**		

Source: (MoWR 2004a)

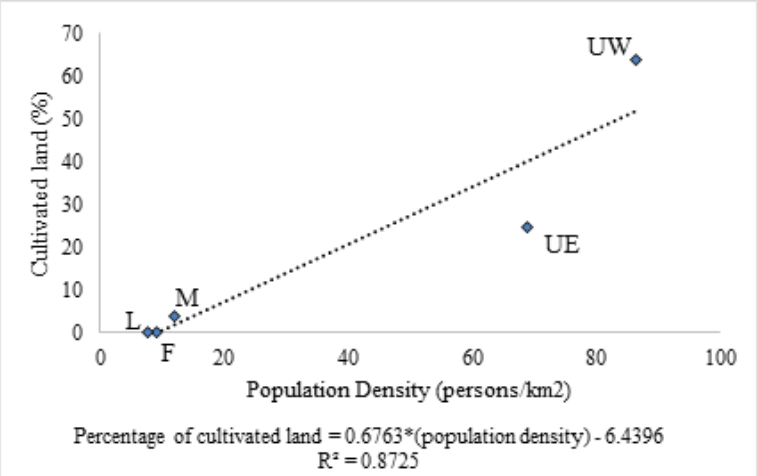

Figure 6-8 Correlation of population density and cultivated land in Wabi Shebele basin in 1997: UW= western upper basin, UE=eastern upper basin, M= middle basin, F= Fafen watershed, and L= lower Wabi Shebele basin

6.5. Conclusion

In this chapter, changes in the flood series are analyzed, and the dominant variability driving factors are attributed using model-based simulation. Swat model is used to generate stream flow data. Both exploratory data analysis (EDA) and non-parametric tests (i.e., Mann-Kendal trend test and quantile perturbation (QPM) methods) are used to see temporal variabilities in flood discharge. The risk level used was 5 %. The p-value of the MK statistic S for sample data is used to measure the significance of trend value; if $p \leq 0.050$ (significance level), then the existing trend is assessed to be statistically significant.

The multi-temporal trend analysis at 5, 10, 15, 25, and 30-year intervals starting from 1980 in annual maximum discharge showed increasing trends for most recent periods in all sample stations while decreasing tendency of flood discharges is observed before the 2000s, particularly in eastern and lower catchments in the basin. Peak over threshold (3^{rd} quartile) values of discharge analysis using QPM show significant positive anomalies (outside confidence interval) in the early 1990s & 2000s and negative anomalies in the 1980s, particularly in upper and middle catchments. In eastern catchments, the 1980s is the decade in which significant positive anomalies were observed and negative anomalies in the 1990s and 2000s.

The Pearson's correlation test between extreme discharge and precipitation indicates that in the annual and wet seasons, moderate (0.1-0.5) positive correlation values are observed between flood discharge and precipitation extremes. The correlation analysis performed between precipitation extremes and four global climate indices indicates the strong influence of Pacific and Atlantic Ocean indices, i.e., Pacific Decadal Oscillation (PDO) and Atlantic Multidecadal Oscillation (AMO) on the highland part and Indian Ocean Index (IOD) influence in the eastern and lowland part of Wabi Shebele River Basin. Similarly, Atlantic and Indian Ocean indices have considerable influence on extreme streamflow in Wabi Shebele River Basin. Among environmental background conditions factors: elevation, soil, and slopes are identified sensitive attributes of flood generations in the study area. Human activities and population densities are also potential driving factors of flood frequency identified in the Wabi Shebele River Basin, particularly in recent decades. Generally, the interplay of atmospheric and terrestrial changes drives the hydrological variability in the river basin.

7. FLOOD HAZARD ATTRIBUTION AND UNCERTAINTY ANALYSIS WITH CLIMATE CHANGE AND LAND USE CHANGES

Abstract

The interaction of the land surface and the atmosphere is vital in hydrological processes. In this chapter, climate change and land use land cover change impacts on streamflow is explored using SWAT model in Wabi Shebele River Basin. Regional Climate Model (RCM) from CORDEX-Africa region is used to analyze the basin's hydrological responses to climate forcing in the projected period. Land use and land cover maps at three different periods (i.e., 1986, 1997 and 2016) are used to see the impact of land cover change on generated stream flow using SWAT model. The result indicates that, flood hazard indices showed larger value at downstream of the river station (i.e., Gode) and smaller value at the upper and middle stations with no change in climate variables (i.e., the baseline scenario, T+0 ^{o}C, P+0 %). The basin is likely to experience an increase in flood hazard with an increase in precipitation in the future as temperatures increase less than 2^{o}C. The impact of LULC changes on streamflow also indicates significance, particularly in the middle and upper part of the study area. Based on separation method analysis, the climate change has greater impact factor on the streamflow and flood hazards in Wabi Shebele River Basin during the last four decades. Model uncertainty analysis reveals that simulated seasonal streamflow using RCMs has similar oscillation patterns to streamflow simulated using observed climate data within uncertainty bands (UB) in the study area with NSE and R^2 values greater than 0.75 and 0.92 respectively.

Key Words: Climate Change Impact, Land Use Changes, Uncertainty Analysis, Flood hazard, Swat Model, Sensitive Parameters

7.1. Introduction

Flood hazard is the probability occurrence of a potentially damaging flood phenomena within specified period of time in a given area (Assefa 2018). Climate change refers to a change in the state of the climate that can be identified by changes in the mean and the variability of its properties that persists for extended periods, decades, or longer (IPCC 2007). Both natural internal dynamics and anthropogenic factors are known to cause climate change. Natural forcing has occurred over thousands of years and interactions between the ocean and atmosphere has caused climate

variations on yearly, decadal, and century time scales. In contrast, anthropogenic factors are due to human intervention activities (i.e., deforestation, agriculture, urbanization) that have contributed, amongst other effects, to increases in greenhouse gases (GHG) concentration in the atmosphere (IPCC, 1996). The changing climate would bring changes to hydrological parameters like temperature, precipitation, evapotranspiration, and discharge both in magnitude and frequency (Jain and Kumar 2012; Bhatt and Mall 2015). Rainfall can produce widespread surface flooding where water encounters dry ground and infiltrates, raising the groundwater volumes (Gumbricht et al., 2004; Adnan, 2010). Temperature increases can lead to increases in evapotranspiration on rivers, dams, and other water reservoirs. Consequently, water availability for agricultural irrigation, domestic and non-domestic usage, and hydropower generation decreases (Adnan, 2010). In tropical regions, annual flooding is associated with high intensity of rainfall and heat in the atmosphere (Dettinger et al., 2009; Hall et al., 2014; Williams et al., 2012).

Several studies used different approaches to understand and quantify the effects of climate change on flooding. Studies, i.e., (Taye and Willems 2012; Fleming and Clarke 2002; Chen et al. 2012; Ntegeka and Willems 2008; Sheng and Wang 2002; Yue et al., 2002; Li et al. 2020; Yue et al., 2003; Seleshi and Zanke 2004) analyzed time-series trends exhibited in the historical hydrological data. Others analyzed historical or current meteorological data coupled with hydrological models, e.g., (Gebrechorkos et al., 2018; Dile et al., 2013; Adnan 2010) and others used a combination of climate models (i.e., a general circulation model, GCM and regional climate models, RCMs) with hydrological data for future projections e.g., (Adnan 2010; Ruiz-Villanueva et al. 2016; Endris et al. 2013; Mulugeta et al., 2020).

The interaction of the land surface and the atmosphere is vital in hydrological processes such as infiltration, evapotranspiration, runoff generation, and flooding. The behavior of a natural catchment system over time may change due to several factors. Increased growth in human populations will increase food demand and caused deforestation that replaces forests with agricultural land and settlement. For example, Hailemariam et al. (2016) analyzed that a large area of forest land decreased due to farmland and urban settlement expansion in the Bale Mountain Eco-Region of Ethiopia from 1985 to 2015. Similarly, over-exploitation of resources due to an increase in population and demand for food supply has caused land degradation in western Kenya (Githui et al., 2009). However, deforestation and land development for agriculture has not necessarily led to an equal increase in food production but has often led to land erosion in the

upstream area and triggered heavy floods in the downstream areas as presented in Vandaele and Poesen (1995) and Adnan (2010).

Understanding LULC changes is essential in supporting decisions of land planning at different scales: global, regional, and local. LULC change analysis can reflect the dimensions, potential impacts, and interactions of the relationship between human activity and the environment (Armenteras et al., 2019; Sutfin and Wohl 2019; Yulianto et al., 2020). Increased runoff as a result of LULC changes can affect the frequency of flooding, base flow, and annual average discharge in such a way as to alter the hydrological cycle (Sutfin and Wohl 2019; Yulianto et al. 2020). The recent history of the Wabi Shebele River Basin is marked by frequent destructive floods (MoWR, 2003; Tadesse et al., 2016; UNDP, 1999). In the basin, magnitudes and frequency of flood events, particularly in the middle part, showed an increasing trend in recent decades as indicated under section 6.4.2 and 6.4.3.

The main objective of this chapter is to quantify the impacts of climate change and land-use/land cover change on streamflow and flood hazard in the Wabi Shebele River Basin using a model-based approach. The specific objectives of the study are: to test the performance of SWAT and identify sensitive parameters in flood prediction; to test climate sensitivity in flood hazard prediction; to analyze uncertainties of a climate model in streamflow prediction; to analyze LULC change and impact on flood occurrences in terms of magnitude, volume, frequency, and hydrograph in the Wabi Shebele basin; and to quantify the share of impact between climate change and LULC change on flood value in the river basin.

7.2. Materials and Methods

7.2.1. Regional Climate Moles (RCMs)

The spatial resolution of GCMs (currently 100–250 km) is too coarse for the direct outputs to be used in hydrological impact assessments on the catchment scale (Mulugeta et al., 2020; Veijalainen et al., 2010). Although climate change is a worldwide concern, its impact on the hydrologic system is at the regional level that needs to be downscaled to appropriate scales. There are two groups of downscaling methods: dynamical and statistical downscaling (Fowler et al., 2007). In dynamical downscaling, a Regional Climate Model (RCM) or Limited Area Model (LAM) of the higher spatial resolution set for a region (Hay et al., 2002; Veijalainen et al., 2010). RCMs use boundary conditions from the GCMs, but capture geographical details more precisely than GCMs (Hay et al., 2002). Few studies in the East African region used RCMs from dynamic

downscaling (Endris et al., 2013; Mulugeta et al., 2020). An ensemble of historical and future climate projections generated by the Coordinated Regional Downscaling Experiment (CORDEX) is available from the World Climate Research Program (Giorgi et al., 2009). CORDEX-Africa (http://cordex.org/domains/region-5-africa/) provides regionally-downscaled climate data for the continent at a spatial resolution of 0.44°×0.44°. Future projections of precipitation and temperature investigated using CORDEX-Africa datasets. There are two methods commonly used to transfer the climate signal to the hydrological model: the delta change approach (Fowler and Kilsby 2007) and the direct RCM data approach. In using direct RCM data, the daily bias-corrected results from RCM are used as input to the hydrological model (Veijalainen et al., 2010). The delta change approach is classified as the simplest statistical downscaling method. However, the direct RCM data relies on dynamically downscaled by the RCM with an additional bias-corrected step.

The CORDEX Africa, downscaled from five GCMs of Climate Model Inter-comparison Project Phase 5 (CMIP5) to quantify the influence of future changes in regional climate on the hydrology of the Wabi Shebele River Basin. The latest version of the regional climate model, developed by the Swedish Ross Centre Regional Atmospheric model (RCA4), is selected for this study (Samuelsson et al., 2011). In addition, two different scenarios of the Representative Concentration Pathways (RCPs) are considered for all models. For the model, climate data belonging to two RCPs emission scenarios (i.e., RCP4.5 and RCP8.5) are extracted for 20^{th} century climate (historical runs; 1981–2005) and future climate (2006– 2100). These RCMs were selected in studies (Diro et al., 2011; Gebrechorkos et al., 2018; Mulugeta et al., 2020; Näschen et al., 2019) have shown that each model can reasonably reproduce the regional climate over the East Africa region. The simulations cover the period from 1951 to 2100, divided into a historical period from 1951 to 2005 and future projections from 2006 to 2100. The details of the RCA4 simulations used in this study are presented in Table 7-1.

Table 7-1 Description of the CORDEX-AFRICA, regional climate model (RCAs) used in this study and their driving Global Climate Models (GCMs)

GCM	RCM	Institution	Country	GCM Resolution
CanESM2	RCA4_v1	Canadian Centre for Climate Modeling and Analysis	Canada	2.8º x 2.8º
CNRM-CM5	RCA4-v1	Centre National de Recherches Meteorolo-Giques/Centre Europeen de Recherche et Formation Avanceesencalcul scientifique	France	1.4º x1.4º
GFDL-ESM2M	RCA4-v1	NOAA Geophysical Fluid Dynamic Laboratory	USA	2.5º x 2.0º
MIROC5	RCA4-v1	Atmosphere and Ocean Research Institute (University of Tokyo), National Institute for Environmental Studies and Japan Agency for Marine-Earth Science and Technology	Japan	1.4º x 1.4º
IPSL-CM5A-MR	RCA4-v1	Institut Pierre-Simon Laplace	France	1.25º x 2.5º

Bias adjustment method

Climate models often provide biased representations of observed time series which needs correction procedures (Teutschbein and Seibert 2012). Among different methods described in Teutschbein and Seibert (2012), Quantile Mapping Method (QMM) has been widely used in hydrological applications (Boé et al., 2007; Ngai et al., 2017) and bias correction of RCMs (Piani et al., 2010; Teutschbein and Seibert 2012; Worku et al., 2020). In the quantile mapping method, the cumulative distribution function (CDF) of RCM-simulated rainfall and temperature values are adjusted with the CDF of observed values. The method adjusts the mean, standard deviation, extremes, and distribution of rainfall and temperature events of RCM outputs (Teutschbein and Seibert 2012). Distribution mapping uses the Gamma distribution (Gudmundsson et al. 2012) and the Gaussian distributions (Mathews and Walker 1970) to fit the distribution of rainfall and temperature of RCMs with observational data. In the distribution mapping, the transformation between observed and modeled rainfall is given as:

$$V_o = F_o^{-1}\left(F_m(V_m)\right) \quad (7.1)$$

where:

V_o = observed variable,

V_m = modeled variable

F_m is the CDF related to Vm and

F_o^{-1} is the inverse CDF of Vo

In this study, I used the CMhyd tool (Rathjens 2016) to execute the bias correction techniques. The tool compares the raw RCM output with observed data, calculates the variation between observed and RCM simulated data, and applies different bias correction methods to correct historical and future climate model output. The bias correction algorithms derived from historical RCM simulation and observed data are applied for future RCM bias correction processes. Temperature and rainfall data at 14 stations in the Wabi Shebele basin are used for the bias correction of the RCA4 climate data.

7.2.2. Land-use and land cover (LULC) changes

Land use means the use to which the land is being put or the utilization of land devoted to human activities, and land cover is the physical surface of the land (Tali and Kanth 2011). Land cover is continually molded and transformed by land-use changes, for example, when a forest is converted to pasture or agricultural land. Land use and land cover map information for 1986, 1997, and 2016 were collected from different sources (Table 7-2) and analyzed. The detail land-use and land cover distribution of the basin is described under section 2.5.

Table 7-2 Overview of land use land cover maps, their resolution, source, and the required parameters in this study

LULC Dataset	Resolution/scale	Source	Required parameter
• 1986	1:250000	Water and Land Resource Center (WLRC), Addis Ababa University, Ethiopia	Land uses and cover classes
• 1997		Ethiopian Ministry of Water, Irrigation, and Energy (MoWIE')	
• 2016		Water and Land Resource Center (WLRC), Addis Ababa University, Ethiopia	

7.2.3. Climate sensitivity test and Uncertainty analysis

I generated an ensemble of potential climate data from the historical station record (1981-2000) and analysis climate sensitivity. In the climate change impact assessment using climate sensitivity tests (Cheng et al., 2013; Ficklin et al., 2009), a combination of two weather variables is examined in this study: mean temperature (0, +1, +2, +3˚C) and mean precipitation (0, +10, +20%). Eleven total climate change conditions, including the current condition (0,0,0), are applied to the calibrated SWAT model. Flood indices were calculated on 18 years of data because the first two years are considered to spin up the SWAT model. The historical record is used as the baseline condition for comparison within the climate sensitivity datasets. Several studies (i.e., Xu et al.

2017: Yang et al. 2016) used climate sensitivity analyses for uncertainty analysis in climate change impact. The set of possible future temperature and precipitation conditions allows us to determine which factors and at what range of values affect environmental outcomes (Pianosi et al., 2016).

Based on simulated streamflow using available observed data, 95%PU analysis is performed in SUFI-2 of SWAT-CUP interface and taken as baseline uncertainty bound. For the climate model approach, the ensemble of five regional climate models (RCMs) are selected for optimistic case emission scenarios (RCP 4.5) and business-as-usual emission scenarios (RCP 8.5) based on their general performance in the study area and region. For each model, I selected historical (1981-2000) and futures at mid and last 21st century (i.e., at 2041-2060 and 2081-2100) conditions for comparison. In both future climate approaches, I changed the only temperature and precipitation inputs in the SWAT model to automatically generate the other three weather inputs: solar radiation, relative humidity, and wind speed, as I had during the historical calibration and verification periods. Similar to observed data, streamflow simulated using historical time series of RCMs in Arc SWAT. If simulated streamflow values lie within the range of baseline uncertainty bound (95PPU) value obtained using observed climate data, the candidate RCMs can be used in the attribution process of flood change in the study area. If the simulated discharge falls outside the uncertainty bound, the climate model is rejected from candidate RCMs for future climate impact analysis.

Climate models meeting the above criteria were assumed to be suitable as members of the ensemble in the climate change impacts on hydrology. An ensemble means of discharges and other water balance components simulated using the selected climate models can be used to assess the projected climate change impacts on the flood events of the Wabi Shebele River Basin.

7.2.4. SWAT Model and Separation strategy

The SWAT model is a watershed-scale and physically based distributed hydrological model (Arnold et al., 1998; Neitsch et al., 2005; Abbaspour et al., 2007), developed to simulate the impact of land management practices on hydrology and water quality under complex watersheds with heterogeneous soil and land use conditions. In recent decades, it has been widely used for water cycle simulation and water resources management, especially for the analysis of streamflow variation under climate change and LULC change (Adamu 2014; Guo et al., 2016; Näschen et al., 2019; Camici et al., 2014; Schulze 2000; Gaur et al., 2020). In this study, the hydrologic model is used to see the impact of LULC change in the Wabi Shebele basin. Three different land use and

land cover map information from different decades are fed to the model to simulate streamflow. The changes in flood discharge due to LULC change are used for analysis. The optimum parameters of the SWAT model are determined by sensitivity analysis, which assesses the sensitivity between a parameter and other parameters in different areas. Based on parameters available for water production identified by Arnold et al. (2012) and preliminary identification in the SWAT model (Appendix E), SWAT-CUP global sensitivity analysis is conducted to select the most sensitive parameters for watersheds. The p-value and t-statistic were used to eliminate non-sensitive parameters from the calibration process. The higher the absolute value of t-stat and the smaller the value of p-value, the more sensitive is the parameter (Abbaspour et al., 2007; Moreira et al., 2018).

Separation Strategy

In this chapter, the SWAT model is combined with a separation method to separate the contributions of LULC change and climate change to the streamflow as proposed by Guo et al. (2016). Simulation results and measured data under different conditions of climate and land use are compared using this strategy. For instance, taking two conjoint periods (defined as the period I and II) and two land use conditions (defined as land use A and B) into consideration, four annual streamflow obtained under four conditions with different climate change and LULC change in the SWAT simulation, as following: Q1 for the period I and land use A; Q2 for the period I and land use B; Q3 for period II and land use A; Q4 for period II and land use B. Therefore, the difference between Q1 and Q2 is caused by the different conditions of land use, defined as ΔQL. Similarly, the difference between Q1 and Q3 is caused by the different conditions of climate, defined as ΔQC, and ΔQ is used to evaluate the difference caused by both climate change and land-use change, here the difference between Q1 and Q4 is used, and yields:

$$\Delta Q_L = Q_2 - Q_1 \tag{7.2}$$

$$\Delta Q_C = Q_3 - Q_1 \tag{7.3}$$

$$\Delta Q = Q_4 - Q_1 \tag{7.4}$$

$$\Delta Q_m = Q_L + Q_C \tag{7.5}$$

Theoretically, $\Delta Q = \Delta Q_m$. Subsequently, the impact of climate change on streamflow η_C and that of land-use change η_L can be separately calculated by:

$$\eta_C = \left(\frac{\Delta Q_C}{\Delta Q_m}\right) * 100\% \tag{7.6}$$

$$\eta_L = \left(\frac{\Delta Q_L}{\Delta Q_m}\right) * 100\% \quad (7.7)$$

Six flood variables are extracted from simulated discharges under different climate changes and LULC change conditions. The impact level of climate change and LULC change are analyzed in each index. These flood indices are: Annual maximum discharge (AMAX), Peak over threshold (3rd quartile) frequency (POTF), Peak over threshold (3rd quartile) magnitude, Seasonal peak discharge for winter (SMW), spring (SMSp), and summer (SMSu) used to define the extreme river flow.

7.2.5. Flood Indices analysis

To quantify flood hazard, I calculated three flood indices from simulated daily flow rate at each sub-basin outlet: flood exceedance probability index (FEPI), flood hazard index (HI), and flood frequency index (FFI). These indices represent the magnitude, duration and frequency of flood hazard respectively. Flood characteristics can be derived from time series of observed or simulated hydro-meteorological variables using a user-defined threshold level. A peak over the threshold of a 2-year return period for wet season streamflow was used in all indices because it was used as a proxy to bank full discharge and threshold for flood events in past studies (BCEOM 1973; IWMI 2015).

Following Cheng et al. (2013) and Xu et al. (2017), flood exceedance probability index is defined as the probability of daily discharges above the 2-year flood, calculated as the fraction of days with simulated streamflow above or equal to 2-year flood in a given year (January-December), then averaged across the simulation period, expressed as a percentage (Equation 7.8). Flood hazard Index (HI) is the probability of several days in a study period of 18 years when the stream outflow (Qi) in respective climate change conditions would exceed the bank full discharge volume (Qo) in current climate conditions (Equation 7.9). The flood frequency index (FFI) is the average number of flood events in a water year across the observation period (Equation 7.10). For historical and the two different future climate approaches, I calculated 2-year return period flood values based on the present climate simulation (the baseline or historical scenario output of each climate model). The flood exceedance probability index (FEPI) is calculated using:

$$FEPI = \frac{\sum_{i=1}^{N} FEPi}{N} * 100 \quad (7.8)$$

$$FEPi = \frac{D_i}{D_y}$$

$$HI = P(Q_i > Q_o) = \frac{Days\ when\ Q_i > Q_o}{365\ days\ a\ year * 18\ years} \quad (7.9)$$

$$FFI = \frac{\sum_{i=1}^{N} FFi}{N} \quad (7.10)$$

Where: FEPi is the flood exceedance probability of year i; Di is the number of days when a flood happens (discharge is greater or equal to the 2-year flood) in the year i; Dy is a total number of days in one year (365 for non-leap year, 366 for leap year); FEPI is an average flood exceedance probability for a sub-basin; P is probability; Qi is stream outflow in climate change conditions; Qo is stream bank full discharge in current climate conditions; FFi represent a quantity of flood events in water year i; FFI is the average Flood Frequency Index for a sub-basin and N is a total number of years in simulation period and.

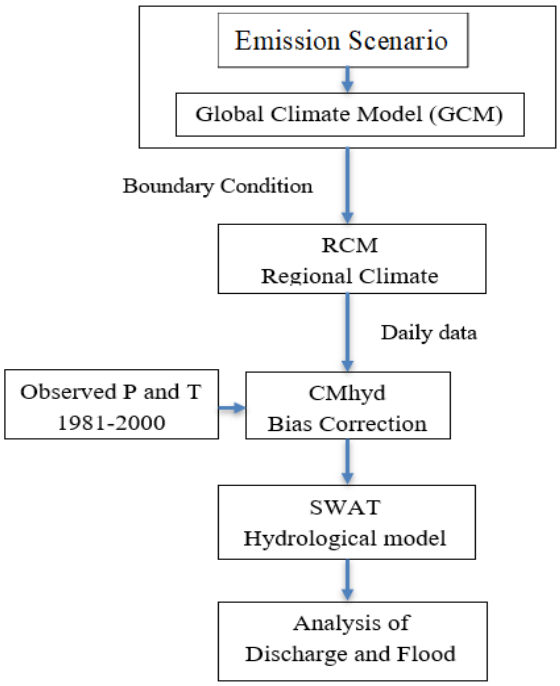

Figure 7-1 The study methodologies used in the paper. T is the air temperature, and P is the precipitation

Flood indices for each of the 11 climate change scenarios are compared to the 18-year baseline condition to test climate sensitivity. For each model in the climate model ensemble, I compared the flood indices under future conditions (2041-2060 and 2081-2100) to the historical station record (1981-2000). Findings are presented as a percentage change in flood indices between future and historical conditions to assess if the flood hazard of each sub-basin increases or decreases under climate change. Overall methodology used in this section is summarized in Figure 7-1.

7.3. Results and Discussions

7.3.1. SWAT Model Calibration and Parameter sensitivity analysis

For model calibration and validation, the observed monthly streamflow data were used from 1988 to 2000 with three years warming period. Figure 7-2 (a–c) presents the time series plot for corresponding observed and calibrated/validated simulated streamflow and uncertainty bands with statistical values at gauging stations. The values of performance measures for the calibration of Wabi at Dodola station were NSE = 0.74, R^2=0.74, and Pbias=-3.0%, respectively. The values of uncertainty measures for the calibration at Dodola station were p-factor =0.50 and r-factor = 0.76. For the validation at Dodola station the values of performance measures were NSE=0.74, R^2=0.74, and Pbias =-2.1% and uncertainty measures were p-factor = 0.70 and r-factor= 0.92, respectively. The negative value of Pbias shows the underestimation of simulated streamflow at Dodola station during calibration and validation. At Legehida station, the values of performance measures during calibration were NSE=0.61, R^2=0.64, and Pbias =-4.3% (underestimation) and uncertainty measures were p-factor=0.48 and r-factor=0.65, respectively. However, during validation the values of performance measures NSE=0.65, R^2=0.62, and Pbias=-0.27% (underestimation) and uncertainty measures were p-factor=0.46 and r-factor =0.38, respectively. At Gode station, the values of performance measures during calibration were R^2=0.40, NSE=0.20 and Pbias =-29.4% (underestimation) and uncertainty measures were p-factor=0.28 and r-factor=0.54, respectively. However, during validation the values of performance measures R^2=0.26, NSE=0.01 and Pbias=-37.6% (underestimation) and uncertainty measures were p-factor=0.18 and r-factor =0.61 respectively.

a)

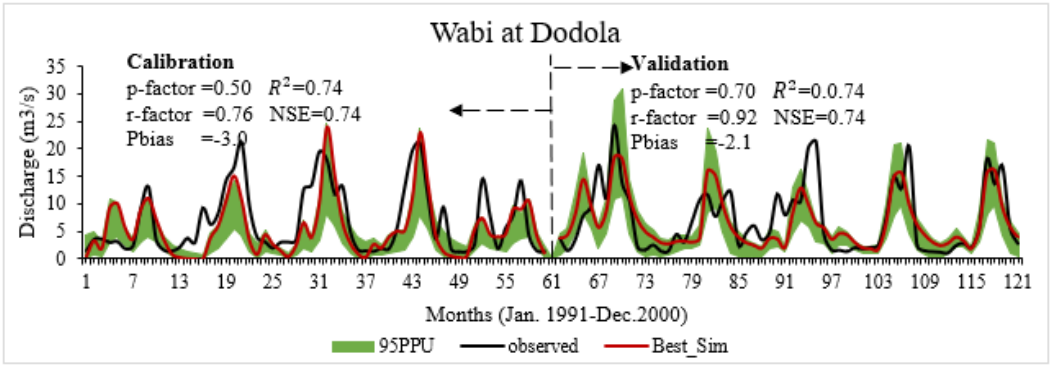

b)

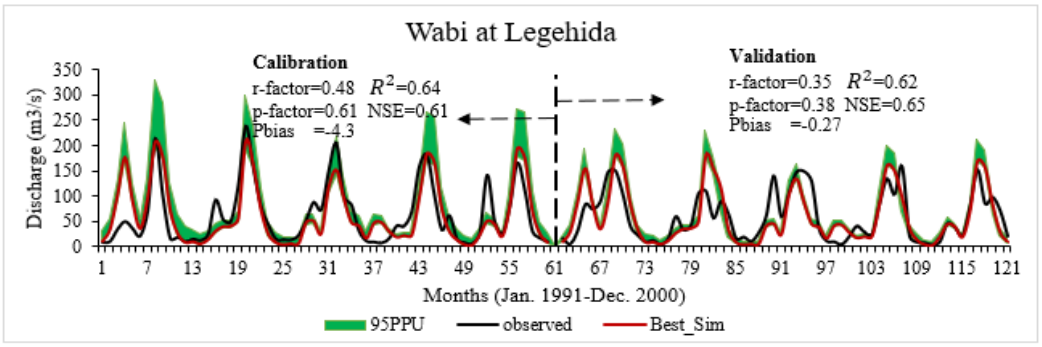

c)

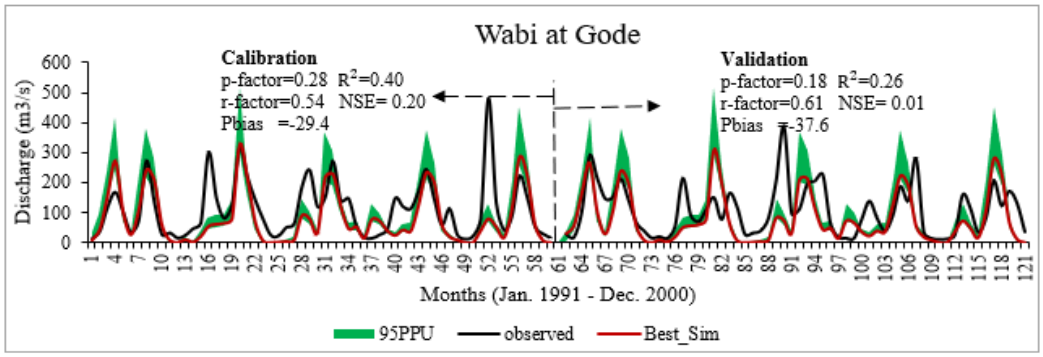

Figure 7-2 Observed, best-simulated hydrographs and 95PPU band in calibration and validation periods

The results indicate that most of the observations with different parameters are bracketed by the 95PPU (i.e., p-factor ≥ 0.5 and r-factor < 1.5), signifying SUFI-2 captures the model behavior. In terms of R^2 and NSE, the simulations give the value related to 0.6, which indicates that the SWAT model looks better for the prediction of discharge in the Wabi Shebele River Basin (as per Abbaspour et al., 2007), and the final parameter ranges were the best solution obtained for the basin. Most of the observed values during the calibration and validation were within the boundaries of 95PPU, which indicates that SWAT model uncertainties were falling within the permissible limits.

Parameter sensitivity analysis

The sensitivity of streamflow to the model parameters is checked through global sensitivity analysis performed using SUFI-2 of SWAT-CUP out of 20 model parameters identified for streamflow prediction in literature (i.e., Moreira et al., 2018; Narsimlu et al., 2015; Neitsch et al., 2005) (Table 7-4). The upper/lower limit of parameters used in the SWAT model selected from Swat- user manual by Arnold et al. (2012) (Appendix E).

Based on the results obtained from the global sensitivity analysis, the first six parameters are found to be very sensitive (p-value< 0.05) in Wabi Shebele River Basin (Table 7-4). Griensven et al. (2006) classified parameters regarding their sensitivity based on their increasing hierarchical parameters position. They categorized parameters as very important (1^{st}), important (2^{nd} -6^{th}), slightly important (7^{th} -14^{th}), and not important (15^{th} -20^{th}). From Table 7-4, it is evident that model parameters contributed to water production distributed at three parts of Wabi Shebele basin watersheds: in the northwestern highland of the basin surface parameters (i.e., SLSUBBSN.hru, HRU_SLP.hru, and CANMX.hru) and groundwater parameters (i.e., GWQMN.gw, RCHRG_DP.gw, and GWREVAP.gw) are the most significant parameters in water production; in the middle and northeastern part of the basin soil parameters (i.e., ESCO.hru, SOL_K sol and SOL_Z.sol) and surface parameters (i.e., SLSUBBSN.hru and HRU_SLP.hru) are the most significant parameters; and in the lower downstream part of the basin surface parameters (i.e., SLSUBBSN.hru, HRU_SLP.hru, CANMX.hru) and soil parameters (i.e., SOL_K sol and SOL_Z.sol) are the most significant water production parameters identified in this study.

Table 7-3 Sensitive parameters at watersheds

Station	Rank of Parameter	Parameter	Fit	minimum	maximum	t-stat	p-value
Wabi at Dodola	1	V__SLSUBBSN.hru	108.68	81.81	130.52	11.03	0.00
	2	V__RCHRG_DP.gw	0.13	0.11	0.34	-6.09	0.00
	3	R__HRU_SLP.hru	0.53	0.19	0.56	-4.01	0.00
	4	V__CANMX.hru	0.05	0.00	1.57	-3.25	0.00
	5	R__SOL_K(..).sol	0.08	0.03	0.25	-3.04	0.00
	6	R__CN2.mgt	-0.07	-0.16	0.02	-2.21	0.03
Maribo	1	A__GWQMN.gw	-347.46	-659.74	21.60	-18.40	0.00
	2	V__ESCO.hru	0.99	0.71	1.00	7.65	0.00
	3	V__ALPHA_BNK.rte	0.21	0.00	0.45	7.09	0.00
	4	V__SLSUBBSN.hru	142.52	80.97	150.00	-4.06	0.00
	5	R__SOL_AWC(..).sol	-0.15	-0.16	0.01	-4.03	0.00
	6	V__CANMX.hru	2.57	1.91	7.30	-2.16	0.03
Robe	1	V__SLSUBBSN.hru	53.95	25.53	78.00	4.19	0.00
	2	V__CH_N2.rte	0.28	0.14	0.42	2.16	0.03
	3	V__ALPHA_BNK.rte	0.90	0.67	1.00	1.84	0.07
	4	V__RCHRG_DP.gw	0.02	0.00	0.28	1.56	0.12
	5	A__GWQMN.gw	-363.99	-1000.00	-324.60	-1.25	0.21
	6	A__GW_REVAP.gw	0.00	-0.01	0.02	-1.19	0.23
Wabi at Legehida	1	R__SOL_AWC(..).sol	-0.02	-0.16	0.02	23.39	0.00
	2	V__SLSUBBSN.hru	140.29	125.20	150.00	9.09	0.00
	3	V__RCHRG_DP.gw	0.00	0.00	0.15	-8.57	0.00
	4	R__SOL_K(..).sol	-0.03	-0.07	0.07	-7.73	0.00
	5	R__HRU_SLP.hru	0.05	0.00	0.16	-7.17	0.00
	6	V__ESCO.hru	0.07	0.00	0.16	-2.87	0.00
Erer	1	V__ESCO.hru	0.04	0.00	0.27	-10.46	0.00
	2	R__SOL_Z(..).sol	0.20	0.06	0.24	7.84	0.00
	3	R__HRU_SLP.hru	0.01	0.00	0.32	-5.95	0.00
	4	V__RCHRG_DP.gw	0.54	0.02	0.55	-5.22	0.00
	5	V__SLSUBBSN.hru	99.11	77.07	125.52	5.15	0.00
	6	R__SOL_AWC(..).sol	0.21	0.12	0.25	3.78	0.00
Jijiga	1	R__SOL_Z(..).sol	-0.08	-0.11	0.03	7.35	0.00
	2	V__ESCO.hru	0.13	0.09	0.27	-5.75	0.00
	3	R__SOL_AWC(..).sol	-0.14	-0.21	-0.12	4.52	0.00
	4	V__SLSUBBSN.hru	144.51	118.84	150.00	3.78	0.00
	5	V__ALPHA_BF.gw	0.39	0.28	0.53	-2.34	0.02
	6	A__REVAPMN.gw	-8.13	-28.99	11.32	1.78	0.08
Wabi at Gode	1	V__SLSUBBSN.hru	140.81	112.98	150.00	24.01	0.00
	2	R__HRU_SLP.hru	0.21	0.00	0.32	-18.34	0.00
	3	R__SOL_K(..).sol	-0.25	-0.25	-0.11	-13.25	0.00
	4	V__CANMX.hru	2.77	0.00	3.33	6.13	0.00
	5	R__SOL_Z(..).sol	0.18	-0.07	0.19	4.05	0.00
	6	R__SURLAG.bsn	-0.10	-0.19	0.01	2.20	0.03

V is the existing parameter value to be replaced by a given value. R is the existing parameter value * (1 + a given value) whereas A represents additional value to be added to the existing parameter value (Abbaspour et al. 2007).

7.3.2. Performance of RCMs in predicting climate variables for the study area

The daily precipitation and temperature simulations of the climate models from the CORDEX-Africa, RCMs datasets are averaged over the watershed area, and their performance is evaluated

using statistical parameters. Table 7-5 shows the absolute values and differences of RCMs from the meteorological observations of these parameters.

Precipitation: All of the CORDEX-Africa RCMs, bias-corrected data sets using the meteorological observation overestimated the number of rainy days (Table 7-5). Although the differences in values to the gauge observation are considerably less, almost all the CORDEX-Africa RCMs underestimated average daily precipitation and standard deviation. However, most RCMs, except GFDL-ESM2M/ RCA4 and MIROC-MIROC5/RCA4, overestimated maximum daily rainfall. The regional climate models such as GFDL-ESM2M/ RCA4 and MIROC-MIROC5/RCA4 showed underestimation on extreme values of the average maximum daily precipitation.

Temperature: All bias-corrected RCMs on temperature showed similar to average maximum temperature with ground-based observed maximum temperature in the study area (Table 7-5). However, extremely high temperatures decrease from the observed temperature in CanESM2/RCA4, CM5A-MR/RCA4, and CNRM-CM5/RCA4 while indicates the increment in GFDL-ESM2M/RCA4, and MIROC-MIROC5. Further, the standard deviation of maximum temperatures is estimated underestimation in all RCMs.

Table 7-4 RCMs daily precipitation (mm) and Temperature (^{o}c) parameter values and differences to gauged values from the period 1981-to 2000

Variable	Model	Absolute values				Differences to gauge values			
		nDays > 1mm	Ave.	Max.	SD	nDays > 1mm	Ave.	Max.	SD
Precipitation	Gauge observed data	96.4	8.3	73.0	8.3	0	0	0	1
	CORDEX AFRICA RCA4 RCMs								
	CanESM2	109.9	7.8	109.4	7.6	13.6	-0.5	36.4	-0.7
	CM5A-MR	111.4	7.7	76.7	7.3	15	-0.6	3.7	-1.0
	CNRM-CM5	112.2	7.7	82.3	7.5	15.9	-0.6	9.3	-0.8
	GFDL-ESM2M	112.9	7.6	63.0	7.6	16.6	-0.7	-10.0	-0.7
	MIROC-MIROC5	111.4	7.4	70.1	7.8	15	-0.9	-3.0	-0.5
Tmax	Gauge observed data		23.2	27.4	1.9		0	0	1
	CORDEX AFRICA RCA4 RCMs								
	CanESM2		23.2	26.4	1.4		0	-0.9	-0.5
	CM5A-MR		23.2	26.5	1.4		0	-0.9	-0.5
	CNRM-CM5		23.2	26.7	1.4		0	-0.7	-0.5
	GFDL-ESM2M		23.2	27.6	1.5		0	0.2	-0.4
	MIROC-MIROC5		23.2	28.2	1.5		0	0.8	-0.4

nDays > 1mm=Average number of days in a year with precipitation > 1 mm; Ave. = average daily precipitation; Max. =maximum daily precipitation; SD = standard deviation, Differences are computed by division (SDsim/SDgauge) for SD and subtraction for the other parameters. Where SDsim and SDgauge are the standard deviations of the climate models' and gauge precipitation, respectively.

Streamflow: Hydrologic evaluations of the climate models are performed in the Wabi Shebele River Basin. Figure 7-3 shows the analysis results in Wabi Shebele at Dodola station. The performance of the RCMs in simulating average monthly discharges varied quite considerably for the watershed. Statistical performance indicators are used to compare the model streamflow using observed meteorological data to the discharges simulated using the climate models. All streamflow simulations using RCMs datasets underestimated the average annual discharges with small negative Pbias values (Figure 7-3). MIROC-MIROC5 shows the maximum deviation with Pbias of - 26.626% for the watershed. However, all other RCMs resulted in reasonable streamflow simulations with small negative Pbias of less than -20%. Furthermore, all the RCMs can represent seasonal streamflow patterns for the Wabi Shebele watershed with NSE and R^2 values greater than 0.75 and 0.92 respectively.

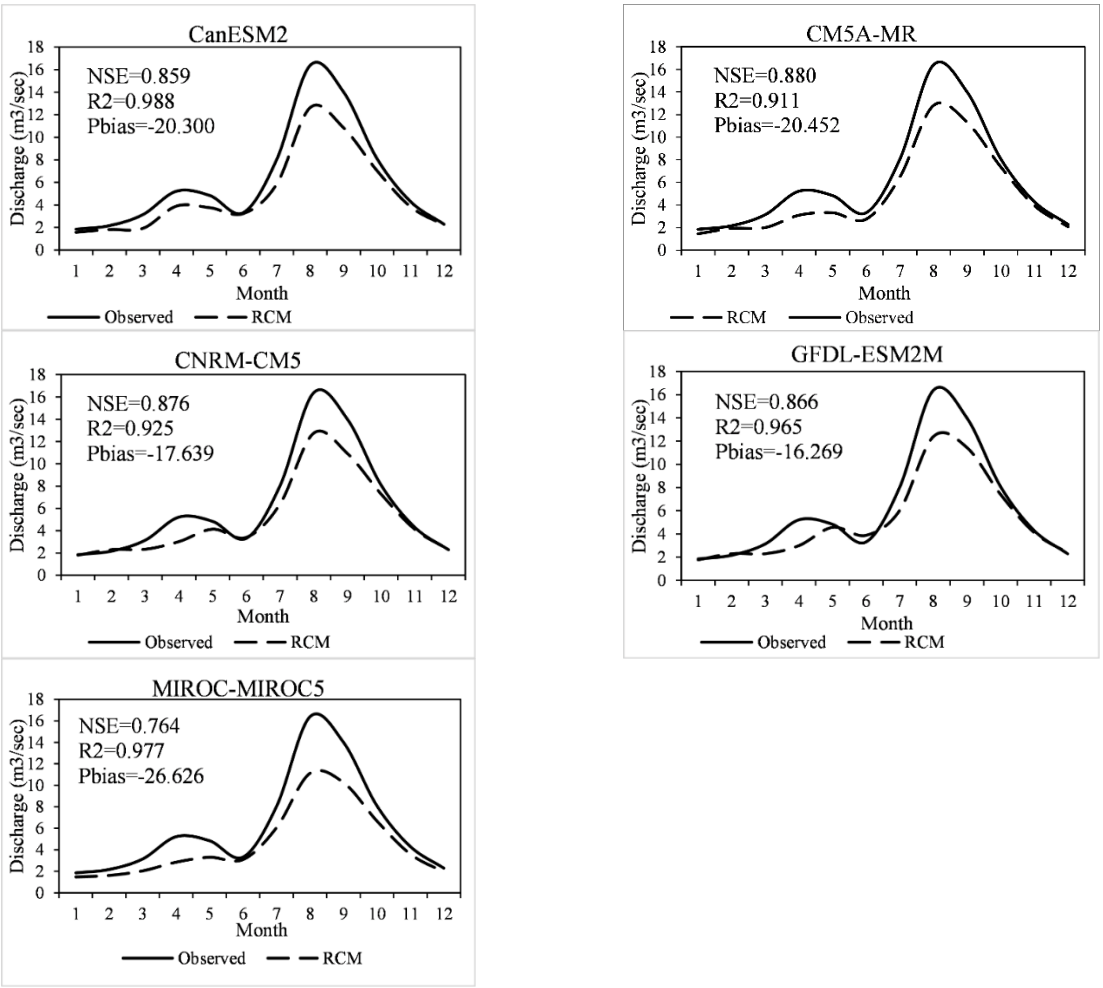

Figure 7-3 Average monthly streamflow simulated in Wabi Shebele at Dodola gauging station using the climate models from CORDEX RCMs datasets during the reference period from 1981 to 2000

7.3.3. Uncertainty analysis

Uncertainties of climate change impact on hydrology arise from different sources: data quality, climate models and emission scenarios selected, the downscaling method used, and the hydrological model applied. Data scarcity and reliability to calibrate the hydrological model is the first source of uncertainty in the analysis. To minimize this uncertainty, checking and filling missed data using weather generators were carried out before calibration and validation of the hydrological model in this study.

Climate model uncertainty arises due to the response of different climate models to produce dis-similar changes in climate in the presence of the same radiative forcing. Relative to GCMs outputs, RCM output reduces uncertainties since it gives high-resolution climate information and provides a better description of orographic, land-surface contrast, and land-surface characteristics. Scenario uncertainty arises due to imperfect knowledge of the external factors affecting the climate system, e.g., future emission of greenhouse gasses. There are four groups of individual scenarios developed by IPCC in 2014 to supersede SRES (IPCC 2014). Each scenario consists of a specific radiative forcing projection and makes assumptions about future population, GDP, and energy use, based on the radiative forcing. Hence, choosing among the scenarios also adds to the uncertainty.

The assumptions involved in the hydrologic model simulations are also a portion of the uncertainty. As described in section 7.3.1, the determination of the impacted streamflow is only based on the precipitation and temperature changes in the future. The other climatic variables: such as wind speed, solar radiation, and relative humidity, were assumed to be constant throughout the future simulation periods. Even though it is definite that land-use changes in the future, it is also assumed constant. But these assumptions can lead to a certain level of additional uncertainty. Therefore, all types of uncertainties discussed above propagated on the future predicted discharge volume. Thus, the uncertainty presented in the model and model outputs kept on cumulating while progressing towards the final result of the study.

The historical record of five RCMs ensembles is used as the baseline condition for comparison within the climate datasets with observed climate data sets. Based on simulated flow using available observed data, 95%PU uncertainty analysis is performed in SUFI-2 of SWAT-CUP interface and taken as reference values. The 95%PU performed based on RCMs that fall within the range of reference values are identified as the candidate RCMs and used in the attribution process of flood change. From Figure 7-4 all simulated streamflow using RCMs falls within 95%

probable uncertainty bands, estimated using gauged meteorological data. All RCMs incorporated in this study can show similar variability patterns with simulated streamflow from observed meteorological data. It indicates that all RCMs sampled in this study can be used for climate impact analysis of hydrology in the study area.

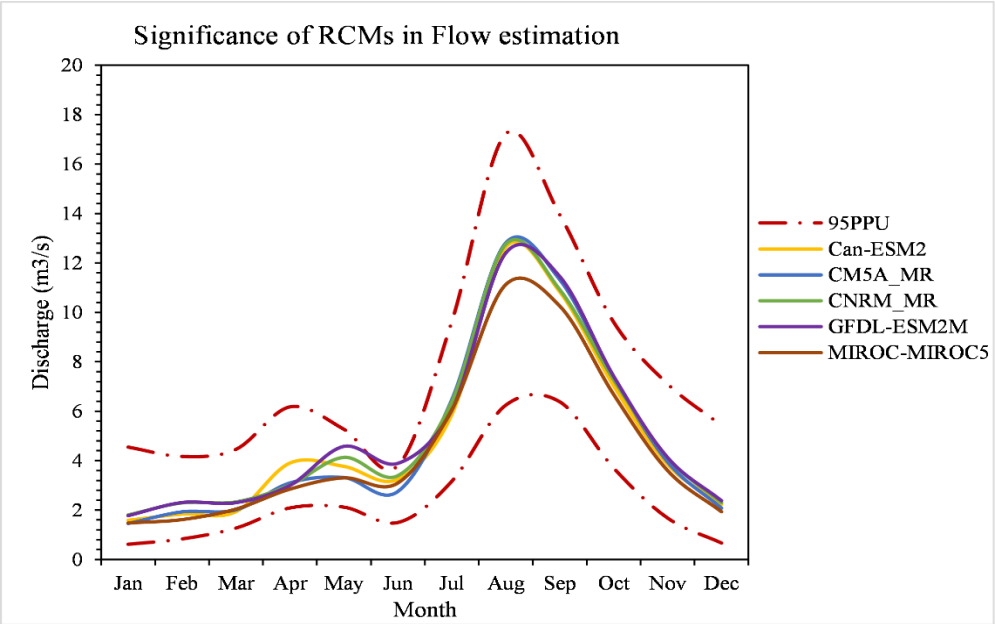

Figure 7-4 Significance of climate models in the river flow estimation at baseline period (1981-2000) and uncertainty bands of Wabi Shebele river

The future streamflow of the Wabi Shebele river is significantly impacted by climatic change in most of the months (Figure 7-5). The future streamflow predicted at seasonal and annual flows at the 2050s and 2090s are falls outside the hydrologic model uncertainty bands. In all gauging stations, future flows at the 2050s fall below lower uncertainty bands. In the winter season (ONDJ), flows are estimated above upper uncertainty bands in all sample gauging stations in the 2090s. However, future flows are estimated below lower uncertainty bands in the spring (FMAM) and summer (JJAS) seasons at all gauging stations. For Wabi Shebele at Dodola station (upstream), the future river flows in January, February, and September varies within uncertainty bands. However, predicted future flows in the middle and lower Wabi Shebele river change outside uncertainty bands. Furthermore, flood season peak month shifted for future case following rainfall pattern in the future. It means that the future flow of the Wabi Shebele river will be under the impact of climatic change. Therefore, it might be possible to conclude that the climatic change impact will be significant for future river flows in the Wabi Shebele river in all seasons, especially

in the middle and downstream of the river. The cumulative uncertainty propagation is the worst in predicted future flow volume in seasonal and annual aggregation levels.

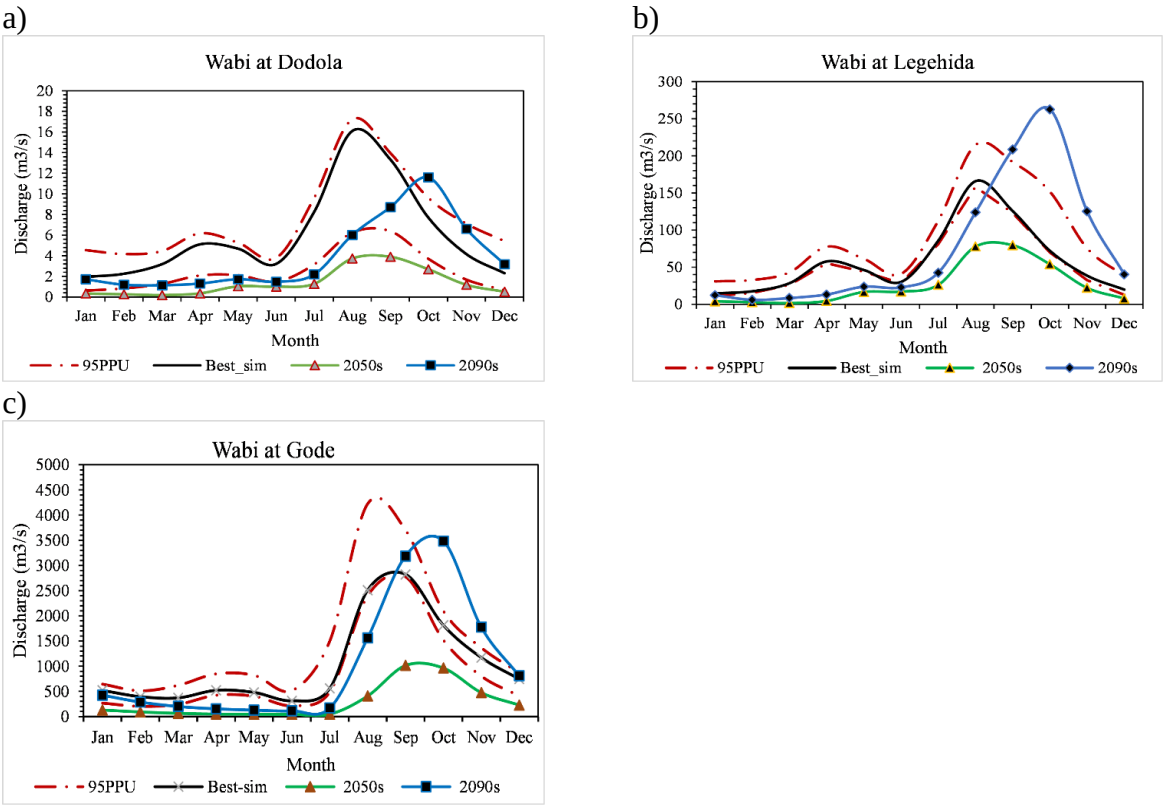

Figure 7-5 Significance of future impacted river flow and uncertainty bands of Wabi Shebele river at three stations

7.3.4. Flood hazard under climate change

Flood hazard under the baseline condition

The spatial distribution of all flood indices for the baseline case (T+0 ^{o}C, P+0%) agrees across the basin and relatively shows greater flood hazard in the downstream part of the Wabi Shebele river (Table 7-6). The relatively high flood indices in the downstream gauging station at Gode may be explained by drainage size, where most of the main tributaries contribute flood discharges to this subbasin, Appendix B (Figure B.1). Drainage size is one of the major driving factors for flood discharge increment confirmed in different studies, e.g., (Al-Rawas and Valeo 2010; Huang 2020). The spatial distribution of flood hazard under baseline conditions confirms with the SWAT model captured the impact of drainage size on stream discharge and the downstream area of the Wabi Shebele River Basin could be a focus area for flood mitigation.

Table 7-5 Flood indices at baseline scenario (T +0^{o}C, P+0%) (1983-2000)

Subbasin	FEPI (%)	HI (%)	FFI
Wabi at Dodola	25.17	1.36	91.9
Wabi at Legehida	24.32	1.35	88.8
Wabi at Gode	25.30	1.40	91.9

Future flood hazard under climate sensitivity testing

The climate sensitivity test reveals overall flood hazard under different scenarios and areas sensitive to climate change. As expected, all gauging stations exhibited the highest discharges when precipitation increased by 20% with no increase in temperature (scenario T+0^{o}C, P+20%), and all indices increased (Figure 7-6). In contrast, all indices are indicated to decreasing when temperatures increased by 3^{o}C (scenario T+3^{o}C P+0%) with index value less than or equal to zero. As shown in Figure 7-6 a gradual change is observed in flood discharge between scenario T+0^{o}C P+20% and scenario T+1^{o}C P+20%. It is also evident that increasing the mean precipitation resulted in a trend with a steep slope, whereas increasing the mean temperature resulted in a trend with a gentle slope (Figure 7-6). Flood hazards in sub-basins are summarized for each index in Table 7-7. Generally, more precipitation tended to perpetuate flood hazard, while warmer temperatures reduce flood hazard. Furthermore, this demonstrates the need to evaluate flood hazard concerning both temperature and precipitation change.

When precipitation increased by 10% or 20%, almost all subbasins saw flood index increases from the baseline. Warmer temperatures caused a decrease in water yield, which counteracted the increase in precipitation. Therefore, in the sub-basins more sensitive to temperature change, flood indices were lower compared to the baseline scenario despite precipitation increases. Exceptionally in the upper subbasin at Wabi Dodola station, flood exceedance probability and flood hazard indices exhibited increasing tendency when temperature increased, indicating that headwaters were more sensitive to higher temperatures in terms of these two components of flood hazard. However, for both downstream gauging stations, Wabi at Legehida and Wabi at Gode, the level of change seems to be consistent across the watershed, suggesting that precipitation change has more impact on flood indices than temperature.

a)

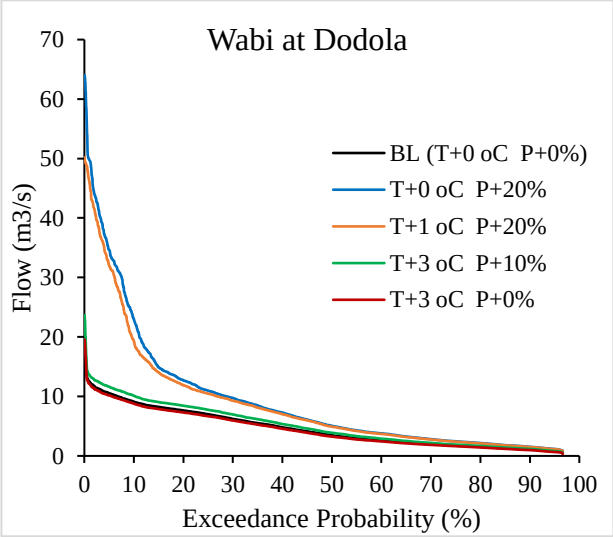

b)

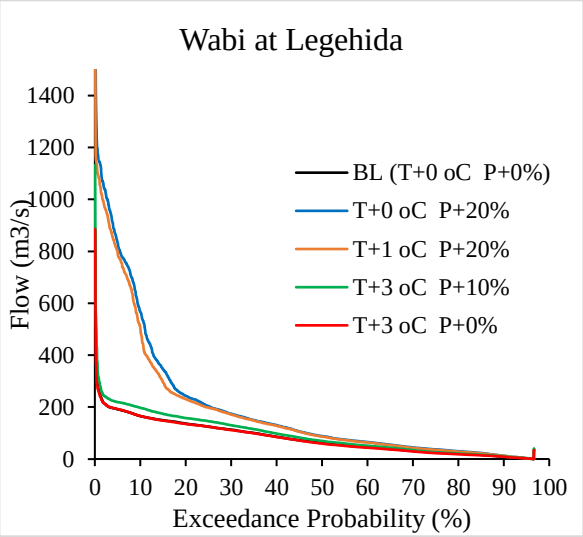

c)

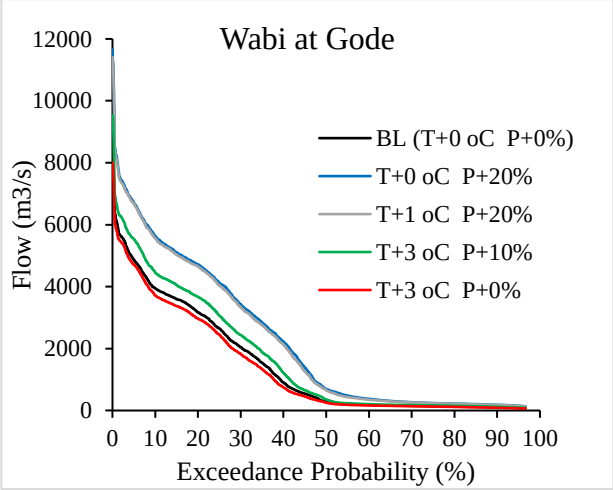

Figure 7-6 Comparison between exceedance probability of daily streamflow for baseline scenario (T+0^{o}C P+0%) and different climate scenarios

Table 7-6 Summary of flood indices under climate change conditions (condition of climate variables of temperature & precipitation)

Sub basin	Climate Change Condition		Flood Indices			Difference to Baseline flood indices (T+0°C, P+0%)		
	Temp. (+°C)	Prec. (+ %)	FEPI (%)	HI (%)	FFI	FEPI (%)	HI (%)	FFI
Wabi at Dodola	0	0	25.17%	1.36%	91.9	0	0	0.00
	1	0	25.17%	1.39%	91.9	0.000%	0.030%	0.00
	2	0	25.17%	1.40%	91.9	0.000%	0.040%	0.00
	3	0	25.17%	1.40%	91.9	0.000%	0.040%	0.00
	0	10	25.17%	1.40%	91.9	0.000%	0.040%	0.00
	0	20	25.17%	1.40%	91.9	0.000%	0.040%	0.00
	1	10	25.17%	1.40%	91.9	0.000%	0.040%	0.00
	1	20	25.17%	1.40%	91.9	0.000%	0.040%	0.00
	3	10	25.17%	1.40%	91.9	0.000%	0.040%	0.00
	3	20	25.17%	1.40%	91.9	0.000%	0.040%	0.00
Wabi at Legehida	0	0	24.32%	1.35%	88.8	0	0	0.00
	1	0	24.30%	1.35%	88.7	-0.020%	0.000%	-0.10
	2	0	24.30%	1.35%	88.7	-0.020%	0.000%	-0.10
	3	0	24.30%	1.35%	88.7	-0.020%	0.000%	-0.10
	0	10	24.30%	1.35%	88.8	-0.020%	0.000%	0.00
	0	20	24.40%	1.35%	89.0	0.080%	0.000%	0.20
	1	10	24.30%	1.35%	88.7	-0.020%	0.000%	-0.10
	1	20	24.35%	1.35%	88.9	0.030%	0.000%	0.10
	3	10	24.31%	1.35%	88.7	-0.010%	0.000%	-0.10
	3	20	24.33%	1.35%	88.8	0.010%	0.000%	0.00
Wabi at Gode	0	0	25.30%	1.40%	91.9	0	0	0.00
	1	0	25.17%	1.40%	91.9	-0.130%	0.000%	0.00
	2	0	25.17%	1.40%	91.9	-0.130%	0.000%	0.00
	3	0	25.17%	1.40%	91.9	-0.130%	0.000%	0.00
	0	10	25.17%	1.40%	91.9	-0.130%	0.000%	0.00
	0	20	25.17%	1.40%	91.9	-0.130%	0.000%	0.00
	1	10	25.17%	1.40%	91.9	-0.130%	0.000%	0.00
	1	20	25.19%	1.40%	92.0	-0.110%	0.000%	0.10
	3	10	25.17%	1.40%	91.9	-0.130%	0.000%	0.00
	3	20	25.17%	1.40%	91.9	-0.130%	0.000%	0.00

Future flood change under climate model prediction

The flow duration curves (FDC) for gauging stations are drawn to compare the exceedance probability of daily discharges between the observed (1981–2000) and projected climate to assess the flow patterns during 2041-2060 and 2081-2100 (Figure 7-7).

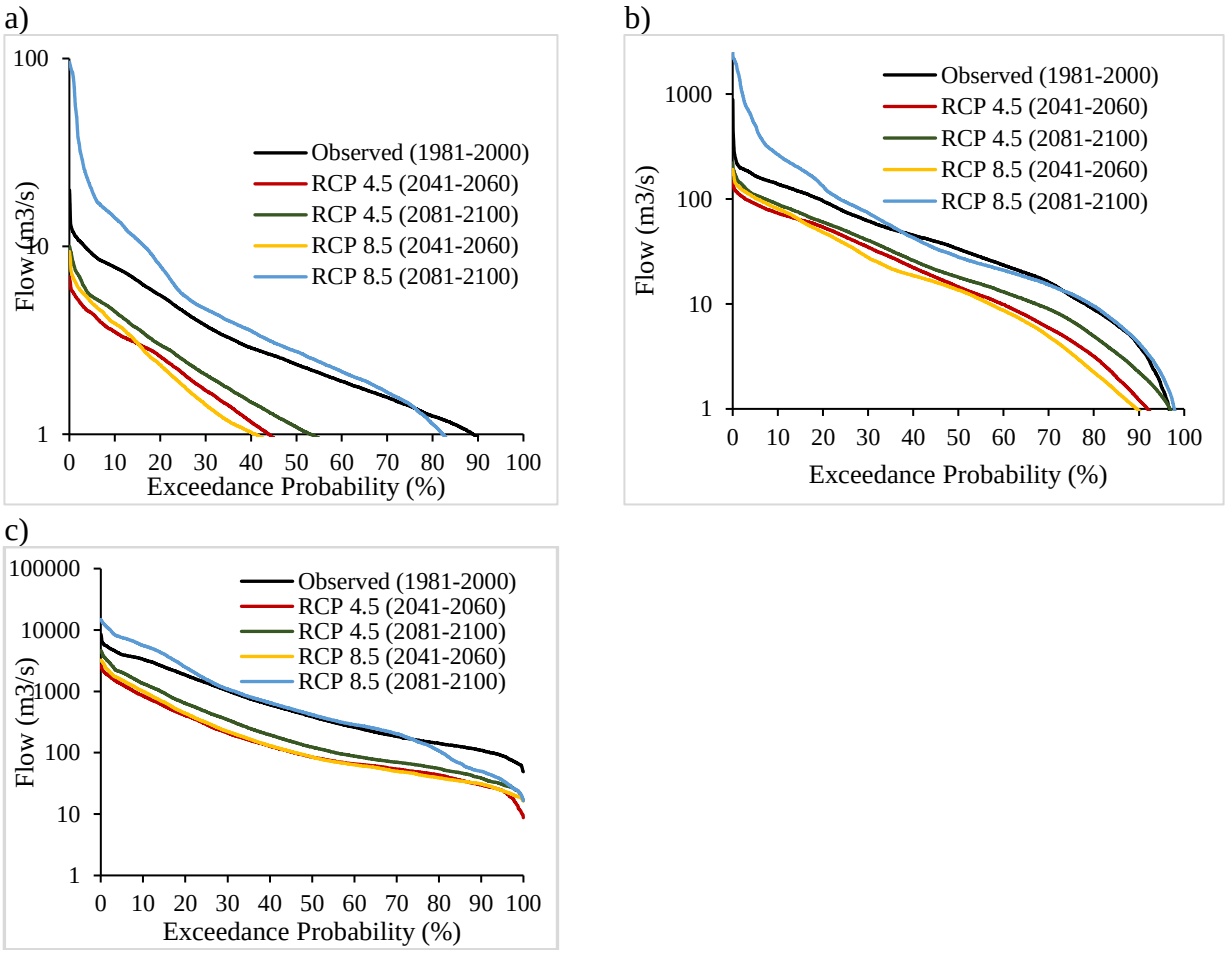

Figure 7-7 Comparison between exceedance probability of daily streamflow for observed and projected climate through flow duration curves (FDCs) using RCP 4.5 and RCP 8.5 scenarios at three gauging stations: a) Wabi at Dodola, b) Wabi at Legehida, and c) Wabi at Gode

It is evident from the figure that under the RCP 8.5 emission scenario, the magnitude of streamflow increases in 2081-2100 when all others are estimated below the observed scenarios. FDCs at upper gauging stations at Dodola and Legehida become steep slope, while FDCs at Wabi at Gode station show relatively flatter during Q30-Q90 (medium flows). A flat curve indicates that groundwater contributions to the stream reach are significant, that sustain the flow throughout the year (Chambers et al., 2017; Gaur et al., 2020). Additionally, FDCs at Gode station show a considerable increase in high flows (10% exceedance) during 2081-2100 relative to observed discharges (1981-2000).

A 2-year return period flood value is used as a threshold level to estimate flood characteristics during the reference period 1981-2000 and future climate scenarios. From extracted flood values,

three flood indices are estimated and compared in between all scenarios. As presented in Table 7-8, most of the flood simulated under future climate scenarios estimated flood indices below the reference period, except flood in the upper basin at Wabi at Dodola station, in which flood exceedance probability index (FEPI) increases in most of the future climate scenarios. Furthermore, the flood frequency index at Wabi Gode station shows a considerable increment between 2081-2100 in both scenarios.

Table 7-7 Summary of flood indices under future climate change conditions

Sub basin	Climate Change Condition (climate scenarios)	Flood Indices			Difference to Observed flood indices (1981-2000)		
		FEPI (%)	HI (%)	FFI	FEPI (%)	HI (%)	FFI
Wabi at Dodola	Observed (1981-2000)	49.98%	2.78%	182.6	0	0	0.0
	RCP 4.5 (2041-2060)	49.99%	2.78%	182.6	0.006%	0.000%	0.1
	RCP 4.5 (2081-2100)	49.96%	2.78%	182.5	-0.021%	-0.001%	-0.1
	RCP 8.5 (2041-2060)	49.99%	2.78%	182.6	0.006%	0.000%	0.1
	RCP 8.5 (2081-2100)	49.99%	2.78%	182.6	0.009%	0.000%	0.1
Wabi at Legehida	Observed (1981-2000)	50.00%	2.78%	182.6	0	0	0.0
	RCP 4.5 (2041-2060)	49.99%	2.78%	182.6	-0.006%	0.000%	0.0
	RCP 4.5 (2081-2100)	49.99%	2.78%	182.6	-0.003%	0.000%	0.0
	RCP 8.5 (2041-2060)	49.99%	2.78%	182.6	-0.007%	0.000%	0.0
	RCP 8.5 (2081-2100)	49.96%	2.78%	182.5	-0.032%	-0.002%	-0.1
Wabi at Gode	Observed (1981-2000)	50.00%	2.78%	182.6	0	0	0.0
	RCP 4.5 (2041-2060)	49.99%	2.78%	182.6	-0.005%	0.000%	0.0
	RCP 4.5 (2081-2100)	49.98%	2.78%	193.3	-0.019%	-0.001%	10.7
	RCP 8.5 (2041-2060)	50.00%	2.78%	182.6	-0.001%	0.000%	0.0
	RCP 8.5 (2081-2100)	49.99%	2.78%	193.4	-0.006%	0.000%	10.7

7.3.5. LULC changes and their impacts on Flood occurrence

The effects of LULC change on streamflow are distinguished by simulations of multi-year daily discharges using 1986, 1997, and 2016 land covers as presented in Table 7-9 and Figure 7-9. I used two different conditions to see effects of land use and cover changes on streamflow: condition one, streamflow change under LULC change at a short period of 12 years in between 1986 and 1997 and condition two, streamflow change under LULC change long period of 31 years in between 1986 and 2016.

Condition one

During the 12-years of LULC observation from 1986 to 1997 (Figure 7-8a and 7-8c), LULC is dominated by grassland, shrubland, bare land, and forest entire the basin. Increases in LULC

during this period occurred are in grassland, agricultural land, and barren land. These increments are occurred in three watersheds: Wabi at Dodola, Wabi at Legehidha, and Wabi at Gode. Exceptionally, the coverage of agricultural land increases almost in all sub-basins of the Wabi Shebele River Basin during this period. However, the coverage of forest, woodland, and shrubland steeply decreased in the period. The forest coverage is significantly dropped in the Erer watershed (Figure 7-8c), one of the main watersheds that contributes a large number of annual floods to the Wabi Shebele River Basin (MoWR 2003). From Table 7-9, flow simulated under condition one increases in those watersheds their agricultural land showed an increase, and decrease in forest coverage. The Wabi at Dodola, Maribo, Robe, and Erer watersheds exhibits this situation. In the upper Wabi Shebele basin at Dodola station, annual streamflow increases by 7% when the agricultural land increased by 2.66 factors.

Condition two

In the long period of 31 years of LULC observation from 1986 and 2016 (Figure 7-8b and 7-8d), LULC is dominated by woodland, shrubland, agricultural land, grassland, bare land, and forest entire the basin. Increases in LULC during this period occurred in shrubland, agricultural land, grassland, and barren land, whereas forest and woodland are LULC which shows decreases in this period. A significant change in this condition is observed on shrubland coverage. The shrubland showed increases in the long period from 1986 to 2016. However, it showed decreases during a short period in between 1986 and 1997. But others followed similar trends as condition one.

Out of ten LULC types analyzed in the study area, only three of them: agricultural land, grassland, and bare land showed growth in both conditions. The coverage of agricultural land was increased by 47.56% in condition one and by 48.63% in condition two. However, the forest coverage indicates a significant decrement in conditions one & two by 86.4% and 49.1%. Similarly, the study conducted by IWMI (2015) revealed that the forest degradation in the western upper Wabi Shebele basin by an average annual deforestation rate of 0.25%. The data analysis in Bale Eco-Region (i.e., upper Wabi Shebele basin) indicates a reduction in forest area (forest, woodlands, Erica forest) of about 2.3% between 2010 and 2014 (IWMI 2015). It is known that the deforestation and forest degradation in Ethiopia are mainly for the expansion of subsistence agriculture and grazing land. The reduction of forest cover amplifies flood events, as more rainfall directly turns into runoff instead of being slowed down or buffered by forests (IWMI 2015; Bradshaw et al., 2007). In the northeastern and downstream of the Wabi Shebele basin (i.e., Erer and Wabi at Gode

watersheds), simulated streamflow doesn't show significant changes with land-use change in both conditions as presented in Table 7-9 and Figure 7-9.

Flood indices calculated from simulated daily streamflow under different land-use and land-cover maps indicate a similar situation with annual average flow variations in the basin. In the middle and northwestern part of the basin, flood indices like AMAX, SMW, SMSp, SMSu, and volume indicated increasing as forest coverage showed decreasing trends (Table 7-10).

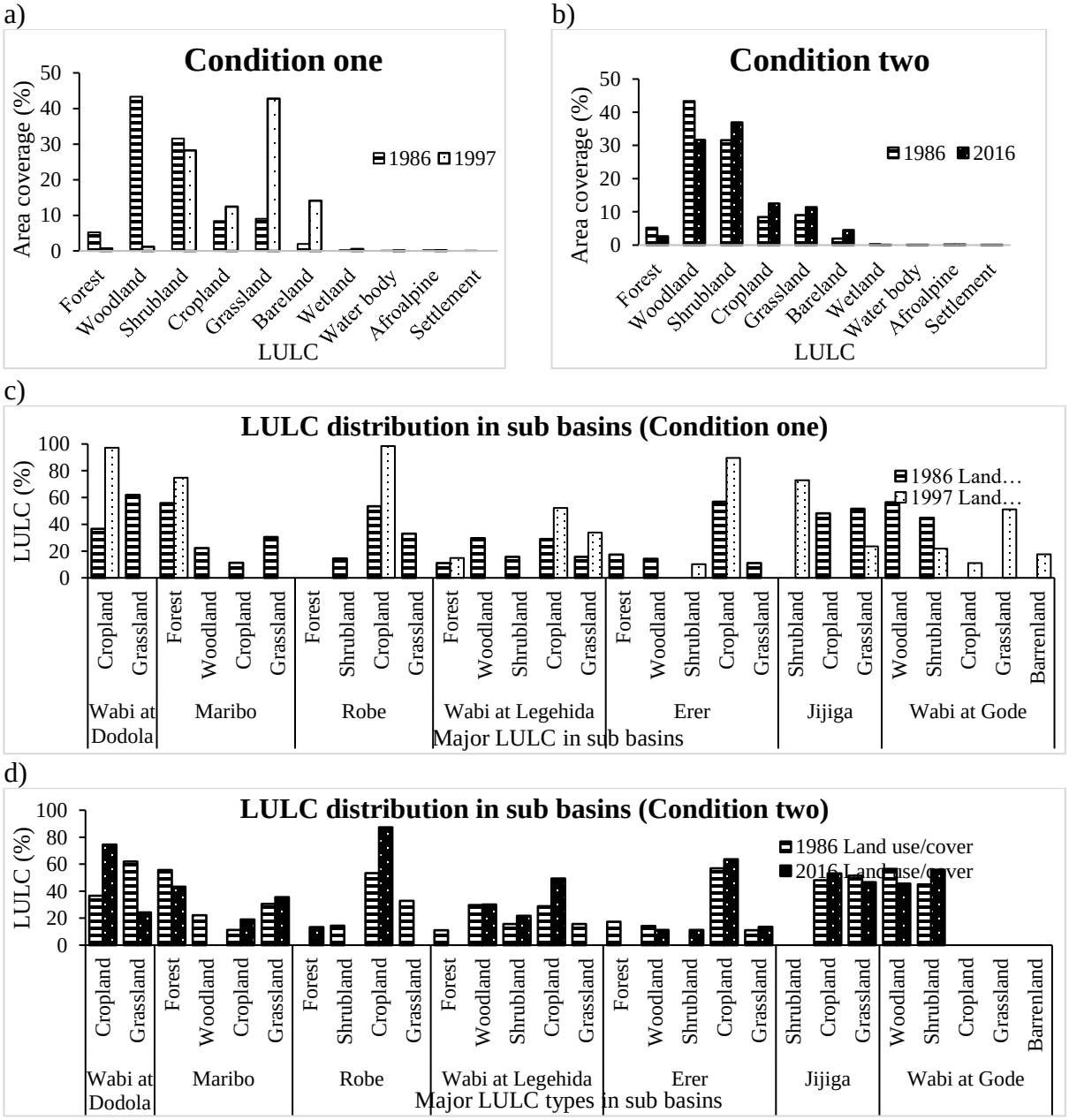

Figure 7-8 Major LULC distribution in Wabi Shebele basin and its sub-basins at two various conditions: condition one (a and c) in the short period between 1986 and 1997 and condition two (b and d) in the long period between 1986 and 2016

Table 7-8 Simulated average annual surface runoff (m^3/s) from different LULC maps under two conditions

S. No	Sub-basin	Condition one		change (m^3/s)	change (%)	Condition two		change (m^3/s)	change (%)
		1986	1997			1986	2016		
1	Wabi at Dodola	3.76	4.04	0.28	7%	3.76	3.82	0.06	2%
2	Maribo	2.59	2.68	0.09	3%	2.59	2.58	-0.01	0%
3	Robe	1.59	1.61	0.02	1%	1.59	1.6	0.01	1%
4	Wabi at Legehida	65.56	65.77	0.21	0%	65.56	67.18	1.62	2%
5	Erer at Babile	3.07	3.10	0.03	1%	3.07	3.07	0.00	0%
6	Jijiga	3.90	3.90	0.00	0%	3.90	3.91	0.01	0%
7	Wabi at Gode	143.42	125.42	-18	-2%	143.42	143.09	-0.34	0%

Table 7-9 Flood indices obtained from daily simulations for 1986, 1997, and 2016 land cover

Item	Maribo watershed			Wabi at Legehida watershed			Erer watershed			Wabi at Gode watershed		
	1986	1997	2016	1986	1997	2016	1986	1997	2016	1986	1997	2016
Maximum daily flow (m^3/s)	8.9	9.1	8.8	281	273	286	8.59	8.53	8.47	4181	4120	4176
Seasonal maximum discharge for Winter (m^3/s)	2.7	2.8	2.7	68.1	70.5	70.8	3.20	3.23	3.22	1459	1454	1462
Seasonal maximum discharge for Spring (m^3/s)	1.8	1.9	1.9	60.5	59.5	60.9	3.38	3.36	3.34	786	671	680
Seasonal maximum discharge for Summer (m^3/s)	5.9	6.2	5.9	161	158	164	5.96	5.97	5.91	2782	2828	2881
Frequency of Peak over threshold (3rd quartile) (POTF)	91.0	91.0	91.0	91.0	91.0	91.0	91.0	91.0	91.0	95.0	95.0	95.0
Volume of discharge (BMC)	0.8	0.9	0.9	2.1	2.1	2.2	0.96	0.98	0.97	38.3	37.8	38.3

a)

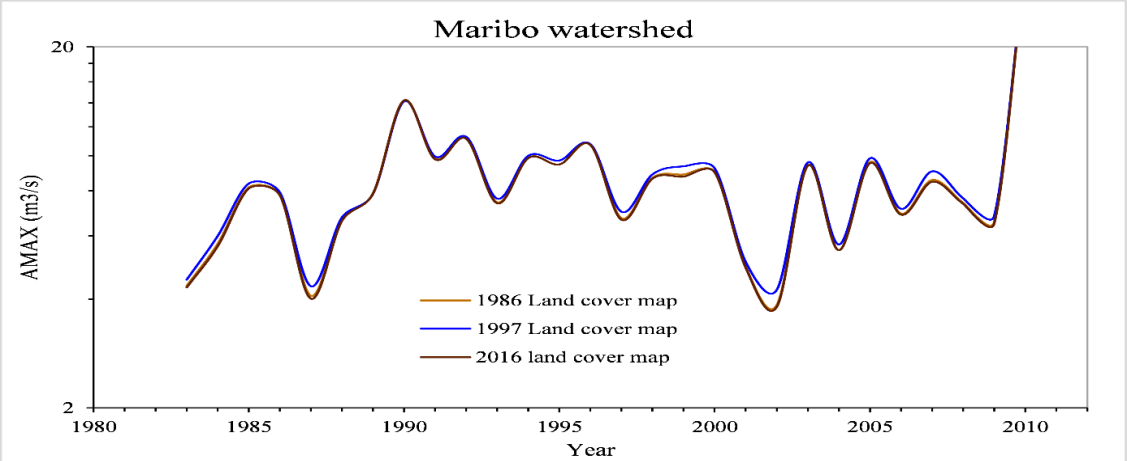

b)

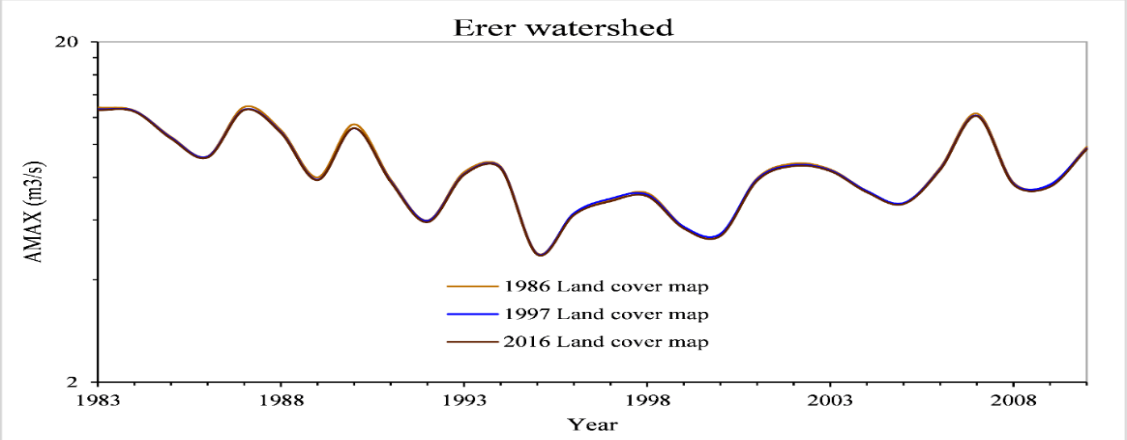

c)

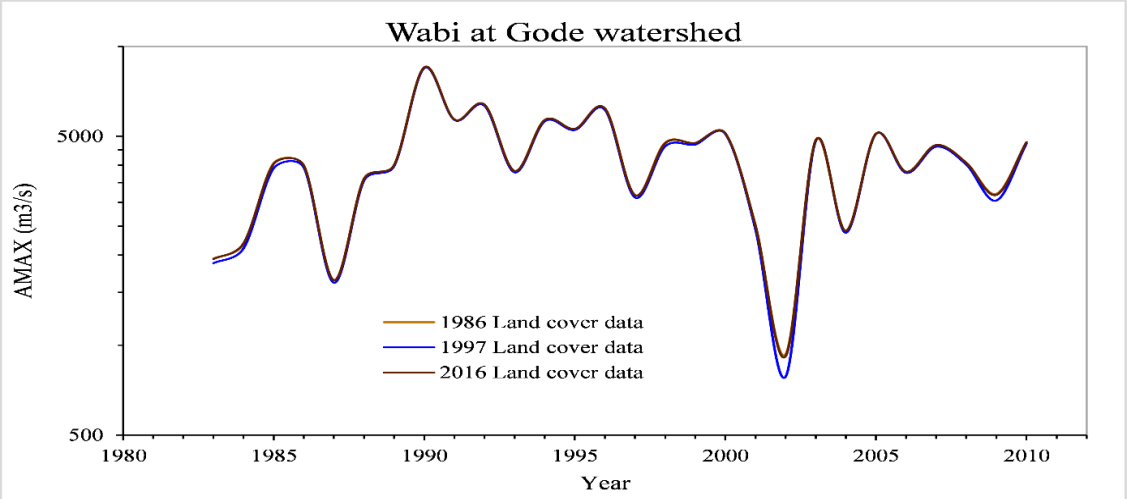

Figure 7-9 Comparison of simulated maximum daily discharges for 1986, 1997, and 2016 land cover data at three gauging stations: a) western upper basin (Maribo watershed), b) eastern upper basin (Erer watershed), and c) downstream lower basin (Wabi at Gode watershed)

7.3.6. Quantitative measure of the influence of Climate Change and LUCC change on Flood occurrence

The influence level of LULC and climate change on streamflow is estimated using the separation method. As presented in Table 7-11, the response of the discharges to climate change is higher than that of LULC change in the Wabi Shebele basin. However, LULC change has also a significant impact in middle and upper watersheds like Wabi at Legehida, Wabi at Dodola, Maribo, and Robe. Annual maximum discharge (AMAX) decreases in watersheds where forest and shrubland coverage increase in the study period. For instance, in Wabi at Legehida and Erer watersheds, the magnitude of floods decreases while the coverage of forest increases in condition one. In watersheds like Wabi at Dodola, Maribo, Robe, and Wabi at Legehida, flood discharge estimated using LULC of 2016 are more than flood estimate using LULC of 1986 by 3.91, 2.33, 1.92, and 128.66 m^3/s respectively. As a result, flood magnitude increases by 0.18%, 1.83%, 0.57%, and 0.44% in watersheds respectively. In Wabi at Gode watershed, flood discharge under condition one is more than flood magnitude in condition two by a value of 1285.18 m^3/s which is contributed by climate change and LUCC, accounting for 105.12%, and 5.12%, respectively. The results indicated that climate change is the main factor influencing the streamflow and flood values in Wabi Shebele River Basin between 1980 and 2010, which is similar to the conclusion drawn by Akola et al. (2018).

Table 7-10 Impact of LULC and Climate change on annual maximum streamflow in Wabi Shebele River Basin under two different conditions defined by the pre-set scenario. A *Bold* number indicates the significance of drivers influence on streamflow

Subbasin	Condition one (1980-1999)			Condition two (1980-2010)		
	Variation in AMAX (m^3/s)	Impact of LULC change (ηL) (%)	Impact of Climate change and others (ηc) (%)	Variation in AMAX (m^3/s)	Impact of LULC change (ηL) (%)	Impact of Climate change and others (ηc) (%)
Wabi at Dodola	1.86	2.55	**97.45**	3.91	0.18	**100.18**
Maribo	1.94	**6.45**	**93.46**	2.33	1.83	**101.83**
Robe	0.95	0.66	**99.34**	1.92	0.57	**100.57**
Wabi at Legehida	-14.37	**45.95**	**54.05**	128.66	**0.44**	**99.56**
Erer	-4.51	**3.07**	**96.63**	-2.71	**6.44**	**93.56**
Jijiga	-18.57	0.54	**100.54**	-12.31	0.11	**99.89**
Gode	1285.18	5.12	**105.12**	-115.08	**3.37**	**96.63**

7.4. Conclusion

This chapter addressed three main works: first is to analyze the potential impacts of climate change on streamflow simulation along with quantification of projected flood characteristics; the second is to analyze LULC change and its impact on flood hazards in the Wabi Shebele basin; and the third is related to the quantification of uncertainty in streamflow projections. A semi-distributed hydrological model (i.e., SWAT) is used to carry out, analysis and account for the spatial variability of streamflow. Model calibration/validation and parameter sensitivity analysis are performed through the SUFI-2 algorithm in SWAT-CUP. Model uncertainty analysis is done to establish the uncertainty bounds of the model using observed meteorological data, which is taken as a boundary limit to evaluate the significance of the climate change impact. The overall calibration and validation of the SWAT model were good in the basin except for Wabi at Gode station. At Gode station, the percentage of the simulated data within the uncertainty bound is only 28%. But for the other two sub-basins, the percentage of simulated flow within the uncertainty limit is more than 48%.

The model produced similar patterns of change in flooding due to temperature and precipitation drove either by RCMs or climate sensitivity tests. All simulated discharges using RCMs fall within 95% probable uncertainty bands. Three flood indices are used in analysis, showed higher risk in lower basin areas (i.e., at Gode stations) and lower risk in the upper and middle part of the basin areas at baseline scenario (T+0 ^{o}C, P+0 %). The Wabi Shebele River Basin is likely to experience an increase in flood hazard with an increase in precipitation in the future as temperature increase less than 2^{o}C. When precipitation increased by above 20%, flood hazard most likely be escalated in sub-basins. Out of the ten LULC types analyzed in the study area, three of them: agricultural land, grassland, and bare land showed increases in their coverage during the last 36 years. Streamflow simulated under LULC change indicates increases in those watersheds show significant agricultural land increases and forest coverage decreases, particularly in Wabi at Dodola, Maribo, Robe, and Erer watersheds. The influence level of LULC change and climate change on streamflow analyzed using the separation method indicates that climate change is the main factor influencing the streamflow and flood values in Wabi Shebele River Basin. However, LULC change has also significant impact in middle and upper watersheds like Wabi at Legehida, Wabi at Dodola, Maribo, and Robe. These findings could provide information on extreme weather events and provides early warning alarms.

8. MANAGEMENT IMPLICATION OF UNDERSTANDING FLOOD VARIABILITIES IN TRANSBOUNDARY RIVER BASINS

Abstract

Floods are among the most severe hydrological extremes in terms of social impact and potential economic damage. Flood variability impacts and managements are investigated in the Wabi Shebele River Basin. The basin has shown an increased flood frequency and magnitude. Between 1981 and 2010, the annual peak flood discharge showed increasing trends in the upper and the middle while decreases in eastern and lower catchments of Wabi Shebele Basin. Flood variability and socio-economic damages follow a similar trend tendency in the basin. Like variability analysis results in the early 21st century, the number of people affected indicates an increasing trend in the study area. In such cases, development-based climate adaptation mechanisms and flood risk management strategies need to placed. Integrated Flood Management (IMF) approaches needs to be placed in the context of socio-economic development. Due to its nature, flooding in the transboundary river basins has transboundary consequences. This indicates that the need for cooperation between riparian countries for Integrated Flood Management (IMF). IMF is an approach that adopts the best mix of both structural and non-structural strategies by ensuring a participatory approach and adopting integrated hazard management approaches.

Keywords: Mann-Kendall test, Quantile Perturbation method, Flood risk, Endemism, Expectations, Integrated Flood Management (IMF)

---

[5] F. A. Wudineh, S. A. Moges and B. B. Kidanewold (2021) Management Implication of Understanding Flood Variabilities in Transboundary Rivers for Future: A Case of Wabi Shebele River Basin, Ethiopia. Pp 151-179 in: Melesse, Assefa M., Abtew, Wossenu, Moges, Semu A. (Eds.) Nile and Grand Ethiopian Renaissance Dam; Past, Present and Future. Springer Geography, https://doi.org/10.1007/978-3-030-76437-1_9 .

8.1. Introduction

Floods are among the most severe hydrological extremes in terms of social impact and potential economic damage. Although the application of science and medicine has improved humankind's ability to predict, alleviate and survive flood disasters to some extent. There is a high probability of increase human exposure and vulnerability to floods in the future since population growth, urbanization, and social, economic, and political processes have been increasing over the globe.

Flood variabilities highly affect the poorest regions of the world (World Bank 2006), where insufficient investments are made in the hydraulic and institutional infrastructures to provide a reasonable measure of water security. Changes in climate or human interventions in catchments and river systems may change flood hazards and then flood risk. Due to this, floods are evaluated from a hazard perspective, focusing on hydrologic/ hydraulic parameters such as discharge, water level, or inundation extent neglecting societal processes, which implicitly means they are assumed to be constant or, if random, a stationary process, e.g., (Assefa 2018; Bissolli et al., 2011; World Bank 2006). However, some socio-economic processes, like population growth and economic development, may change fast than long-term physical changes (e.g., the impacts of climate change on discharge), and exposure and vulnerability to floods can be highly dynamic. Therefore, societal processes need to be addressed within a risk-based approach, where next to the hazard, societal exposure and vulnerability play a decisive role in the flood management process.

A critical question raising in recent years in extreme hydrology is how space-time variations in flood hazard that may be related to climate variability and change intersect with the changing nature of the flood exposure and vulnerability. To understand climate-flood linkage, some researchers conducted a robust study on the area. Among these, Merz et al. (2014) contrast the traditional narrow framing of floods with the broader perspective, emerging from an improved understanding of the climate context of flood generation (Table 8-1). Accordingly, they identify perspectives in floods as traditional and emerging perspectives. For instance, they explain the traditional approach for linking atmospheric components to flood analysis has been primarily hydro-meteorological. However, the emerging view of climate-flood linkages is process-driven and seeks to understand and analyses flood events in the context of their long-term history of variation in magnitude, frequency, and seasonality within the climate framework of the global and regional atmospheric circulation patterns and processes that drive changing combinations of meteorological elements at the catchment scale. Therefore, long-term climate trends, catchments characteristics like geology, topography, vegetation, and humans have to be disentangled to understand flood. In the case of data-sparse watersheds like the Wabi Shebele River Basin, obtaining long period observed extreme data for variability analysis is difficult. Thus, hydrologic models to generate flow from weather and catchment variables is required.

Table 8-1 Contrasting traditional views with emerging perspectives on flood hazard and risk

	Aspect	Traditional view	Emerging perspective
Understanding climate–flood linkages	Randomness	**Random:** Floods are random events with flood magnitude quantified by a probability distribution.	**Causal:** Flood occurrence and magnitude depend on a causal network of processes in the atmosphere, catchment, and river system.
	Spatial perspective	**Local:** Floods are events that can be described fully by processes on a catchment scale.	**Global:** Floods occur within the spatial framework of largescale circulation patterns and global climate mechanisms.
	Natural variability and floods	**Stationary:** Flood characteristics are stationary and represent the long-term natural variability of the climate-catchment system.	**Time-varying:** Flood characteristics change in time due to climate variability at different time scales.
	Temporal perspective	**Recent:** Flood characteristics result from current catchment characteristics and are derived from recent observations.	**Long-term:** Flood characteristics result from the long-term interplay of climate, geology, topography, vegetation (biology), and humans.
Exploiting climate flood linkages	Flood estimation	**Process-neutral:** Flood estimation does not differentiate between different flood event types and processes. Flood frequency analysis is based on assumptions.	**Process-based:** Flood events of different types occur in a given catchment. Knowledge of flood generation processes informs flood probability estimation.
	Flood projections under climate change	**Model chain:** Flood scenarios are the result of model chains, from emission scenarios through climate models to flood frequency estimation.	**Model chain augmented:** In addition to model chains, a range of approaches for assessing climate-related flood changes are used, such as assessing historical climate variability or using ocean source – atmospheric moisture transport – flood linkages.
	Flood risk management	**Hazard-focused, static:** Flood management focuses on flood hazard reduction within a static framework, principally using structural or zoning floodproofing or insurance.	**Risk-oriented, dynamic:** Risk management takes into account changing hazards, exposure and vulnerability, and the combined application of financial, structural, and non-structural measures.

Source: (Merz et al. 2014)

Ethiopia has seven transboundary rivers, of which the Wabi Shebele river is the one frequently affected basin in the country by flood disaster (Amer et al., 2013; MoWR 2003; NDRMC 2018). Due to its nature, the floods in transboundary rivers basins often have transboundary consequences. It indicates the need for cooperation between riparian countries. Recognizing this, Ethiopia has started to promote cooperative development and management of its shared rivers with riparian countries, particularly in the Nile Basin Initiative (NBI).

Flood Risk management should have taken into account changing hazards, exposure and vulnerability, and the combined application of financial, structural, and non-structural measures

(Merz et al., 2014). The best way to mitigate floods depends on how changes in flood risk, can be predicted at short and long-time scales. This chapter aims to investigate associated impacts and management implication of understanding flood variabilities in the transboundary river basins, a case of Wabi Shebele River Basin, Ethiopia. Based detected annual and seasonal variabilities in floods the first task, assessment of associated impacts and management of flood risk is performed in this chapter.

8.2. Severity of Floods in Wabi Shebele basin

There are two main types of flood events that regularly occur in the Wabi Shebele River Basin: Riverine floods and flash floods. The first type of flood is mainly in the lower valley of Wabi Shebele basin, when the Wabi Shebele river overflows, during torrential rains on the upper and middle highland of the basin, and localized heavy rainfall in the lower Wabi Sheble Basin. This type of flood occurs mainly during the first (March-May) and second (July-December) rainy seasons. These floods were reported in April 1995, October 1999, April 2002, May 2003, April 2005, April - December 2006, August 2008, November 2008, March 2010, April 2016 (MoWR 2003; Tadesse et al., 2016). Floods in Wabi Shebele, particularly in the lower basin, are favored by the topography, land cover, runoff from highland, and intensive rainfall conditions.

The other type is flash flooding, which occurs from heavy localized rainfall, specifically in the Fafen watershed. In Fafen watersheds, floods reduced in the channel, and the floods of the tributaries do not directly meet the Fafen River but flow in the alluvial plains in both seasons (March-May and September-November) comparably (MoWR 2003). These floods were reported in October- November 1999, May 2003, April-June 2005. Flash floods with a rainfall intensity of above 12.5 mm/h can cause high peak discharge, capable of inflicting hazards depending on the type of topography, soil property, the effect of rainfall over upstream, establishing the occurrence of floods over flood-sensitive areas (Akola et al. 2018).

8.3. Summary of flood changes in Wabi Shebele River Basin

The presented results under sections 6.4.2 and 6.4.3 revealed that there has been an increasing trend in the flood magnitude and frequency since the early 21st century over the river basin. A similar result is reported in the literature that the scale and frequency of floods indicate an increasing trend in Wabi Shebele River Basin since 2000 (IWMI 2015; MoWR 2003; Tadesse et al., 2016). For the period 1981 to 2010, the annual peak flood discharge shows an upward trend in the upper and middle catchments, while downward trends in the eastern and lower catchments of

Wabi Shebele River Basin. The annual maximum streamflow for middle catchments (i.e., Erer at Hamaro and Gololcha at Wabi junction) shows a significant positive trend because the computed p-value is in both watersheds are lower than the significance level (α0.05). However, a significant decreasing trend in annual maxima is observed in the Fafen watershed at Jijiga and Kebridehar gauging stations. Seasonal trend analysis reveals a similar pattern with annual maximum streamflow almost in all stations during the past 30 years.

Extreme discharge variability analysis using peak over the threshold (3rd quartile) based on QPM showed a significant increasing trend in the early 1990s and 2000s and decreasing trends in the 1980s, particularly in upper and middle catchments (Table 6-8). Over eastern catchments, the 1980s is the decade in which a significant increasing trend is observed and decreasing trends in the 1990s and 2000s. The lower Wabi Shebele river stations indicate a general decreasing trend in the analyses period, 1980-2010. In seasonal flow analysis, significant anomaly occurrence season varies with catchments (Table 6-6). In upper and middle catchments, the highest flows occurred in the spring season; in eastern catchments, the highest discharge anomalies occurred in the winter season; and in lower Wabi Shebele catchments highest extreme values occurred during the summer season. It is known, the Wabi Shebele basin is characterized by two rainfall regimes (NMA 1996): bimodal type I, the area known by a quasi-double maximum rainfall pattern, with a small peak in April and maximum in August (covers the west-east highland of the basin); and bimodal type II, the area dominated by double peak rainfall pattern with peaks during April and October (covers the south-eastern lowland areas of the basin).

8.4. Associated Impacts and Management of Flood

8.4.1. Associated impacts of flood variability

In countries where hydrological variability is high and investments to achieve water security are inadequate, variability is a constant economic risk to small investors (such as farm families) and large ones (such as industries) as well as to the nation. The seasonality of streamflow and cost of extreme weather events has been shown a rapid upward trend, in recent decades, throughout the world (Allamano et al., 2009; Bates et al., 2008; Tadesse et al., 2016; Kundzewicz et al., 2018; Ruiz-Villanueva et al., 2016; IPCC 2013). As shown in Figure 8-1, the number of people with flood disasters in Wabi Shebele basin increased since 2000s, similar to flood discharge trend analysis (section 6-4) in the early 21st century. Similarly, some studies, e.g., (MoWR 2003; Seleshi and Zanke 2004), showed high temporal and spatial variation in hydrologic parameters,

precipitation, and discharges in the basin. There is a perception in people prevailing that flooding in Ethiopia is linked with torrential rainfall (NDRMC 2018; Tadesse et al., 2016) which may not be true always. Because, short-time precipitation, even a less-than-a-day rainfall event can also create floods (Bissolli et al., 2011; Liu et al., 2017).

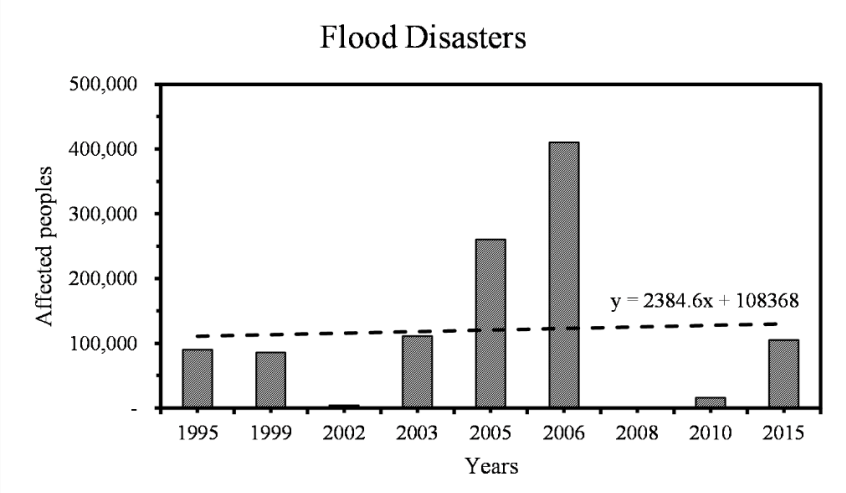

Figure 8-1 Flood disasters in Wabi Shebele River Basin since 1995 (Adapted from Assefa, 2018 and Tadesse et al., 2016)

The satellite image (Figure 8-2a and 8-2b) showed an extent of flooding in April and May 2005, which was very stressful to the locals and damaged properties (http:// earthobservatory.nasa.gov) in the southeast of Ethiopia. As of May 5, 2005, 154 people have been reported dead in the wake of severe flooding along the Wabi Shebele river in the southeast of Ethiopia (Tadesse et al. 2016). UNOCHA reported that at least 100,000 people have been affected by the flooding (https://www.un.org/press/en/2005/afr1145.doc.htm). In addition to the direct flood impacts, the swollen river has also extended the reach of crocodiles and water snakes. The reports revealed that 19 of the deaths were caused by crocodiles. The floods have also brought diseases, like malaria and diarrhea, to the region. On May 4, skies were clear when the Moderate Resolution Imaging Spectroradiometer (MODIS) flew overhead on NASA's Terra satellite to capture the top image. According to UNOCHA reports, Heavy rains pounded down over the Ahmar Mountains and the desert-dry plain to their south and east on April 23 and 24, 2005. Rivers flowing out of the mountains overflow far beyond their banks on April 27, 2005. The lower Wabi Shebele basin is a region affected by drought, and that may have contributed to the flooding because the hard and sunbaked ground cannot easily absorb heavy rain, so the water tends to run off, filling depressions and riverbeds. After two days of heavy rainfall on April 23 and 24, 2005, the drought-shrunken

Shebele River banks swelled and resulted in more flood events that swept away more than 35 villages in the region. In general, environmental and economic impacts of too much rain and extreme rainfall variability are shown in Table 8-2.

a)

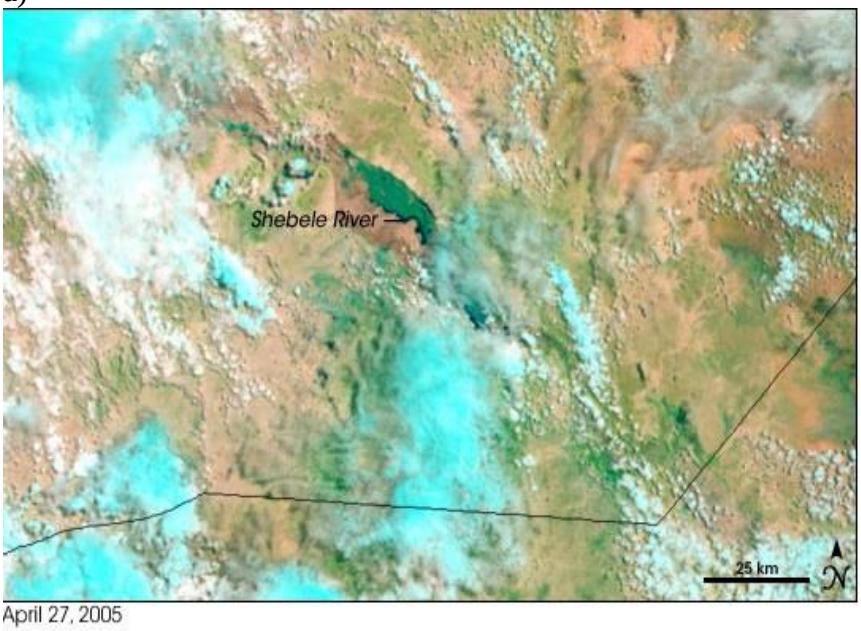

April 27, 2005

b)

May 4, 2005

Figure 8-2 Satellite pictures showing Wabi Shebelle valley floods; a) April 27, 2005; b) May 4, 2005. Water is blue and blue-green, vegetation is bright green, bare ground is pinkish-tan, and clouds are light blue

Table 8-2 Flood disasters in Wabi Shebele River Basin, 1980-2019

Date	Disaster event	Causalities Reported	Source
July 1993	Flooding: 120,000 affected	Heavy Rain	http://floodobservatory.colorado.edu/Archives/index.html
1995	Flooding: 89,902 affected, 27 deaths	Heavy Rain	http://floodobservatory.colorado.edu/Archives/index.html
1999	Flooding: 85,789 affected, 34 deaths.	Torrential rain	http://floodobservatory.colorado.edu/Archives/index.html
2003	Floods: 119 people died	Heavy Rain	ERCS: http://ifrc.org/where/country/check.asp/countryid=65
2005	Flooding: 103,000 affected, 177 deaths	Heavy Rain	ERCS: http://ifrc.org/where/country/check.asp/countryid=65
2006	Flooding: 410,132 affected, 132 deaths	Heavy Rain	http://floodobservatory.colorado.edu/Archives/index.html
May 2008	Flooding: 11 deaths, 52,000 people abandoned, 164 hectares farmland washed away.	Heavy seasonal rains	http://www.irinnews.org/report/81526/ethiopia thousands-displaced-by-floods-in-Somalia-region.
2010	Flooding: 16,000 affected	Heavy Rain	http://floodobservatory.colorado.edu/Archives/index.html
2015	Flooding: 105,000 affected	Heavy Rain	http://floodobservatory.colorado.edu/Archives/index.html

These high resources and human losses indicate the importance of flood risk management practice in the basin. Also, there is now a pressing need for decision-makers to understand the ongoing changes in hydrologic extremes to make preparations for the possibility of changing conditions. The recent study of the World Bank (2006) on the environmental analysis of Ethiopia revealed that the challenges in the country involve complex cross-sectoral linkages. The two main links in environmental development identified by the study relate to the challenges posed by Ethiopia's hydrology are the lack of integrated water resources management and the "land degradation-food insecurity-energy access-livelihood" nexus. The latter includes unsustainable agricultural land management practices and heavy reliance on biomass energy. The consequences of both deforestation and degraded soil structure are: decrease infiltration, which diminishes groundwater recharge, increase runoff, which contributes to erosion and siltation; and reduced water storage capacity in the soil, which makes crops less able to withstand drought.

8.4.2. Endemism and Expectations of Flood Variability

If the effects of the flood are not well recognized, expectations of high variability and endemism can affect the economic performance and structure of the economy. The expectations of variability and the unpredictability of rainfall and runoff will make economic actors focus on minimizing their downside risks rather than maximizing their potential gains (World Bank, 2006). Because they think they could lose everything in a single flood. The farm families will not invest in land improvements, advanced technologies, or agricultural inputs and constrain agricultural output and productivity gains. Lack of such investments can lead to land degradation and desertification, which result in a vicious circle of reducing production and deteriorating assets. Understanding and mitigating the full impact of hydrological variability on economic performance require a better understanding of the role of expectations and the incentives created by entirely rational risk aversion. In risk assessment, three elements are involved, i.e., vulnerability, exposure, and threats. Risk assessment in flood-prone areas of Ethiopia is a challenging task due to a shortage of adequate and reliable water and soil data.

In Ethiopia, flood assessments done by some researchers (Assefa 2018; NDRMC 2018) indicate the severity of flood risk in the country. According to the studies, parts of Oromia and Afar regions lying along the upper, middle, and down-stream plains of the Awash River; parts of Somali region along the Wabi Shebele, Genale Dawa Rivers; low-lying areas of Gambella along the Baro and Akobo Rivers; down-stream areas along the Omo and Bilate Rivers in southern Ethiopia and the extensive floodplains surrounding Lake Tana and the banks of Gumara, Rib and Megech Rivers have been recognized as flood-prone areas. However, there were no adequate protection measures done to decrease these flood disasters in the areas. Assefa (2018) proposed structural and non-structural measures to mitigate flood risk in the country. The best-known structural measures are concrete, earthen, or other engineering structures. However, these measure types focus on flood prevention by reducing the discharge amount running down a river, for example, Reservoirs, Retention ponds, River training, dams, and floodwalls. Flood risk mapping is proposed as a non-structural flood management technique in reducing flood damages in areas frequented by the flood. In general, flood mitigation actions fall into the following categories: Preventative Measures, Property Protection Measures, Natural Resource Protection Activities, Emergency Services (ES) Measures, Structural Mitigation Projects, Public Education, and Awareness Activities.

8.4.3. Flood management in Transboundary River Basin

Flood management is a complicated task in river basins controlled by a single authority and becomes more challenging when dealing with transboundary floods. Transboundary floods are floods that originated in one country and then propagate downstream to another country (Bakker, 2009). Ethiopia has seven transboundary rivers (Table 8-3), of which the Wabi Shebele river is part Shebele-Juba basin. It is one of the frequently affected basins in the country by hydrological extremes (Amer et al., 2013; Awass 2009). Due to the nature of transboundary rivers, flooding often has transboundary consequences. This indicates the need for cooperation between riparian countries. To prevent and resolve potential conflicts and avoid severe effects of flooding in transboundary waters, countries sharing a water resource need to agree on common rules and procedures of cooperation to jointly manage the water resources (Bakker, 2009).

Table 8-3 Transboundary Rivers

River	Total basin area (km^2)	% Of basin within Ethiopia	Sharing countries
Nile basin	3,112,369	12	**Burundi, Democratic Republic of Congo, Egypt, Eritrea, Kenya, Rwanda, South Sudan, Sudan, Uganda, Tanzania**
• *Abbay*			*Sudan*
• *Baro-Akobo*			*South Sudan*
• *Tekeze*			*Sudan*
• *Mereb*			*Eritrea*
Rift Valley Basin	637,593	49	**Kenya**
• *Gibe-Omo*			
Shebelle-Juba basin	810, 427	46	**Kenya, Somalia**
• *Wabi Shebele*			*Somalia*
• *Genale -Dawa*			*Kenya, Somalia*

Source: http://www.fao.org/nr/water/aquastat/countries_regions/eth/print1.stm.

United Nations sustainable flood prevention guides (UN 2000) state that, considering the evolution and trends of floods, one must shift from defensive action against hazards to managing the risk. Flood protection is never absolute. Therefore, risk management will be the appropriate method to deal with this challenge. Therefore, a holistic approach based on multilateral cooperation, including interdisciplinary planning for the whole catchment area including international cooperation in the case of transboundary rivers is necessary to take into account the whole river basin.

8.4.4. Integrated Flood Risk Management

Integrated flood management (IFM) refers to the integration of land and water management in a river basin using a combination of measures (UN 2000). IFM is a holistic approach to address the water cycle, integrating land and water management. The idea is to adopt the best mix of structural and non-structural strategies by ensuring a participatory approach and adopting integrated hazard management approaches. IFM requires adopting a river basin approach in planning that involves many disciplines and stakeholders in efforts to reduce flood vulnerability and risk and to preserve ecosystems. Unite Nation Convention on the protection and use of transboundary rivers and international lakes proposed four main principles for integrated flood management (IMF) (UN 2000):

- **River basin management:** Water management should be based on the boundaries of the river basin, not on administrative areas or country borders, thus taking into account a river system as a whole, from source to mouth.
- **Solidarity:** Problems should not be shifted to neighboring countries or regions. Negative effects between upstream and downstream areas should be prevented, and positive effects should be stimulated.
- **Sustainability:** Principles of sustainable development involve ensuring livelihood and security among different population groups as well as the viability of ecosystems and floodplain functions, including in the long term.
- **Public participation:** Active public involvement in the development and implementation of water management strategies and plans.

8.5. Conclusion

In this study, variabilities in flood and their implication in flood risk management are assessed. Similar to flood discharge, the impact of floods on human beings and resources indicates an increasing trend in the 21st century in the Wabi Shebele River Basin. In countries where high hydrological variability is observed and investments to achieve water security are inadequate, variability is a constant economic risk. Understanding and mitigating the full impact of hydrological variability on economic performance will require a better understanding of the role of expectations and the incentives created by entirely rational risk aversion. Flood risk management in transboundary river basins needs the involvement of complex cross-sectoral linkages and is more challenging when dealing with transboundary rivers.

9. CONCLUSION AND RECOMMENDATIONS

9.1. Conclusion

The core of the research in this thesis is to detect changes in flood discharge and attribute them to its driving forces in data-scarce watersheds. During the past few years, investigating trends in streamflow time series has evolved from just providing information to decision-makers in water resource management. Providing the information on the causes of changes in flood events assures one to work on specific drivers to control disasters that come from changes in flood events. The emphasis taken in this study are understanding flood generation mechanisms and potential drivers in the Wabi Shebele basin of Ethiopia; detecting trends and variabilities in flood discharge and attribution to potential drivers using both observed and model-based simulation data; analyzing flood risks and uncertainties with climate change, and land use and cover change, and investigating management implication of understanding flood variabilities in transboundary rivers in future. Both statistical time series analysis and hydrologic model are used in the detection and attribution process. Mainly, two non-parametric statistical tests (i.e., Mann Kendall trend test and Quantile Perturbation Method) are applied to detect trends and variabilities in the hydroclimatic variables. SWAT hydrologic model used for streamflow simulation and to identify the effects of different causes of changes in flood hazards (cause-effect relationships). The calibration of the SWAT model in the Wabi Shebele basin presented "good" performances with the statistical values of NSE= 0.64 and 0.34 in average at upstream and downstream stations respectively. Considering the representativeness of the watershed and data scarcity for hydrological modeling, the results are satisfactory and offer an understanding of the flood variabilities and potential drivers, which is valuable in flood risk management of river basins.

The study provides an overview of the increasing situation of floods throughout the river basin during the 21st century. Extreme streamflow analysis based on observed data indicates a significant increasing trend in the northwestern and eastern watersheds, i.e., Maribo and Erer river when most extreme discharge anomalies vary within confidence intervals in Wabi at Dodola and Robe gauging stations. Precipitation extremes analysis also indicates increasing trends and periodicities over the northwestern and eastern part of the basin at two to five years intervals. However, the middle part of Wabi Shebele basin showed a decreasing trend in all extreme precipitation indices. Flood events in the watersheds exhibit less variability in flood-peak discharges, which shows that most flood events in the Wabi Shebele basin fall under the category of riverine floods except for

flood events in the northeastern part of the basin around the Jijiga area, which is identified as potential flash flood areas. The assessment upon driving forces of floods: climate factor (i.e., rainfall); watershed factors (i.e., Drainage Area (DA), Basin Elevation (BE), Basin Slope (BS), a fraction of sand coverage); human activity factors (i.e., Population Density (PD), agricultural, and forest coverage) are the most sensitive attributes in generations and changes of flood discharge in the Wabi Shebele basin. Multi-temporal trend analysis at 5-, 10-, 15-, 25- and 30-years intervals in annual maximum discharge showed increasing trends for most recent periods (since 1996) in the river basin. The influence of natural variabilities on extreme weather events reveals the strong impact of Pacific and Atlantic Ocean indices, i.e., Southern Oscillation Index (SOI), Pacific Decadal Oscillation (PDO) and Atlantic Multidecadal Oscillation (AMO) on rainfall and streamflow of Wabi Shebele basin at the highland part and Indian Ocean index influence in the eastern and lowland part of basin with correlation value of R^2>0.5. The impact of climate change on flood hazard indicates higher in the downstream stations, particularly on Gode station at baseline scenario (i.e., with no change in temperature and precipitation, T+0 ^{o}C, P+0 %). The Wabi Shebele River Basin is likely to experience an increase in flood hazard with an increase in precipitation in the future as temperature increase less than 2^{o}C. Streamflow simulated under LULC change indicates increases in those watersheds show a significant increase in agricultural land and decrease in forest coverage (i.e., Wabi at Dodola, Maribo, Robe, and Erer). The study also observed that the impact of floods on human beings and resources indicates an increasing trend in the 21st century similar to the extreme discharge trend in the river basin. In countries like Ethiopia, where investments to achieve water security are inadequate, hydrologic variability is a constant economic risk. Due to its nature, flooding in the transboundary river basins has transboundary consequences. Therefore, riparian countries need to jointly manage these water resources using Integrated Flood Management (IFM) principles: river basin management, solidarity, sustainability, and public participation.

Generally, this study explores the hydrological variability and understandings of flood generation mechanisms using a statistical and model-based approach. The result highlights that the dominant hydrological variability and flooding in Wabi Shebele River Basin are not attributed to a single dominant factor. It is caused by the interplay of climate change/climate variability, physical and anthropogenic factors such as population increase and land-use changes. In short, this study

underscores a new effort to bring a methodological framework for detection and attribution of flood changes in data-scarce watersheds context.

9.2. Recommendations

Lack of studies showing hydrological situation is one of the major problems frustrating policymakers in their attempt to adopt sustainable development in the river basin. The decline in the number of stations and data quality has made water resources less studied and used for operational purposes. Hence, a new ground-based water resources monitoring system design and implementation are required in the Wabi Shebele River Basin.

The detected trends and variabilities are attributed to only major external drivers like anthropogenic climate change, watersheds characteristics, and land-use change. Further studies on attribution of changes to natural internal variability can provide a better insight into the cause of devastating flood events in the river basin.

The climate model used in the study is RCMs; the Cordex-Africa model is a dynamic downscaling model from GCM. Projections of future climate from different methods like statistical downscaling and different emission scenarios can provide analysis more related to reality in forecasting hydrological responses due to climate change.

Furthermore, land-use change impact analysis was observed only based on historical land use map information. Projection of land-use map using land-use dynamics model may provide better insights on the impact of land-use change in the basin for the future hydrologic response.

In river basins like Wabi Shebele, where climate change is the leading cause for high hydrologic variability, development-based climate change adaptation mechanisms and flood risk management strategies is needed.

REFERENCES

Abbaspour, Karim C, Jing Yang, Ivan Maximov, Rosi Siber, Konrad Bogner, Johanna Mieleitner, Juerg Zobrist, and Raghavan Srinivasan. 2007. "Modelling Hydrology and Water Quality in the Pre-Alpine/Alpine Thur Watershed Using SWAT." *Journal of Hydrology* 333 (2–4): 413–30.

Abebe, Adane, and Gerd Förch. 2006. "Catchment Characteristics as Predictors of Base Flow Index (BFI) in Wabi-Shebele River Basin, East Africa." *Conference on International Agricultural Research for Development, University of Siegen, Germany*.

Adamu, T.A. 2014. "Impacts of climate change, land-cover change and reservoir operation on the hydrology of Rib-Gumera catchments, Upper Blue Nile, Ethiopia." Delft: UNESCO-IHE.

Admassu, Habtamu, Mezgebu Getinet, and Abebe Kirub. 2010. "Impacts of Climate Variability and Change in Agricultural Systems of Semi-Arid Areas of Ethiopia," 107.

Adnan, N.A. 2010. *Quantifying the Impacts of Climate and Land Use Changes on the Hydrological Response of a Monsoonal Catchment. University of Southampton*. University of Southampton.

Ahmad, Ijaz, Deshan Tang, TianFang Wang, Mei Wang, and Bakhtawar Wagan. 2015. "Precipitation Trends over Time Using Mann-Kendall and Spearman's Rho Tests in Swat River Basin, Pakistan." *Advances in Meteorology* 2015 (January): e431860. https://doi.org/10.1155/2015/431860.

Akola, Juliet, Joseph Binala, and Jimmy Ochwo. 2018. *Guiding Developments in Flood-Prone Areas: Challenges and Opportunities in Dire Dawa City, Ethiopia*. OASIS. http://hdl.handle.net/10394/33660.

Allamano, P, P Claps, and F Laio. 2009. "An Analytical Model of the Effects of Catchment Elevation on the Flood Frequency Distribution." *WATER RESOURCES RESEARCH* 45 (1): W01402.

Al-Rawas, Ghazi A., and Caterina Valeo. 2010. "Relationship between Wadi Drainage Characteristics and Peak-Flood Flows in Arid Northern Oman." *Hydrological Sciences Journal* 55 (3): 377–93. https://doi.org/10.1080/02626661003718318.

Amer, Alain Gachet, Wayne R. Belcher, James R. Bartolino, and Candice B. Hopkins. 2013. *Groundwater Exploration and Assessment in the Eastern Lowlands and Associated Highlands of the Ogaden Basin Area, Eastern Ethiopia: Phase 1 Final Technical Report*. USA: USAID and USGS.

Andréassian, Vazken, Eric Parent, and Claude Michel. 2003. "A Distribution-Free Test to Detect Gradual Changes in Watershed Behavior." *WRCR Water Resources Research* 39 (9).

Armenteras, Dolors, Uriel Murcia, Tania Marisol González, Oscar Javier Barón, and Jorge Eliecer Arias. 2019. "Scenarios of Land Use and Land Cover Change for NW Amazonia: Impact on Forest Intactness." *Global Ecology and Conservation* 17.

Arnold, D. N. Moriasi, P. W. Gassman, K. C. Abbaspour, M. J. White, R. Srinivasan, C. Santhi, et al. 2012. "SWAT: Model Use, Calibration, and Validation." *Transactions of the ASABE* 55 (4): 1491–1508.

Arnold, J. G, R Srinivasan, R. S Muttiah, and J. R Williams. 1998. "Large Area Hydrologic Modeling and Assessment Part I: Model Development." *Journal of the American Water Resources Association* 34 (1): 73–89.

Assefa, Tesfay Hailekiros. 2018. "Flood Risk Assessment in Ethiopia." *Civil and Environmental Research* 10 (1): 35–40.

Awass, Adane Abebe. 2009. “Hydrological Drought Analysis - Occurrence, Severity, Risks: The Case of Wabi Shebele River Basin, Ethiopia.” *University of Siegen, Germany*, 217.

Awulachew, Seleshi Bekele, Aster Denekew Yilma, Makonnen Loulseged, W. Loiskandl, M. Ayana, and T. Alamirew. 2007. “Water Resources and Irrigation Development in Ethiopia.” Working Paper. International Water Management Institute. https://cgspace.cgiar.org/handle/10568/39349.

Bakker, Marloes H. N. 2009. “Transboundary River Floods and Institutional Capacity1.” *JAWRA Journal of the American Water Resources Association* 45 (3): 553–66. https://doi.org/10.1111/j.1752-1688.2009.00325.x.

Bates, Bryson C, Zbigniew Kundzewicz, Jean Palutikof, Wu Shaohong, World Meteorological Organisation (WMO), United Nations Environment Programme (UNEP), and Intergovernmental Panel on Climate Change. 2008. *Climate Change and Water [Electronic Resource]: IPCC Technical Paper VI.* Geneva: IPCC Secretariat.

BCEOM. 1973. *BCEOM_ORSTOM_EDF, 1973 Hydrological Survey of the Wabi Shebele Basin, Ethio-France Cooperative Program*.

Belay, Getachew Welelaw, Mulugeta Azeze, and Assefa M. Melesse. 2019. “Chapter 16 - Reservoir Operation Analysis for Ribb Reservoir in the Blue Nile Basin.” In *Extreme Hydrology and Climate Variability*, edited by Assefa M. Melesse, Wossenu Abtew, and Gabriel Senay, 191–211. Elsevier. https://doi.org/10.1016/B978-0-12-815998-9.00016-6.

Bhatt, Diva, and R.K Mall. 2015. “Surface Water Resources, Climate Change and Simulation Modeling.” *Aquatic Procedia* 4: 730–38.

Bissolli, Peter, Karsten Friedrich, Jörg Rapp, and Markus Ziese. 2011. “Flooding in Eastern Central Europe in May 2010 – Reasons, Evolution and Climatological Assessment.” *Weather* 66 (6): 147–53. https://doi.org/10.1002/wea.759.

Bloch, Jha, and Lamond. 2011. “Cities and Flooding: A Guide to Integrated Urban Flood Risk Management for the 21st Century, Washington DC: World Bank.”

Boé, J, L Terray, F Habets, and E Martin. 2007. “Statistical and Dynamical Downscaling of the Seine Basin Climate for Hydro-Meteorological Studies.” *JOC International Journal of Climatology* 27 (12): 1643–55.

Bradshaw, C. J. A., N. S. Sodhi, K. S. H. Peh, and B. W. Brook. 2007. *Global evidence that deforestation amplifies flood risk and severity in the developing world*. Blackwell Publishing. http://espace.cdu.edu.au/view/cdu:2749.

Broxton P, Troch P.A, Schaffner M, Unkrich C, and Goodrich D. 2014. “AN All-Season Flash Flood Forecasting System for Real-Time Operations.” *Bulletin of the American Meteorological Society* 95 (3): 399–407.

Camdevyren, H, N Demyr, A Kanik, and S Keskyn. 2005. “Use of Principal Component Scores in Multiple Linear Regression Models for Prediction of Chlorophyll-a in Reservoirs.” *ECOLOGICAL MODELLING* 181 (4): 581–89.

Camici, S., L. Brocca, F. Melone, and T. Moramarco. 2014. “Impact of Climate Change on Flood Frequency Using Different Climate Models and Downscaling Approaches.” *Journal of Hydrologic Engineering* 19 (8): 04014002. https://doi.org/10.1061/(ASCE)HE.1943-5584.0000959.

Campozano, L, E Sanchez, A Aviles, and E Samaniego. 2014. “Evaluation of Infilling Methods for Time Series of Daily Precipitation and Temperature: The Case of the Ecuadorian Andes” 5 (1): 17.

Chambers B.M, Pradhanang S.M, and Gold A.J. 2017. “Simulating Climate Change Induced Thermal Stress in Coldwater Fish Habitat Using SWAT Model.” *Water (Switzerland)* 9 (10).

Charles, J. V., R. B. Victor, P. L. Dennis, P. L. Daniel, P. David, F. S. George, H. S. Emily, Z. Chunmiao, J. H. Laura, and H. Anita. 2011. *Global Change and Extreme Hydrology: Testing Conventional Wisdom, National Academies Press (U. S.)*. National Academies Press.

Chen, Z.Q.R, Kavvas M.L, Ohara N, Anderson M.L, and Yoon J. 2012. “Coupled Regional Hydroclimate Model and Its Application to the Tigris-Euphrates Basin.” *Journal of Hydrologic Engineering* 16 (12): 1059–70.

Cheng, CHINGWEN, E. Brabec, Y. Yang, and R. Ryan. 2013. “Rethinking Stormwater Management in a Changing World: Effects of Detention for Flooding Hazard Mitigation under Climate Change Scenarios in the Charles River Watershed.” In *Proceedings of 2013 CELA Conference, Austin, Texas*, 27–30.

Chow, Ven Te, David R Maidment, and Larry W Mays. 2013. *Applied Hydrology*. New York; London: McGraw-Hill Professional; McGraw-Hill [distributor.

Dankers, Rutger, Nigel W. Arnell, Douglas B. Clark, Pete D. Falloon, Bal�zs M. Fekete, Simon N. Gosling, Jens Heinke, et al. 2014. “First Look at Changes in Flood Hazard in the Inter-Sectoral Impact Model Intercomparison Project Ensemble.” *Proceedings of the National Academy of Sciences of the United States of America* 111 (9): 3257–61.

Delgado, Apel H, and Merz B. 2009. “Flood Trends and Variability in the Mekong River.” *Hydrology and Earth System Sciences Discussions* 6 (5): 6691–6719.

Dettinger, M. D, California Energy Commission, California Environmental Protection Agency, and California Climate Change Center. 2009. *Projections of Potential Flood Regime Changes in California: Final Paper*. http://bibpurl.oclc.org/web/39425 http://www.energy.ca.gov/2009publications/CEC-500-2009-050/CEC-500-2009-050-F.PDF.

Devia, Gayathri, B.P. Ganasri, and G.S. Dwarakish. 2015. “A Review on Hydrological Models.” *Aquatic Procedia* 4 (December): 1001–7. https://doi.org/10.1016/j.aqpro.2015.02.126.

Dile, Yihun Taddele, Ronny Berndtsson, and Shimelis G. Setegn. 2013. “Hydrological Response to Climate Change for Gilgel Abay River, in the Lake Tana Basin - Upper Blue Nile Basin of Ethiopia.” *PLOS ONE* 8 (10): e79296. https://doi.org/10.1371/journal.pone.0079296.

Dinku, T, J Hansen, A Rose, B Damen, and M Sheinkman. 2020. “Enhancing National Climate Services (ENACTS) Approach to Support Climate Resilience in Agriculture.” November 16, 2020. https://ccafs.cgiar.org/resources/publications/enhancing-national-climate-services-enacts-approach-support-climate.

Dinku, Tufa, Paul Block, Jessica Sharoff, Kinfe Hailemariam, Daniel Osgood, John del Corral, Rémi Cousin, and Madeleine C. Thomson. 2014. “Bridging Critical Gaps in Climate Services and Applications in Africa.” *Earth Perspectives* 1 (1): 15. https://doi.org/10.1186/2194-6434-1-15.

Diro, G.T, D.I.F Grimes, and Black E. 2011. “Teleconnections between Ethiopian Summer Rainfall and Sea Surface Temperature: Part I-Observation and Modelling.” *Climate Dynamics* 37 (1): 103–19.

Doocy, S, A Daniels, S Murray, and Kirsch TD. 2013. “The Human Impact of Floods: A Historical Review of Events 1980-2009 and Systematic Literature Review. PLOS Currents Disasters. Edition 1.”

Eleutério, Julian, Anne Rozan, Robert Mosé, Sandrine Spaeter-Loehrer, Nilo De Oliveira Nascimento, Bruno Tassin, Roland Nussbaum, et al. 2012. *Flood Risk Analysis: Impact of Uncertainty in Hazard Modelling and Vulnerability Assessments on Damage Estimations*.

EM-DAT. 2021. "The OFDA/CRED International Disaster Database, Www.Em-Dat.Net - Université Catholique de Louvain - Brussels - Belgium". Created on: Jun-19-2021. - Data Version: V03.07." 2021. https://public.emdat.be/mapping.

Emeribe, Ali Butu, and Chukwudi. 2019. "Trend Analysis, Cycles and Periodicities in Annual Maximum Daily Rainfall Distributions over Southern Nigeria." *Journal of the Nigerian Association of Mathematical Physics* 52 (November): 299–312.

Endris, Hussen Seid, Philip Omondi, Suman Jain, Christopher Lennard, Bruce Hewitson, Ladislaus Chang'a, J. L Awange, et al. 2013. "Assessment of the Performance of CORDEX Regional Climate Models in Simulating East African Rainfall." *Journal of Climate* 26 (21): 8453–75.

Enzel, Y, L. L Ely, P. K House, and V. R Baker. 1993. "Paleo flood Evidence for a Natural Upper Bound to Flood Magnitudes in the Colorado River Basin." *Water Resources Research* 29 (7): 2287.

ERCS. 2005. "ERCS (Ethiopian Red Cross Society) ETHIOPIA: HEAVY RAINS AND FLOODS; Information Bulletin No. 2/2005." Addis Ababa, Ethiopia. http://www.ifrc.org/where/country/check.asp?countryid=65.

Erena and Worku. 2018. "Flood Risk Analysis: Causes and Landscape-Based Mitigation Strategies in Dire Dawa City, Ethiopia," Geo-environmental Disasters, .

Fenicia, F., H. H. G. Savenije, and Y. Avdeeva. 2009. "Anomaly in the Rainfall-Runoff Behavior of the Meuse Catchment. Climate, Land-Use, or Land-Use Management?" *Hydrology and Earth System Sciences* 13 (9): 1727–37. https://doi.org/10.5194/hess-13-1727-2009.

Ficklin, D.L, Luo Y, Luedeling E, and Zhang M. 2009. "Climate Change Sensitivity Assessment of a Highly Agricultural Watershed Using SWAT." *Journal of Hydrology* 374 (1–2): 16–29.

Fleming, Sean W., and Garry K.C. Clarke. 2002. "Autoregressive Noise, Deserialization, and Trend Detection and Quantification in Annual River Discharge Time Series." *Canadian Water Resources Journal* 27 (3): 335–54. https://doi.org/10.4296/cwrj2703335.

Fowler, H. J, and C. G Kilsby. 2007. "Using Regional Climate Model Data to Simulate Historical and Future River Flows in Northwest England." *Climatic Change* 80 (3–4): 337–67.

Funk, Chris, Pete Peterson, Martin Landsfeld, Diego Pedreros, James Verdin, Shraddhanand Shukla, Gregory Husak, et al. 2015. "The Climate Hazards Infrared Precipitation with Stations; a New Environmental Record for Monitoring Extremes." *Scientific Data*. https://doi.org/10.1038/sdata.2015.66.

Gaur, Srishti, Arnab Bandyopadhyay, and Rajendra Singh. 2020. "Modelling Potential Impact of Climate Change and Uncertainty on Streamflow Projections: A Case Study." *Journal of Water and Climate Change*.

Gebrechorkos, Solomon Hailu, Stephan Hülsmann, and Christian Bernhofer. 2018. "Evaluation of Multiple Climate Data Sources for Managing Environmental Resources in East Africa." *Hydrology and Earth System Sciences* 22 (8): 4547–64. https://doi.org/10.5194/hess-22-4547-2018.

Gebru, Shishay Yemane. 2016. "The Role of Reservoirs in Drought Mitigation in Ethiopia, Awash River Basin." Undefined. 2016. http://www.secheresse.info/spip.php?article58143.

Getahun, YS, and SL Gebre. 2015. "Flood Hazard Assessment and Mapping of Flood Inundation Area of the Awash River Basin in Ethiopia Using GIS and HEC-GeoRAS/HEC-RAS Model." *Civil & Environmental Engineering* 5: 179. https://doi.org/10.4172/2165-784X.1000179.

Githui, F, F Mutua, and W Bauwens. 2009. "Estimating the Impacts of Land-Cover Change on Runoff Using the Soil and Water Assessment Tool (SWAT): Case Study of the Nzoia Catchment, Kenya." *Hydrological Sciences Journal.* 54 (5): 899–908.

Griensven, A van, T Meixner, S Grunwald, T Bishop, M Diluzio, and R Srinivasan. 2006. "A Global Sensitivity Analysis Tool for the Parameters of Multi-Variable Catchment Models." *Journal of Hydrology* 324 (1–4): 10–23.

Grubb, A, and A Robson. 2000. "Exploratory/Visual Analysis." *Detecting Trend and Other Changes in Hydrological Data*, 19–47.

Gudmundsson L, Bremnes J.B, Haugen J.E, and Engen-Skaugen T. 2012. "Technical Note: Downscaling RCM Precipitation to the Station Scale Using Statistical Transformations – A Comparison of Methods." *Hydrology and Earth System Sciences* 16 (9): 3383–90.

Gumbricht, T, P Wolski, P Frost, and T S Mccarthy. 2004. "Forecasting the Spatial Extent of the Annual Flood in the Okavango Delta, Botswana." *Journal of Hydrology*. 290 (3): 178.

Guo, Jing, Xiaoling Su, Vijay Singh, and Jiming Jin. 2016. "Impacts of Climate and Land Use/Cover Change on Streamflow Using SWAT and a Separation Method for the Xiying River Basin in Northwestern China." *Water* 8 (5): 192.

GWI. 2010. "Assessing Climate Change Vulnerability in East Africa A Case Study on the Use of CARE's Climate Change Vulnerability and Capacity Assessment (CVCA) Methodology within the Global Water Initiative1 East Africa Program." In *Assessing Climate Change Vulnerability in East Africa*. CARE International. care.or.ke/images/PDF/GWI_CVCA_CS_Sept11.pdf.

Gyau-Boakye, P, and G. A Schultz. 1994. "Filling Gaps in Runoff Time Series in West Africa." *Hydrological Sciences Journal* 39 (6): 621–36.

Hailemariam, S.N, Soromessa T, and Teketay D. 2016. "Land Use and Land Cover Change in the Bale Mountain Eco-Region of Ethiopia during 1985 to 2015." *Land* 5 (4).

Hall, J, B Arheimer, M Borga, R Brázdil, P Claps, A Kiss, T R Kjeldsen, et al. 2014. "Understanding Flood Regime Changes in Europe: A State-of-the-Art Assessment." *Hydrol. Earth Syst. Sci.*, 39.

Hamlet, A. F, and D. P Lettenmaier. 2007. "Effects of 20th Century Warming and Climate Variability on Flood Risk in the Western U.S. (DOI 10.1029/2006WR005099)." *Water Resources Research* 43 (6): W06427.

Hargreaves, George H., and Zohrab A. Samani. 1985. "Reference Crop Evapotranspiration from Temperature." *Applied Engineering in Agriculture* 1 (2): 96–99.

Hay, L. E., M. P. Clark, R. L. Wilby, W. J. Gutowski, G. H. Leavesley, Z. Pan, R. W. Arritt, and E. S. Takle. 2002. "Use of Regional Climate Model Output for Hydrologic Simulations." *Journal of Hydrometeorology* 3 (5): 571–90. https://doi.org/10.1175/1525-7541(2002)003<0571: UORCMO>2.0.CO;2.

Higashino, Makoto, and Heinz G Stefan. 2019. "Variability and Change of Precipitation and Flood Discharge in a Japanese River Basin." *Journal of Hydrology: Regional Studies* 21: 68–79.

Houghton-Carr, H. A., C. R. Print, M. J. Fry, H. Gadain, and P. Muchiri. 2011. "An Assessment of the Surface Water Resources of the Juba-Shabelle Basin in Southern Somalia."

Hydrological Sciences Journal 56 (5): 759–74. https://doi.org/10.1080/02626667.2011.585470.
Huang, P.-C. 2020. "Analysis of Hydrograph Shape Affected by Flow-Direction Assumptions in Rainfall-Runoff Models." *Water (Switzerland)* 12 (2).
Hundecha, Yeshewatesfa, and Bruno Merz. 2012. "Exploring the Relationship between Changes in Climate and Floods Using a Model-Based Analysis." *Water Resources Research* 48 (4).
IPCC. 1996. *Climate Change 1995: The Science of Climate Change: Contribution of Working Group I to the Second Assessment Report of the Intergovernmental Panel on Climate Change*. New York: Cambridge University Press.
IPCC. 2001. "Climate Change 2001: The Scientific Basis. Contribution of Working Group I to the Third Assessment Report of the Intergovernmental Panel on Climate Change [Houghton, J.T., Ding, Y., Griggs, D.J, Nouguer, M., van Der Linden, P.J., Dai, X., Maskell, K., Johnson C.A. (Eds.)]." In , 881.:881. Cambridge, UK. and New York, NY, USA: Cambridge University Press.
IPCC. 2007. *Climate Change 2007: Impacts, Adaptation and Vulnerability*. Cambridge [England]; New York; Melbourne, Australia; Madrid: Cambridge University Press.
IPCC. 2010. *IPCC Expert Meeting on Detection and Attribution Related to Anthropogenic Climate Change: The World Meteorological Organization, Geneva, Switzerland, 14-16 September 2009: Meeting Report*. Bern, Switzerland: IPCC Working Group I Technical Support Unit.
IPCC. 2013. *Climate Change 2013: The Physical Science Basis: Working Group I Contribution to the Fifth Assessment Report of the Intergovernmental Panel on Climate Change*.
IPCC. 2014. *Climate Change 2014: Synthesis Report. Contribution of Working Groups I, II and III to the Fifth Assessment Report of the Intergovernmental Panel on Climate Change*. IPCC.
IWMI. 2015. "Drivers of Hydrological Dynamics in the Bale Eco-Region In SHARE Bale Eco-Region Research Report Series No. 7." In. https://phe-ethiopia.org/pdf/7.%20Drivers-20-of-hydrological-20dynamics-%2020i n-20the-20BER.pdf.
Jain, Sharad K, and Vijay Kumar. 2012. "Trend Analysis of Rainfall and Temperature Data for India." *Current Science* 102 (1): 37–49.
Jenkins, G. J, Matthew Perry, John Prior, UKCIP09, and UK Climate Impacts Program. 2009. *The Climate of the United Kingdom and Recent Trends*. Exeter: Met Office Hadley Centre. http://www.ukcip.org.uk/images/stories/08_pdfs/Trends.pdf.
Jia Y, Ding X, Wang H, Zhou Z, Qiu Y, and Niu C. 2012. "Attribution of Water Resources Evolution in the Highly Water-Stressed Hai River Basin of China." *Water Resources Research* 48 (2).
Kay, S.M. Crooks, P. Pall, and D.A. Stone. 2011. "Attribution of Autumn/Winter 2000 Flood Risk in England to Anthropogenic Climate Change: A Catchment-Based Study." *Journal of Hydrology* 406 (1–2): 97–112. https://doi.org/10.1016/j.jhydrol.2011.06.006.
Keast, and Joanna Ellison. 2013. "Magnitude Frequency Analysis of Small Floods Using the Annual and Partial Series." *Water* 5 (4): 1816–29.
Kendall, M.G. 1975. "Rank Correlation Methods, Charles Griffin, London, UK."
Kerr, R. A. 1992. "Unmasking a Shifty Climate System." *Science* 255 (5051): 1508–10.
Kloos, Helmut, and Worku Legesse, eds. 2010. *Water Resources Management in Ethiopia: Implications for the Nile Basin*. Amherst, NY: Cambria Press.
Kundzewicz, Zbigniew W., and Alice J. Robson. 2004. "Change Detection in Hydrological Records—a Review of the Methodology / Revue Méthodologique de La Détection de

Changements Dans Les Chroniques Hydrologiques." *Hydrological Sciences Journal* 49 (1): 7–19. https://doi.org/10.1623/hysj.49.1.7.53993.
Kundzewicz, Zbigniew W, and Markus Stoffel. 2016. "Anatomy of Flood Risk."
Kundzewicz, Zbigniew W, Markus Stoffel, Tadeusz Niedźwiedź, Bartłomiej Wyżga, and Springer International Publishing AG. 2018. *Flood Risk in the Upper Vistula Basin.*
LCRDB. 2013. "Livestock and Crop Rural Development Bureau (LCRDB): The Lower Shebelle Irrigation Scheme in Ethiopia: An Assessment of Productive Options." Jijiga: Ethiopian Somali Regional State. https://dlci-hoa.org/assets/upload/combined-documents/20200804035015352.pdf.
Li, Linchao, Yufeng Zou, Yi Li, Haixia Lin, and De Li Liu. 2020. "Trends, Change Points and Spatial Variability in Extreme Precipitation Events from 1961 to 2017 in China." *Hydrology Research* 51 (3): 484–504.
Linsley, Ray K, Max A Kohler, and Joseph L. H Paulhus. 1988. *Hydrology for Engineers*. London: McGraw-Hill Book Company.
Liu, Ximin Yuan, Liang Guo, Yaohuan Huang, and Xiaolei Zhang. 2017. "Driving Force Analysis of the Temporal and Spatial Distribution of Flash Floods in Sichuan Province," August. https://doi.org/doi:10.3390/su9091527.
Malamud, B. D, and D. L Turcotte. 2006. "The Applicability of Power-Law Frequency Statistics to Floods." *Journal of Hydrology -Amsterdam-* 322 (1–4): 168–80.
Mann, Henry B. 1945. "Nonparametric Tests against Trend." *Econometrical: Journal of the Econometric Society*, 245–59.
Mathews, Jon, and R. L Walker. 1970. *Mathematical Methods of Physics*. New York: W.A. Benjamin.
McCuen, Richard H. 2003. *Modeling Hydrologic Change: Statistical Methods*. Boca Raton, Fla: Lewis Publishers.
Meng, Fanhao, Tie Liu, Yue Huang, Min Luo, Anming Bao, and Dawei Hou. 2016. "Quantitative Detection and Attribution of Runoff Variations in the Aksu River Basin." *Water* 8 (8): 338.
Merz, B., J. Aerts, K. Arnbjerg-Nielsen, M. Baldi, A. Becker, A. Bichet, G. Blöschl, et al. 2014. "Floods and Climate: Emerging Perspectives for Flood Risk Assessment and Management." *Natural Hazards and Earth System Sciences* 14 (7): 1921–42. https://doi.org/10.5194/nhess-14-1921-2014.
Merz, B., S. Vorogushyn, S. Uhlemann, J. Delgado, and Y. Hundecha. 2012. "HESS Opinions "More Efforts and Scientific Rigour Are Needed to Attribute Trends in Flood Time Series"" *Hydrology and Earth System Sciences* 16 (5): 1379–87. https://doi.org/10.5194/hess-16-1379-2012.
Merz, J. Aerts, K. Arnbjerg-Nielsen, M. Baldi, A. Becker, A. Bichet, and G. Blöschl. 2014. "Floods and Climate: Emerging Perspectives for Flood Risk Assessment and Management." https://doi.org/doi:10.5194/nhessd-2-1559-2014.
Mfwango, Lusajo H, Catherine J Salim, and Shija Kazumba. 2018. "Estimation of Missing River Flow Data for Hydrologic Analysis: The Case of Great Ruaha River Catchment." *Hydrology: Current Research* 09 (02).
Mi, Egigu. 2020. "Techniques of Filling Missing Values of Daily and Monthly Rain Fall Data: A Review" 3: 5.
Moes, Denika. 2015. *Power-Law Flood Frequency Analysis of Selected Queensland Stream Gauges*. http://eprints.usq.edu.au/29294/1/Moes_D_Brodie.pdf.

Moges, S.A., M.T. Taye, P. Willems, and M. Gebremichael. 2014. "Exceptional Pattern of Extreme Rainfall Variability at Urban Centre of Addis Ababa, Ethiopia." *Urban Water Journal* 11 (7): 596–604. https://doi.org/10.1080/1573062X.2013.831914.

Moges, Semu, Yirga Aleemu, Stuart McFeeters, and Worku Legesse. 2010. "Flooding in Ethiopia, Recent History and the 2006 Flood." *Cambria Press*.

Monteith. 1965. "Evaporation and Environment." *Symposia of the Society for Experimental Biology* 19: 205–34.

Moreira, Luana Lavagnoli, Daniel Rigo, and Dimaghi Schwamback. 2018. "Sensitivity Analysis of the Soil and Water Assessment Tools (SWAT) Model in Streamflow Modeling in a Rural River Basin." *Ambiagua Revista Ambiente & Água* 13 (6).

Moriasi, Arnold, M. W. Van Liew, R. L. Bingner, R. D. Harmel, and T. L. Veith. 2007. "Model Evaluation Guidelines for Systematic Quantification of Accuracy in Watershed Simulations." *Transactions of the ASABE* 50 (3): 885–900.

MoWR. 1998. *Ethiopian Ministry of Water Resources (MoWR) Wabi Shebele River Basin Integrated Development Master Plan Project, Reconnaissance Phase: Socio Economic*. Vol. II. Ethiopia: Ethiopian Ministry of Water Resources.

MoWR. 2003. *Ethiopian Ministry of Water Resources (MoWR) Wabi Shebele River Basin Integrated Master Plan Study Project. Vol. VII Water Resources, Part 2 Hydrology, Part. Ethiopia.* Part 2. Ethiopia: Ministry of Water Resources.

MoWR. 2004a. *Wabi Shebele River Basin Integrated Development Master Plan, Land Use/ Land Cover Study, Part. Ethiopia.* Part 8. Ethiopia: Ministry of Water Resources.

MoWR. 2004b. "The Federal Democratic Republic of Ethiopia, Ministry of Water Resources, Wabi Shebele River Basin, Integrated Development Master Plan Study Project, Volume III – Natural Resources, Part 7 – Soils (No. II), Addis Ababa, Ethiopia." II. Addis Ababa, Ethiopia: Ministry of Water Resources.

Mulugeta, Muise, Sen Sumit, and Puneet. 2020. "Application of CORDEX-AFRICA and NEX-GDDP Datasets for Hydrologic Projections under Climate Change in Lake Ziway Sub-Basin, Ethiopia | Elsevier Enhanced Reader." 2020. https://doi.org/10.1016/j.ejrh.2020.100721.

Narsimlu, Boini, Ashvin K Gosain, Baghu R Chahar, Sudhir Kumar Singh, Prashant K Srivastava, and SpringerLink (Online service). 2015. *SWAT Model Calibration and Uncertainty Analysis for Streamflow Prediction in the Kunwari River Basin, India, Using Sequential Uncertainty Fitting*. https://doi.org/10.1007/s40710-015-0064-8.

Näschen, Kristian, Bernd Diekkrüger, Constanze Leemhuis, Larisa Seregina, and Roderick van der Linden. 2019. "Impact of Climate Change on Water Resources in the Kilombero Catchment in Tanzania." *Water* 11 (4): 859.

Nash, J.E, and J.V Sutcliffe. 1970. "River Flow Forecasting through Conceptual Models, Part I - a Discussion of Principles." https://doi.org/doi.org/10.1016/0022-1694(70)90255-6.

NDRMC. 2018. "Federal Democratic Republic of Ethiopia National Disaster Risk Management Commission, Early Warning and Emergency Response Directorate."

Neitsch, S. L, J. Arnold, J. Kiniry, and J. Williams, 2005. *Soil and Water Assessment Tool: Theoretical Documentation: Version 2005*. Temple (Texas): Grassland, Soil and Water Research Laboratory; Blackland Research Center.

Newson, Malcolm David. 2005. *Hydrology and the River Environment*. Oxford; New York: Clarendon Press; Oxford University Press.

Ngai, Sheau Tieh, Fredolin Tangang, and Liew Juneng. 2017. “Bias Correction of Global and Regional Simulated Daily Precipitation and Surface Mean Temperature Over Southeast Asia Using Quantile Mapping Method.” *GLOBAL and Planetary Change* 149: 79–90.

Nied, Hundecha Y, and Merz B. 2013. “Flood-Initiating Catchment Conditions: A Spatio-Temporal Analysis of Large-Scale Soil Moisture Patterns in the Elbe River Basin,” Hydrol Earth Syst Sci 17:1401–1414, .

Niedźwiedź, Tadeusz, and Ewa Łupikasza. 2016. “Change in Atmospheric Circulation Patterns,” 189–208.

NMA. 1996. “Climatic and Agroclimatic Resources of Ethiopia.” *NMSA Meteorological Research Report Series (Ethiopia)*. https://agris.fao.org/agris-search/search.do?recordID, ET9700128.

Ntegeka, Victor, and Patrick Willems. 2008. “Trends and Multidecadal Oscillations in Rainfall Extremes, Based on a More than 100-Year Time Series of 10 Min Rainfall Intensities at Uccle, Belgium: Oscillations IN RAI.” *Water Resources Research* 44 (7). https://doi.org/10.1029/2007WR006471.

Onyutha, Charles. 2016. “Statistical Analyses of Potential Evapotranspiration Changes over the Period 1930–2012 in the Nile River Riparian Countries.” *Agricultural and Forest Meteorology* 226–227 (October): 80–95. https://doi.org/10.1016/j.agrformet.2016.05.015.

Patra, K. C. 2010. *Hydrology and Water Resources Engineering*. Oxford: Alpha Science International.

Perrin, C, C Michel, and V Andreassian. 2001. “Does a Large Number of Parameters Enhance Model Performance? Comparative Assessment of Common Catchment Model Structures on 429 Catchments.” *Journal of Hydrology.* 242 (3): 275.

Piani C, Coppola E, and Haerter J.O. 2010. “Statistical Bias Correction for Daily Precipitation in Regional Climate Models over Europe.” *Theoretical and Applied Climatology* 99 (1–2): 187–92.

Pianosi, Francesca, Keith Beven, Jim Freer, Jim W. Hall, Jonathan Rougier, David B. Stephenson, and Thorsten Wagener. 2016. “Sensitivity Analysis of Environmental Models: A Systematic Review with Practical Workflow.” *Environmental Modelling & Software* 79 (May): 214–32. https://doi.org/10.1016/j.envsoft.2016.02.008.

Pickford, John, ed. 1999. *Integrated Development for Water Supply and Sanitation: Proceedings of the 25th WEDC Conference, Addis Ababa, Ethiopia, 1999*. Loughborough: WEDC, Water, Engineering and Development Centre.

Podesta, J., and J Holdren. 2014. “The U.S. and China Just Announced Important New Actions to Reduce Carbon Pollution.” Whitehouse.Gov. 2014. https://obamawhitehouse.archives.gov/blog/2014/11/12/us-and-china-just-announced-important-new-actions-reduce-carbon-pollution.

Prachansri, Saowanee. 2007. “Analysis of Soil and Land Cover Parameters for Flood Hazard Assessment,” 106.

Priestley, C.H.B. 1972. “On the Assessment of Surface Heat Flux and Evaporation Using Large-Scale Parameters.” *Monthly Weather Review* 100 (2): 81–82.

Rahman, A.S. 2020. “Application of Principal Component Analysis and Cluster Analysis in Regional Flood Frequency Analysis: A Case Study in New South Wales, Australia.” *Water (Switzerland)* 12 (3): 1–26.

Rathjens, Hendrik. 2016. “CMhyd User Manual,” 17.

Razavi, Saman, and Richard Vogel. 2018. “Pre-whitening of Hydroclimatic Time Series? Implications for Inferred Change and Variability across Time Scales.” *Journal of Hydrology* 557 (February): 109–15. https://doi.org/10.1016/j.jhydrol.2017.11.053.

Ruiz-Villanueva, Virginia, Bartłomiej Wyżga, Zbigniew W Kundzewicz, Tadeusz Niedźwiedź, Ewa Łupikasza, and Markus Stoffel. 2016. “Variability of Flood Frequency and Magnitude During the Late 20th and Early 21st Centuries in the Northern Foreland of the Tatra Mountains.”

Salas, J. D, J Obeysekera, and R. M Vogel. 2018. “Techniques for Assessing Water Infrastructure for Nonstationary Extreme Events: A Review.” *Hydrological Sciences Journal.* 63 (3): 325–52.

Samuelsson, Patrick, Colin G. Jones, Ulrika Will´En, Anders Ullerstig, Stefan Gollvik, Ulf Hansson, Erik Jansson, Christer Kjellstro¨M, Grigory Nikulin, and Klaus Wyser. 2011. “The Rossby Centre Regional Climate Model RCA3: Model Description and Performance.” *Tellus A: Dynamic Meteorology and Oceanography* 63 (1): 4–23. https://doi.org/10.1111/j.1600-0870.2010.00478.x.

Schreider, S.Yu, A.J Jakeman, R.A Letcher, R.J Nathan, B.P Neal, and S.G Beavis. 2002. “Detecting Changes in Streamflow Response to Changes in Non-Climatic Catchment Conditions: Farm Dam Development in the Murray–Darling Basin, Australia.” *Journal of Hydrology* 262 (1–4): 84–98.

Schulze. 2000. “Modelling Hydrological Responses to Land Use and Climate Change: A Southern African Perspective.” *Ambio* 29 (1): 12–22.

Segele, Z T, and P J Lamb. 2005. “Characterization and Variability of Kiremt Rainy Season over Ethiopia.” *Meteorology and Atmospheric Physics.* 89 (1): 153.

Seibert, J, and J.J McDonnell. 2010. “Land-Cover Impacts on Streamflow: A Change-Detection Modelling Approach That Incorporates Parameter Uncertainty.” *Hydrological Sciences Journal.* 55 (3): 316–32.

Seleshi, Yilma, and Ulrich Zanke. 2004. “Recent Changes in Rainfall and Rainy Days in Ethiopia.” *International Journal of Climatology* 24 (8): 973–83.

Sen, Pranab Kumar. 1968. “Estimates of the Regression Coefficient Based on Kendall’s Tau.” *Journal of the American Statistical Association* 63 (324): 1379–89.

Sheng, Yue, and Chun Y Wang. 2002. “Regional Streamflow Trend Detection with Consideration of Both Temporal and Spatial Correlation.” *International Journal of Climatology*, 0899–8418.

Shiferaw, Andualem, Jemal Seid Ahmed, Tesfaye Gisella, Temesgen Gebremariam, Aklilu Amsalu, and Gebru Jember. 2015. *Ethiopian Panel on Climate Change (2015), First Assessment Report, Working Group I Physical Science Basis*. Ethiopia: Ethiopian Academy of Sciences.

Siam, Mohamed S, Guiling Wang, Marie-Estelle Demory, and Elfatih A. B Eltahir. 2014. “Role of the Indian Ocean Sea Surface Temperature in Shaping the Natural Variability in the Flow of Nile River.” *Climate Dynamics: Observational, Theoretical and Computational Research on the Climate System* 43 (3–4): 1011–23.

Slater, Louise J, Bailey Anderson, Marcus Buechel, Simon Dadson, Shasha Han, Shaun Harrigan, Timo Kelder, et al. 2021. “Nonstationary Weather and Water Extremes: A Review of Methods for Their Detection, Attribution, and Management.” *Hydrology and Earth System Sciences* 25 (7): 3897–3935.

Stoffel, Markus, Bartłomiej Wyżga, Tadeusz Niedźwiedź, Virginia Ruiz-Villanueva, Juan Antonio Ballesteros-Cánovas, and Zbigniew W Kundzewicz. 2016. “Floods in Mountain Basins,” 23–37.

Sutfin, Nicholas A., and Ellen Wohl. 2019. “Elevational Differences in Hydrogeomorphic Disturbance Regime Influence Sediment Residence Times within Mountain River Corridors.” *Nature Communications* 10 (1): 2221. https://doi.org/10.1038/s41467-019-09864-w.

Tabari, Hossein, Amir AghaKouchak, and Patrick Willems. 2014. “A Perturbation Approach for Assessing Trends in Precipitation Extremes across Iran.” *Journal of Hydrology* 519 (November): 1420–27. https://doi.org/10.1016/j.jhydrol.2014.09.019.

Tadesse, Tsegaye, Tonya Haigh, Nicole Wall, Andualem Shiferaw, Ben Zaitchik, Shimelis Beyene, Getachew Berhan, and Jacob Petr. 2016. “Linking Seasonal Predictions to Decision-Making and Disaster Management in the Greater Horn of Africa.” *Bulletin of the American Meteorological Society* 97 (4): ES89–92. https://doi.org/10.1175/BAMS-D-15-00269.1.

Talchabhadel, Rocky, Ramchandra Karki, Bhesh Raj Thapa, Manisha Maharjan, and Binod Parajuli. 2018. “Spatio-Temporal Variability of Extreme Precipitation in Nepal.” *JOC International Journal of Climatology* 38 (11): 4296–4313.

Tali, P.Ahmed, and T. A. Kanth. 2011. “Land Use/Land Cover Change and Its Impact on Flood Occurrence: A Case Study of Upper Jhelum Floodplain, Dissertation Submitted to University of Kashmir, Srinagar - 190 006, Kashmir.” Search.Myway.Com. September 2011. https://search.myway.com/web.

Taye, M. T., and Patrick Willems. 2012a. “Temporal Variability of Hydroclimatic Extremes in the Blue Nile Basin:” *Water Resources Research* 48 (3). https://doi.org/10.1029/2011WR011466.

Teshome, Asaminew, and Jie Zhang. 2019. “Increase of Extreme Drought over Ethiopia under Climate Warming.” *AMETE Advances in Meteorology* 2019.

Teutschbein, Claudia, and Jan Seibert. 2012. “Bias Correction of Regional Climate Model Simulations for Hydrological Climate-Change Impact Studies: Review and Evaluation of Different Methods.” *Journal of Hydrology* s 456–457 (August): 12–29. https://doi.org/10.1016/j.jhydrol.2012.05.052.

UN. 2000. “Meeting of The Parties to The Convention on The Protection and Use of Transboundary Watercourses and International Lakes.”

UNDP. 1999. “Drought and Floods Stress Livelihoods and Food Security in the Ethiopian Somali Region - Ethiopia.” ReliefWeb. 1999. https://reliefweb.int/report/ethiopia/drought-and-floods-stress-livelihoods-and-food-security-ethiopian-somali-region.

UNOCHA. 2015. “The State of Response to El-Nino in the Horn of Africa.” https://www.unocha.org/sites/dms/Documents/2016_11_Elnino_Africa_Breakfast_meeting_FINAL.pdf.

USACE. 2000. *HEC-HMS Hydrologic Modeling System: User’s Manual*. Davis, California: US Army Corps of Engineers, Hydrologic Engineering Center.

Vandaele, K, and J Poesen. 1995. “Spatial and temporal patterns of soil erosion rates in an agricultural catchment, central Belgium.” *CATENA -GIESSEN THEN AMSTERDAM-* 25 (1/4): 213.

Veijalainen, Noora, Eliisa Lotsari, Petteri Alho, Bertel Vehviläinen, and Jukka Käyhkö. 2010. "National Scale Assessment of Climate Change Impacts on Flooding in Finland." *HYDROL Journal of Hydrology* 391 (3–4): 333–50.

Viglione, Alberto, Bruno Merz, Nguyen Viet Dung, Juraj Parajka, Thomas Nester, and Günter Blöschl. 2016. "Attribution of Regional Flood Changes Based on Scaling Fingerprints." *WRCR Water Resources Research* 52 (7): 5322–40.

Villarini, G, J. A Smith, F Serinaldi, J Bales, P. D Bates, and W. F Krajewski. 2009. "Flood Frequency Analysis for Nonstationary Annual Peak Records in an Urban Drainage Basin." *Advances in Water Resources.* 32 (8): 1255–66.

Von Storch, Hans. 1999. "Misuses of Statistical Analysis in Climate Research." In *Analysis of Climate Variability*, 11–26. Springer.

Wanders, Niko. 2015. *Hydrological Extremes: Improving Simulations of Flood and Drought in Large River Basins*. http://dspace.library.uu.nl/bitstream/handle/1874/310177/Wanders.pdf?sequence=1.

Welch, B. L. 1959. "The Advanced Theory of Statistics: Vol. I—Distribution Theory." *RSSA Journal of the Royal Statistical Society: Series A (General)* 122 (1): 99–100.

Wilby, R. L, C. W Dawson, and E. M Barrow. 2002. "Sdsm — a Decision Support Tool for the Assessment of Regional Climate Change Impacts." *Environmental Modelling & Software* 17 (2): 145–57. https://doi.org/10.1016/S1364-8152(01)00060-3.

Williams, A. Park, Chris Funk, Joel Michaelsen, Sara A. Rauscher, Iain Robertson, Tommy H. G. Wils, Zewdu Eshetu, and Neil J. Loader. 2012. "Recent Summer Precipitation Trends in the Greater Horn of Africa and the Emerging Role of Indian Ocean Sea Surface Temperature" 39 (9–10): 2307–28. https://doi.org/10.7916/D8R78C8F.

Williams and Funk. 2011. "A Westward Extension of the Warm Pool Leads to a Westward Extension of the Walker Circulation, Drying Eastern Africa." *Climate Dynamics* 37 (11–12): 2417–35.

WMO. 2013. "World Meteorological Organization (WMO No. 8): Guide to Meteorological Instruments and Methods of Observation." *MET Education* (blog). December 7, 2013. https://metmalaysiaeducation.wordpress.com/wmo-no-8-guide-to-meteorological-instruments-and-methods-of-observation/.

WMO, 2014. *Atlas of Mortality and Economic Losses from Weather, Climate and Water Extremes (1970-2012)*.

Woldegebrael, Surafel Mamo, Belete Kidanewold, and Assefa Melesse. 2019. "Historical Flood Events and Hydrological Extremes in Ethiopia." In *Extreme Hydrology and Climate Variability: Monitoring, Modelling, Adaptation and Mitigation, Editors, Melesse, AM, Abtew, W and Senay,G (Pp.379-384)*, 379–84. https://doi.org/10.1016/B978-0-12-815998-9.00029-4.

Worku, Gebrekidan, Ermias Teferi, Amare Bantider, and Yihun T Dile. 2020. "Statistical Bias Correction of Regional Climate Model Simulations for Climate Change Projection in the Jemma Sub-Basin, Upper Blue Nile Basin of Ethiopia." *Theoretical and Applied Climatology* 139 (3–4): 1569–88.

WORLD BANK. 2006. *Ethiopia: Managing Water Resources to Maximize Sustainable Growth*. The World Bank Agriculture and Rural Development Department.

World Bank. 2020. "Climate Risk Country Profile: Ethiopia | PreventionWeb.Net." 2020. https://www.preventionweb.net/publications/view/74339.

Xu, Xin, Yu-Chen Wang, Margaret Kalcic, Rebecca Muenich, Yi-Chen Yang, and Donald Scavia. 2017. "Evaluating the Impact of Climate Change on Fluvial Flood Risk in a Mixed-Use Watershed." *Environmental Modelling & Software* 122 (August). https://doi.org/10.1016/j.envsoft.2017.07.013.

Yang, Y. C. Ethan, Sungwook Wi, Patrick A. Ray, Casey M. Brown, and Abedalrazq F. Khalil. 2016. "The Future Nexus of the Brahmaputra River Basin: Climate, Water, Energy and Food Trajectories." *Global Environmental Change* 37 (March): 16–30. https://doi.org/10.1016/j.gloenvcha.2016.01.002.

Yue, Kundzewicz, and Wang. 2019. *Detection of Changes*. *Changes in Flood Risk in Europe*. CRC Press. https://doi.org/10.1201/b12348-22.

Yue, Sheng, Paul Pilon, and Bob Phinney. 2003. "Canadian Streamflow Trend Detection: Impacts of Serial and Cross-Correlation." *Hydrological Sciences Journal* 48 (1): 51–63.

Yue, Sheng, paw Pilon, and George Cavadias. 2002. "Power of the Mann-Kendall and Spearman's Rho Tests for Detecting Monotonic Trends in Hydrological Series." *Elsevier, Journal of Hydrology*. www.elsevier.com/locate/jhydrol.

Yulianto, Fajar, Suwarsono Suwarsono, Udhi Catur Nugroho, Nunung Puji Nugroho, Wismu Sunarmodo, and Muhammad Rokhis Khomarudin. 2020. "Spatial-Temporal Dynamics Land Use/Land Cover Change and Flood Hazard Mapping in the Upstream Citarum Watershed, West Java, Indonesia." *Quaestiones Geographicae (Poznań ; 2010).*, 125–46.

Zhang, Xuebin, Lucie A Vincent, WD Hogg, and Ain Niitsoo. 2000. "Temperature and Precipitation Trends in Canada during the 20th Century." *Atmosphere-Ocean* 38 (3): 395–429.

Zuo, Qiting, Heng Zhao, Cuicui Mao, Junxia Ma, and Guotao Cui. 2015. "Quantitative Analysis of Human-Water Relationships and Harmony-Based Regulation in the Tarim River Basin." *Journal of Hydrologic Engineering* 20 (8): 05014030.

APPENDICES

Appendix A: Historical Flood Events in Ethiopia

Table A.1: Historical flood events and distributions in Ethiopia (1980-2021)

Year	Occurrence	Origin	Location	River Basin
1981	1		Kalafo	Wabi Shebele
1985	2		Ogaden and Rift Valley region	Wabi Shebele, Rift Valley basin
1988	2		Gambela and Sidamo province	Baro and Genale dawa
1990	1	Heavy rain	Gambela region	Baro Akobo
1993	2	"	Addis Abeba, Gojjam, Gonder	Awash, Abbay
1994	1	Heavy rain	North Shoa, South Welo, Gonder	Awash and Abbay
1995	1	Heavy rain	Kelafo, Mustahil, Ferfer, Burukur, Eastern Ogaden	Webi Shebelle
1996	2	Heavy rains	Gambella region, East-Shoa, Wanji provinces	Baro and Awash
1997	2	Heavy rain	Somali region; Dollo, Arba Minch	Wabi Shebele, Awash and Omo gibe
2001	3		Dubti, Asaita, Gambela region; Himora in Tigray region	Awash, Baro and Tekeze
2002	1	Heavy rain	Afar, Oromia, Somali regions	Wabi Shebele and Awash
2003	1	Heavy rains	Somali region	Wabe Shebelle
2005	4	Heavy rains	Dire Dawa, Somali, Tigray, Amhara, Oromia region	Wabi Shebele, Awash and Tekeze
2006	7	Heavy rain	Dire Dawa, Addis Ababa, Somali, Tigray, Amhara, Gambela and Afar regions	Awash, Tekeze, Omo gibe, Wabi Shebelle and Baro
2007	2	Heavy rain	Gambela, Amhara, SNNPR, Addis Ababa, Afar, Tigray, Somali regions	Awash, Tekeze, Omo gibe, Wabe Shebelle and Baro
2008	3	Heavy rains	Somali; SNNPR; Oromia; Amhara and Gambela region	Wabe Shebele
2010	2	Heavy rains	Somali region; Afar, Amhara, Tigray regions	Wabi Shabelle, Awash, Tekeze
2011	1		Mustahil, Kelafo and Shabelle in Somali	Wabi Shabelle
2013	1		Somali region; SNNPR region.	Wabi Shabelle, Omo
2015	1		Shabelle district in Somali region	Wabishabelle, Genale/Dawa, and Omo
2016	2	Torrential rains	SNNPR and district in Oromia region.	Wabi Shebele
2019	1		Somali region	Wabi Shebele
2020	2	Heavy rains	Dire Dawa City, SNNPR, Amhara Region	Wabi Shabelle, Abbay

Source: "EM-DAT: The OFDA/CRED International Disaster Database, www.em-dat.net

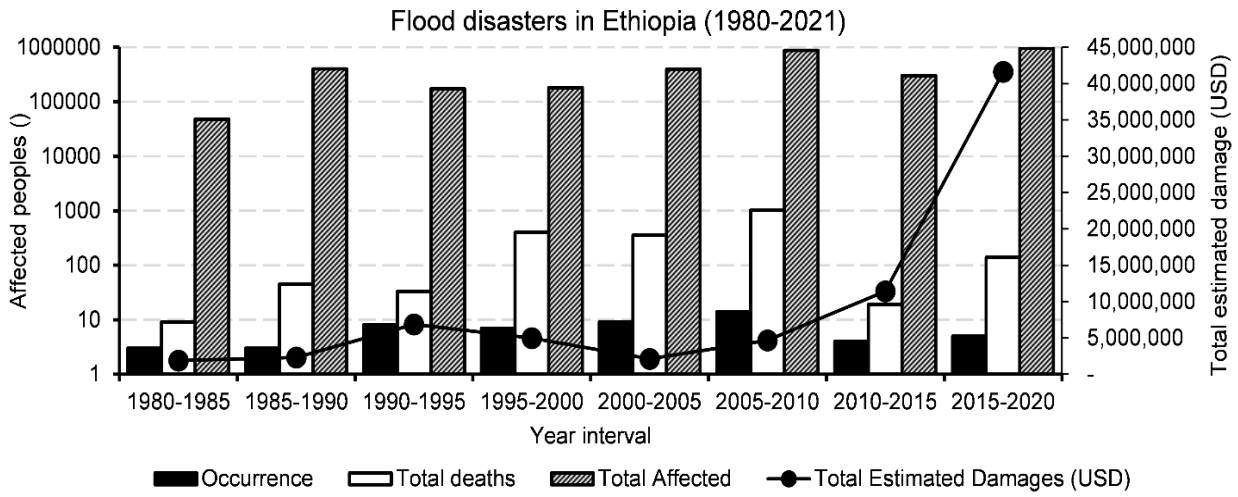

Figure A.1: Flood disasters trend in Ethiopia

Appendix B: Spatial and temporal information of meteorological stations used in the study

Table B.1: Spatial and temporal information of meteorological stations used in the study

S.No	Station Name	Latitude (Degree)	Longitude (Degree)	Altitude (m)	Period of Records	Missing (%)
1	Adaba	7.00	39.40	2420	1980-2013	21.12%
2	Adele	7.80	39.9	2420	1980-2013	29.80%
3	Arsi Robe	7.86	39.63	2400	1980-2013	1.70%
4	Bale Robe	7.13	40.00	2500	1980-2013	14.90%
5	D/Dawa	9.60	41.86	1260	1980-2013	1.92%
6	Deder	9.32	41.45	2350	1980-2013	22.40%
7	Degehabour	8.22	43.55	1070	1980-2013	5.64%
8	Dodola	6.98	39.18	3000	1988-2006	14.72%
9	Gode	5.90	43.58	295	1980-2011	8.62%
10	Gursum	9.35	42.4	1900	1984-2013	6.82%
11	Haromaya	9.40	42.03	2020	1980-2011	14.12%
12	Hawassa	7.07	38.48	1750	1980-2013	0.60%
13	Jara	7.46	40.81	1474	1986-2017	3.92%
14	Jijiga	9.33	42.78	1775	1980-2011	2.87%
15	Kebriderhar	6.73	44.30	505	1980-2011	27.97%
16	Kofele	7.07	38.80	2620	2000-2018	6.40%
17	Mararo	7.45	39.36	2940	1980-2013	27.80%
18	Seru	7.67	40.20	2480	1980-2013	14.20%
19	Sinana	7.04	40.13	2400	1980-2013	27.50%

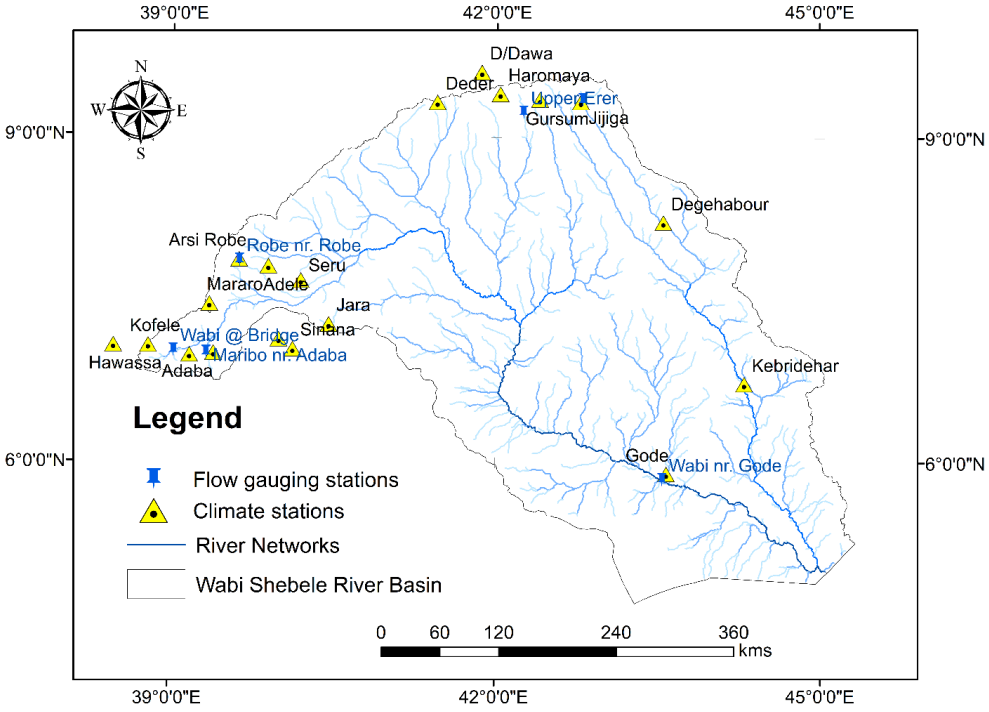

Figure B.1: Locations of selected hydro climatic gauging stations considered in the study

Appendix C: Data quality and missing data estimation

Before further analysis and simulations, the quality of hydrological and meteorological data is checked. Different data quality checks like filling gaps, inconsistency adjustments, and non-homogeneity analysis are conducted in this study. Several methods used for filling missed data precipitation and flow are given in Mi (2020) and Gyau-Boakye and Schultz (1994) in detail. In this study, values with a short length of gap (<10%) of flow, precipitation, temperature, sunshine hour, relative humidity, and wind speed data are filled using the long-year average method at each station. But to fill missing data for long period gaps (> 10%), a multiple Regression analysis with nearby gauging stations is used. The method has the ability to outperform the other methods in estimation of missed data, on annual and in seasons flow time series in different studies (Campozano et al. 2014; Mfwango et al., 2018).

Homogeneity and consistency tests are performed for selected gauging stations and plotted for comparison (Figure C.1 and C.2). In this study, a relative homogeneity test is conducted to select the representative meteorological stations. Monthly precipitation is non-dimensionalized using Equation (C.1) at each station, following Linsley et al. (1988) and Belay et al. (2019).

$$P_i = \frac{(\overline{p_i})}{\bar{P}} * 100\% \qquad (C.1)$$

Where Pi is the non-dimensionalized value of precipitation for the month i, $P_i$bar is the average monthly precipitation for the station i, and Pbar is the average yearly precipitation of the station. For illustration, From Figure C.1, similar precipitation mode and pattern of the stations observed in most of the gauging stations and, hence the group of stations selected is homogenous. However, the gauging station located in the downstream lowland of the basin indicates different rainfall patterns, the second peak in the area shifts to October month.

The double mass curve technique is used to adjust precipitation records of non-representative factors such as a change in location or exposure of rain gage. The accumulated totals of rainfall in each station are compared with the corresponding sum of annual rainfall in a group of nearby stations. If a significant change in the regime of the curve is observed, it should be corrected. The consistency test using the double-mass curve at gauging stations indicates that all stations were consistent (Figure C.2).

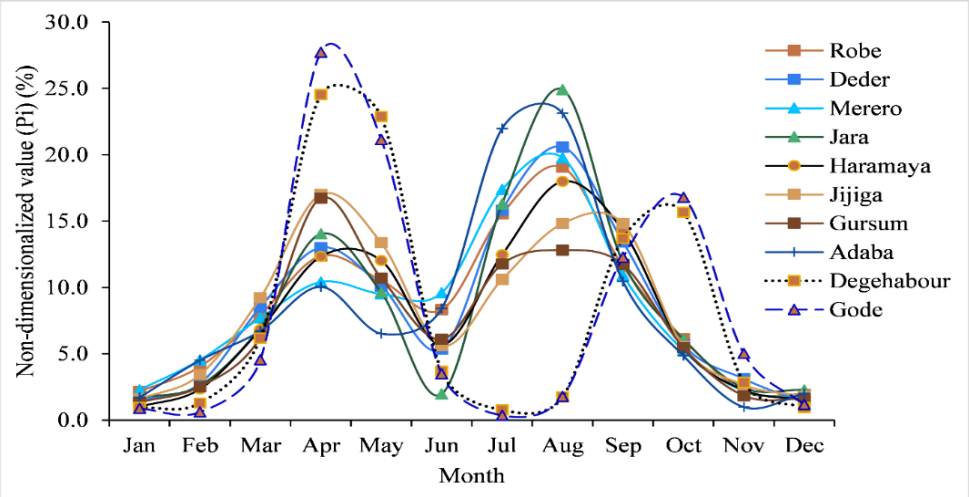

Figure C.1: non-dimensionalized rainfall from five stations and their average used for Wabi Shebele River Basin

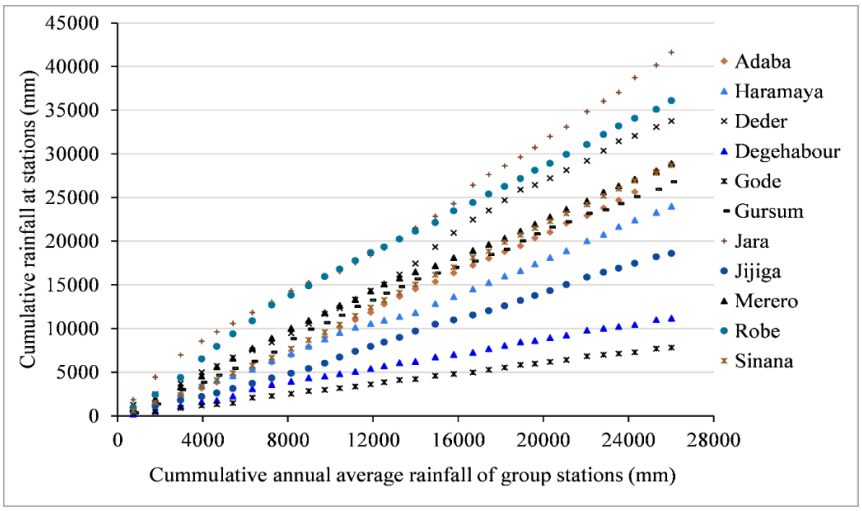

Figure C.2: Double mass curve of rainfall in Wabi Shebele River Basin for selected stations

Table C.1. Goodness-of fit test on Cumulative Distribution Function (CDF) of reanalysis climate products relative to ground based observed data using Chi-square (X^2) statistics

Station	ENACTS	CHIRPS
Adaba	74.68	151.94
Kofele	40.47	16.81
Robe (Arsi)	116.21	96.4
Jara	276.76	79.52
Deder	71.5	135.13
Diredawa	7.88	3.63
Jijiga	14.5	62.57
Gode	63.08	22.83
Degehabour	17.62	7.29
Kebridehar	106.4	134.52

Appendix D: Potential Drivers of Flood Events

Climate factors

The annual average depth of rainfall (P) over the watershed area (km^2) of the study area is estimated by the Thiessen method (Equation D.1) from the precipitation (Pi) observed at each of the rain gauges in and around watersheds.

$$P = \frac{\sum_{i=1} P_i a_i}{A} \qquad (D.1)$$

where a_i is the area or weighting factor for each station i, respectively.

Watershed characteristics factors

An accurate, 90-m DEM is used, to extract watershed characteristics representing the geomorphologic properties of the six watersheds under investigation. Also, DEM reconditioning

is implemented using GIS ArcMap; this system adjusts the surface elevation of the DEM to be consistent with vector coverage of drainage streams provided by the Ministry of Water, Irrigation, and Energy (MoIE). Stream networks, elevation, stream networks, and slope parameters were generated directly by the GIS, and the rest of drainage density is calculated from these. All the variables were transformed later by taking the common logarithms for the regression analysis.

Drainage area (DA; km^2): is assumed to be the same area of the bounded watershed that contributes to surface runoff. DA was delineated from the DEM by computing the flow direction.

Mean basin elevation (BE; m): is measured in meters above sea level and is the mean watershed altitude.

Basin slope (BS; %): is the mean basin slope and is measured by calculating the average rate of change between each cell partitioned as a hydrologic response unit in each watershed.

Basin perimeter (BP; km): is the distance measured around a basin boundary.

The basin shape factor (SF; dimensionless): is expressed as the ratio of the square of the valley length to the watershed area. SF was computed by dividing the squared valley length by basin area:

$$SF = \frac{VL^2}{DA} \qquad (D.2)$$

The SF is expected to be <1 if the watershed is long and narrow and SF=1 if the watershed is square (Patra 2010).

Drainage density (DD; km/km^2): is computed by dividing the total sum of all stream lengths (SL; km) in the watersheds by the drainage area:

$$DD = \frac{\sum SL}{DA} \qquad (D.3)$$

Valley slope (VS; m/km): was calculated by determining the elevations at the gauge station (E_{gauge}) and 85% of the distance along with VL ($E_{0.85VL}$), and then dividing the difference in elevation between these two points by the length of that valley channel connecting the two points:

$$VS = \frac{E_{0.85VL} - E_{gsuge}}{0.85VL} \qquad (D.4)$$

The elongation ratio (ER; no units): originally proposed by Schumm (1956), is the ratio of the diameter of a circle with the same area to the maximum length of the valley:

$$ER = \left(\frac{4DA}{\pi VL\text{^}2}\right)^{0.5} = 1.13\left(\frac{1}{SF}\right)^{0.5} \qquad (D.5)$$

Soil type: the soil infiltration rate is another sensitive variable in flood generation. Soils containing a large amount of sand and silt have a habit of forming a crust and become more compacted that significantly reduces the infiltration rate. In the Wabi Shebele basin, soil distributions vary spatially; loamy sand in the east and downstream, clay in the middle, sandy loam in the middle, and silty clay in the northwest (Figure 2-4).

Human activities factor

The percentage of land use and land cover in the Wabi Shebele basin was taken and analyzed from the basin master plan report (MoWR, 2004a.). The land use and land cover coverage area are estimated using the watershed boundary and land use map information. Another potential driver of floods in watersheds is population density. The population growth and cultivated land density have a strong correlation

Multiple regression Analysis

Multiple linear regression analysis was also performed on watershed characteristics with QMPF, and the weakest predictor, i.e., highest p-value, was removed in each step. The regression is recalculated until only useful predictor variables remain in the model. For each model, the significance analysis was evaluated and in the independent variable.

The regression equation takes the following form:

$$Y = a + b_1X_1 + b_2X_2 + b_3X_3 + \cdots + b_iX_i \qquad (D.6)$$

Where: Y is the value of the Dependent variable (i.e., QMPF in m^3/s), what is being predicted or explained; X_1, X_2, X_3, … Xi are independent variables that explain the variance in Y; a (Alpha) is the constant or intercept; b_1, b_2, b_3, …, bi are the slope (Beta coefficient) for independent variables.

Principial Component Analysis

Principal Component Analysis (PCA) is used in this study to see multivariate relationships between potential driving factors and mean peak flow discharge (QMPF). If the number of predictor variables increases and they are highly correlated, Multiple linear regression (MLR) models gets more unstable. In PCA, different types of variables: hydrologic and watershed variables are treated together. The original dataset of n variables, which are correlated to various degrees are transformed to n numbers of uncorrelated PCs. The PCs are linear transformation of the original variables in such a way that the original and the new variables have equal sums of the variances. Although the number of PCs and original variables are equal, the first few PCs explain the majority of the variance in the data set, reducing the dimensionality of the original data set.

The PCs are sequenced from the highest to the lowest variance, i.e., the first PC describes the data's highest variance proportion. The next highest variance is explained by the second PC and so on. The values of PCs can be obtained from Equations (D.7) and (D.8):

$$PC1 = a_{11}x_1 + a_{12}x_1 + \cdots + a_{1n}x_n = \sum_{j=1}^{n} a_{1j}x_j \qquad (D.7)$$

$$PC2 = a_{21}x_1 + a_{22}x_2 + \cdots + a_{2n}x_n = \sum_{j=1}^{n} a_{2j}x_j \qquad (D.8)$$

where x_1, x_2, … x_n are the original variables and a_{jj} are the eigenvectors. The eigenvalues are the variances of the PCs. The covariance or correlation matrix of the data set is used to derive the coefficients a_{jj}, which are the eigenvectors. The eigenvalues of the data matrix can be calculated by Equation (D.9):

$$|C - \lambda I| = 0 \qquad (D.9)$$

where C is the correlation/covariance matrix, λ is the eigenvalue, and I is the identity matrix. The PC coefficients or the weights of the variables in the PCs are then calculated by Equation (D.10):

$$|C - \lambda I|a_{jj} = 0 \qquad (D.10)$$

Appendix E: Model Parameters selected for Water production in SWAT model

Table E.1: The parameter descriptions, physical properties, and lower/upper limits (Source: Arnold et al. (2012))

Parameter	Description	LL	LU	Method of Variation
CN2.mgt	Initial SCS runoff curve number for moisture condition II	-0.25	0.25	Relative
ALPHA_BF.gw	Baseflow alpha factor (day)	0	1	Replace
GW_DELAY.gw	Groundwater delay time (day)	-10	10	Add
GWQMN.gw	Threshold depth of water in the shallow aquifer required for return flow to occur (mm)	-1000	1000	Add
CANMX	Maximum canopy storage (mm)	0	10	Replace
REVAPMN.gw	Threshold depth of water in the shallow aquifer for "revap" or percolation to the deep aquifer (mm)	-100	100	Add
SOL_AWC (1).sol	Available water capacity of the soil (mm mm^{-1})	-0.25	0.25	Relative
SOL_K (1).sol	Saturated hydraulic conductivity (mm h^{-1})	-0.25	0.25	Relative
SOL_Z	Depth from soil surface to bottom of layer (mm)	-0.25	0.25	Relative
SURLAG	Surface runoff lag coefficient (day)	-0.25	0.25	Relative
ESCO.hru	Soil evaporation compensation factor	0	1	Replace
EPCO.hru	Plant uptake compensation factor	0	1	Replace
BIOMIX	Biological mixing efficiency	0	1	Replace
GW_REVAP.gw	Groundwater "revap" coefficient	-0.036	0.036	Add
CH_K2.rte	Effective hydraulic conductivity in the main channel alluvium (mm h^{-1})		150	Replace
CH_N2.rte	Manning's "n" value for the main channel (s m^{-3})	0	1	Replace
SLSUBBSN.hru	Average slope length (m)	10	150	Replace
OV_N.hru	Manning's n value for overland flow	0.01	30	Replace
HRU_SLP.hru	Average slope steepness (m m^{-1})	0	1	Relative
ALPHA_BNK.rte	Baseflow alpha factor for bank storage (days)	0	1	Replace